Research Report
KTC-07-07/SPR246-02-6F

KENTUCKY TRANSPORTATION CENTER

SEISMIC-HAZARD MAPS AND TIME HISTORIES FOR THE COMMONWEALTH OF KENTUCKY

UNIVERSITY OF KENTUCKY
College of Engineering

OUR MISSION

We provide services to the transportation community through research, technology transfer and education. We create and participate in partnerships to promote safe and effective transportation systems.

OUR VALUES

Teamwork
Listening and communicating along with courtesy and respect for others.

Honesty and Ethical Behavior
Delivering the highest quality products and services.

Continuous Improvement
In all that we do.

Research Report
KTC-07-07/SPR246-02-6F

SEISMIC-HAZARD MAPS AND TIME HISTORIES FOR THE COMMONWEALTH OF KENTUCKY

by

Zhenming Wang
Seismologist and Head, Geologic Hazards Section
Kentucky Geological Survey

Issam E. Harik
Professor of Civil Engineering and Program Manager, Structures and Coatings Section,
Kentucky Transportation Center

Edward W. Woolery
Assistant Professor, Department of Earth and Environmental Sciences

Baoping Shi
Seismologist, Kentucky Geological Survey

and

Abheetha Peiris
Doctoral Research Student, Kentucky Transportation Center

Kentucky Transportation Center
College of Engineering, University of Kentucky

in cooperation with

Transportation Cabinet
Commonwealth of Kentucky

and

Federal Highway Administration
U.S. Department of Transportation

June 2008

Technical Report Documentation Page

1. Report No.	2. Government Accession No.	3. Recipient's Catalog No.
KTC-07-07/SPR246-02-6F		

4. Title and Subtitle

SEISMIC HAZARD MAPS AND TIME HISTORIES FOR THE COMMONWEALTH OF KENTUCKY

5. Report Date
June 2008

6. Performing Organization Code

7. Author(s): Wang Z., Harik I.E., Woolery E.W., Shi B. and Peiris A.

8. Performing Organization Report No.
KTC-07-07/SPR246-02-6F

9. Performing Organization Name and Address

Kentucky Transportation Center
College of Engineering
University of Kentucky
Lexington, KY 40506-0281

10. Work Unit No. (TRAIS)

11. Contract or Grant No.

12. Sponsoring Agency Name and Address

Kentucky Transportation Cabinet
State Office Building
Frankfort, KY 40622

13. Type of Report and Period Covered
Final

14. Sponsoring Agency Code

15. Supplementary Notes
Prepared in cooperation with the Kentucky Transportation Cabinet and the U.S. Department of Transportation, Federal Highway Administration.

16. Abstract

The ground-motion hazard maps and time histories for three earthquake scenarios, *expected earthquakes*, *probable earthquakes*, and *maximum credible earthquakes* on the free surface in hard rock (shear-wave velocity >1,500 m/s), were derived using the deterministic seismic hazard analysis. The results are based on (1) historical observations, (2) instrumental records, and (3) current understanding of the earthquake source, recurrence, and ground-motion attenuation relationship in the central United States. It is well understood that there are uncertainties in the ground-motion hazard maps because of the uncertainties inherent in parameters such as earthquake location, magnitude, and frequency used in the study. This study emphasizes the earthquakes that would have maximum impacts on humans and structures. The ground-motion parameters, including time histories, are intended for use in the recommended zone (not site-specific) where the structure is assumed to be situated at the top of a bedrock foundation. For sites underlain by soils, and in particular for sites underlain by poorly consolidated soils, it is recommended that site-specific investigations be conducted by qualified professionals in order to determine the possibilities of amplification, liquefaction, slope failure, and other considerations when subjected to the ground motions.

17. Key Words	18. Distribution Statement
Earthquake, Seismic Hazards, Ground Motion, Response Spectra, Time Histories	Unlimited with approval of Kentucky Transportation Cabinet

19. Security Classif. (of this report)	20. Security Classif. (of this page)	21. No. of Pages	22. Price
Unclassified	Unclassified	148	

EXECUTIVE SUMMARY

Background

Earthquakes, such as the June 8, 2003, Bardwell, Ky., earthquake (M4.0), have periodically occurred in and around Kentucky throughout history. The most widely felt and damaging earthquakes in the state are the great earthquakes that occurred in the winter of 1811-1812 and were centered in northeastern Arkansas, northwestern Tennessee, southwestern Kentucky, and southeastern Missouri–the New Madrid Seismic Zone. The 1811-1812 earthquakes are reported to have caused damage (i.e., modified Mercalli intensity VII–IX) throughout much of the commonwealth. The 1980 Sharpsburg earthquake caused significant damage (MMI VII) in Maysville, Ky. Since earthquakes are not well understood in the central United States, it is very difficult to predict them. Still, they continue to occur in and around Kentucky, and will affect humans, buildings, and bridges (i.e., they are seismic hazards) and pose risk to society.

Although seismic hazard and risk have often been used interchangeably, they are two fundamentally different concepts. Seismic hazard is a natural phenomenon generated by earthquakes, such as a surface rupture, ground motion, ground-motion amplification, liquefaction, and induced landslide, that has the potential to cause harm, and is quantified by two parameters: a level of hazard and its recurrence interval. Seismic risk, on the other hand, describes a probability of occurrence of a specific level of seismic hazard over a certain time (i.e., 50 or 75 years), and is quantified by three parameters: probability, a level of hazard, and exposure time. These differences are significant for policy consideration by engineers and decision-makers. High seismic hazard does not necessarily mean high seismic risk, and vice versa. For example, San Francisco, CA, and Paducah, KY, experienced similar intensity (MMI VII and greater) during the 1906 and 1811-1812 earthquakes, respectively. This does not necessarily mean that Paducah has similar seismic hazard as San Francisco because the recurrence intervals of the large earthquake are quite different: about 500 to 1,000 years in the central United States and about 100 years in the San Francisco Bay area. The differences in the recurrence intervals are important because any highway structure, such as a bridge, has a life, normally about 75 years. A bridge would likely experience a large earthquake or ground motion generated by the large earthquake over its lifetime (75 years) in San Francisco, but would be unlikely to experience a large earthquake or ground motion generated by the large earthquake over several life-cycles (couple of hundred years) in Paducah. In terms of seismic risk, the probability that a bridge could be struck by at least one large earthquake or ground motion generated by the large earthquake in San Francisco is about 53 percent over its lifetime (75 years), and about 7% to 14% in Paducah.

In this study, ground-motion hazard maps depicting a level of ground motion on the free surface in hard rock (shear-wave velocity >1,500 m/s) with a recurrence interval were developed, along with time histories, from all potential earthquake sources in and around Kentucky. Two approaches to determine seismic hazard, probabilistic seismic hazard analysis (PSHA) and deterministic seismic hazard analysis (DSHA), are widely used in seismic-hazard mapping. The two approaches use the same data sets, earthquake sources (where and how big), earthquake occurrence frequencies (how often), and ground-motion attenuation relationship (how strong),

but are fundamentally different in final products. PSHA uses a series of probabilistic computations to combine the uncertainties in earthquake source, occurrence frequency, and the ground-motion. PSHA predicts a relationship between a ground-motion value, such as peak ground acceleration (PGA), and the annual probability with which that value will be exceeded (hazard curve). PSHA addresses the frequency of exceeding a level of ground motion from all possible earthquakes. The ground motion derived from PSHA does not have a clear physical and statistical meaning and is not associated with any individual earthquake. DSHA develops a particular seismic scenario upon which a ground-motion hazard evaluation is based. The scenario consists of the postulated occurrence of an earthquake of a specified size at a specified location. The advantage of DSHA is that it provides a seismic-hazard estimate from earthquakes that have the most significant impact, and the estimate has a clear physical and statistical meaning. This advantage is of significance in engineering design and analysis.

The engineering seismic designs and standards in the United States, as well as in most countries around the world, are based on experience learned in California. The ground motion specified for bridge design in California is the deterministic ground motion from the maximum credible earthquake. Also, the ground motion from the maximum considered earthquake was recommended for building seismic design in California. In engineering practice in California, DSHA, not PSHA, is being used to develop design ground motion.

Study Objective

The objective of this study is to develop ground motions, including peak values and time histories, for seismic analysis and design of highway structures in Kentucky using the deterministic seismic hazard analysis (DHSA).

Study Tasks

The objective of this study is achieved by conducting the following tasks:

Task 1: Develop the expected earthquake (EE) ground motion
Task 2: Develop the probable earthquake (PE) ground motion
Task 3: Develop the maximum credible earthquake (MCE) ground motion

Ground-motion hazards associated with three earthquake scenarios, the expected earthquakes (EE), probable earthquakes (PE), and maximum credible earthquakes (MCE), on the free surface in hard rock (shear-wave velocity >1,500 m/s) were developed in this project, along with corresponding time histories. Time histories were developed using the composite source model for each earthquake scenario. The composite source model takes into account the source effects, including directivity and asperity, and three-dimensional wave propagation, and provides three-component ground motions that are physically consistent. Selection of time histories and response spectra for use in design depends on (1) the earthquake scenario and (2) the zone being considered. The time histories and response spectra developed in this project are not site-specific.

Task 1: Expected Earthquake (EE) Ground Motion

EE is defined in this study as the earthquake that could be expected to occur any time in the bridge lifetime of 75 years (Fig. 1-EE in Appendix ES-I)). The probability that EE ground motion could be exceeded over the bridge life of 75 years is about 50% (risk). EE peak ground-motion hazard maps are equivalent to the maps of horizontal peak-particle acceleration at the top of rock with a 90% probability of not being exceeded in 50 years, which were defined by Street et. al. [5-ES]. EE is equivalent to the "*small earthquake*" defined in the 2002 American Association of State Highways and Transportation Officials (AASHTO) provisions [4-ES] and is similar to the "*expected earthquake*" defined in the 2003 Recommended LRFD Guidelines for the Seismic Design of Highway Bridges [2-ES]. EE ground motion is also equivalent to the *"lower-level earthquake"* ground motion specified in the 2006 Seismic Retrofitting Manual for Highway Structures [3-ES].

The maximum median peak (horizontal) ground acceleration, and short-period (0.2 s) and long-period (1.0 s) response accelerations $\mathbf{S_S}$ and $\mathbf{S_1}$ with 5% damping, for the EE were developed in this study (Figs. 2-EE to 4-EE in Appendix ES-I). Figure 5-EE shows the recommended zones of time histories and response spectra for EE.

The data and guidelines for generating the time histories and response spectra can be downloaded by following these steps: (1)- Go to web site: http://www.ktc.uky.edu/ ; (2)- Click on "Research", (3)- Click on "Reports by Section"; and (4)- Go to "Structures" and Report Number "KTC-07-07/SPR246-02-6F".

The derivation of the "Acceleration Design Response Spectrum" is presented in Appendix ES-IV and the derivation of the “Time History” is presented in Appendix ES-V.

Task 2: Probable Earthquake (PE) Ground Motion

PE is defined as the earthquake that could be expected to occur in the next 250 years (Fig. 1-PE in Appendix ES-II). The probability that PE ground motion could be exceeded over the bridge life of 75 years is about 26% (risk). PE peak ground-motion hazard maps are equivalent to the maps of horizontal peak-particle acceleration at the top of rock with a 90% probability of not being exceeded in 250 years, which were defined by Street et. al. [5-ES]. PE is equivalent to the "*moderate earthquake*" defined in the 2002 AASHTO provisions [4-ES] and is similar to the "*moderate earthquake*" defined in the 2003 Recommended LRFD Guidelines for the Seismic Design of Highway Bridges [2-ES]. PE ground motion is also equivalent to the *"moderate-level earthquake"* ground motion specified in the 2006 Seismic Retrofitting Manual for Highway Structures [3-ES].

The maximum median peak (horizontal) ground acceleration, and short-period (0.2 s) and long-period (1.0 s) response accelerations $\mathbf{S_S}$ and $\mathbf{S_1}$ with 5% damping, for the PE were developed in this study (Figs. 2-PE to 4-PE in Appendix ES-II). Figure 5-PE shows the recommended zones of time histories and response spectra for PE.

The data and guidelines for generating the time histories and response spectra can be downloaded by following these steps: (1)- Go to web site: http://www.ktc.uky.edu/ ; (2)- Click on "Research", (3)- Click on "Reports by Section"; and (4)- Go to "Structures" and Report Number "KTC-07-07/SPR246-02-6F".

The derivation of the "Acceleration Design Response Spectrum" is presented in Appendix ES-IV and the derivation of the "Time History" is presented in Appendix ES-V.

Task 3: Maximum Credible Earthquake (MCE) Ground Motion

MCE is defined as the maximum event considered likely in a reasonable amount of time (Fig. 1-MCE in Appendix ES-III). The phrase "reasonable amount of time" is defined by the historical or geological records. For instance, the reasonable amount of time for the maximum earthquake in the New Madrid Seismic Zone is about 500 to 1,000 years, based on paleoseismic records. The reasonable amount of time for the maximum earthquake in the Wabash Valley Seismic Zone is about 2,000 to 4,000 years. Thus, the probability that MCE ground motion could be exceeded over the bridge life of 75 years varies from zone to zone, about 7% to 14% in the New Madrid Seismic Zone, 2% to 4% in the Wabash Valley Seismic Zone, and less than 2% percent in other zones. MCE is equivalent to the "*large earthquake*" defined in the 2002 AASHTO provisions [4-ES], and similar to the "*maximum considered earthquake*" defined in the 2003 Recommended LRFD Guidelines for the Seismic Design of Highway Bridges [2-ES]. MCE ground motion is also equivalent to the "*upper-level earthquake*" ground motion specified in the 2006 Seismic Retrofitting Manual for Highway Structures [3-ES].

The maximum median peak (horizontal) ground acceleration, and short-period (0.2 s) and long-period (1.0 s) response accelerations $\mathbf{S_S}$ and $\mathbf{S_1}$ with 5% damping, for the MCE were developed in this study (Figs. 2-MCE to 4-MCE in Appendix ES-III). Figure 5-MCE shows the recommended zones of time histories and response spectra for MCE.

The data and guidelines for generating the time histories and response spectra can be downloaded by following these steps: (1)- Go to web site: http://www.ktc.uky.edu/ ; (2)- Click on "Research", (3)- Click on "Reports by Section"; and (4)- Go to "Structures" and Report Number "KTC-07-07/SPR246-02-6F".

The derivation of the "Acceleration Design Response Spectrum" is presented in Appendix ES-IV and the derivation of the "Time History" is presented in Appendix ES-V.

Appendix ES-I

Expected Earthquake (EE) for the Commonwealth of Kentucky

Notes on the Expected Earthquake (EE) for the Commonwealth of Kentucky

1- The Expected Earthquake (EE) is defined as the earthquake that could be expected to occur in the next 100 years.

2- EE is equivalent to the "*Expected Earthquake*" defined in the 2003 "Recommended LRFD Guidelines for the Seismic Design of Highway Bridges" [2-ES].

3- EE ground motion is equivalent to the "*Lower-Level Earthquake*" ground motion specified in the 2006 "Seismic Retrofitting Manual for Highway Structures" [3-ES], which is derived from a probabilistic approach and has a 50% probability of exceedance in 75 years or 100-year return period.

4- EE is equivalent to the "*Small Earthquake*" defined in the 2002 AASHTO Standard Specifications [4-ES].

5- EE peak ground-motion hazard maps are equivalent to the maps of horizontal peak-particle acceleration at the top of rock with a 90 percent probability of not being exceeded in 50 years as defined by Street et. al. [5-ES].

6- The Probability of exceedance of the Expected Earthquake (EE) in 75 years is 50% (or 100-year return period).

7- It should be noted that, due to the consideration of the local (or background) earthquakes in this study, the maximum accelerations in the response spectra in the counties highlighted in Fig. 1-EE may exceed the maximum accelerations derived from the USGS, AASHTO, or NEHRP.

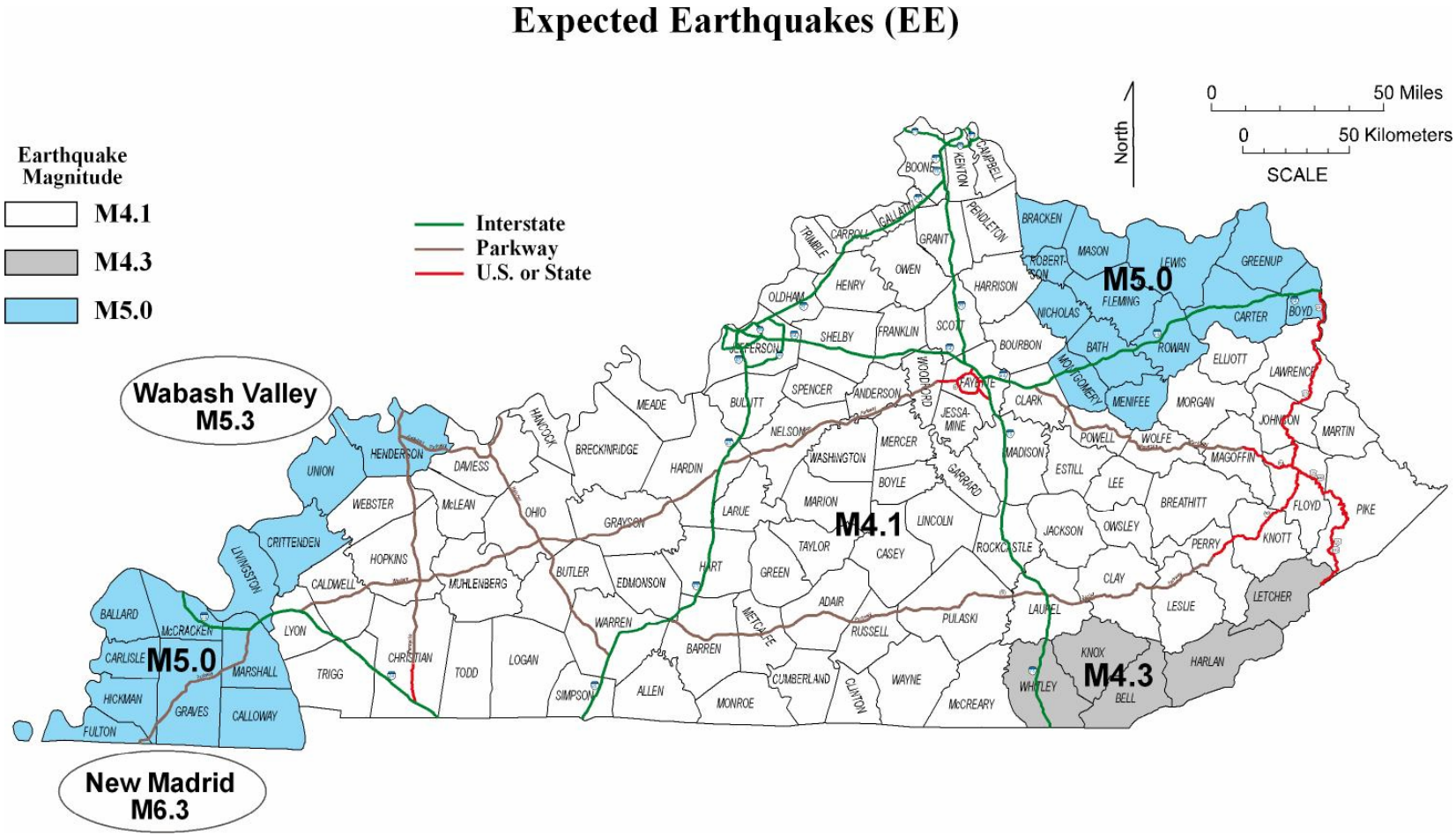

Figure 1-EE. Expected Earthquakes (EEs) for Seismic Zones in and Surrounding the Commonwealth of Kentucky

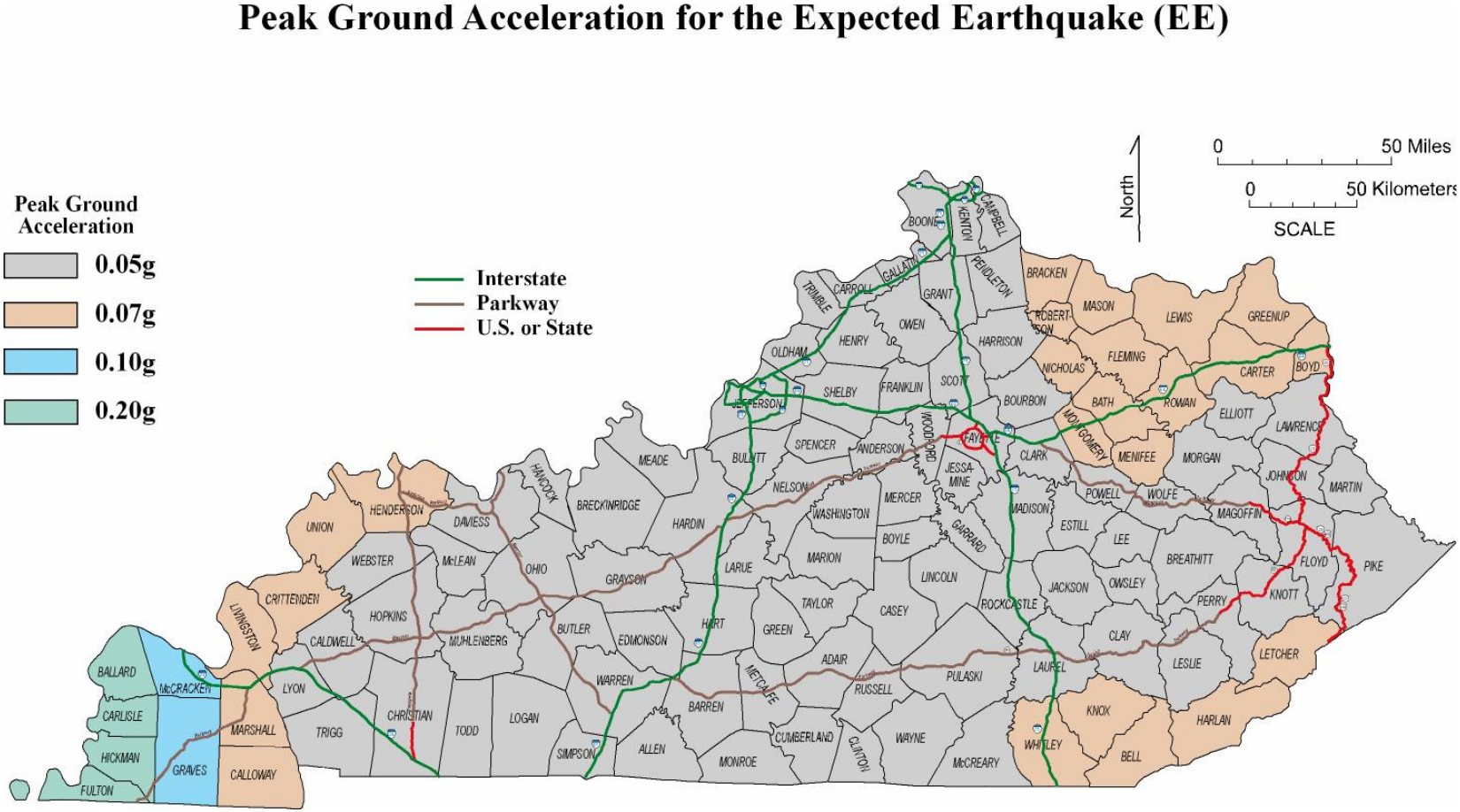

Figure 2-EE. Expected Earthquake (EE) Peak Ground Acceleration for the Commonwealth of Kentucky, Site Class A (Hard Rock)

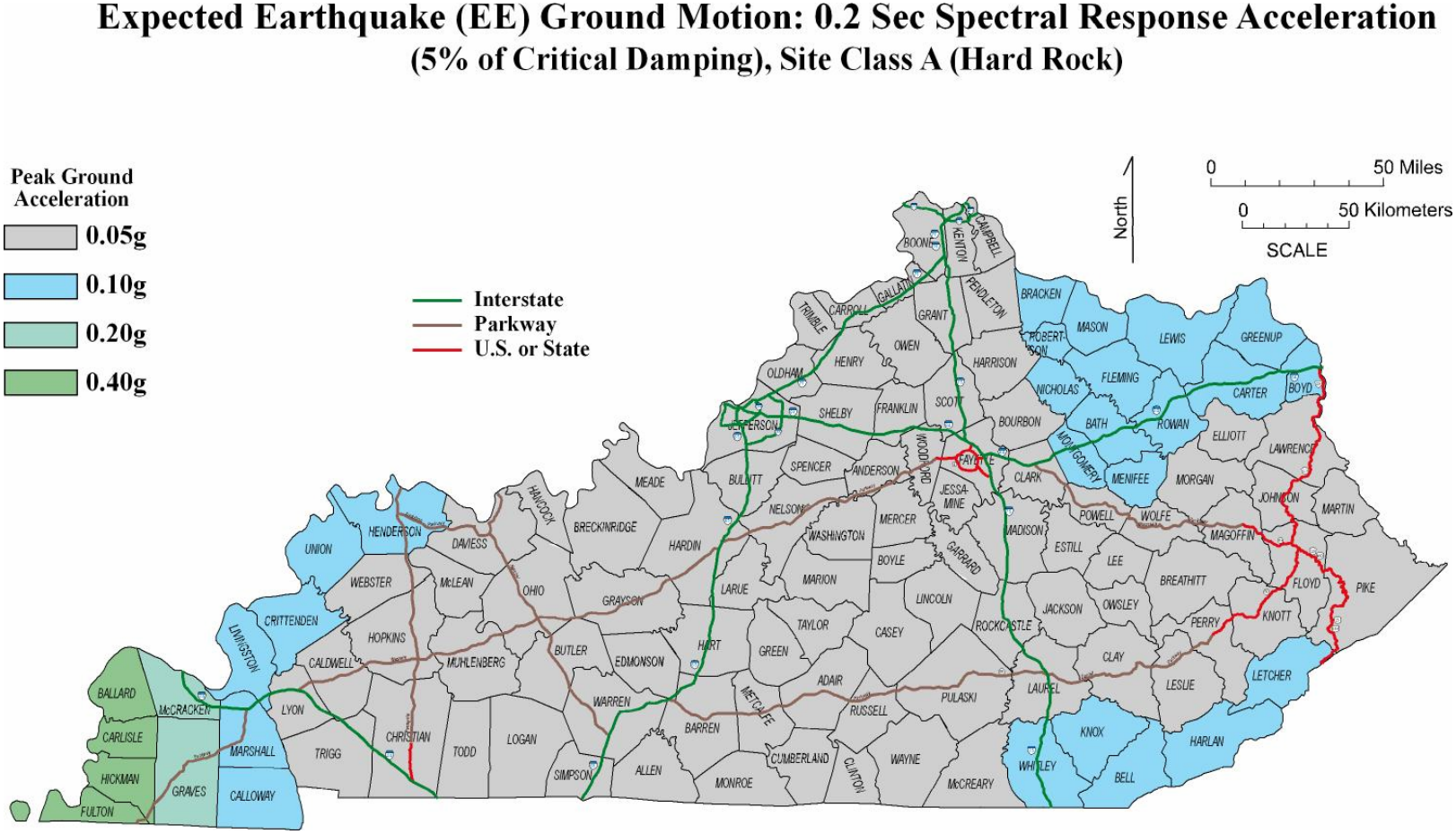

Figure 3-EE. Expected Earthquake (EE) Ground Motion for the Commonwealth of Kentucky: 0.2-Sec Spectral Response Acceleration, S_s (5% of Critical Damping), Site Class A (Hard Rock)

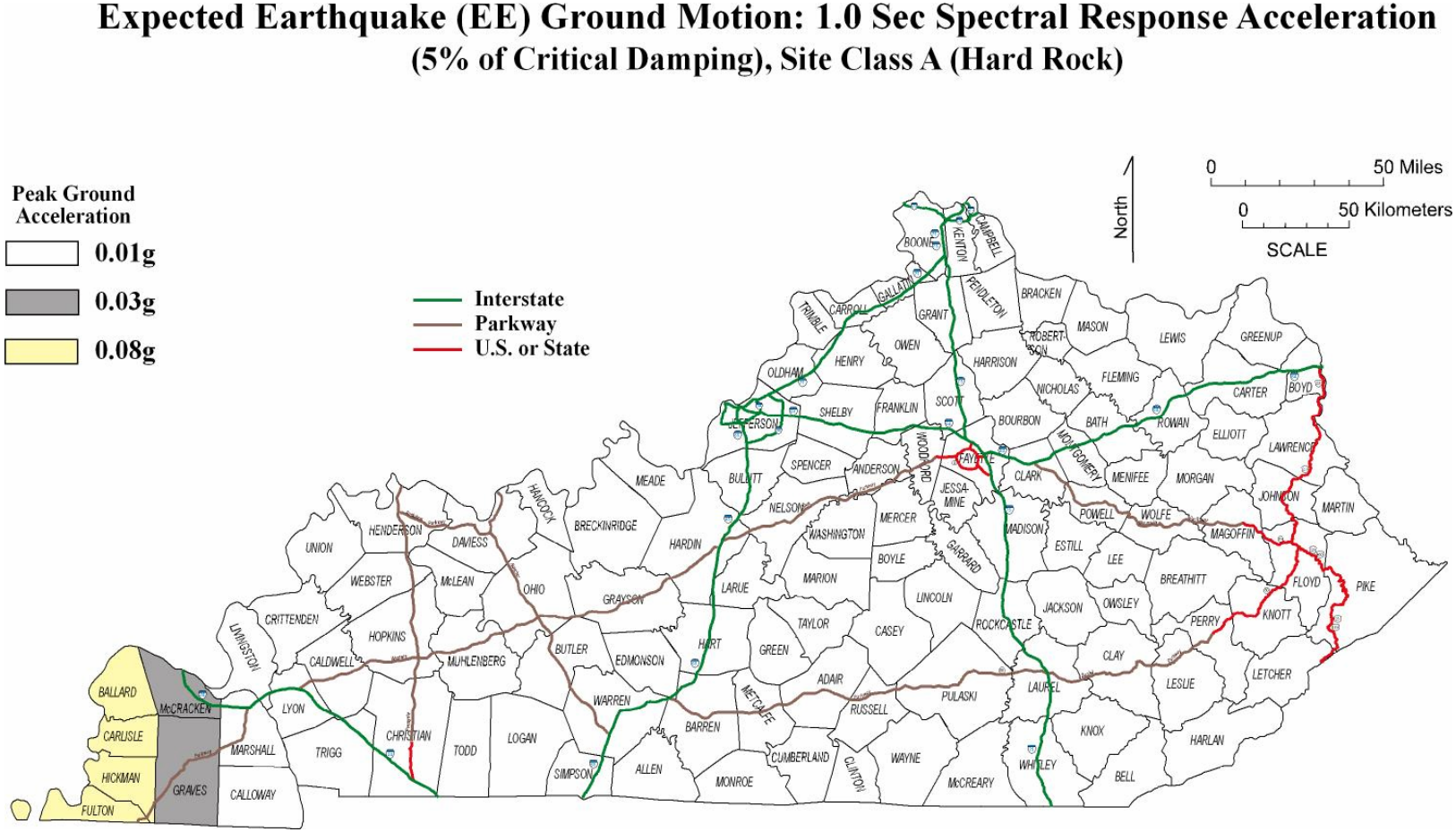

Figure 4-EE. Expected Earthquake (EE) Ground Motion for the Commonwealth of Kentucky: 1.0-Sec Spectral Response Acceleration, S_1 (5% of Critical Damping), Site Class A (Hard Rock)

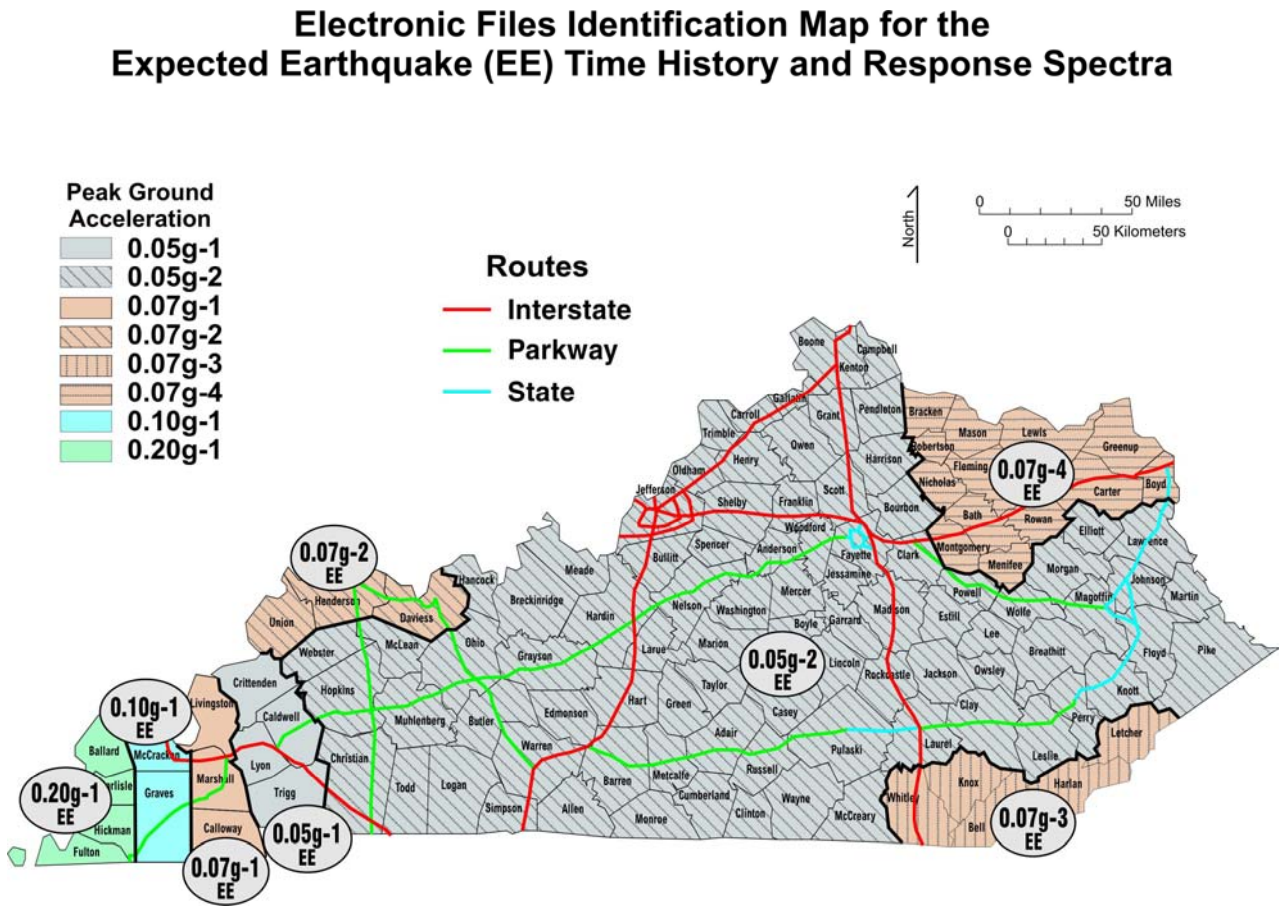

Figure 5-EE. Electronic Files Identification Map for the Expected Earthquake (EE) Time History and Response Spectra for the Commonwealth of Kentucky

(Note: The data and guidelines for generating the time histories and response spectra can be downloaded by following these steps: (1)- Go to web site: http://www.ktc.uky.edu/ ; (2)- Click on "Research", (3)- Click on "Reports by Section"; and (4)- Go to "Structures" and Report Number "KTC-07-07/SPR246-02-6F")

Appendix ES-II

Probable Earthquake (PE) for the Commonwealth of Kentucky

Notes on the Probable Earthquake (PE) for the Commonwealth of Kentucky

1 - The Probable Earthquake (PE) is defined as the earthquake that could be expected to occur in the next 250 years.

2- PE is equivalent to the "*Moderate Earthquake*" defined in the 2003 "Recommended LRFD Guidelines for the Seismic Design of Highway Bridges" [2-ES].

3- PE ground motion is equivalent to the "*Moderate-Level Earthquake*" ground motion specified in the 2006 "Seismic Retrofitting Manual for Highway Structures" [3-ES], which is derived from a probabilistic approach and has a 26% probability of exceedance in 75 years or 250-year return period.

4- PE is equivalent to the "*Moderate Earthquake*" defined in the 2002 AASHTO Standard Specifications [4-ES].

5- PE peak ground-motion hazard maps are equivalent to the maps of horizontal peak-particle acceleration at the top of rock with a 90 percent probability of not being exceeded in 250 years as defined by Street et. al. [5-ES].

6- The Probability of exceedance of the Probable Earthquake (PE) in 75 years is 26% (or 250-year return period).

7- It should be noted that, due to the consideration of the local (or background) earthquakes in this study, the maximum accelerations in the response spectra in the counties highlighted in Fig. 1-PE may exceed the maximum accelerations derived from the USGS, AASHTO, or NEHRP.

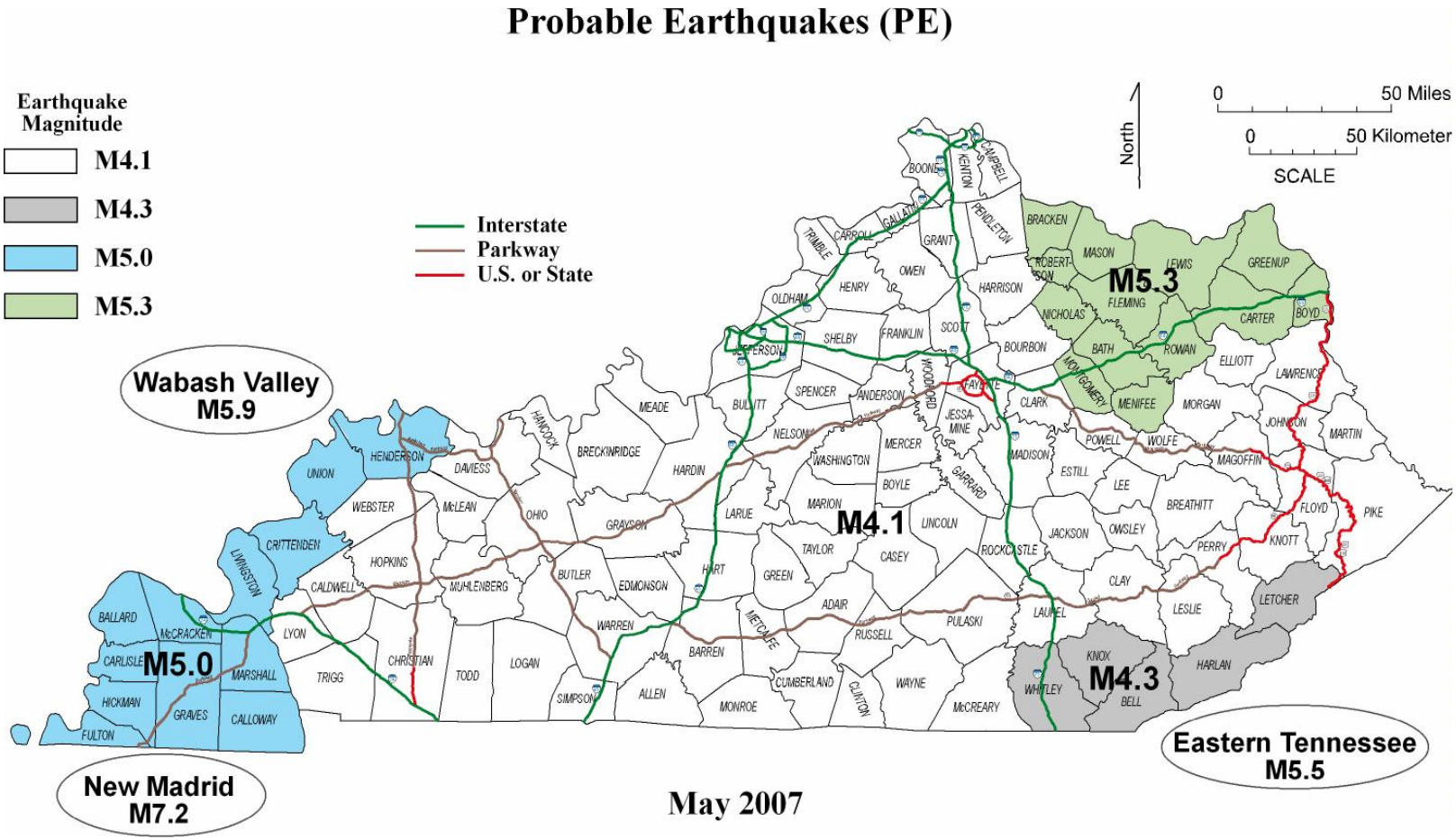

Figure 1-PE. Probable Earthquakes (PEs) for Seismic Zones in and Surrounding the Commonwealth of Kentucky

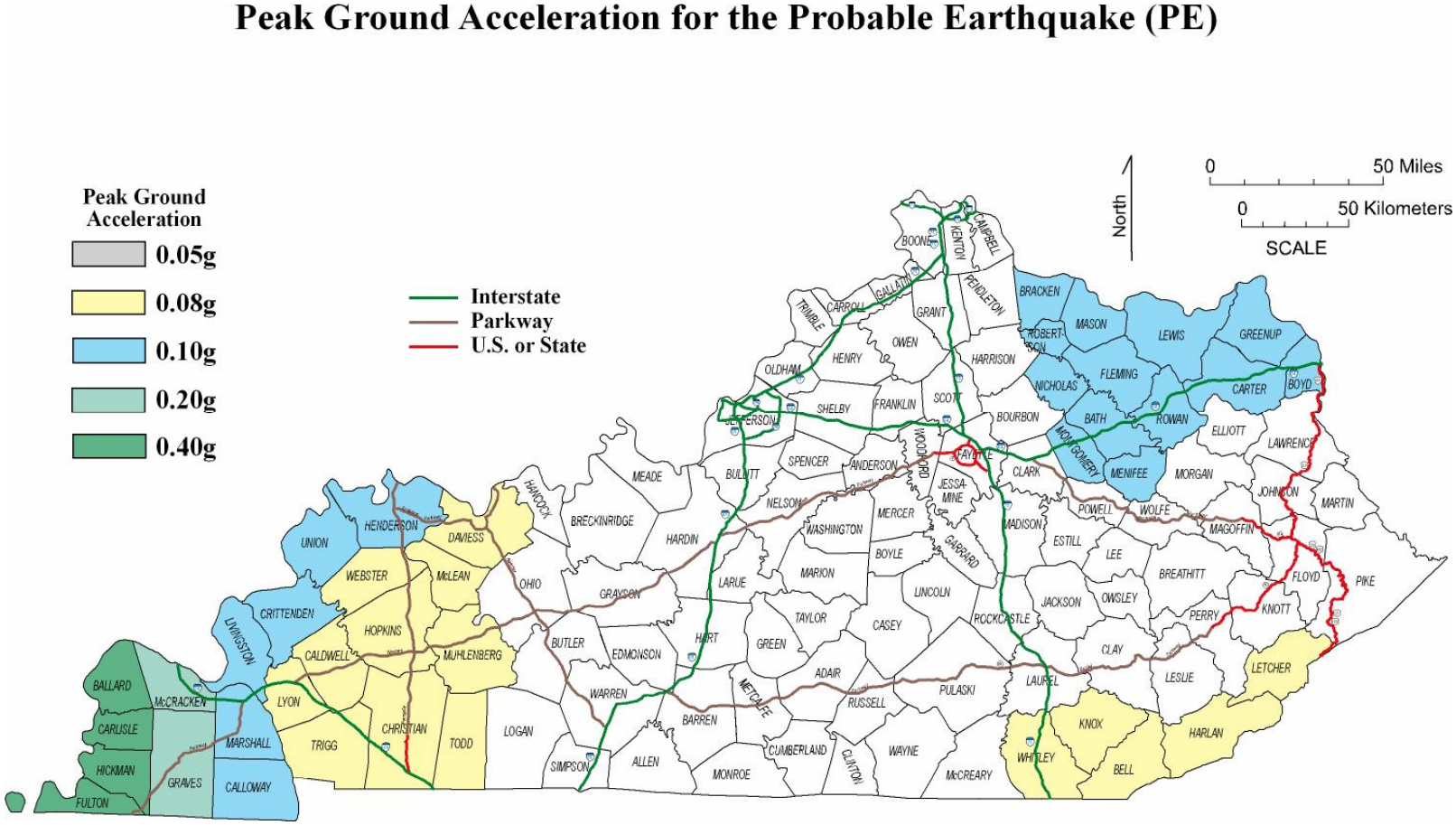

Figure 2-PE. Probable Earthquake (PE) Peak Ground Acceleration for the Commonwealth of Kentucky, Site Class A (Hard Rock)

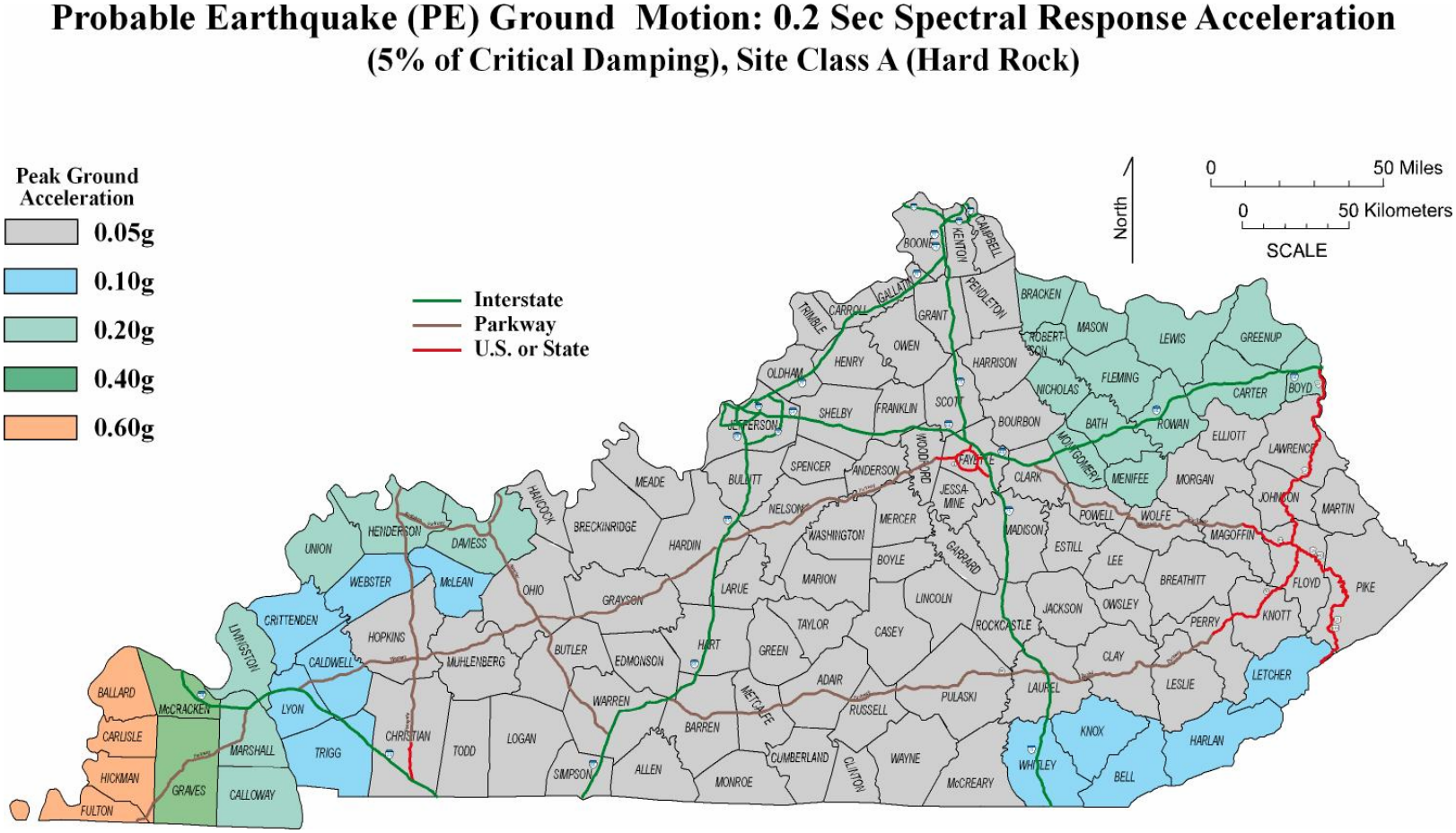

Figure 3-PE. Probable Earthquake (PE) Ground Motion for the Commonwealth of Kentucky: 0.2-Sec Spectral Response Acceleration, S_s (5% of Critical Damping), Site Class A (Hard Rock)

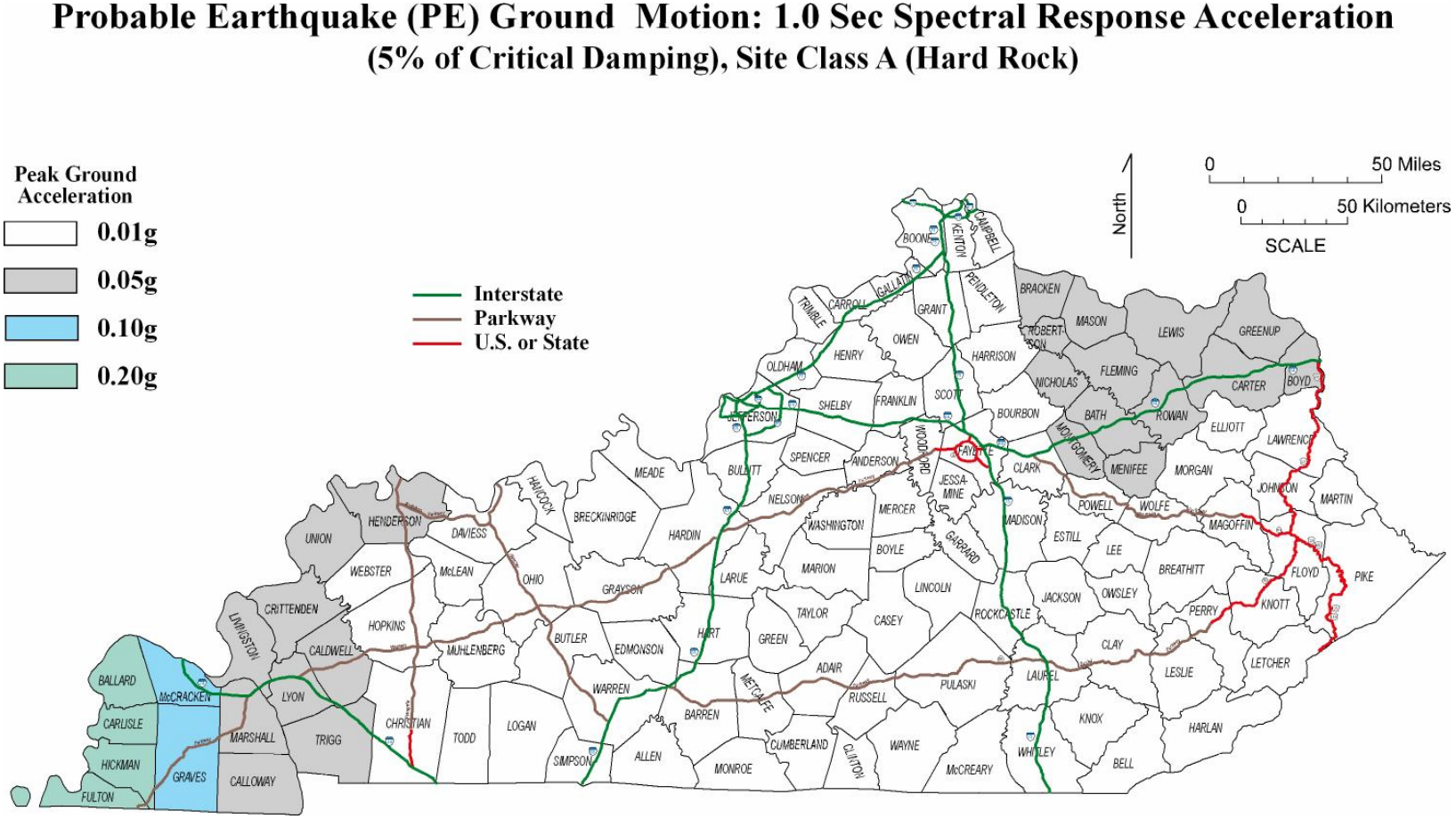

Figure 4-PE. Probable Earthquake (PE) Ground Motion for the Commonwealth of Kentucky: 1.0-Sec Spectral Response Acceleration, S_1 (5% of Critical Damping), Site Class A (Hard Rock)

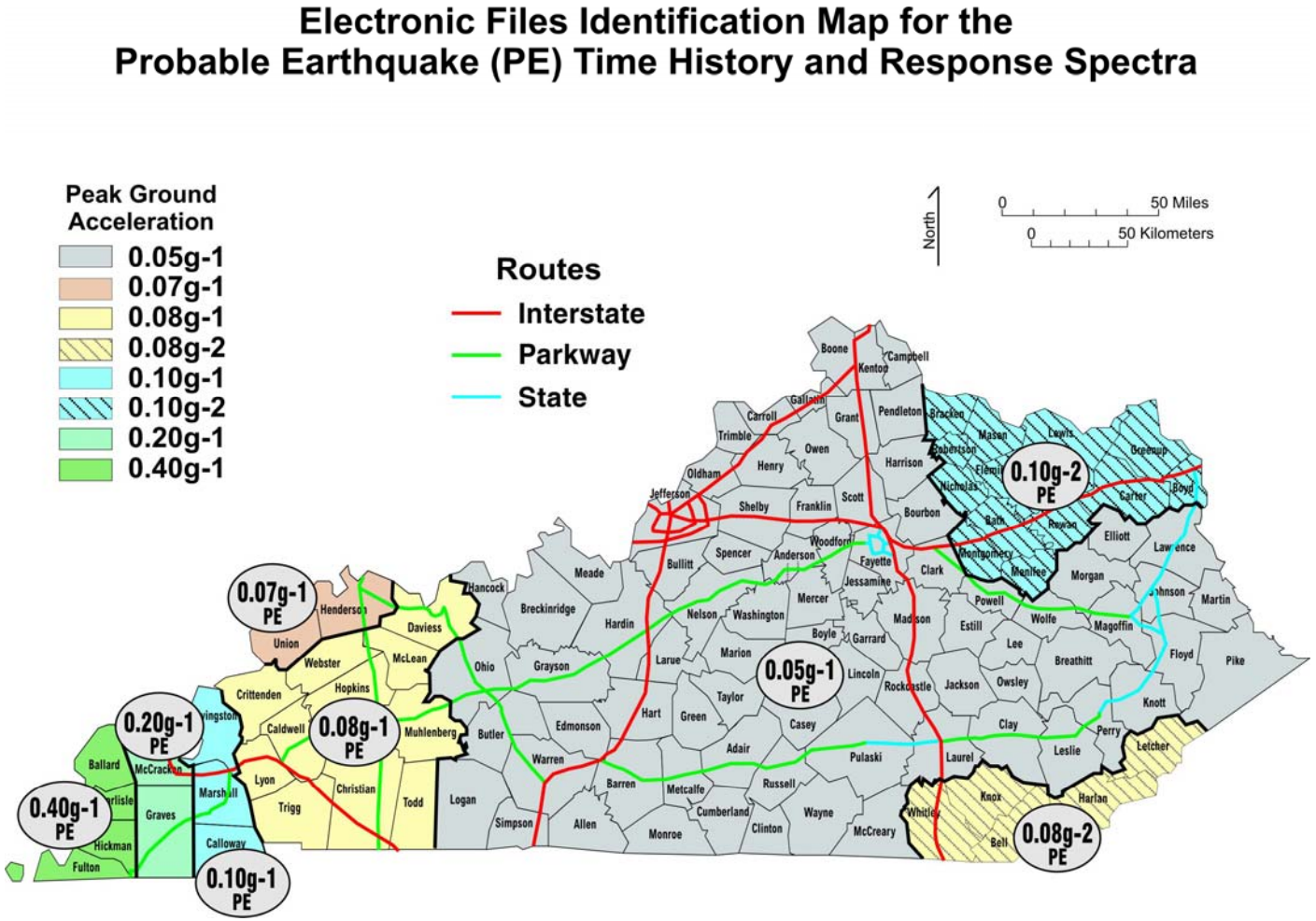

Figure 5-PE. Electronic Files Identification Map for the Probable Earthquake (PE) Time History and Response Spectra for the Commonwealth of Kentucky

(Note: The data and guidelines for generating the time histories and response spectra can be downloaded by following these steps: (1)- Go to web site: http://www.ktc.uky.edu/ ; (2)- Click on "Research", (3)- Click on "Reports by Section"; and (4)- Go to "Structures" and Report Number "KTC-07-07/SPR246-02-6F")

Appendix ES-III

Maximum Credible Earthquake (MCE) for the Commonwealth of Kentucky

Notes on the
Maximum Credible Earthquake (MCE) for the Commonwealth of Kentucky

1- The Maximum Credible Earthquake (MCE) ground motion is the median motion derived from a deterministic approach and is equivalent to 2/3 of the "*Maximum Considered Earthquake*" ground motion defined in the 2003 "Recommended LRFD Guidelines for the Seismic Design of Highway Bridges" [2-ES] which, in turn, is derived from a probabilistic approach and has a 3% probability of exceedance in 75 years or a 2500-year return period. The 2/3 factor is recommended in Chapter 3, section 3.4 of the NEHRP 2003 Provisions [1-ES].

2- MCE ground motion is equivalent to the "*Upper-Level Earthquake*" ground motion specified in the 2006 "Seismic Retrofitting Manual for Highway Structures" [3-ES], which is derived from a probabilistic approach and has a 5% probability of exceedance in 50 years or 1000-year return period.

3- MCE is also equivalent to the "*Large Earthquake*" defined in the 2002 AASHTO Standard Specifications [4-ES].

4- The Probability of exceedance of the Maximum Credible Earthquake (MCE) in 75 years is: 7% (or 1000-year return period) to 14% (or 500-year return period) for New Madrid, 2% (or 4000-year return period) to 4% (or 2000-year return period) for Wabash Valley, and less than 2% (or 4000-year return period) for all other seismic zones.

5- It should be noted that, due to the consideration of the local (or background) earthquakes in this study, the maximum accelerations in the response spectra in the counties highlighted in Fig. 1-MCE may exceed the maximum accelerations derived from the USGS, AASHTO, or NEHRP.

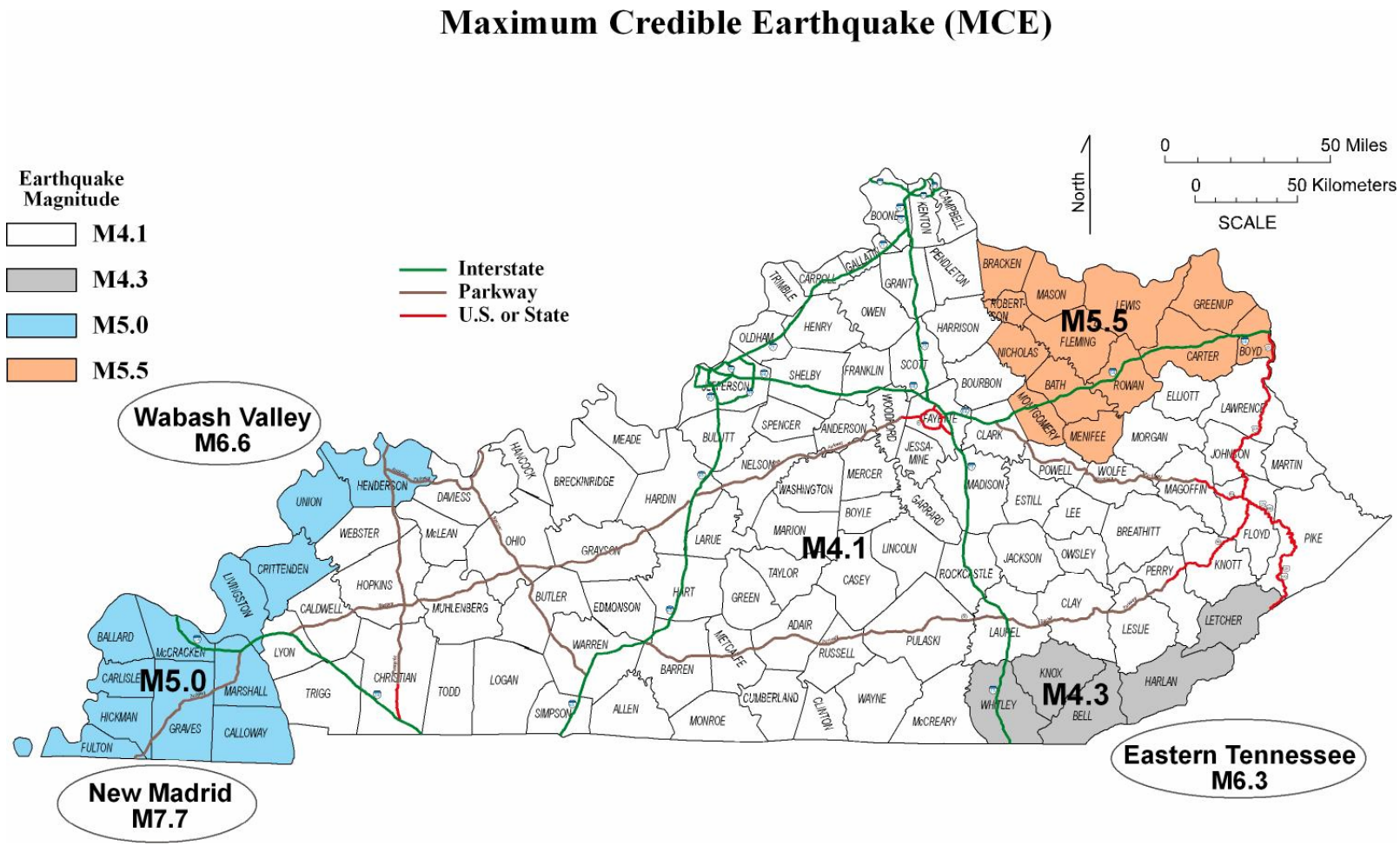

Figure 1-MCE. Maximum Credible Earthquakes (MCEs) for Seismic Zones in and Surrounding the Commonwealth of Kentucky

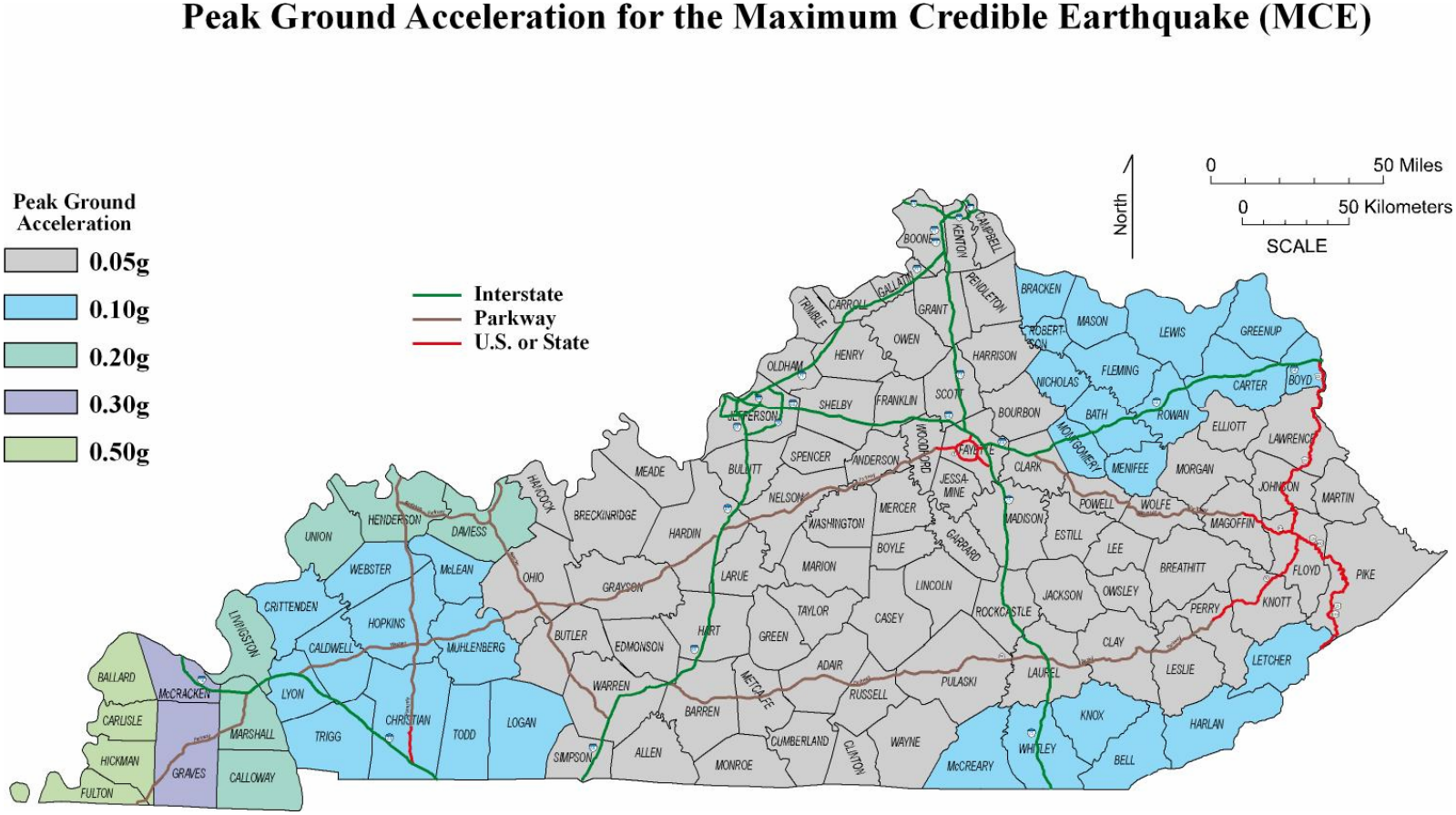

Figure 2-MCE. Maximum Credible Earthquake (MCE) Peak Ground Acceleration for the Commonwealth of Kentucky, Site Class A (Hard Rock)

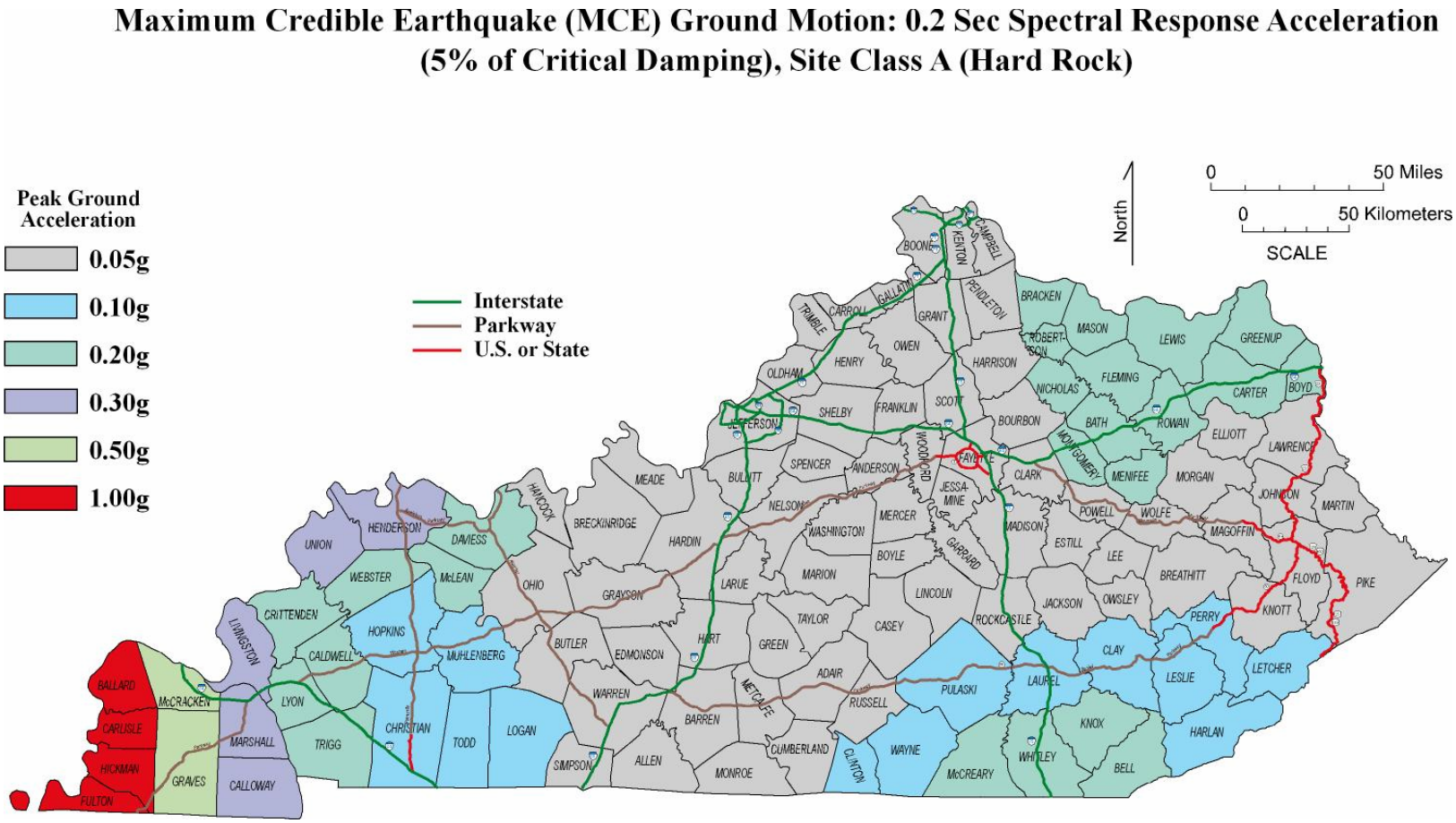

Figure 3-MCE. Maximum Credible Earthquake (MCE) Ground Motion for the Commonwealth of Kentucky: 0.2-Sec Spectral Response Acceleration, S_s (5% of Critical Damping), Site Class A (Hard Rock)

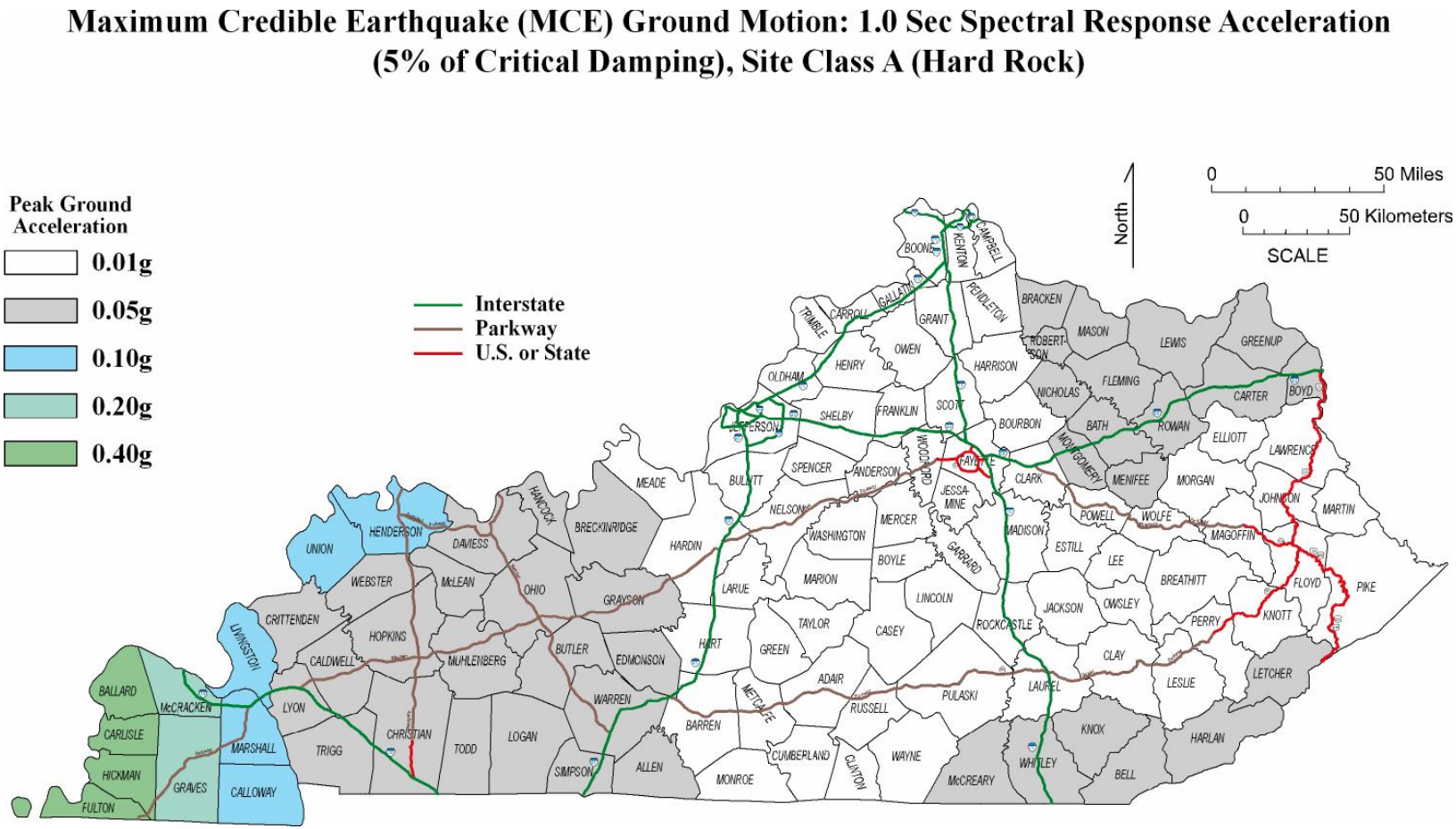

Figure 4-MCE. Maximum Credible Earthquake (MCE) Ground Motion for the Commonwealth of Kentucky: 1.0-Sec Spectral Response Acceleration, S_1 (5% of Critical Damping), Site Class A (Hard Rock)

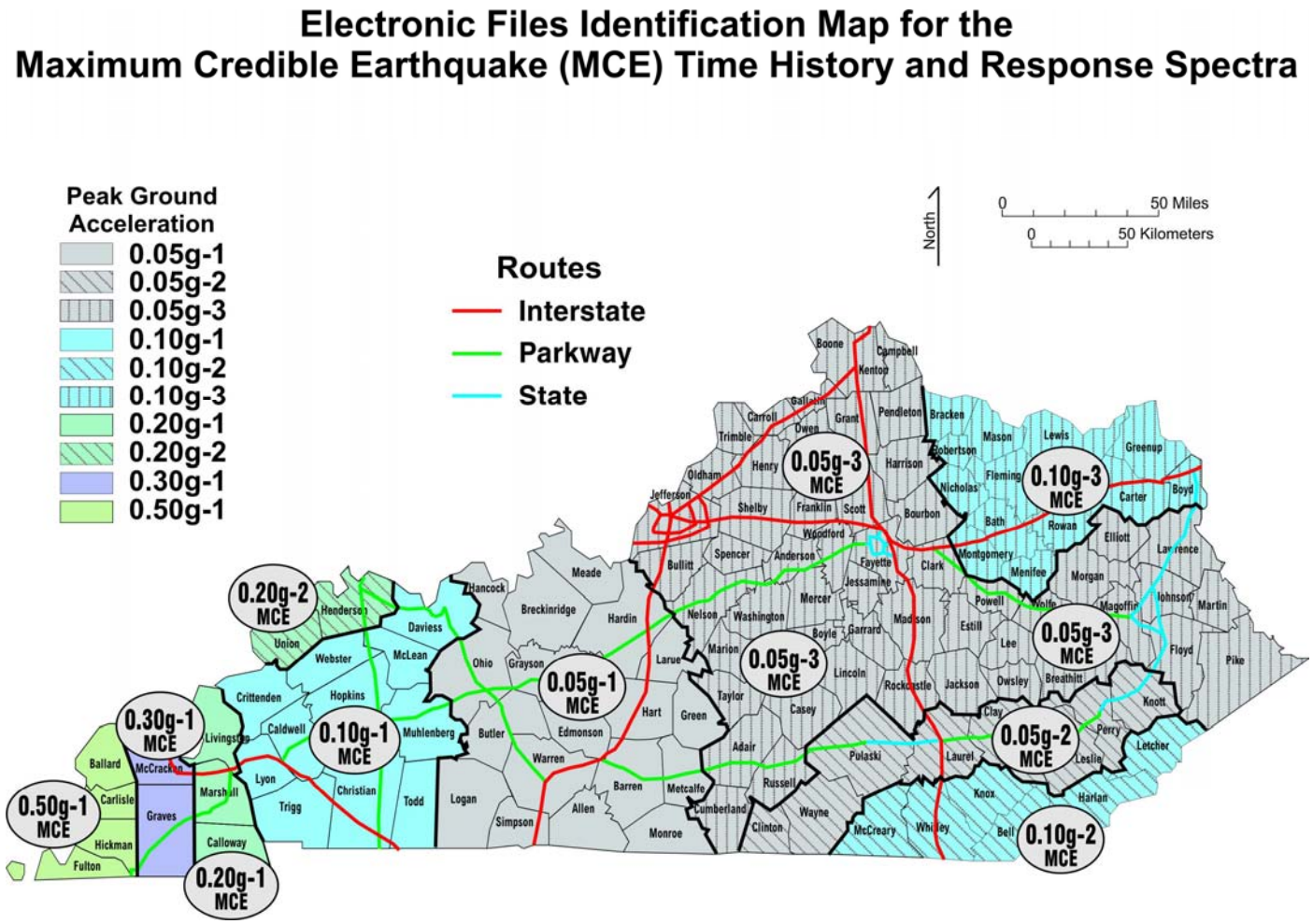

Figure 5-MCE. Electronic Files Identification Map for theMaximum Credible Earthquake (MCE) Time History and Response Spectra for the Commonwealth of Kentucky

(Note: The data and guidelines for generating the time histories and response spectra can be downloaded by following these steps: (1)- Go to website: http://www.ktc.uky.edu/ ; (2)- Click on "Research", (3)- Click on "Reports by Section"; and (4)- Go to "Structures" and Report Number "KTC-07-07/SPR246-02-6F")

Appendix ES-IV

Derivation of the Acceleration Design Response Spectrum

Acceleration Response Spectra Generation
For Counties in the Commonwealth of Kentucky

Example: Generate the Maximum Credible Earthquake Acceleration Response Spectra for McCracken County, KY.

I. Electronic File Identification Map

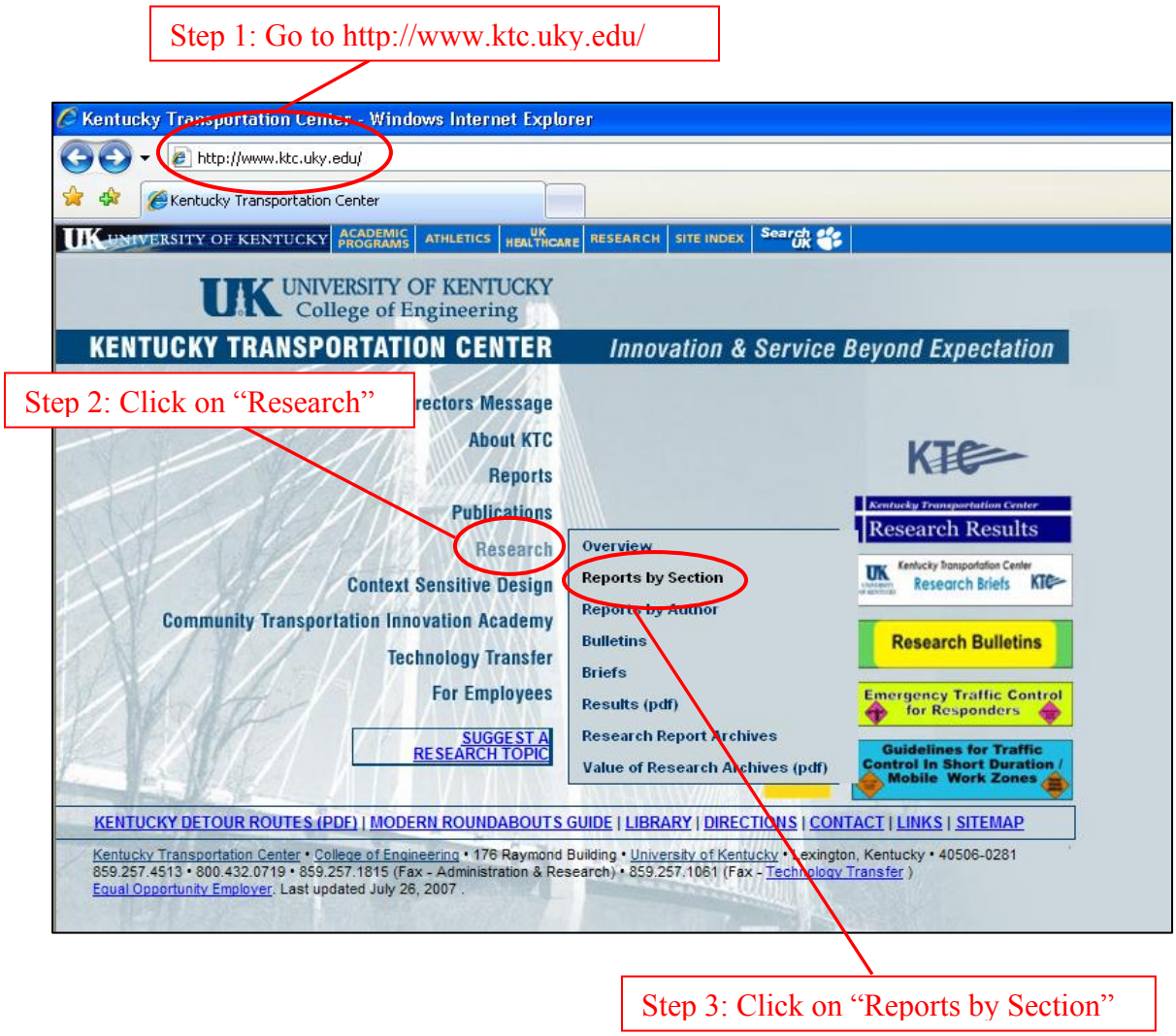

Step 4: Scroll down to “Structures”

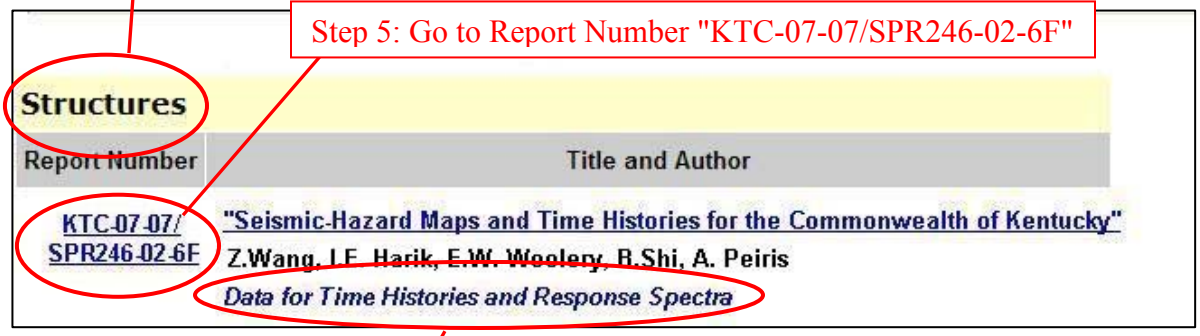

Step 6: Click on “*Data for Time Histories and Response Spectra*”

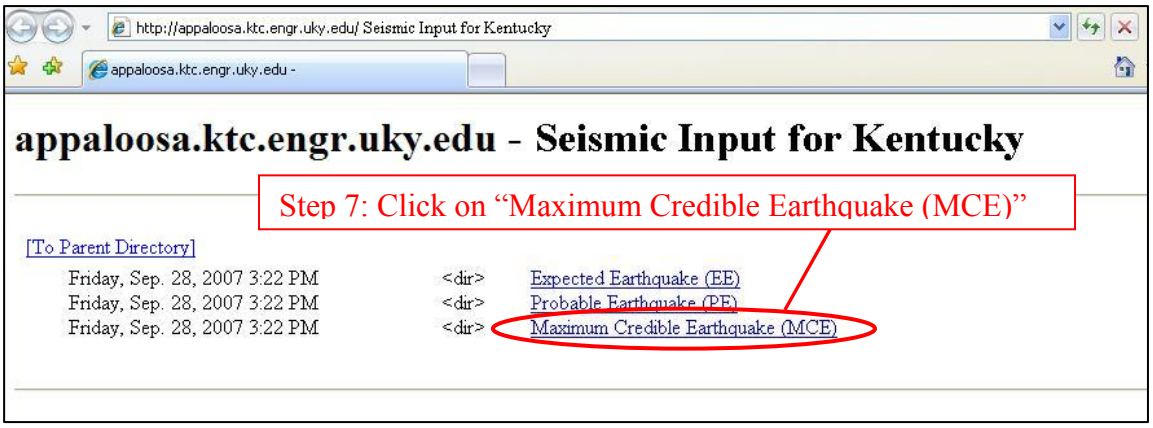

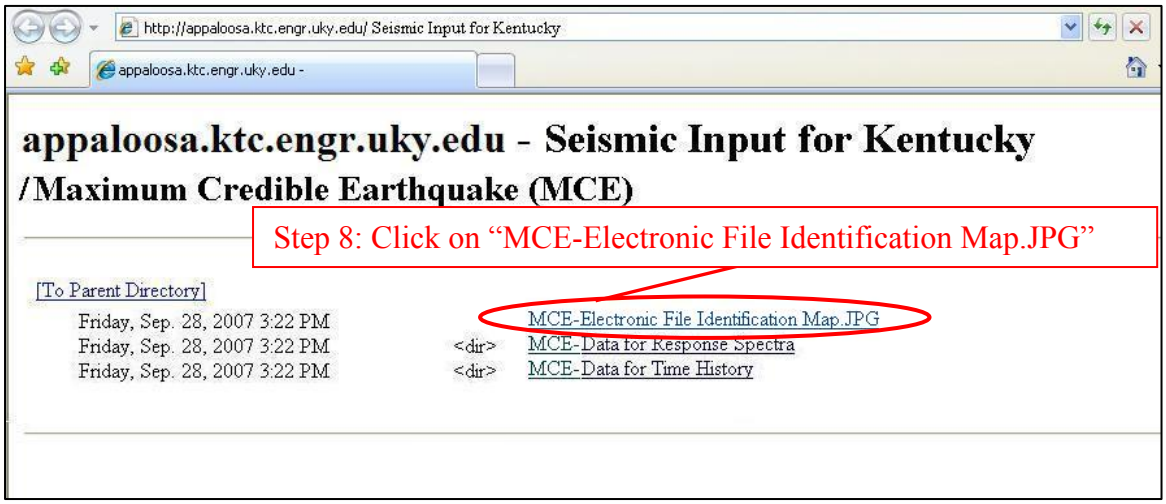

Step 9: Go to Electronic File Identification Map for MCE

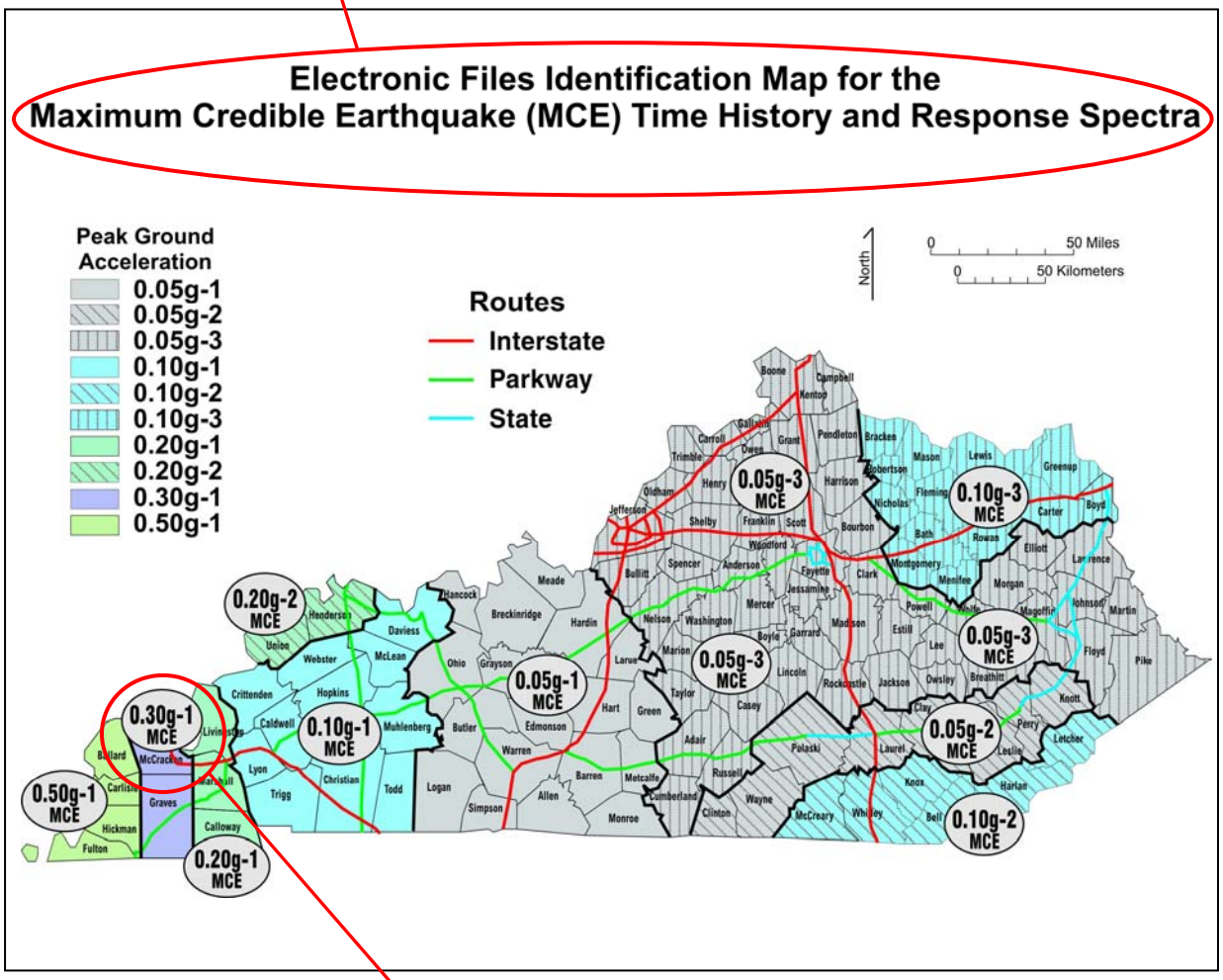

Step 10: Locate "*McCracken County, KY*" and the corresponding "Peak Ground Acceleration" (0.30g-1 MCE for this example)

II. Acceleration Response Spectra

Step 11: Go back to the "Maximum Credible Earthquake (MCE)" Screen

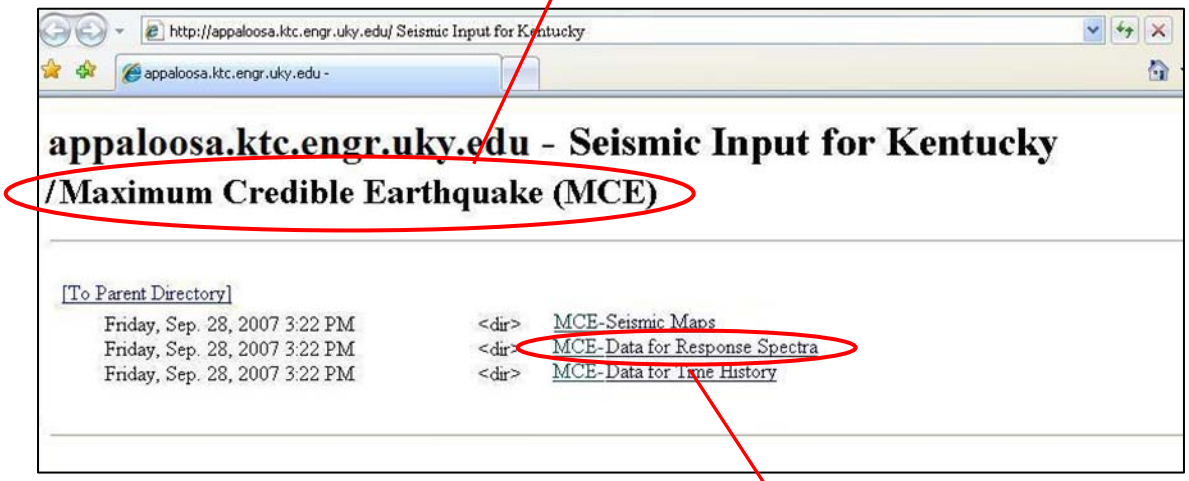

Step 12: Click on "MCE-Data for Response Spectra"

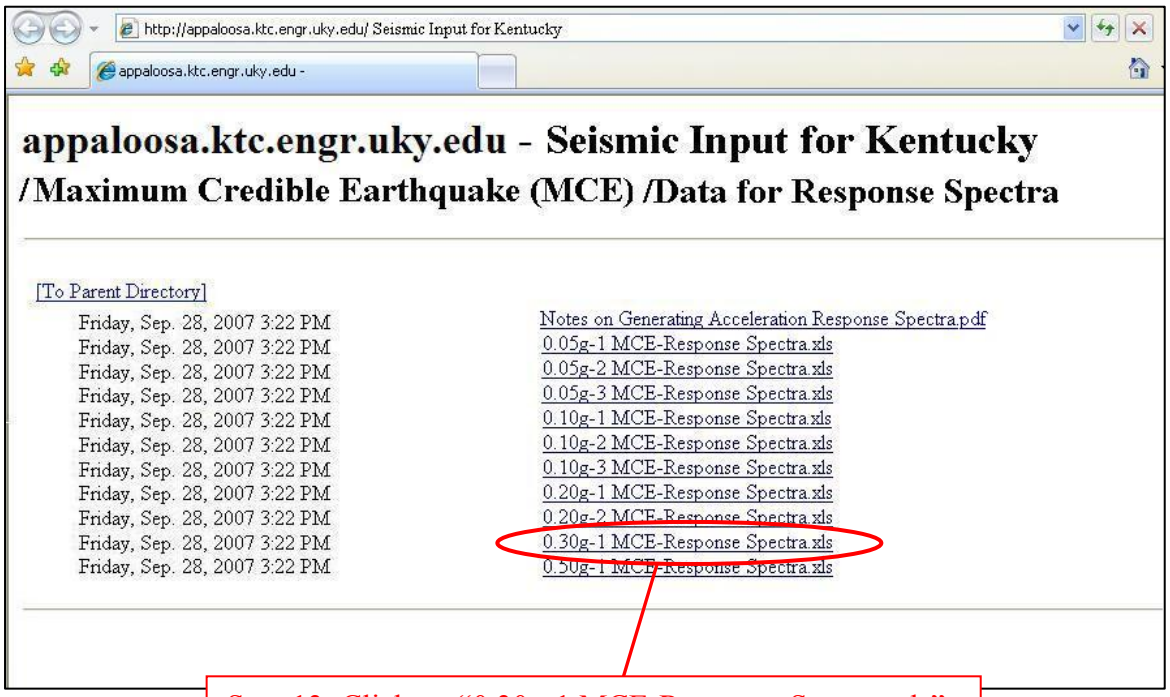

Step 13: Click on "0.30g-1 MCE-Response Spectra.xls"

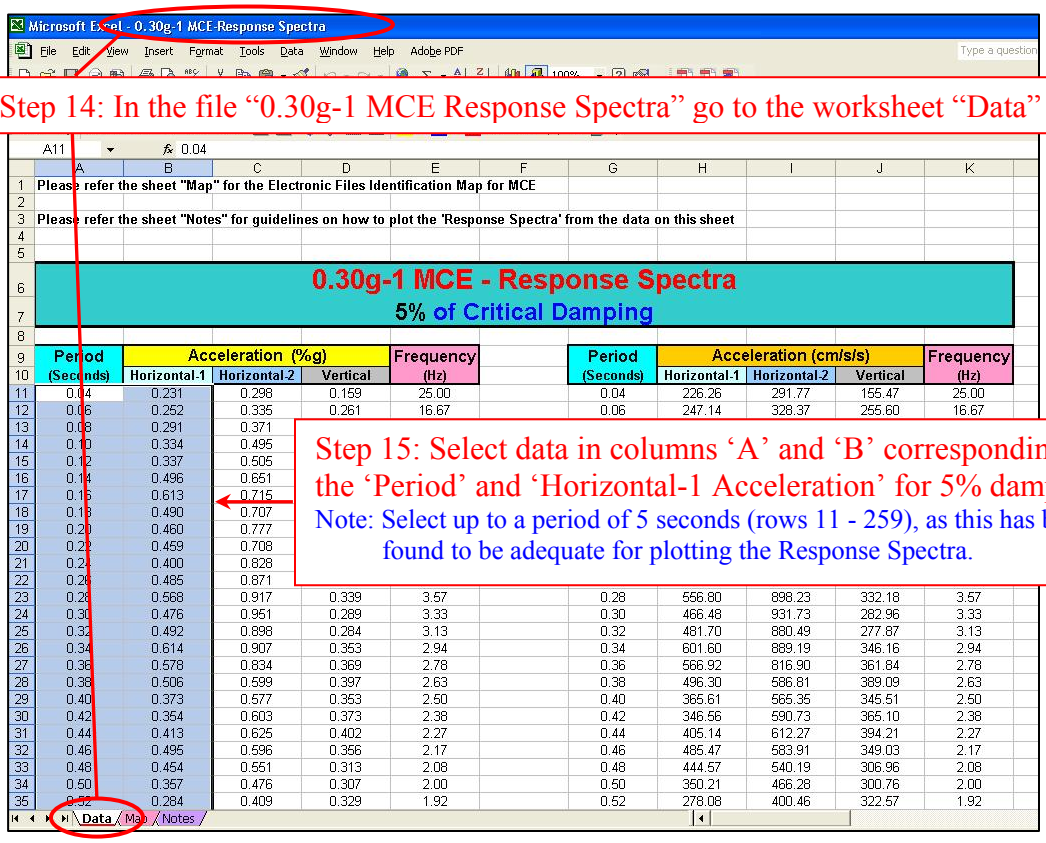

Step 14: In the file "0.30g-1 MCE Response Spectra" go to the worksheet "Data"

Step 15: Select data in columns 'A' and 'B' corresponding to the 'Period' and 'Horizontal-1 Acceleration' for 5% damping

Note: Select up to a period of 5 seconds (rows 11 - 259), as this has been found to be adequate for plotting the Response Spectra.

Step 16: Click "Chart Wizard" button or on the menu click *Insert* → *chart*

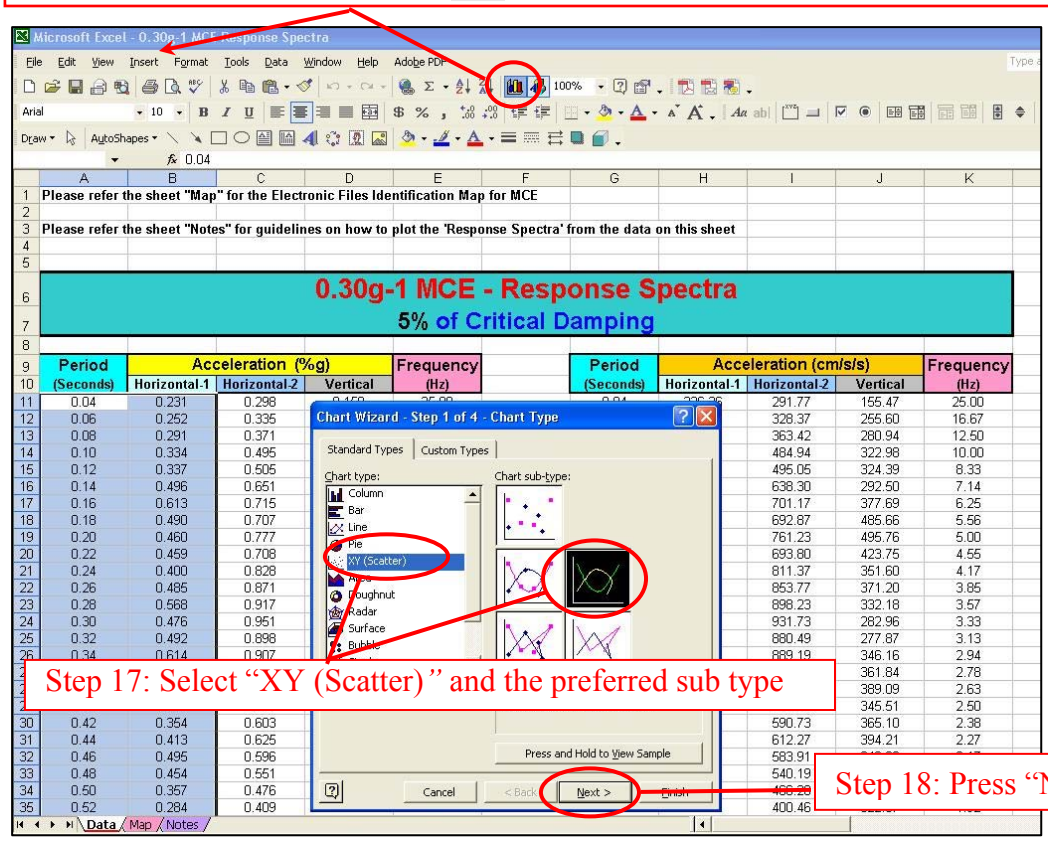

Step 17: Select "XY (Scatter)" and the preferred sub type

Step 18: Press "Next"

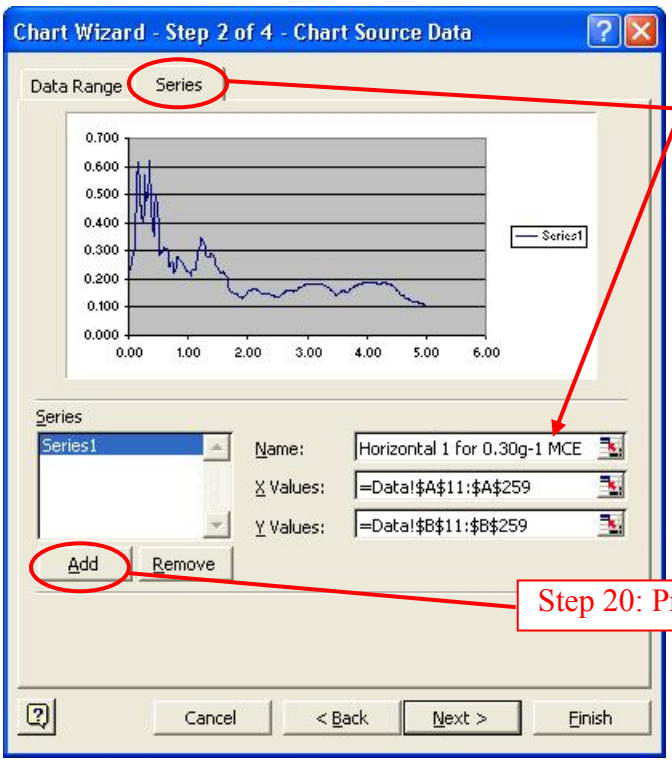

Step 19: Press "Series" tab and enter 'Name' of Series 1

Step 20: Press *"Add"* to enter Series 2

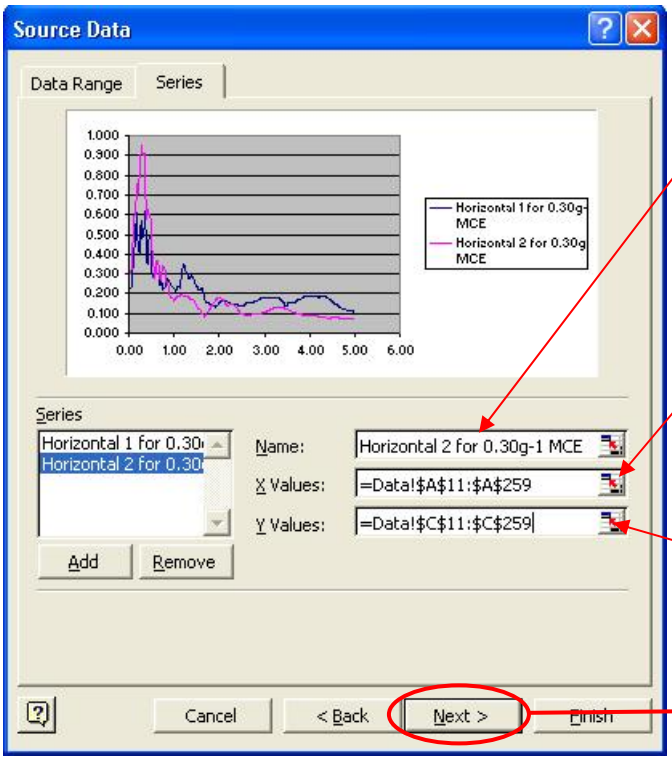

Step 21: Enter 'Name' of Series 2

Step 22: Press and select data for 'Period' in column A (row 11-259) for 'X-Values' (refer to step 14)

Step 23: Press and select data for 'Horizontal-2 Acceleration' in column C (row 11-259) for 'Y-Values' (refer to step 14)

Step 24: Press "Next"

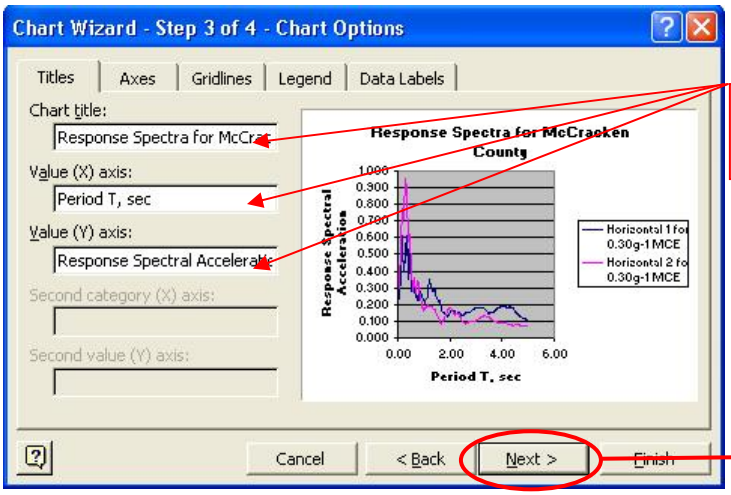

Step 25: Enter 'Chart Title' and X, Y axis titles

Step 26: Press "Next"

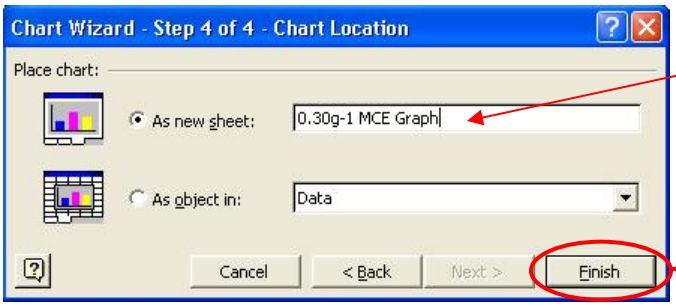

Step 27: Select "As new sheet" and enter name e.g.: 0.30g-1 MCE Graph

Step 28: Press "Finish"

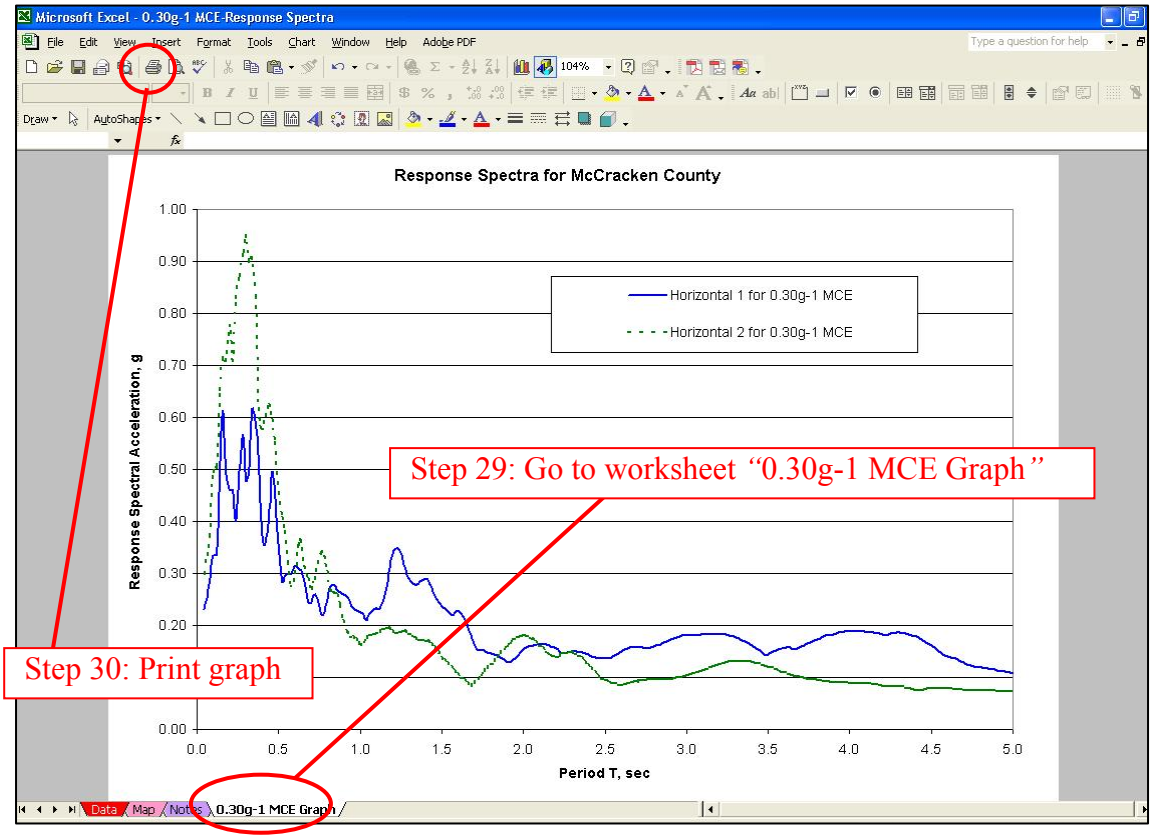

Step 29: Go to worksheet "0.30g-1 MCE Graph"

Step 30: Print graph

III. Design Response Spectra

Step 31: Plot manually or in Microsoft Excel the 'Design Response Spectra'

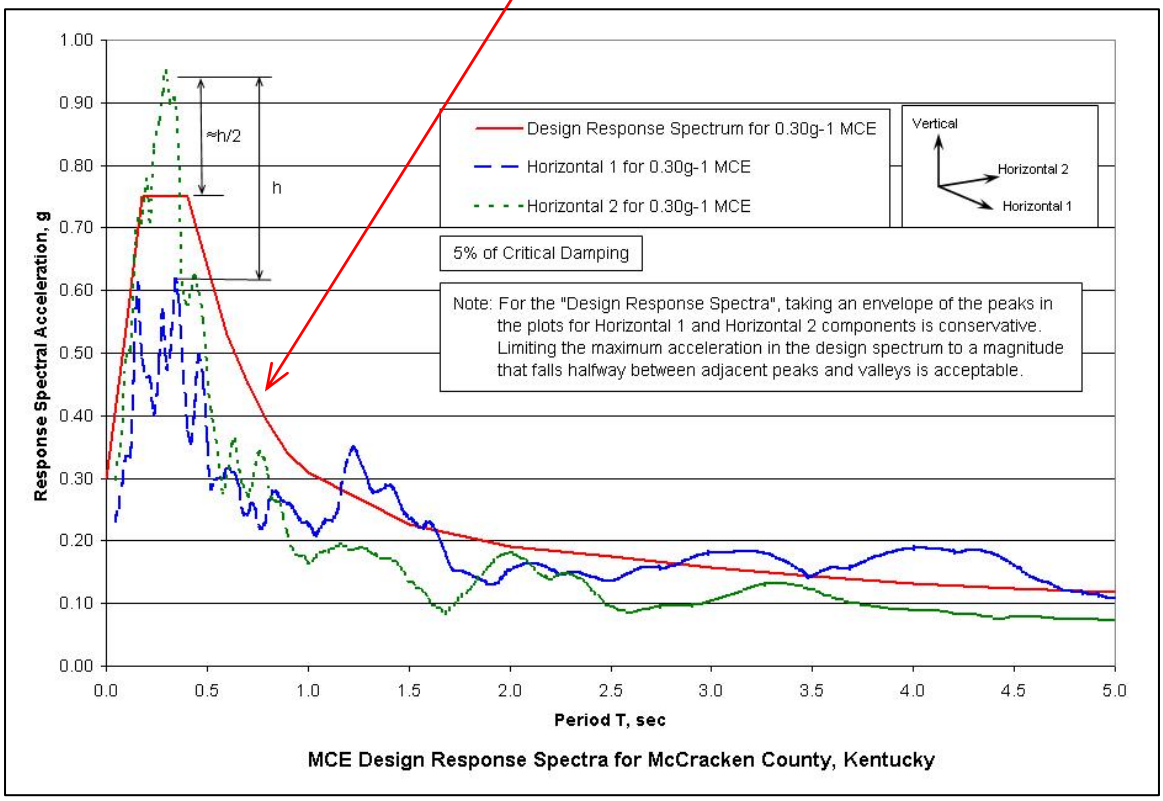

Appendix ES-V

Derivation of the Time History

Time History Generation
For Counties in the Commonwealth of Kentucky

Example: Generate the Expected Earthquake Horizontal-1 Acceleration Time History for McCracken County, KY.

I. Electronic File Identification Map

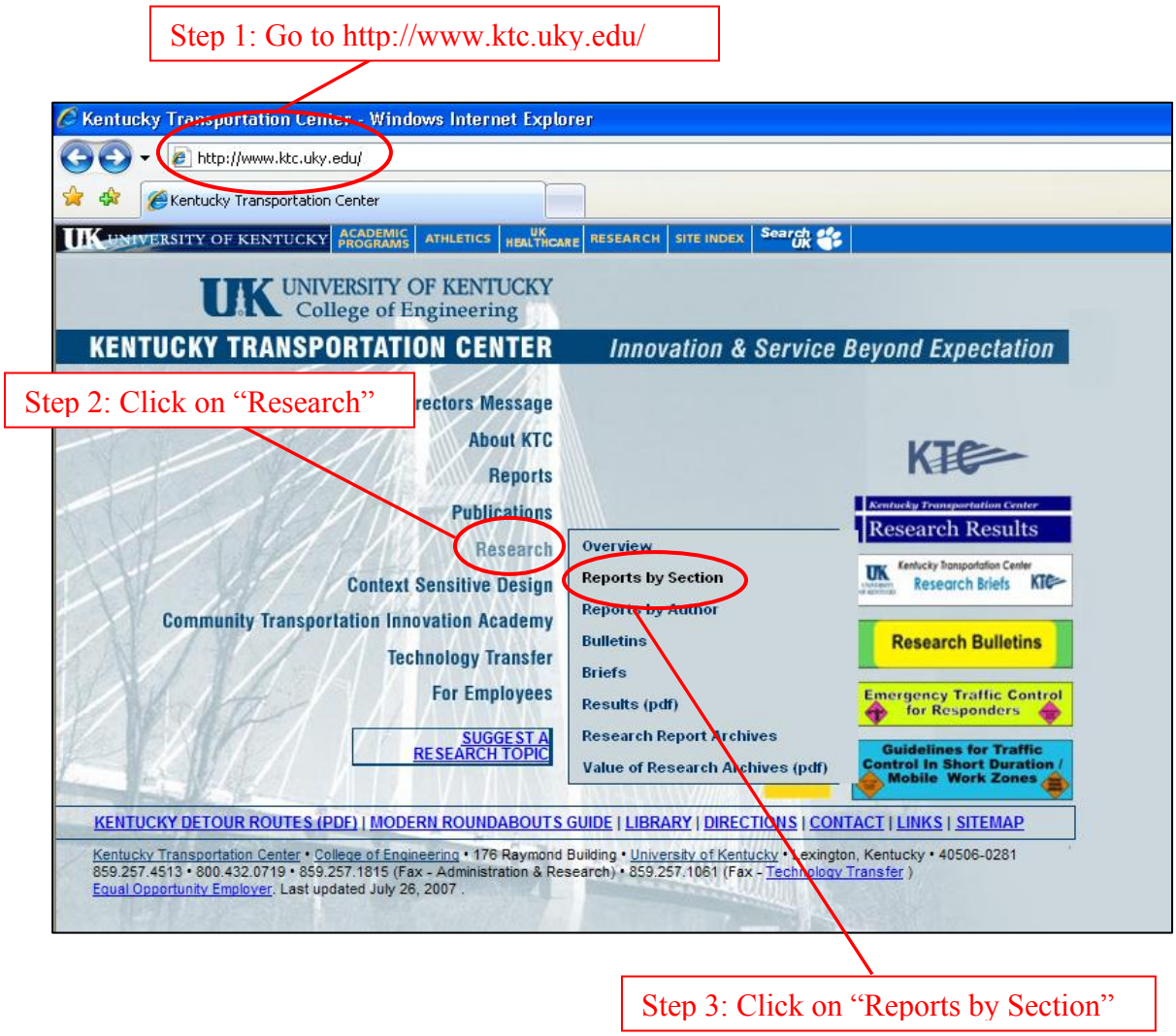

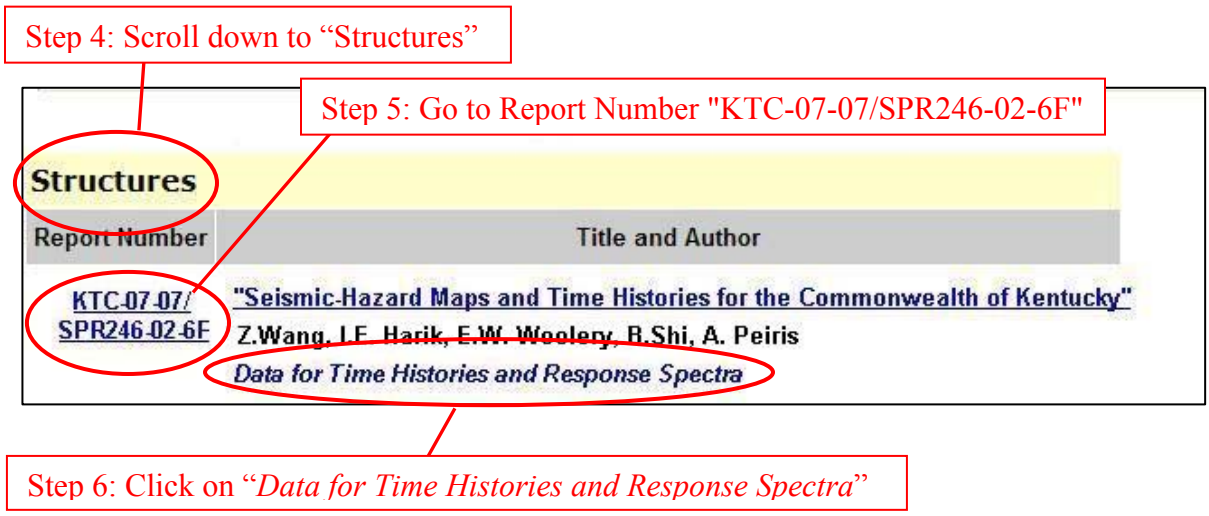
Step 4: Scroll down to “Structures”
Step 5: Go to Report Number "KTC-07-07/SPR246-02-6F"
Structures
Report Number
Title and Author
KTC-07-07/ SPR246-02-6F
"Seismic-Hazard Maps and Time Histories for the Commonwealth of Kentucky"
Z.Wang, I.F. Harik, E.W. Woolery, B.Shi, A. Peiris
Data for Time Histories and Response Spectra
Step 6: Click on “Data for Time Histories and Response Spectra”

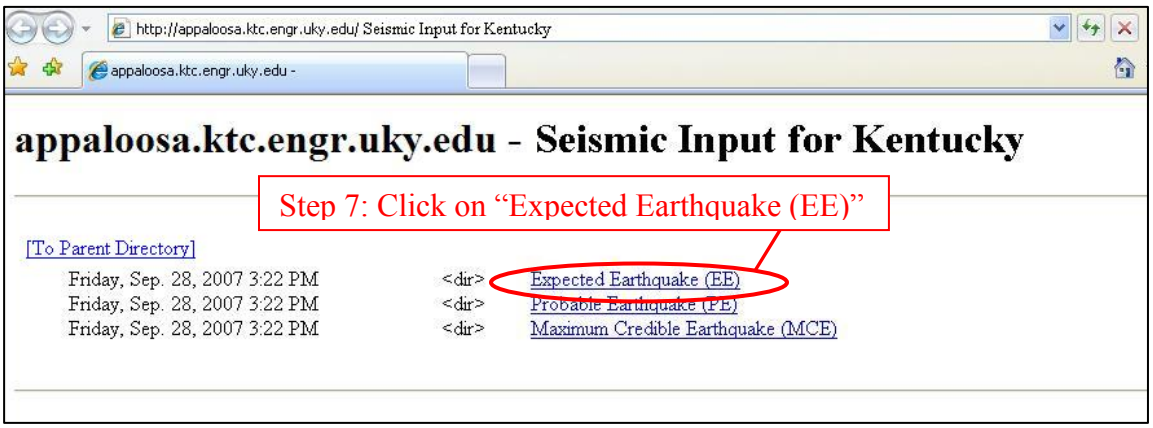
http://appaloosa.ktc.engr.uky.edu/ Seismic Input for Kentucky
appaloosa.ktc.engr.uky.edu -
appaloosa.ktc.engr.uky.edu - Seismic Input for Kentucky
Step 7: Click on “Expected Earthquake (EE)”
[To Parent Directory]
Friday, Sep. 28, 2007 3:22 PM <dir> Expected Earthquake (EE)
Friday, Sep. 28, 2007 3:22 PM <dir> Probable Earthquake (PE)
Friday, Sep. 28, 2007 3:22 PM <dir> Maximum Credible Earthquake (MCE)

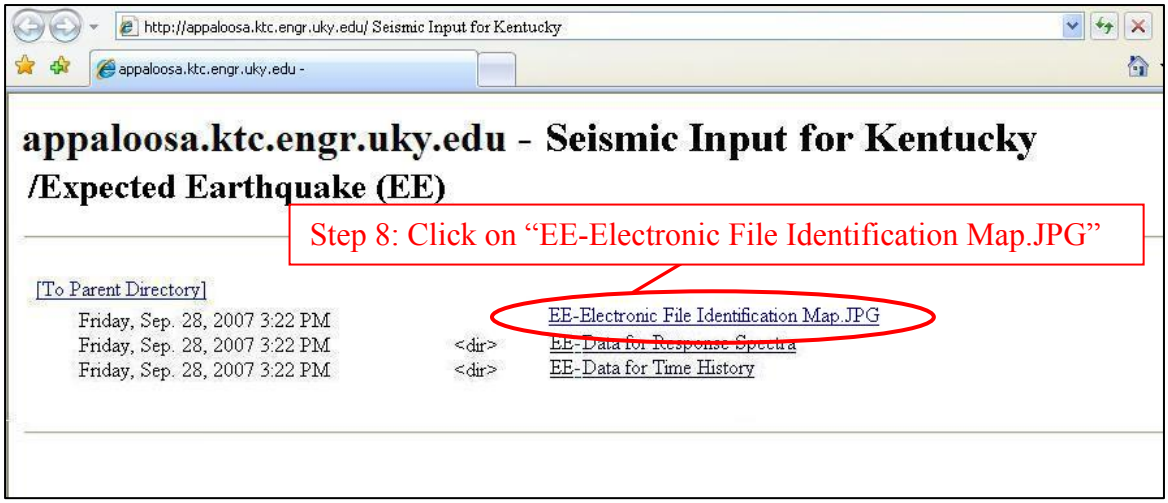
http://appaloosa.ktc.engr.uky.edu/ Seismic Input for Kentucky
appaloosa.ktc.engr.uky.edu -
appaloosa.ktc.engr.uky.edu - Seismic Input for Kentucky
/Expected Earthquake (EE)
Step 8: Click on “EE-Electronic File Identification Map.JPG”
[To Parent Directory]
Friday, Sep. 28, 2007 3:22 PM EE-Electronic File Identification Map.JPG
Friday, Sep. 28, 2007 3:22 PM <dir> EE-Data for Response Spectra
Friday, Sep. 28, 2007 3:22 PM <dir> EE-Data for Time History

Step 9: Go to the Electronic File Identification Map

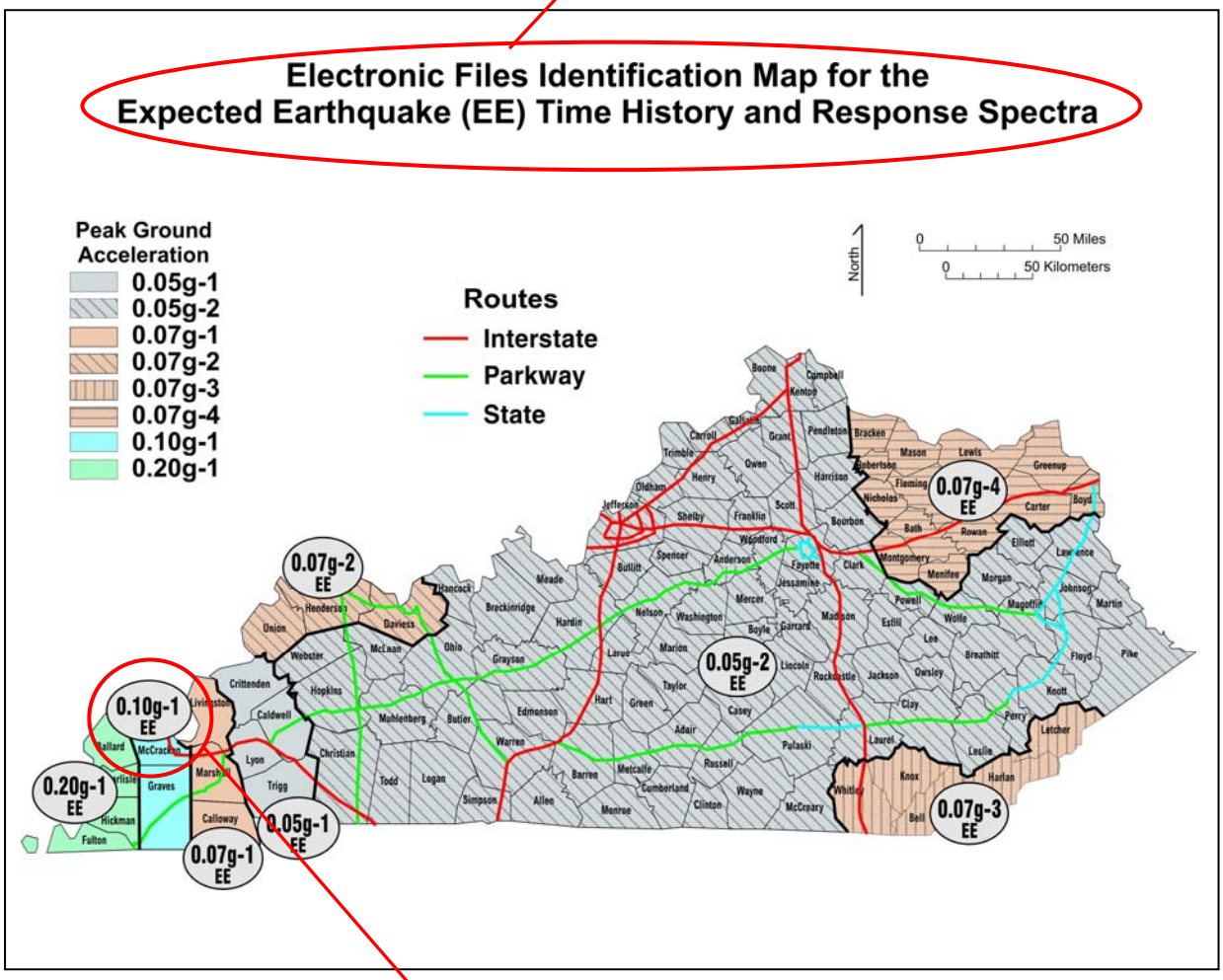

Step 10: Locate "*McCracken County, KY*" and the corresponding "Peak Ground Acceleration" (0.10g-1 EE for this example)

II. Time History

Step 11: Go back to the "Expected Earthquake (EE)" Screen

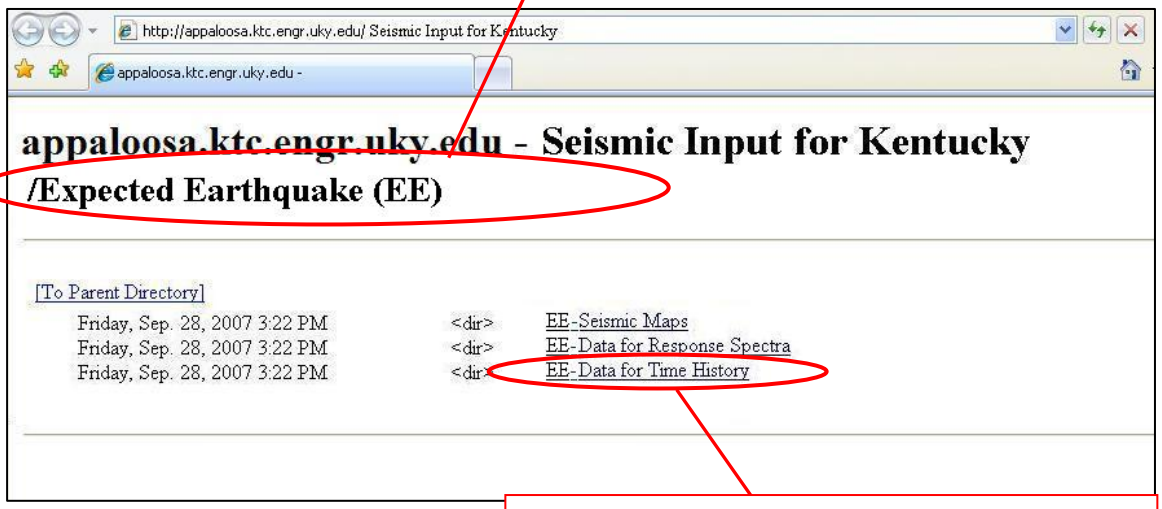

Step 12: Click on "EE- Data for Time History"

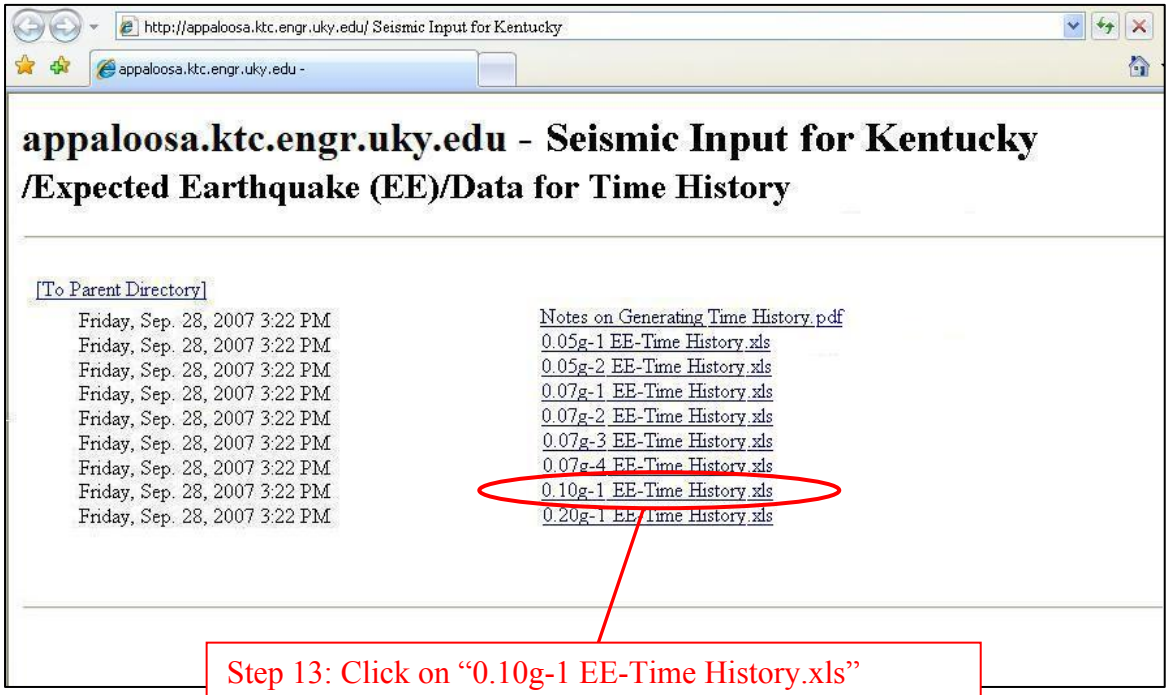

Step 13: Click on "0.10g-1 EE-Time History.xls"

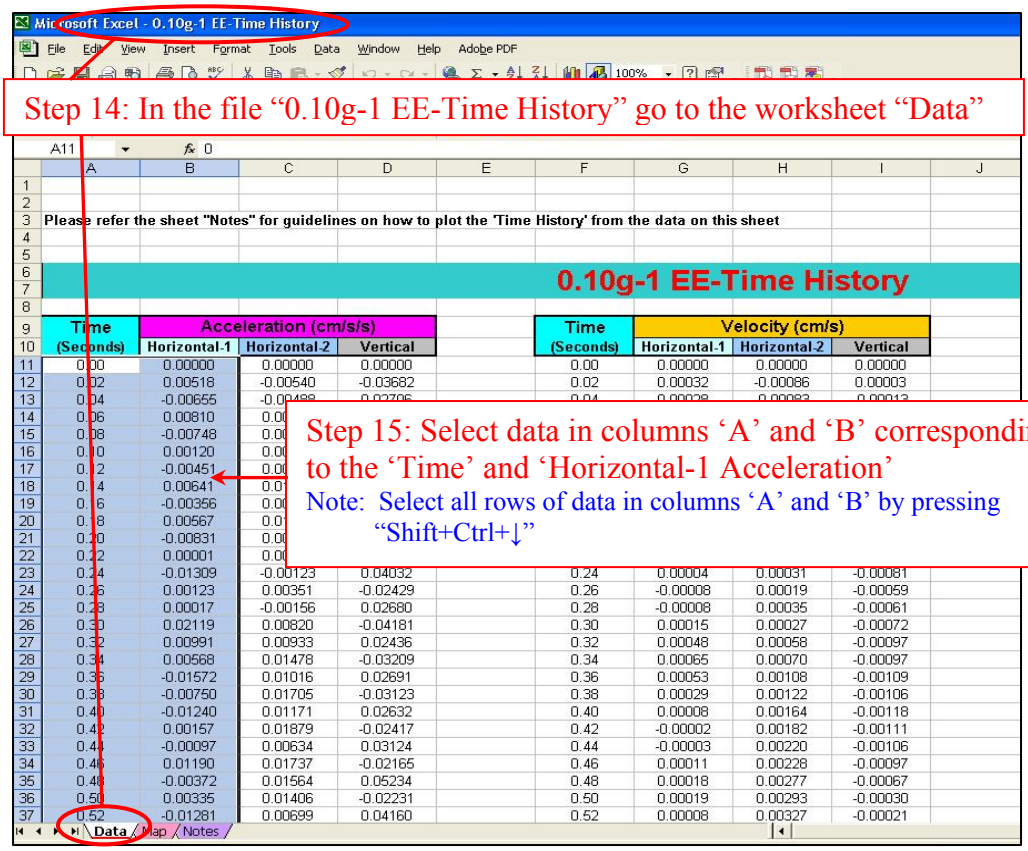
Microsoft Excel - 0.10g-1 EE-Time History
Step 14: In the file "0.10g-1 EE-Time History" go to the worksheet "Data"
Please refer the sheet "Notes" for guidelines on how to plot the 'Time History' from the data on this sheet
0.10g-1 EE-Time History
Time (Seconds)
Acceleration (cm/s/s)
Horizontal-1
Horizontal-2
Vertical
Time (Seconds)
Velocity (cm/s)
Horizontal-1
Horizontal-2
Vertical
Step 15: Select data in columns 'A' and 'B' corresponding to the 'Time' and 'Horizontal-1 Acceleration'
Note: Select all rows of data in columns 'A' and 'B' by pressing "Shift+Ctrl+↓"
Data
Map
Notes

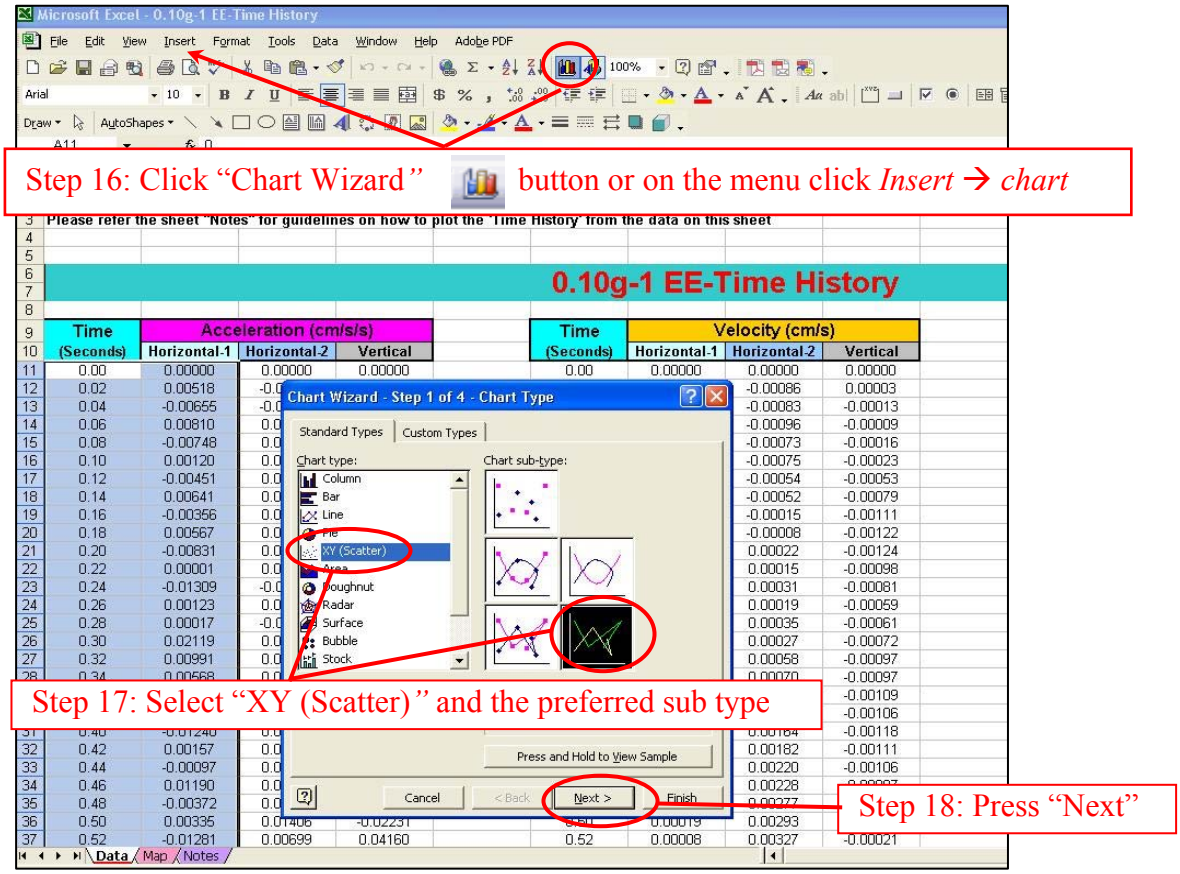
Microsoft Excel - 0.10g-1 EE-Time History
Step 16: Click "Chart Wizard" button or on the menu click *Insert* → *chart*
Please refer the sheet "Notes" for guidelines on how to plot the "Time History" from the data on this sheet
0.10g-1 EE-Time History
Chart Wizard - Step 1 of 4 - Chart Type
Standard Types
Custom Types
Chart type:
Chart sub-type:
Column
Bar
Line
Pie
XY (Scatter)
Area
Doughnut
Radar
Surface
Bubble
Stock
Press and Hold to View Sample
Cancel
< Back
Next >
Finish
Step 17: Select "XY (Scatter)" and the preferred sub type
Step 18: Press "Next"
Data
Map
Notes

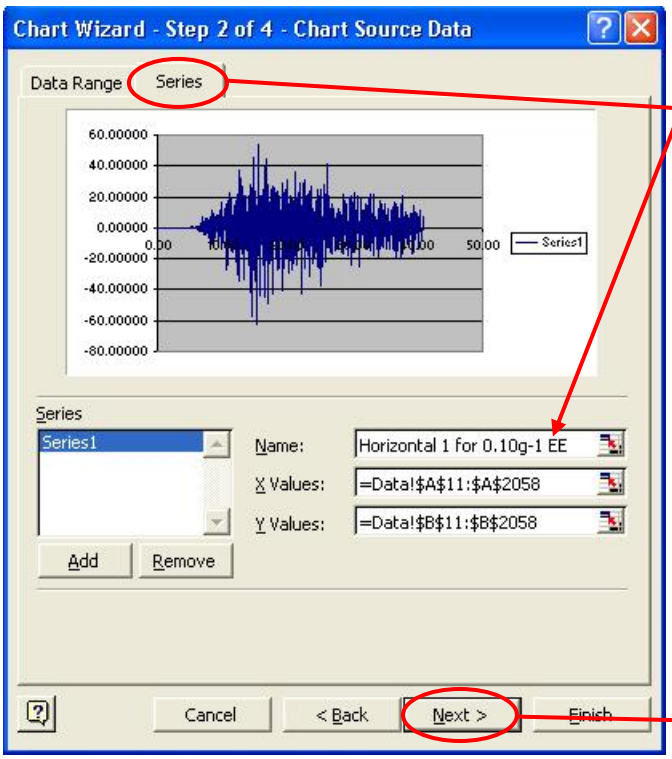

Step 19: Press "Series" tab and enter 'Name' of Series 1

Step 20: Press "Next"

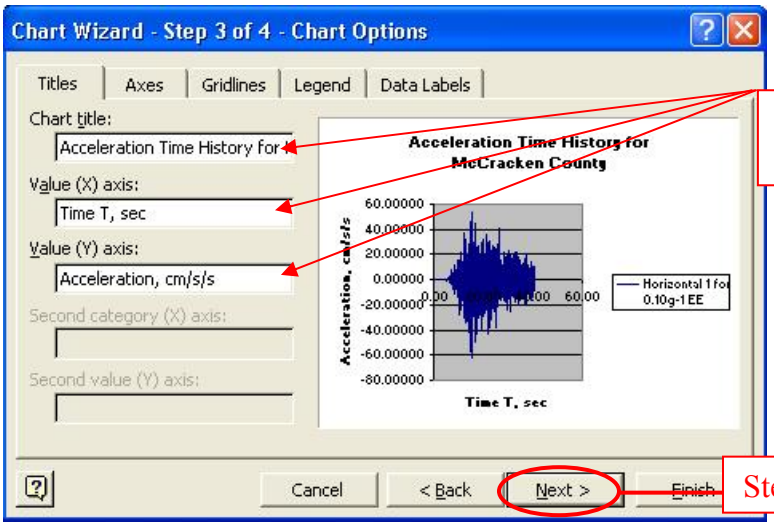

Step 21: Enter 'Chart Title' and X, Y axis titles

Step 22: Press "Next"

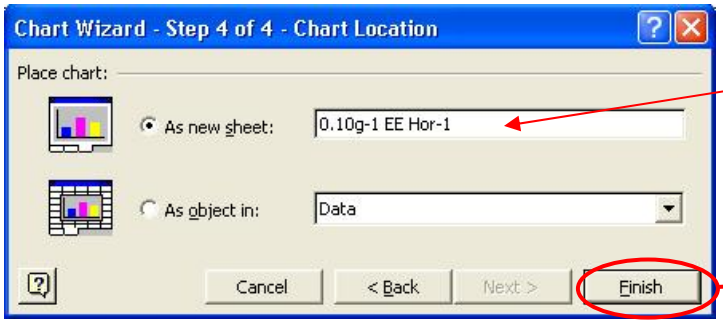

Step 23: Select "As new sheet" and enter name e.g.: 0.10g-1 EE Hor 1

Step 24: Press "Finish"

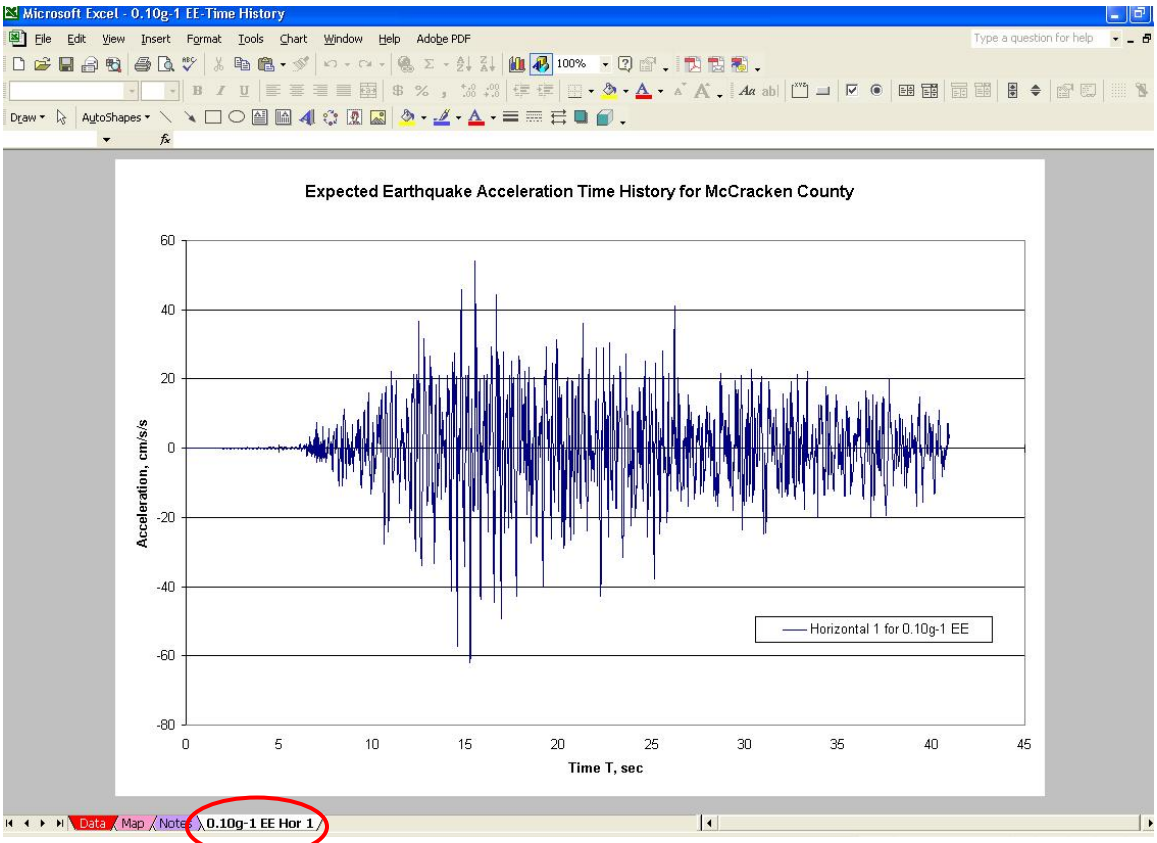

Step 25: Go to worksheet "0.10g-1 EE Hor 1"

Note : To plot any other Time History, for example the Expected Earthquake Horizontal-2 Velocity Time History go back to step 15, select data in columns 'F' and 'H' and repeat the above process.

Executive Summary References

[1-ES]- "NEHRP Recommended Provisions for Seismic regulations for New Buildings and Other Structures (FEMA 450), 2003 Edition, Part 1: Provisions," Building Seismic Safety Council, National Institute of Building Sciences, Washington, D.C., 2004.

[2-ES]- "Recommended LRFD Guidelines for the Seismic Design of Highway Bridges, Part I: Specifications," 2003, MCEER/ATC 49.

[3-ES]- "Seismic Retrofitting Manual for Highway Structures: Part 1-Bridges," 2006, US Department of Transportation, Federal Highway Administration, Publication No. FHWA-HRT-06-032, 656 p.

[4-ES]- "Standard Specifications for Highway Bridges," 2002, American Association of State Highway and Transportation Officials, 17th Edition.

[5-ES]- Street, R., Wang, Z., Harik, I.E., Allen, D.L., and Griffin, J.J., 1996, Source zones, recurrence rates, and time histories for earthquakes affecting Kentucky: Kentucky Transportation Center, KTC-96-4, 187 p.

NOTE: This report is the sixth in a series of six reports for Project SPR 246: "Seismic Evaluation of Bridges along Western Kentucky Parkways." The six reports are:

Report Number:	**Report Title:**
(1) KTC-07-02/SPR246-02-1F	Seismic Evaluation of Bridges on and over the Parkways in Western Kentucky – Summary Report
(2) KTC-07-03/SPR246-02-2F	Site Investigation of Bridges on and over the Parkways in Western Kentucky
(3) KTC-07-04/SPR246-02-3F	Preliminary Seismic Evaluation and Ranking of Bridges on and over the Parkways in Western Kentucky
(4) KTC-07-05/SPR246-02-4F	Detailed Seismic Evaluation of Bridges on and over the Parkways in Western Kentucky
(5) KTC-07-06/SPR246-02-5F	Seismic Evaluation and Ranking of Embankments for Bridges on and over the Parkways in Western Kentucky
(6) KTC-07-07/SPR246-02-6F*	Seismic-Hazard Maps and Time Histories for the Commonwealth of Kentucky

* Denotes current report

ACKNOWLEDGMENTS

The Federal Highway Administration and the Kentucky Transportation Cabinet provided the financial support for this project. The authors would like to acknowledge the cooperation, suggestions, and advice of Dr. Ron Street. We also thank Meg Smath of the Kentucky Geological Survey for editorial help.

TABLE OF CONTENTS

LIST OF TABLES

LIST OF FIGURES

1. INTRODUCTION

1.1 Background

Earthquakes have been periodically felt in Kentucky throughout history. An example is the June 18, 2002, Evansville, Ind., earthquake ($m_{b,Lg}$5.0). The most widely felt and damaging earthquakes in the state are the great earthquakes that occurred in the winter of 1811–1812 and were centered in northeastern Arkansas, northwestern Tennessee, southwestern Kentucky, and southeastern Missouri (Fig. 1-1) (Nuttli, 1973a). The 1811–1812 earthquakes were reported to have caused damage (i.e., modified Mercalli intensity [MMI] VII–IX) throughout much of the Commonwealth (Fig. 1-1). MMI VII effects in Kentucky also occurred as a result of the 6.2 $m_{b,Lg}$ earthquake near Charleston, Mo., on October 31, 1895 (Nuttli, 1976). Figure 1-2 is an isoseismal map for the event. Two other events have resulted in MM intensity VII damage in Kentucky. One is the 5.5 $m_{b,Lg}$ (M_o = 9.7x10^{23} dyne-cm) southern Illinois earthquake of November 9, 1968 (Herrmann and Ammon, 1997), and the other is the 5.2 $m_{b,Lg}$ (M_o = 4.1x10^{23} dyne-cm) northeastern Kentucky earthquake of July 27, 1980 (Herrmann and others, 1982). The 1968 earthquake caused MM intensity VII damage in the Henderson area (Stover and Coffman, 1993) and the 1980 earthquake caused MM intensity VII damage in Sharpsburg and Maysville (Street and Foley, 1982).

Epicenters of historical earthquakes that have occurred in and near Kentucky, and have caused MMI VI or greater damage, are shown in Figure 1-3. As seen in the figure, most of the earthquakes have occurred either in northeastern Arkansas, southeastern Missouri, or southern Illinois and southern Indiana. A few earthquakes have occurred in the general vicinity of Middlesboro, however. The largest of these is the 4.3 $m_{b,Lg}$ earthquake of January 2, 1954. Damage caused by the earthquake included cracked foundations, broken windows, and cracked plaster. A 4.0 $m_{b,Lg}$ earthquake occurred near Barbourville on January 19, 1976. This earthquake resulted in broken windows, cracked roads, and plaster damage. The 1954 and 1976 earthquakes are listed as MMI VI events by Stover and Coffman (1993).

Although most of the earthquake damage in Kentucky is the result of events outside the state, there is a persistent level of low-magnitude (< 4 $m_{b,Lg}$) seismicity in certain areas of the state: Fulton, Hickman, Carlisle, Ballard, and McCracken Counties of western Kentucky; Union and Henderson Counties in northwestern Kentucky; the part of Kentucky north and east of Mount Sterling; and the southeastern counties of Bell, Harlan, Knox, and Whitley.

1.2. Seismic Hazards

Seismic hazard is a natural phenomenon generated by earthquakes, such as surface rupture, ground motion, ground-motion amplification, liquefaction, and induced landslides, that have potential to cause harm. How earthquakes affect humans, buildings, and bridges depends on how strong the ground motion is. Most damage during an earthquake is caused by ground motion. Figure 1-4 shows damage to the I-80 bridge caused by strong ground motion during the 1989 Loma Prieta earthquake. The level of ground motion depends on earthquake magnitude, the distance from the earthquake center (epicenter), and the type of fault on which the earthquake

occurred. The larger an earthquake's magnitude, the stronger the ground motion it will generate. The closer a site is to the epicenter, the stronger the ground motion, and vice versa. The ground motion generated directly by an earthquake is the primary hazard, referred to as the ground motion hazard. This report is focused on the ground-motion hazard and contains detailed discussion on how the ground-motion hazard maps are derived and how they can be used.

Strong ground motion can cause secondary hazards, such as ground-motion amplification, liquefaction, and landslides, under certain local geologic conditions. Soft soils overlying hard bedrock tend to amplify ground motions; this is known as ground-motion amplification. Amplified ground motion caused by loose lake deposits contributed to the heavy damage in Mexico City during the earthquake of September 19, 1985 (Fig. 1-5), even though the city was about 200 km away from the epicenter. Amplified ground motion caused by Ohio River deposits contributed to the damage in Maysville during the Sharpsburg earthquake of July 28, 1980 (Fig. 1-6). Soft sandy soils can be liquefied by strong ground motion, a process called liquefaction. Figure 1-7 shows that sandy soil was liquefied and behaved like fluid during the Nisqually, Wash., earthquake of February 28, 2001. Strong ground motion can also trigger landslides—known as earthquake-induced landslides—in areas with steep slope, such as eastern Kentucky. Figure 1-8 shows a slope failure caused by the Nisqually earthquake. These secondary hazards may be of great concern for bridge engineers. They are site-specific and require detailed investigation. Characterization of these secondary hazards is beyond the scope of this study.

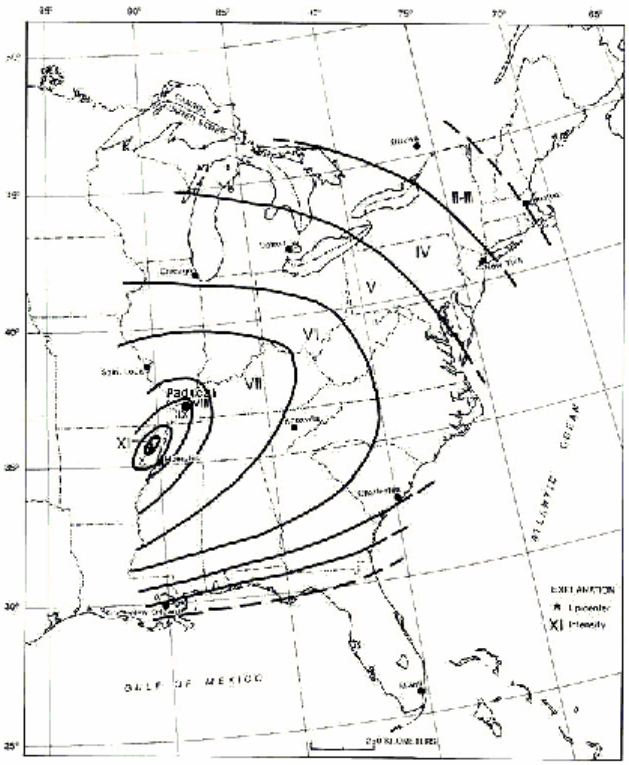

Figure 1-1. Isoseismal map of the Arkansas earthquake of December 16, 1811, 08:15 UTC (first of the 1811–1812 New Madrid series). From Stover and Coffman (1993)

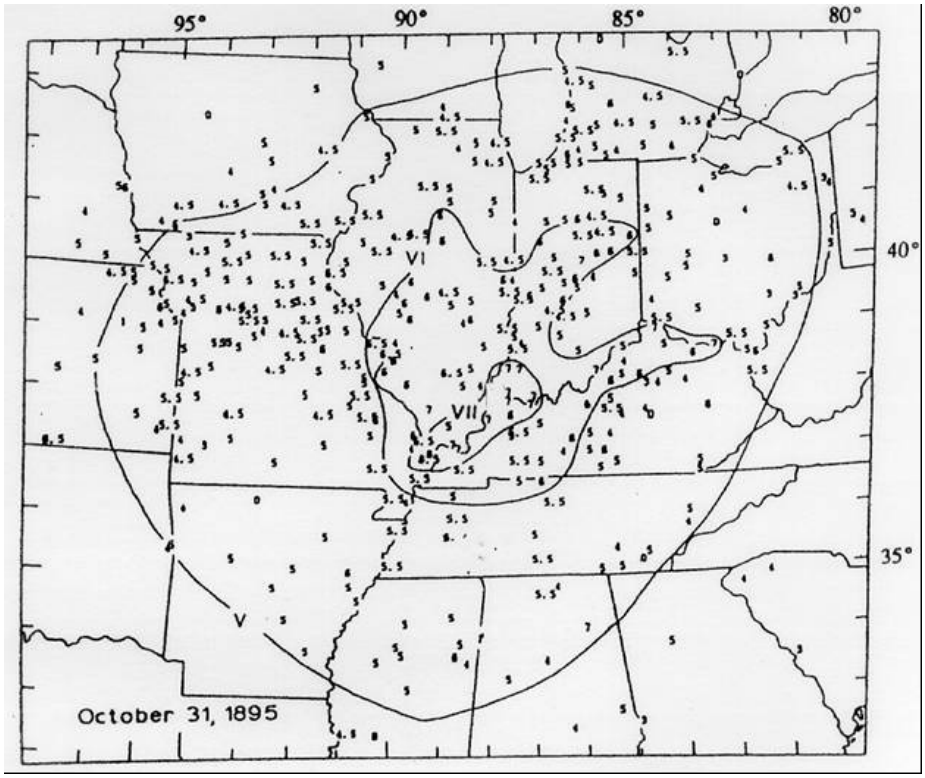

Figure 1-2. Isoseismal map of the Charleston, Mo., earthquake of October 31, 1895. From Nuttli (1976)

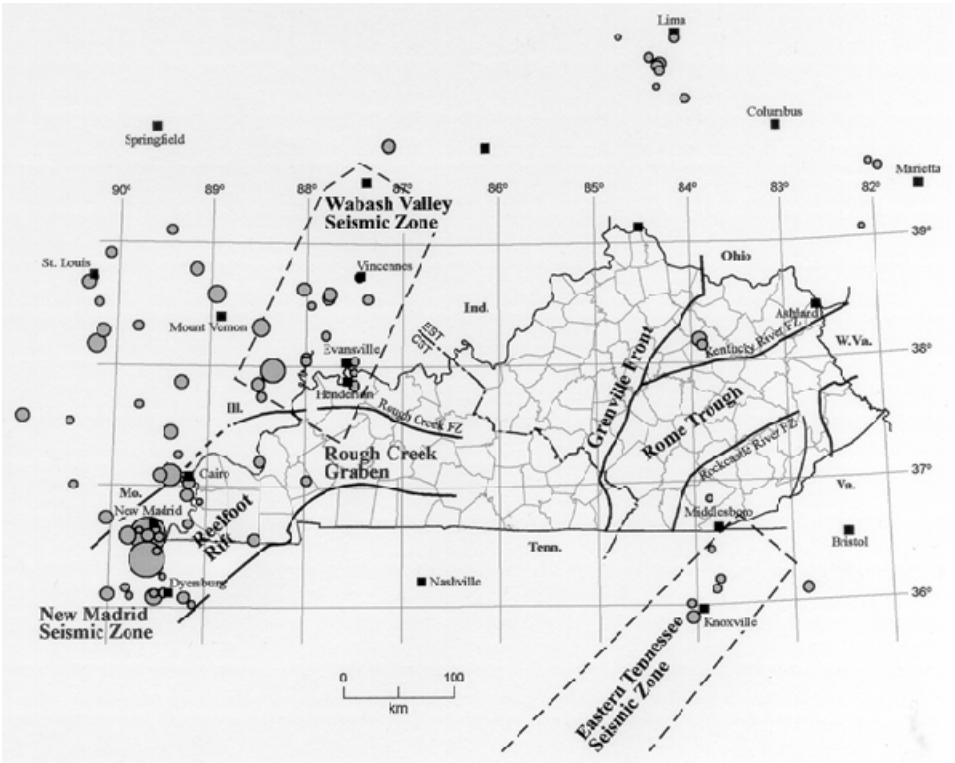

Figure 1-3. Historical earthquakes in and around Kentucky

Figure 1-4. I-80 damage during the 1989 Loma Prieta earthquake

Figure 1-5. Complete destruction of a building caused by amplified ground motion in Mexico City during the 1985 Mexico earthquake

Figure 1-6. High MMI in Maysville was caused by amplified ground motion during the 1980 Sharpsburg earthquake. From Hanson and others (1980)

Figure 1-7. Road damage caused by liquefaction during the 2001 Nisqualy, Wash., earthquake

Figure 1-8. Road damage caused by slope failure during the 2001 Nisqualy, Wash., earthquake

2. EARTHQUAKE MEASUREMENT

2.1. Magnitude

Earthquake size has routinely been given in terms of a magnitude (*M*). Magnitude scales are empirical relations of the form

$$M = B(T) + C(T, D)\log_{10} D + \log_{10}(\frac{A}{T}) \qquad (2\text{-}1)$$

in which *A* is the amplitude of a particular phase on a seismogram, corrected for instrumental response; *T* is the period of the wave corresponding to the amplitude; and *D* is the epicentral distance. The coefficients *B* and *C* are pseudoconstants. *B* is a scaling factor that depends upon the phase and period of the phase used in the magnitude determination. *C* is obtained from the linear approximation of the attenuation with distance of the phase being used in the magnitude scale. As such, *C* is dependent upon the phase, the path of the wave propagation, and is only valid over a limited range of epicentral distances.

The earliest magnitude scale, introduced by Charles Richter in 1935 for southern California earthquakes, is the local magnitude, M_L, often referred to as the "Richter scale." In the central United States, the $m_{b,Lg}$ scale, based on higher-mode *Lg* waves recorded in the central United States (Nuttli, 1973b), is used. *Lg* waves are shear waves that are reflected supercritically between the surface and the Moho. As such, they are a trapped crust wave, and are most strongly developed in areas underlain by ancient crustal shields, such as the central United States. The formulas are:

$$m_{b,Lg} = 3.75 + 0.90\log_{10} D + \log_{10}(\frac{A}{T}) \qquad 0.5^\circ \le D \le 4^\circ \qquad (2\text{-}2)$$

$$m_{b,Lg} = 3.30 + 1.66\log_{10} D + \log_{10}(\frac{A}{T}) \qquad 4^\circ \le D \le 30^\circ \qquad (2\text{-}3)$$

where *D* is the epicentral distance in degrees; *A* is the amplitude in microns of the ~1-s, vertical-component *Lg* wave; *T* is the period; and the ratio *A*/*T* is expressed in microns per second (zero-to-peak amplitude). The standard deviation of a typical $m_{b,Lg}$ estimate is ±0.15 to ±0.2 units, depending upon the number of seismic stations used, the distribution of the seismic stations, and the size of the earthquake.

The most commonly used magnitude is moment magnitude, *M,* which is related to seismic moment, M_o, as follows:

$$M = \frac{2}{3}\log_{10}(M_o) - 10.7 \qquad (2\text{-}4)$$

where seismic moment is in dyne-cm (10^{-7} N-m). Moment magnitude was devised by Hanks and Kanamori (1979) to overcome the shortcomings of saturation of traditional magnitude scales,

such as the *Lg*-magnitude scale. Most traditional magnitude scales depend on the amplitude and period of a particular seismic wave; for example, the *Lg*-magnitude scale is based on a 1-s *Lg* wave. Seismic waves whose wavelengths are much smaller than the earthquake source do not increase in amplitude as the earthquake source size increases. For this reason, seismologists prefer to classify earthquakes by their seismic moment, which can be readily converted to *M* using equation 2-4.

Two commonly cited relationships between Nuttli's (1973b) *Lg*-wave magnitude ($m_{b,Lg}$) and *M* are Johnston's (1996):

$$M = 1.14 + 0.24 m_{b,Lg} + 0.093 m_{b,Lg}^2, \qquad (2\text{-}5)$$

and Atkinson and Boore's (1995):

$$M = 2.75 - 0.277 m_{b,Lg} + 0.127 m_{b,Lg}^2. \qquad (2\text{-}6)$$

Figure 2-1 compares the two M-$m_{b,Lg}$ relationships with the observed data for the earthquakes listed in Table 2-1. Based on the fit of the observed data with Johnston's (1996) M-$m_{b,Lg}$ relationship, equation 2-5 was used in this study for converting $m_{b,Lg}$ to *M*.

Table 2-1. Magnitude $m_{b,Lg}$, seismic moments, and locations of some well-constrained earthquakes in the central United States

Date	Lat/Long (°N/°W)	Depth (km)	Strike (°)	Dip (°)	Rake (°)	$m_{b,Lg}$	Moment (dyne-cm)	Ref.
Feb. 2, 1962	36.37/89.51	7.5	350	84	145	4.3	2.5×10^{22}	1
Mar. 3, 1963	36.64/90.05	15	304	78	-28	4.8	1.1×10^{23}	1
Aug. 14, 1965	37.22/89.31	1.5	280	70	-20	3.8	2.9×10^{21}	1
Nov. 9, 1968	37.91/88.37	22	0	46	79	5.5	9.7×10^{23}	1
Nov. 17, 1970	35.86/89.95	16	220	75	150	4.3	1.6×10^{22}	1
Apr. 3, 1974	38.55/88.07	15	310	70	0	4.2	3.7×10^{22}	1
June 13, 1975	36.54/89.68	9	85	60	-20	4.3	4.6×10^{21}	1
Mar. 25, 1976	35.59/90.48	12	220	65	150	4.9	9.8×10^{22}	1
July 27, 1980	38.17/83.91	8	30			5.2	4.1×10^{23}	3
Jun. 10, 1987	38.71/87.95	10	135	70	15	5.2	3.1×10^{23}	1
Sep. 7, 1988	38.14/83.88	4–7	198	51		4.6	2.0×10^{22}	2
Sep. 26, 1990	37.16/89.58	15	140	75	50	4.5	3.0×10^{22}	1
May 4, 1991	36.56/89.83	8	90	67.5	20	4.5	1.8×10^{22}	1
Feb. 5, 1994	37.36/89.19	16	30	70	170	4.2	6.8×10^{21}	1
Jun. 18, 2002	37.97/87.78	17–19	30	85	180	5.0	8.1×10^{22}	4

(1) Herrmann and Ammon (1997); (2) Street and others (1993); (3) Herrmann and others (1982); Herrmann, R.B., personal communication

Converting $m_{b,Lg}$ to M, or vice versa, implies a level of knowledge about the stress drop associated with the event, which is rarely known for events in the central United States. The seismic moment and moment magnitude of an earthquake are measures of seismic waves having periods between a few to several tens of seconds, depending on the size of the earthquake. For most engineering purposes, seismic waves having periods of several seconds and greater are not of particular concern. The $m_{b,Lg}$ magnitude scale described above, however, is calibrated to a 1-s period wave (the *Lg* wave at distances > 100 km, and the *S* wave at distances < 100 km), a period that is within the general range of engineering interest.

2.2. Modified Mercalli Intensity

In the United States, the assessment of earthquakes based on their effects is done using the abridged modified Mercalli intensity scale (MMI) developed by Wood and Neumann (1931). The scale is a measure of the intensity of the ground motions by means of human perception (such as being awakened from sleep or being unable to stand), by the degree of damage to buildings (such as damage to chimneys and plaster), and by the amount of disturbance to the surface of the ground (such as liquefaction). There is no direct relationship between MMI and magnitude. A larger earthquake will generally generate higher MMI in a larger area, however.

Historical seismicity is seismicity for which there are no or inadequate instrumental records that can be used to assess the size of an earthquake. In the central United States, the first modern seismographs were not installed until the early 1960's with the advent of the St. Louis University Seismograph Network. Prior to the 1960's, miscellaneous seismic stations were in cities such as Chicago, Cincinnati, Cleveland, and St. Louis, but the instruments were not operated in a consistent manner, and were inadequate in number, gain, and resolution to provide well-constrained epicentral locations and magnitudes. Consequently, locations and magnitudes for earthquakes that occurred in the central United States prior to 1960 are generally assessed from MMI data. Street and Turcotte (1977) estimated that the standard deviation of magnitudes based on intensity data is, at a minimum, ±0.3.

For the central United States, Bakun and others (2003) derived a relationship between MMI, moment magnitude (M), and distance (D in km) as follows:

$$MMI = 1.41 + 1.68M - 0.00345D - 2.08\log_{10} D\,. \qquad (2\text{-}7)$$

MMI has also been related to ground-motion measurement (Wald and others, 1999). Table 2-2 shows the relationship between MMI and ground-motion measurement (Wald and others, 1999).

Table 2-2. Relationship between MMI and ground-motion measurement

PERCEIVED SHAKING	Not felt	Weak	Light	Moderate	Strong	Very strong	Severe	Violent	Extreme
POTENTIAL DAMAGE	none	none	none	Very light	Light	Moderate	Moderate/Heavy	Heavy	Very Heavy
PEAK ACC.(%g)	*<.17*	*.17-1.4*	*1.4-3.9*	*3.9-9.2*	*9.2-18*	18-34	34-65	65-124	>124
PEAK VEL.(cm/s)	<0.1	0.1-1.1	1.1-3.4	3.4-8.1	8.1-16	*16-31*	*31-60*	*60-116*	*>116*
INSTRUMENTAL INTENSITY	I	II-III	IV	V	VI	VII	VIII	IX	X+

Although MMI data can be used to evaluate earthquakes and indeed are the only means available for evaluating historical events, epicentral locations and magnitudes derived for earthquakes on the basis of their intensity data are not well constrained. In 1980, for example, a moderately damaging earthquake occurred on July 27, near the community of Sharpsburg. Based on the damage reports, however, some researchers initially concluded that the event had occurred near Maysville, which is ~50 km north of the actual epicenter. Only after several aftershocks had been recorded in the Sharpsburg area was it fully accepted that the event had occurred near Sharpsburg. In this case, site conditions, unconsolidated soils at Maysville and bedrock at Sharpsburg, and the lack of a nearby seismograph station led to the incorrect initial epicentral

location. Based on this example, and other examples involving historical seismicity (Street and Green, 1984), the epicentral locations of noninstrumental events could be mislocated by as much as 50 km.

2.3. Focal Depth, Epicenter, and Epicentral Distance

Earthquakes are caused by sudden movement along a fault. The starting point of the movement is called the *focus* or *hypocenter.* The focus is usually beneath the surface at a certain depth, called the *focal depth*. Surface projection of the focus is called the *epicenter*. The distance between the epicenter and an observation point on the surface is called *epicentral distance*.

The extent of damage in the area of the epicenter of an earthquake can be profoundly affected by the focal depth of the event. For example, the earthquakes in southern Illinois on August 14, 1965, and November 9, 1968, resulted in a maximum MM intensity of VII in both epicentral areas. The magnitudes of the events, however, were very different. The $m_{b,Lg}$ of the 1965 earthquake was 3.8, whereas the $m_{b,Lg}$ of the 1968 earthquake was 5.5. Both events had the same maximum intensity because of their respective focal depths. Herrmann and Ammon (1997) gave the focal depth of the 1965 event as 1.5 km and of the 1968 event as 22 km. As another example, there were two M4.0 earthquakes in the central United States in 2003, the April 30 Blythville, Ark., event and the June 6 Bardwell event. The focal depths for the two quakes were significantly different: about 23.8 km for Blythville and 2.5 km for Bardwell (Wang and others, 2003a). The Blythville earthquake had a larger felt area but lower MMI in the epicenter, whereas the Bardwell earthquake had a smaller felt area but higher MMI in the epicenter.

The focal depths of most earthquakes in the seismic zones around Kentucky range from 5 to 15 km in the New Madrid Seismic Zone, and 10 to 25 km in the Eastern Tennessee and Wabash Valley Seismic Zones. In Kentucky, the only reliable focal depths are the ones for the 5.3 $m_{b,Lg}$ July 27, 1980, Sharpsburg earthquake and its aftershocks (Herrmann and others,, 1982); the 4.6 $m_{b,Lg}$ September 7, 1988, Judy earthquake and its aftershocks (Street and others, 1993); and some of the 1990 Meade County earthquakes (Street and others, 1991). The focal depth of the 1980 Sharpsburg main shock is 12 km (Herrmann and others, 1982), and 47 of the 50 recorded aftershocks were estimated to have focal depths of 8 to 15 km. The focal depth of the 1988 Judy main shock and 22 of its aftershocks ranged from 4 to 10 km. Street and others (1991) estimated focal depths for four of the 1990 Meade County earthquakes at between 5 and 7 km.

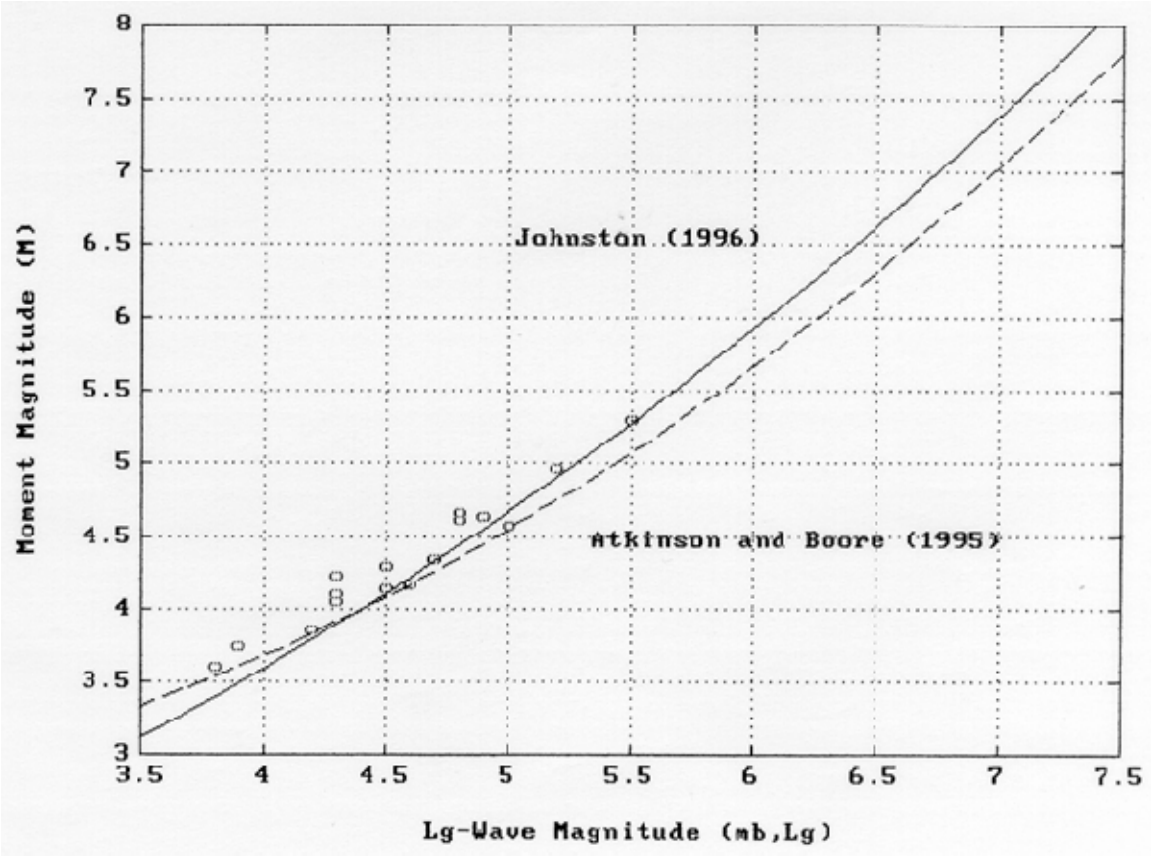

Figure 2-1. Relationship between moment magnitude (M) and $m_{b,Lg}$ (Atkinson and Boore, 1995; Johnston, 1996)

3. SEISMIC-HAZARD MAPPING

3.1. Introduction

Seismic-hazard mapping is an effort to estimate what level of ground motion could be expected in a region over a certain time, for instance 100 or 500 years. Three data sets are required: earthquake sources (where and how big), earthquake occurrence frequencies (how often), and the ground-motion attenuation relationship (how strong). In Kentucky, as well as the rest of the central United States, answers to the questions "where, how big, how often, and how strong" are difficult ones. Except in the New Madrid Seismic Zone, where earthquakes concentrate along active faults, earthquakes in the central United States occur in a large area and are not associated with any specific zone or fault. In comparison to typical plate-boundary seismic zones such as coastal California, the central United States is located in the middle of the continent and has a totally different tectonic setting. The exact boundary of the New Madrid Seismic Zone is still difficult to define, even though it is the most active and well studied in the country. The largest historical earthquakes to have occurred in the central United States were the 1811–1812 New Madrid events. The estimated magnitude ranges from about M7 to M8—a large range, though it has been well studied (Johnston, 1996; Hough and others, 2000; Mueller and Pujol, 2001; Bakun and Hopper, 2004). Earthquakes are also infrequent, especially large earthquakes that have significant impacts on the built environment. Recurrence intervals for large earthquakes are quite long, ranging from about 500 to 1,000 years in the New Madrid Seismic Zone to about 2,000 to 4,000 years in the Wabash Valley Seismic Zone; they are even longer in other zones. These recurrence intervals were primarily determined from paleoseismic studies (Obermeier and others, 1991; Tuttle and Schweig, 1996; Munson and others, 1997; Tuttle and others, 2002; Holbrook and others, 2006). Several ground-motion attenuation relationships are available for the central United States (Atkinson and Boore, 1995; Frankel and others, 1996; Toro and others, 1997; Somerville and others, 2001; Campbell, 2003). All the attenuation relationships were based on numerical modeling and sparse strong-motion records from small earthquakes, however. Thus, these attenuation relationships are uncertain and predict much higher ground motions in comparison with similar-magnitude earthquakes in California.

Two approaches—probabilistic seismic hazard analysis (PSHA) and deterministic seismic hazard analysis (DSHA)—are widely used in seismic-hazard mapping. The two approaches use the same data sets—earthquake sources (where and how big), earthquake occurrence frequencies (how often), and ground-motion attenuation relationship (how strong)—but are fundamentally different in calculations and final results. Before PSHA and DSHA, as well as their results, are discussed in detail, we will briefly discuss seismic risk and the relationship between hazard and risk. Although seismic hazard and risk are two fundamentally different concepts, they have been used interchangeably, which causes confusion and difficulty in understanding seismic hazard and risk (Wnag and Ormsbee, 2005; Wang, 2006).

3.2. Seismic Risk

As discussed in Chapter 1, seismic hazard is a natural phenomenon generated by earthquakes, such as surface rupture, ground motion, ground-motion amplification, liquefaction,

and induced landslides, that have potential to cause harm, and is quatified by two parameters: a level of hazard (i.e., 0.2g PGA and 5 m surface rupture) and its recurrence interval. In contrast to seismic hazard, the definition of seismic risk is more broad and subjective. In general, seismic risk describes a propability of occurrence of a specific level of seismic hazard over certain time (i.e., 50 or 75 years), and is quantified by three parameters: probability, level of hazard or consequence to society, and exposure (McGuire, 2004; Wang and Ormsbee, 2005; Wang and others, 2005; Malhotra, 2006; Wang, 2006). The relationship between seismic hazard and risk is complicated and must be treated very cautiously. Seismic risk depends not only on seismic hazard and exposure, but also on the models (i.e., time-independent [Poisson] and time-dependent ones) that could be used to describe the occurrences of earthquakes. High seismic hazard does not necessarily mean high seismic risk, and vice versa.

It is important to point out that exposure here means both time and societal vulnerability (i.e., buildings, humans, etc.). For example, 75 years (time) is commonly referred to as the normal life of a highway structure (vulnerability). These two elements of the exposure (time and vulnerability) are inseparable. This is analogous to someone driving a car: the driver and car (vulnerabilities) are both exposed to a potential car crash (hazard). The probability that the driver and car could have a car crash cannot be estimated without knowing how long (time) the driver and car will be on the road.

In earthquake engineering, seismic risk was originally defined as the probability that a modified Mercalli intensity or ground motion at a site of interest will exceed a specific level at least once in a given period (Cornell, 1968; Milne and Davenport, 1969), a definition that is analogous to flood and wind risk (Gupta, 1989; Liu, 1991). This definition is based on the assumption that earthquake occurrences follow a Poisson distribution (independent of time and independent of the past history of occurrences or nonoccurrences) (Cornell, 1968; Milne and Davenport, 1969). Although the Poisson model may not be valid for describing earthquake occurrences (Esteva, 1970; Vere-Jones and Ozaki, 1982; Cornell and Winterstein, 1986; Stein and Wysession, 2003), it is the standard model for engineering seismic-risk analysis, as well as for other risk analyses such as for floods and wind (Cornell, 1968; Milne and Davenport, 1969; Gupta, 1989; Liu, 1991; Malhotra, 2006).

According to the Poisson model, the probability of n earthquakes of interest in an area or along a fault occurring during an interval of t years is

$$p(n,t,\tau) = (\tfrac{t}{\tau})^n e^{-\frac{t}{\tau}} / n!, \qquad (3\text{-}1)$$

where τ is the average recurrence interval of earthquakes with magnitudes equal to or greater than a specific size (M). The probability of one or more (at least one) earthquakes with magnitudes equal to or greater than a specific size occurring in t years is

$$p(n \geq 1,t,\tau) = 1 - p(0,t,\tau) = 1 - e^{-\frac{t}{\tau}} \approx \frac{t}{\tau}, \qquad (3\text{-}2)$$

where the Taylor series expansion $e^{t/\tau} \sim 1\text{-}t/\tau$ for $t << \tau$ is used.

Eequation 3-2 determines risk in terms of an earthquake (event) with magnitude *M* or greater. In practice, knowing the consequences of an earthquake (i.e., ground motions or modified Mercalli intensity at a point or in a region of interest is desirable. For example, PGA and response acceleration (S.A.) at a given period are commonly needed for engineering design at a site. This is similar to the situation in flood and wind analyses whereby knowing the consequences of floods and winds, such as peak discharge and 3-s gust wind speed, is desired for a specific site. The ground motions (consequences of an earthquake) and their return periods (i.e., hazard curves) are determined through seismic-hazard analyses (Cornell, 1968; Milne and Davenport, 1969; Stein and others, 2005; Frankel, 2004), PSHA in particular (Frankel and others, 1996, 2002; McGuire, 2004; Malhotra, 2006). For example, for ground motions with 500-, 1,000-, and 2,500-year return periods, equation 3-2 gives exceedance probabilities of about 10, 5, and 2 percent in 50 years, respectively (Frankel and others, 1996, 2002; Malhotra, 2006). Equation 3-2 also gives exceedance probabilities of about 15, 7.5, and 3 percent in 75 years for these ground-motion hazard levels (MCEER, 2001; FHWA, 2006). This example illustrates the relationship between seismic hazard (i.e., ground motion with a return period) and seismic risk (probability of ground motion being exceeded in a period): seismic risk depends not only on seismic hazard, but also on exposure and model (i.e., time-independent [Poisson] or time-dependent) that could be used to describe the occurrences of earthquakes.

Thus, seismic hazard and risk are fundamentally different: seismic hazard describes ground motion and its associated return period, whereas seismic risk describes propability of a ground motion being exceeded in a period. These differences are significant for policy consideration by engineers and decision-makers that can be illustrated by a comparison of seismic hazard and risk between San Francisco, Calif., and Paducah, Ky. (Fig. 3-1 and Table 3-1). As shown in Figure 3-1, San Francisco and Paducah both experienced similar intensity (MMI VII and greater) during the 1906 earthquake and 1811 earthquake, respectively, which suggests that San Francisco and Paducah have similar seismic hazard without consideration of the recurrence intervals. However, the mean recurrence intervals (MRI) for the large earthquakes are quite different, about 100 years in San Francisco and 500 years in Paducah. MRI is also an important parameter for policy consideration. A bridge would likely experience at least one large earthquake over its life of 75 years in San Francisco Bay area, whereas a bridge would unlikely experience one large earthquake over its few life circles in the central United States. With the MRIs, the seismic hazard comparison between San Francisco and Paducah, either earthquake magnitude with an MRI or intensity with an MRI, may not be so traightforward because the mitigation policy is normally made over few years to several decades, but not over huntred to several hundred years (Table 3-1). If occurrence of earthquakes follows the Poisson model, we can calculate seismic risk in terms of magnitude M7.8 or MMI VII and greater over 75 years. The risk comparison (Table 3-1), either M7.8 or MMI VII and greater with a probability in 75 years, is straightforward for engineers and policy-makers. Table 3-1 shows that the differences between seismic hazard and risk in San Francisco and Paducah. Clearly, San Francisco has much higher seismic risk than Paducah. That is why we have to spend more recources and efforts to mitigate seismic hazard in San Francisco than Paducah.

Table 3-1. Seismic hazard and risk comparison between San Francisco and Paducah

	Seismic Hazard	Seismic Risk
San Francisco	1) M7.8 with ~100 years MRI* 2) MMI VII and greater with ~100 years MRI	1) M7.8 with ~53% in 75 years 2) MMI VII and greater with ~53% in 75 years
Paducah	1) M7.7 with ~500 years MRI 2) MMI VII and greater with ~500 years MRI	1) M7.7 with ~14% in 75 years 2) MMI VII and greater with ~14% in 75 years

*MRI: mean recurrence interval

3.3. Probabilistic Seismic Hazard Analysis

The purpose of PSHA is to estimate ground motion hazard using a series of probabilistic computations to combine the uncertainties in earthquake source, occurrence frequency, and ground-motion attenuation relationship. PSHA consists of four basic elements (Reiter, 1990):

(1) Determination of earthquake sources
(2) Determination of earthquake occurrence frequencies—selecting controlling earthquake(s): the maximum magnitude, maximum credible, or maximum considered earthquake
(3) Determination of ground-motion attenuation relationships
(4) Determination of seismic-hazard curves.

Mathematically, PSHA uses a triple integration over earthquake sources, occurrence frequencies, and ground-motion attenuation relationships (Figs. 3-2a through 3-2c):

$$\gamma(y) = \sum_{N} \nu_i \iiint_{M,R,\mathrm{E}} f_M(m) f_R(r) f_{\mathrm{E}}(\varepsilon) P[Y > y | m, r, \varepsilon] dm dr d\varepsilon \ . \qquad (3\text{-}3)$$

The results from PSHA are commonly expressed in a series of curves, *seismic hazard curves*, which compare ground-motion value (peak acceleration, peak velocity, response acceleration, etc.) with the annual probability or return period (reciprocal of annual probability) that the ground motion will be exceeded at a specific site or sites (Fig. 3-2d). Figure 3-3 shows 0.2 s response spectral acceleration hazard curves for seven selected cities in the United States (Leyendecker and others, 2000). The hazard curves provide a range of ground-motion values, from 0.01 to 8.0 g, with corresponding annual frequencies of a ground motion being exceeded (or return period) from 0.1 to 0.00001 (10- to 100,000-year return periods). What level of ground motion or return period should be selected for bridge design from the curves? Currently, three levels of ground motion associated with 500-, 1,000-, and 2,500-year return periods are commonly used. These represent only three specific points on the hazard curves. All other points on the curves would also be equally valid choices. Therefore, in terms of PSHA, the choices of ground motion for bridge design are not one, not two, not three, but infinite (Wang and others, 2003b). This is one of the reasons that the selection of a hazard level is so difficult for engineering design and anlysis. The ground motion with different return periods have been selected or recommended for engineering design of buildings and bridges in the New Madrid Seismic Zone by different communities and organizations. For example, the city of Memphis has

selected the ground motion with a return period of 500 years (Frankel and others, 1996) for building seismic design (i.e., the 2005 MSC Building Code of the 2005 Technical Codes for Mephis and Shelby County, Tennessee), the State of Kentucky has selected the ground motion with a return period of 1,000 years (Frankel and others, 1996) for residential building seismic design (KRC-2002), and the Federal Highway Administration has also selected the ground motion with a return period of 1,000 years (Frankel and others, 1996, 2002) for seismic retrofitting highway structure (FHWA, 2006).

There is confusion on the national seismic hazard maps (Wang and others, 2005). As shown in Figure 3-3, the ground motions with 500-, 1,000-, and 2,500-year return periods have also been equated to those with 10, 5, and 2 percent probabilities of exceedance in 50 years, respectively (Frankel and others, 1996, 2002; Malhotra, 2006). Although the ground motions themselves are the same, the ground motions with 500-, 1,000-, and 2,500-year return periods are fundemantally different from the ground motions with 10, 5, and 2 percent probabilities of exceedance in 50 years: the former are seismic hazard, whereas the later are seismic risk. Therefore, the three maps produced by the U.S. Geological Survey (Frankel and others, 1996, 2002), depicting the ground motions with exceedance probabilities of about 10, 5, and 2 percent in 50 years, are seismic risk maps by definition, not seismic hazard maps. Unfortunetly, these maps have been labeled and used as seismic hazard maps (Frankel and others, 1996, 2002; Frankel, 2004).

3.4. Deterministic Seismic Hazard Analysis

DSHA is another method that has been widely used in seismic-hazard assessment, especially for engineering purposes. DSHA develops a particular seismic scenario upon which a ground-motion hazard evaluation is based. The scenario consists of the postulated occurrence of an earthquake of a specified size at a specified location. DSHA uses four basic elements (Reiter, 1990):

(1) Determination of earthquake sources
(2) Determination of earthquake occurrence frequencies—selecting controlling earthquake(s): the maximum magnitude, maximum credible, or maximum considered earthquake
(3) Determination of ground-motion attenuation relationships
(4) Determination of seismic hazard from a particular scenario.

DSHA determines the ground motion from a single or several earthquakes that have maximum impact. It addresses the ground motion from individual (i.e., maximum magnitude, maximum probable, or maximum credible) earthquakes. Ground motion derived from DSHA represents the ground motion from an individual earthquake.

3.5. PSHA versus DSHA

PSHA and DSHA use the same data sets on earthquake source, occurrence frequency, and ground-motion attenuation relationship, but the results are fundamentally different. PSHA addresses the probability of a level of ground motion being exceeded from all possible earthquakes. Ground motion derived from PSHA does not have a clear physical and statistical meaning (Wang and others, 2003b, 2005; Wang, 2005, 2006; Wang and Ormsbee, 2005). Figure 3-4 shows a hypothetical region with three seismic sources (*A*, *B*, and *C* faults) and a site of interest. It is assumed that only characteristic earthquakes will repeat along the faults in certain periods (recurrence times). The magnitude (M7.5) and recurrence times (*Ta*, *Tb*, and *Tc*) for the characteristic faults are shown in Figure 3-4, and the ground-motion attenuation relationship of Frankel and others (1996) was used. For each characteristic fault, the annual frequency of a particular ground motion being exceeded at the site is equal to the annual recurrence rate (1/T) times the probability that the ground motion will be exceeded. For example, for characteristic fault ***A***, the annual frequency of the peak ground acceleration of 1.11g being exceeded (0.0004 or a return period of 2,500 years) (Fig. 3-5a) is equal to the annual recurrence rate (1/200) times the probability of 0.08 (shaded area under ground-motion density function shown in Figure 3-5b) that the peak ground acceleration of 1.11g will be exceeded. The total hazard (total annual frequency of a ground motion being exceeded) at the site is the sum of the individual hazards (annual frequency of a ground motion being exceeded) (Fig. 3-5). The total annual frequency of a ground motion being exceeded, of 0.0004 (return period of 2,500 years), is the sum of the individual annual frequencies of 0.00025, 0.0001, and 0.00005 from faults ***A***, ***B***, and ***C***, respectively (Fig. 3-6). The total annual is not associated with any individual earthquake, but with three earthquakes. In contrast to the complicated PSHA, DSHA is straightforward and simple for this example. The median ground motion is 0.5g PGA and median plus a standard deviation is 1.06g PGA. This ground motion represents a scenario earthquake with a magnitude of M7.5 occurring at a distance of 30 km.

In a typical PSHA, the annual frequency of a ground motion being exceeded (total hazard) is contributed by many earthquakes. For example, the 1996 USGS national seismic hazard maps show that the total hazard in Chicago, Ill., is contributed by a series of earthquakes with magnitudes ranging from M5.0 to M8.0 at distances from 0 to 500 km (Harmsen and others, 1999). It is hard to imagine the actual physical model (i.e., a real earthquake) with ground motion that is composed of so many earthquakes. This is one of the disadvantages of PSHA recognized by a panel of scientists (National Research Council, 1988). It is well understood that there is an uncertainty in seismic-hazard assessment because of the uncertainties inherent in the parameters used in the hazard analysis. No matter which method is applied, PSHA or DSHA, the results always contain an uncertainty. The biggest advantage of PSHA, it is claimed, is that it could incorporate a range of uncertainties inherent in earthquake source, occurrence frequency, and ground-motion attenuation relationships. However, recent studies (Wang and others, 2003, 2005; Wang, 2005; Wang and Ormsbee, 2005) showed that PSHA inherences some intrinsic drawbacks, including (1) unclear physical basis; (2) obscure uncertainty; and (3) difficulty in determining a correct choice.

As demonstrated in previous sections, the return period (reciprocal of the annual probability) derived from PSHA is interpreted as the mean (average) time between occurrences of a certain ground motion at a site (McGuire, 2004) and used in seismic risk calculation, Equation 3-2. It has been shown that the return period is different from the recurrence interval of earthquake (Wang and others, 2003, 2005; Wang, 2005; Wang and Ormsbee, 2005, Malhotra, 2005, 2006). Actually, the return period is not a temporal measurement of a ground motion at a site, but a mathematical extrapolation of the recurrence interval of earthquake (temporal measurement) and the ground motion uncertainty (a spatial measurement) (Wang and others, 2003, 2005; Wang, 2005; Wang and Ormsbee, 2005). Use of the return period in seismic risk analysis may be not appropriate (Wang and Ormsbee, 2005).

On the other hand, DSHA, it is claimed, cannot incorporate the range of uncertainties inherent in earthquake source, occurrence frequency, and ground-motion attenuation relationships. The advantage of DSHA is that it provides seismic-hazard estimate, ground motion and recurrence interval, from each individual earthquake that has the most significant impact on a site. This advantage is important because seismic hazard derived from DSHA has a clear physical and statistical meaning. The recurrence interval of a ground motion derived from DSHA is a temporal measure and can be used in seismic risk analysis. As shown by Wang and others (2005), a single characteristic earthquake of M7.7 with a 500-year recurrence interval in the New Madrid Seismic Zone could generates a median ground motion of about 0.3g PGA in Paducah. Because ground motion is a consequence of an earthquake, the median ground motion in Paducah also has a recurrence interval of 500 years. Therefore, estimated hazard from the New Madrid characteristic earthquake will be about 0.3g PGA (median) with a 500-year return period in Paducah. In terms of ground motion, estimated risk is about 10 percent probability that a median PGA of 0.3g could be exceeded in 50 years (Table 3-1).

The engineering seismic designs and standards used in the United States, as well as throughout the world, are based on California. The ground motion specified for bridge design in California is the deterministic ground motion from the maximum credible earthquake (Caltrans, 1999). Also, the ground motion from the maximum considered earthquake ground motion was recommended for building seismic design in California (BSSC, 1998; ICC, 2000). In California, DSHA, not PSHA, is being used to develop the design ground motion. The purpose of this project is to develop ground motions, including peak values and time histories, for seismic analysis and design of highway bridges in Kentucky. We have used DSHA for this project because it is more appropriate.

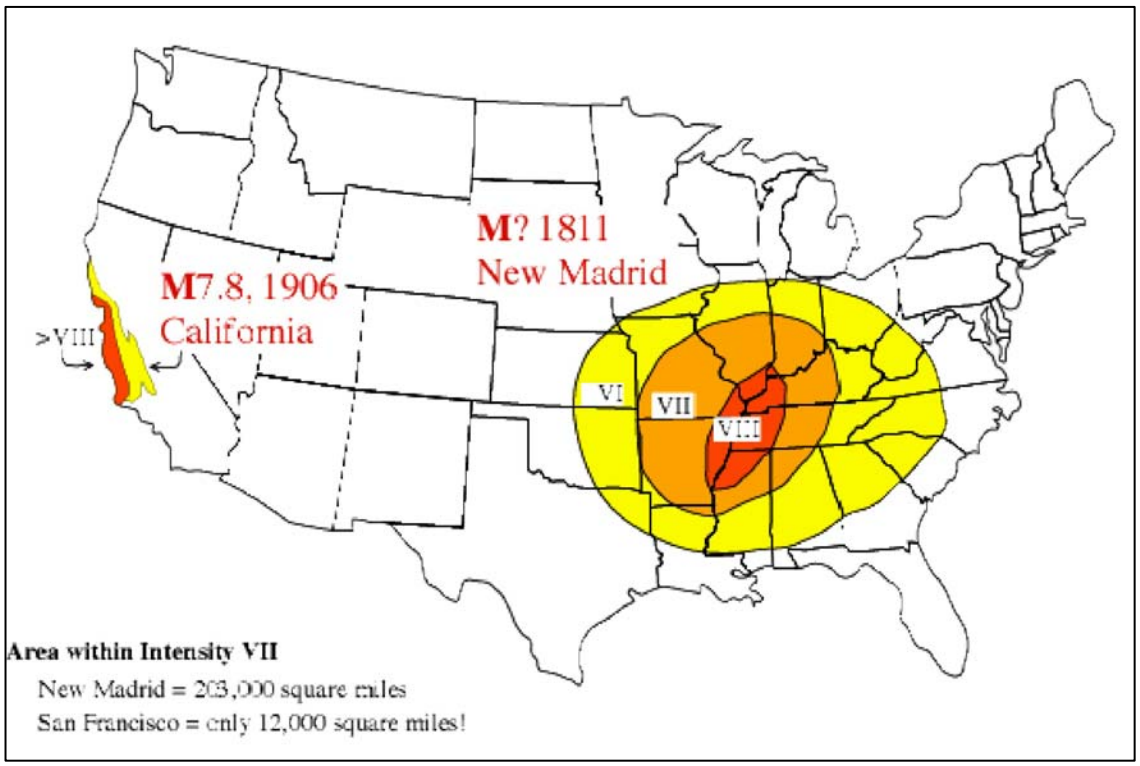

Figure 3-1. Areas affected by the 1906 San Francisco and the 1811 New Madrid earthquakes

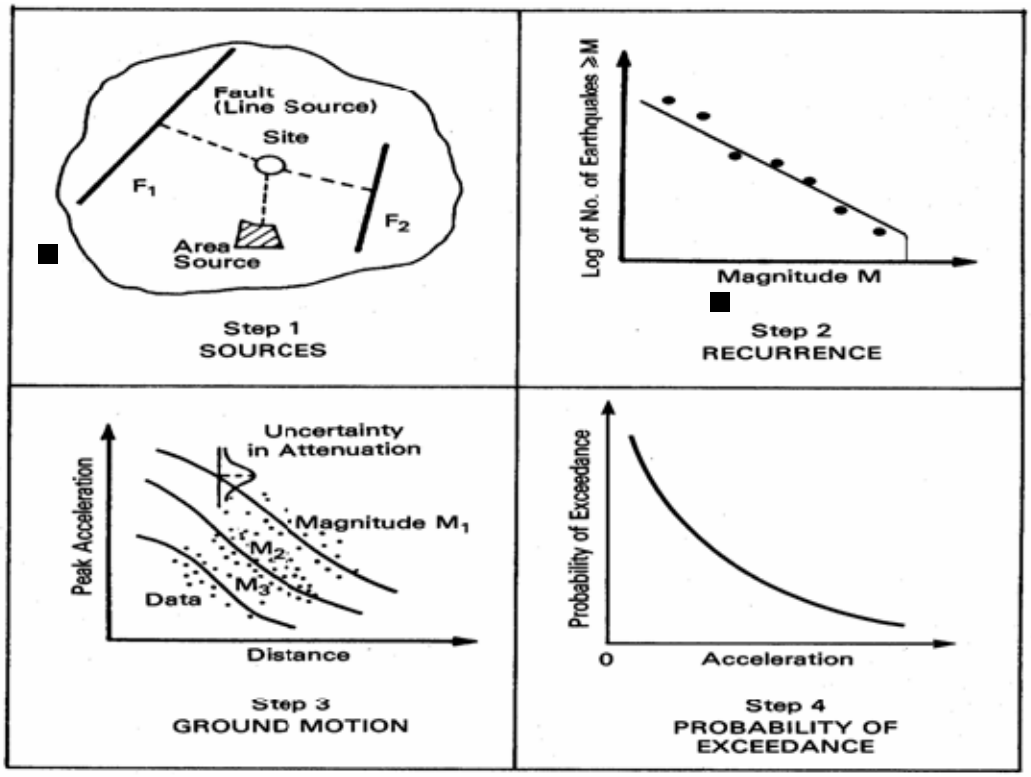

Figure 3-2. Steps involved in PSHA (Reiter, 1990)

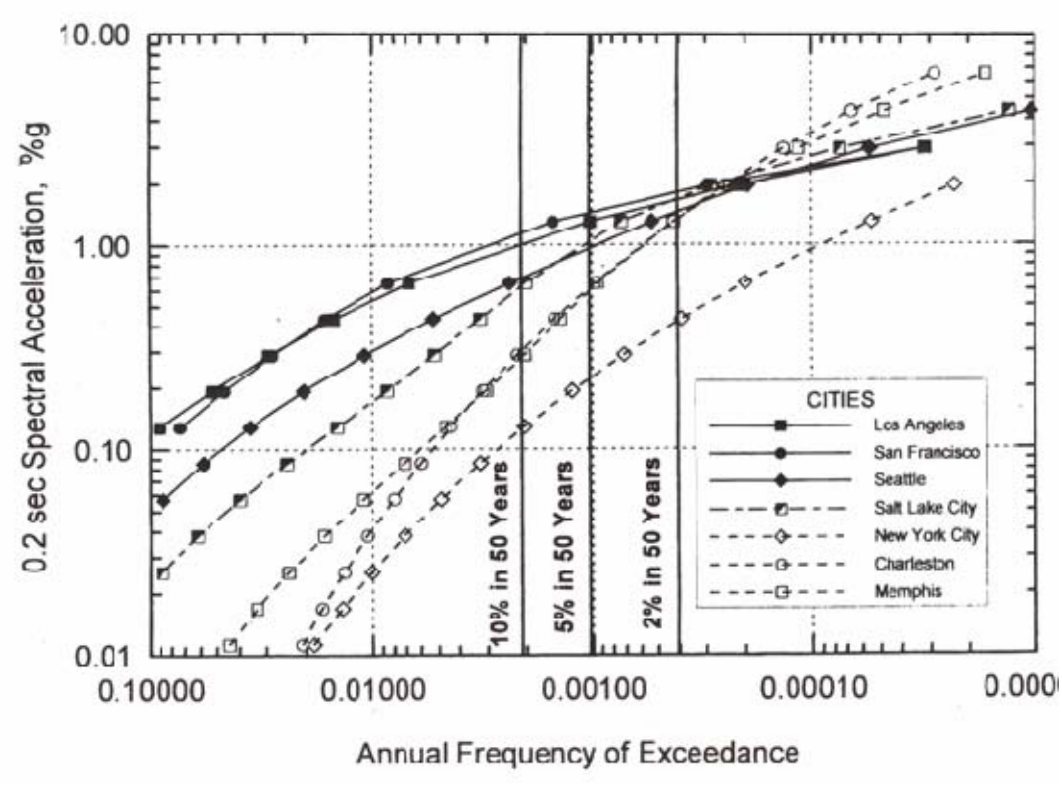

Figure 3-3. Hazard curves for selected cities (Leyendecker and others, 2000)

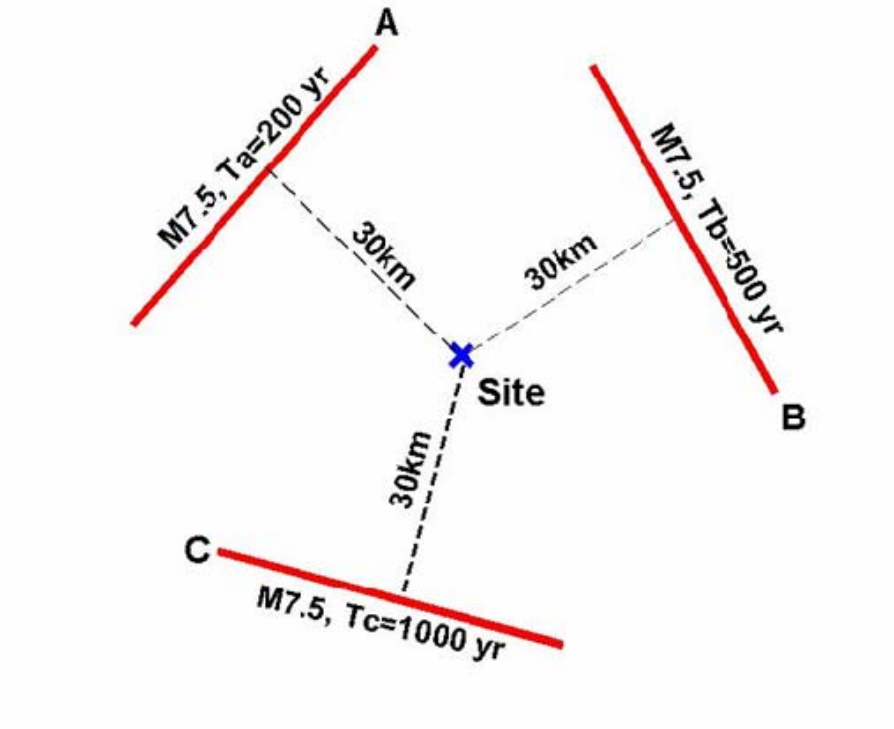

Figure 3-4. Hypothetical region with three seismic sources (A, B, and C faults) and a site of interest within 30 km of the faults

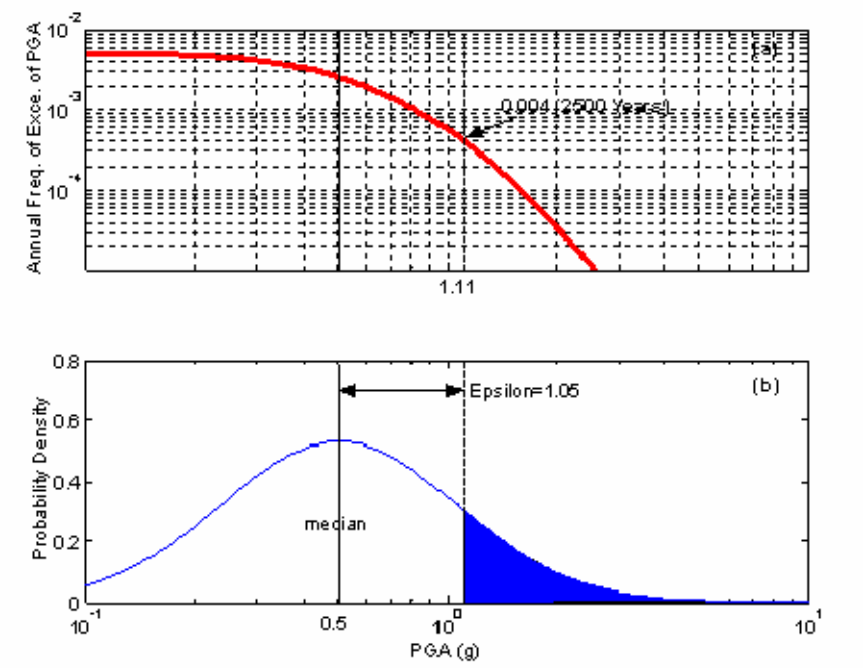

Figure 3-5. (a) Hazard curve for fault A and (b) ground-motion density function (log-normal) for the M7.5 characteristic earthquake with recurrence interval of 200 years. The median ground motion is 0.5g and the standard deviation is 0.75

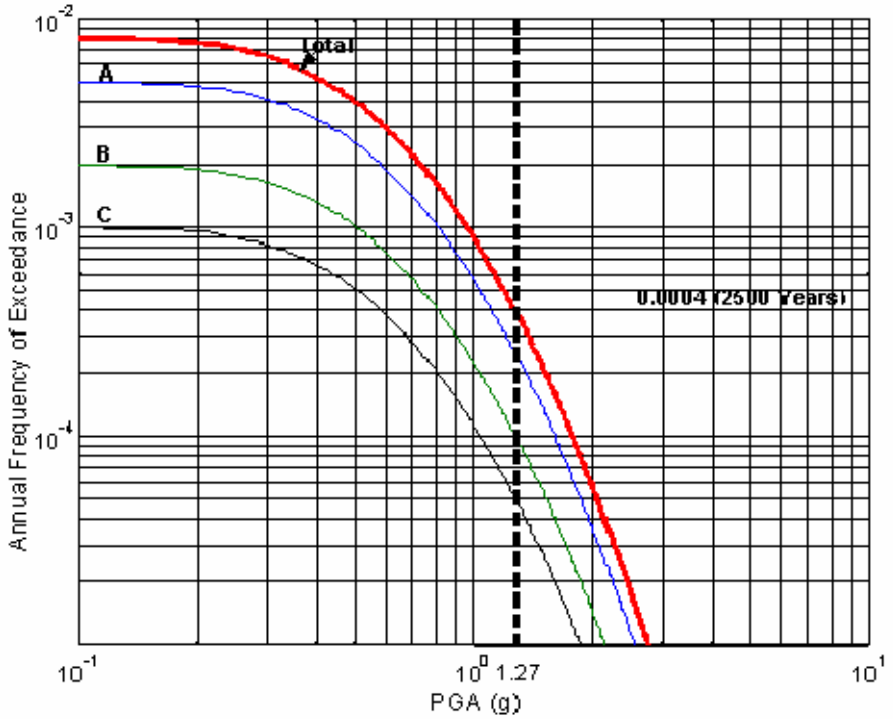

Figure 3-6. Total and individual hazards (annual probabilities of a ground motion being exceeded) at the site

4. SEISMIC SOURCE ZONE

4.1. Introduction

Two hypotheses have been proposed to explain intraplate seismicity: (a) selective reactivation of preexisting faults by local variations in pore pressure, fault friction, or strain localization along favorably orientated lower-crustal ductile shear zones formed during earlier deformation (Zoback and others, 1985) and (b) local stress perturbations that may produce events incompatible with the regional stress field (Zoback and others, 1987). In the central and eastern United States the regional stress field is reasonably well known from well-constrained focal mechanisms (see Herrmann and Ammon, 1997), yet the link between the stress field and the contemporary seismicity remains enigmatic.

Frankel (1995) concluded that historical seismicity could be used to calculate the probabilistic seismic hazard in the central and eastern United States without reference to geology, and thereby avoided the issue of our generally poor knowledge of how the stress field, geology, and seismogenesis are linked. Kafka and Walcott (1998) and Kafka and Levin (1999) arrived at approximately the same conclusion. They used small earthquakes in various locations, including the New Madrid Seismic Zone and the northeastern United States, to test how well the spatial distribution of smaller earthquakes ($2 < m_{b,Lg} < 4$) could be used to forecast the locations of larger earthquakes ($> 4\ m_{b,Lg}$) that have already occurred. They concluded that, on average, larger earthquakes occurred in the vicinity of smaller earthquakes more frequently than would be expected for a random distribution of large earthquakes. They also noted that there were a significant number of large earthquakes that would not have been forecasted based on the distribution of the small earthquakes, but they concluded that many of the missed events were probably the result of incompleteness in the earthquake catalogs. The Sharpsburg, Ky., earthquake of July 27, 1980, might be an example of such an event. It occurred in an area where the earthquake catalogs indicated sparse seismicity, but modern instrumentation installed in the general vicinity of the epicenter of the earthquake after its occurrence suggests that there are more earthquakes in the area then has been generally known (i.e., the earthquake catalog for the area is incomplete).

Seismic source zones considered in this study are those suggested by Bollinger and others (1992), those used by the U.S. Geological Survey in developing the 1996 national seismic-hazard maps (Wheeler and Frankel, 2000), and those suggested by Wheeler and Cramer (2002) for use in the 2002 national seismic-hazard maps. For the purposes of this study, seismic zones based primarily on the historical distribution of earthquakes (Fig. 4-1) were given the most weight, which is in agreement with the studies by Frankel (1995), Kafka and Walcott (1998), and Kafka and Levin (1999).

In this section, the historical maximum magnitude event, focal depths, and type of faulting, if known, are described for the various seismic zones. The rates of seismicity for seismic zones and suggested maximum magnitude earthquakes are presented separately for comparative purposes.

4.2. New Madrid Seismic Zone

The Reelfoot Rift (Fig. 4-2) is the host geologic and tectonic crustal structure for the New Madrid Seismic Zone. The New Madrid Seismic Zone is a tightly clustered pattern of earthquake epicenters that extends from northeastern Arkansas into northwestern Tennessee and southeastern Missouri (Fig. 4-2). Earthquakes along the northeast-trending alignment of the seismic zone in northeastern Arkansas and earthquakes in southeastern Missouri between New Madrid and Charleston, are predominantly right-lateral strike-slip events; whereas earthquakes along the northwest trend of seismicity extending from near Dyersburg, Tenn., to New Madrid, Mo., are predominantly dip-slip events. Focal depths of the earthquakes in the New Madrid Seismic Zone typically range between 5 and 15 km (Chiu and others, 1992).

The northeastern extent of the Reelfoot Rift and, consequently, the northeastern terminus of the New Madrid Seismic Zone are controversial. Wheeler (1997) suggested there are two diffused alignments of northeast-trending seismicity that extend from near New Madrid into western Kentucky and along the Kentucky-Illinois border (Fig. 4-3). He referred to these alignments as trends 1 and 2, and noted that the historical seismicity apparently terminates along the Ohio River near Olmsted, Ill., and Paducah, Ky., respectively. Wheeler (1997) noted that the apparent termination of the seismicity is consistent with the geologic criteria he used to delineate the northeastern extent of the Reelfoot Rift (i.e., the seismicity should terminate either at or southwest of the estimated northeastern boundary of the Reelfoot Rift), based on his examination of (1) the ends of and bends in major faults in the area, (2) the border faults of the Reelfoot Rift and the Rough Creek Graben, and (3) the northeastern limit of the ultramafic rocks in the Reelfoot Rift.

Whether the seismicity in the Jackson Purchase Region of western Kentucky is directly related to the New Madrid Seismic Zone is unclear. The seismicity in the Jackson Purchase Region, like other seismicity outside the primary cluster of earthquakes in the New Madrid Seismic Zone (Fig. 4-2), might be what Bollinger and others (1992) referred to as “off-zone” activity resulting from spatial stress perturbations. Seismicity in the Jackson Purchase Region is not well located because of the lack of instrumentation in the area; epicentral locations could be off by several kilometers, and focal depths are very poorly constrained. A temporary seismic network was deployed in the Jackson Purchase in late 2002. Figure 4-4 shows locations and intensities of earthquakes between January and June 2003. Only one earthquake, the June 6, 2003, Bardwell earthquake (M4.0), has occurred in the area since January 2003 (Wang and others, 2003a). The focal depth of this earthquake was only about 2.5 km, much shallower than those in the central New Madrid Seismic Zone; it is in stark contrast to the 23.7 km focal depth of the April 30, 2003, Blythville, Ark., earthquake. These better-located earthquakes suggest that the active faults of the New Madrid Seismic Zone may not extend into the Jackson Purchase Region. The boundary of the New Madrid Seismic Zone recommended in this study is shown Figure 4-5.

4.3. Wabash Valley Seismic Zone

Nuttli and Herrmann (1978) first proposed the seismic zone on the basis of (1) the number of earthquakes, (2) the occurrence of five ≥ 5 $m_{b,Lg}$ earthquakes in the seismic zone between 1875 and 1975, and (3) the presence of the Wabash Valley Fault Zone. The boundaries of the Wabash Valley Seismic Zone, as drawn by Wheeler and Frankel (2000), are shown in Figure 4-6. Also included in the figure are the epicentral locations of the damaging (MMI ≥ VI) earthquakes in the seismic zone (Stover and Coffman, 1993) and the location of the 5.1 $m_{b,Lg}$ September 27, 1909, earthquake that occurred just north of the seismic zone. Dates, times, and epicentral locations of the damaging earthquakes shown in Figure 4-6 are listed in Table 4-1. Unlike the seismicity in the New Madrid Seismic Zone, which is well defined, seismicity in the Wabash Valley Seismic Zone is diffused over a broad area.

Despite the number of damaging earthquakes in the Wabash Valley Seismic Zone, the number of permanent seismograph stations in the seismic zone is inadequate to derive well-constrained focal depths or focal mechanisms. Of the 18 events listed in Table 4-1, the only ones for which well-determined focal depths and focal mechanisms have been estimated are events 15 through 18. These four earthquakes were large enough to generate sufficient surface-wave data so that their focal depths and focal mechanisms could be estimated using the radiation pattern of their Rayleigh and Love waves (Herrmann and Ammon, 1997).

Table 4-1. Damaging earthquakes in the Wabash Valley Seismic Zone

Event No.	Date (Mo-Day-Yr)	Time (GMT)	Lat./Long. (°N/°W)		Magnitude $m_{b,Lg}$[1]		M_w[2]	Depth[3] (km)
1.	July 5, 1827		38.0/87.5	4.8	4.4			
2.	Aug. 7, 1827	4:30	38.0/88.0	4.8	4.4			
3.	Aug. 7, 1827	7:00	38.0/88.0	4.7	4.3			
4.	Sep. 25, 1876	6:00	38.5/87.8	4.5	4.1			
5.	Sep. 25, 1876	6:15	38.5/87.8	4.8	4.4			
6.	Feb. 6, 1887	22:15	38.7/87.5		4.6	4.2		
7.	July 27, 1891	2:28	37.9/87.5	4.1	3.7			
8.	Sep. 27, 1891	4:55	38.25/88.5	5.5	5.3			
9.	Apr. 30, 1899	2:05	38.5/87.4	4.9	4.6			
10.	Sep. 27, 1909	9:45	39.8/87.2	5.1	4.8			
11.	Nov. 27, 1922	3:31	37.8/88.5	4.8	4.4			
12.	Apr. 27, 1925	4:05	38.2/87.8	4.8	4.4			
13.	Sep. 2, 1925	11:56	37.8/87.5		4.6	4.2		
14.	Nov. 8, 1958	2:41	38.44/88.01		4.4	4.0		
15.	Nov. 9, 1968	17:01	37.91/88.37			5.5	5.3	22
16.	Apr. 3, 1974	23:05	38.55/88.07			4.5	4.3	14
17.	June 10, 1987	23:48	38.71/87.95			5.1	5.0	10
18.	June 18, 2002	18:37	37.98/87.78			4.9	4.5	17-19

1. Magnitudes ($m_{b,Lg}$) are from Stover and Coffman (1993) except for those for events 8 and 15. Street (1980) gave a magnitude range of 5.5 to 5.8 $m_{b,Lg}$ for the September 27, 1891, event, based on an analysis of all the MM intensity data, whereas Stover and Coffman's (1993) $m_{b,Lg}$ of 5.2 is based solely upon the felt area. The 5.5 $m_{b,Lg}$ for event 17, the November 9, 1968, southern Illinois event, is more generally accepted than the 5.3 $m_{b,Lg}$ given by Stover and Coffman (1993). The $m_{b,Lg}$ magnitude, seismic moment, and epicentral location for event 18 are preliminary estimates based on data from the University of Kentucky Seismic and Strong-Motion Network and a personal communication from R. Herrmann at St. Louis University.

2. Except for events 15, 16, and 17, moment magnitudes (M_w) were derived using the m_b to seismic moment (M_o) to moment magnitude conversion outlined in Appendix A. Moment magnitudes for events 17, 18, and 19 were calculated using the seismic moments given in Herrmann and Ammon (1997).

3. Focal depths are from Herrmann and Ammon (1997), except for the depth for event 18, which is based on a personnel communication from R.B. Herrmann of at St. Louis University.

The largest instrumentally recorded historical earthquake in the Wabash Valley Seismic Zone is the November 9, 1968, earthquake (event 15 in Table 4-1). McBride and others (2002) believed that this earthquake occurred as a result of the reactivation of a fault plane within a series of moderately dipping lower crustal reflectors that are decoupled from the overlying Paleozoic structure. The June 18, 2002, Darmstadt, Ind., earthquake (M4.6) was also well located (Table 4-1). Kim (2003) believed that the June 18, 2002, earthquake occurred as a result of the reactivation of a fault within the Wabash Valley Fault System (Fig. 4-7).

The Wabash Valley Fault System illustrated in Figure 4-7 is a series of north-northeast-trending normal faults with right-lateral offsets across the Herald-Phillipstown and New Harmony Faults. The locations and extent of faulting are well known from the extensive set of drill logs and seismic-reflection lines acquired for oil and gas exploration. Between the Albion-Ridgway and New Harmony Faults is the Grayville Graben (Fig. 4-8), so named by Sexton and others (1996) and shown by Bear and others (1997) to exhibit Cambrian extensional slip. Based on Bear and others' (1997) interpretation of the fault movement, Wheeler and Cramer (2002) identified the Grayville Graben as Iapetan. They all but dismissed the graben and the Wabash Valley Fault System as being seismogenic.

Recently, however, Woolery (2005) acquired several kilometers of shallow SH-wave CDP seismic data along an east–west line just south of, but paralleling, the line labeled "Rene 1995" in Figure 4-7. Based on the seismic data, borehole logs, and radiocarbon dating, Woolery (2005) concluded that movement has occurred along the Wabash Island and Hovey Lake Faults (Fig. 4-7) as recently as 40,000 years ago. The possibility that the Wabash Valley faults are seismogenic is also supported by the occurrence of the June 18, 2002, earthquake (Table 4-1). The epicentral location of the event is superimposed on Figure 4-7.

4.4. Eastern Tennessee Seismic Zone

In the central and eastern United States, the Eastern Tennessee Seismic Zone (Fig. 4-9) releases seismic moment at a volume-normalized rate second only to that of the New Madrid Seismic Zone (Powell and others, 1994). The largest earthquake known to have occurred in the seismic zone is the 4.6 $m_{b,Lg}$ event of November 30, 1973, which was centered near Maryville, Tenn. Figure 4-10 is an isoseismal map of the event.

The Eastern Tennessee Seismic Zone is what Wheeler and Frankel (2000) referred to as a seismicity source zone: a cluster of epicenters in which the boundaries of the zone are drawn without reference to the geology. Although the factors responsible for the seismicity in the Eastern Tennessee Seismic Zone are poorly understood, the seismicity seems to be associated in some fashion with the New York–Alabama Magnetic Lineament (Fig. 4-11). The lineament marks a near-vertical boundary between blocks of high- and low-velocity crust, as well as the boundary between areas of relatively high seismicity to the east and low seismicity to the west (Powell and others, 1994; Chapman and others, 1997). The New York–Alabama Magnetic

Lineament is the western boundary of a 300-km-long and 30-km-wide zone that is the source of most of the earthquakes in the seismic zone.

Seismicity in the Eastern Tennessee Seismic Zone typically occurs at a depth of 4 to 22 km and exhibits strike-slip movement involving right-lateral motion along north–northeast-trending faults, or left-lateral motion along east-southeast-trending faults (Johnston and others, 1985; Chapman and others, 1997). A statistical analysis of the spatial distribution of the epicenters of the earthquakes in the Eastern Tennessee Seismic Zone shows that they tend to line up in preferred southwest–northeast directions, which is consistent with the orientations of most focal-mechanism solutions in the seismic zone (Chapman and others, 1997; Hawman and others, 2001). The southwest–northeast trends are interpreted as suggesting a left-stepping pattern of earthquakes that is consistent with what would be expected from wrenching associated with right-lateral strike-slip motion (Hawman and others, 2001).

4.5. Giles County Seismic Zone

The Giles County Seismic Zone (Fig. 4-12) is not included in the U.S. Geological Survey's 1996 or 2002 national seismic-hazard maps because of the lack of seismic activity and the belief that this seismic zone is incapable of producing an earthquake as big as what the U.S. Geological Survey used as their background maximum magnitude earthquake. Nonetheless, the Giles County Seismic Zone has produced one of the larger-magnitude earthquakes in the central or eastern United States in historical times: the Giles County, Va., earthquake of May 31, 1897. It was an MMI VII–VIII event, which was felt from northern Ohio to central Georgia, and from western Kentucky to the Atlantic Coast, as shown in Figure 4-13. Street (1979) estimated its $m_{b,Lg}$ as 5¾(±¼). Bollinger and Wheeler (1983) and Bollinger and others (1992) described the seismogenic zone as an upper crustal feature that strikes northeast–southwest, dips nearly vertically, is 5 to 15 km deep, and has a horizontal extent of approximately 20 to 30 km. Based on a variety of criteria, Bollinger and others (1992) estimated a maximum magnitude earthquake of 6.3 $m_{b,Lg}$ for the seismic zone. Based on equation 2-5 and Bollinger and others' (1992) $m_{b,Lg}$ estimate, the maximum magnitude earthquake for the Giles County Seismic Zone is M6.3.

4.6. The Rough Creek Graben and Rome Trough in Kentucky

In order to account for uncertainty and to obtain a minimum seismic-hazard level, a background earthquake is commonly used in seismic-hazard analyses. Large background earthquakes (M6.5) were used in the 1996 USGS hazard maps; even larger background earthquakes (M7.5) were used for the Rough Creek Graben and Rome Trough in the 2002 USGS hazard maps (Figs. 4-14 and 4-15). In PSHA, the background earthquakes do not contribute to the total hazard calculation because of (1) a large-area source zone and (2) a longer recurrence interval (several thousand years). But if the large earthquakes are possible, they need to be reflected on the hazard maps. For example, the background earthquake of M7.5 was used for the Rough Creek Graben and Rome Trough in Kentucky, but the hazard maps do not include any contribution from the background earthquakes. Use of the large background earthquakes in the NEHRP hazard mapping in the central United States is not necessary, but could cause confusion.

No paleoseismological evidence or historical seismicity supports a suggestion that the Rough Creek Graben and Rome Trough are currently seismogenic. In fact, as noted by Street and others (2002), the Rough Creek Graben and Rome Trough are among the most seismically inactive areas in Kentucky. Based on the lack of paleoseismic and historical activity, as well as the findings of Kafka and Walcott (1998) and Kafka and Levin (1999), the rate of seismicity and maximum magnitude earthquake for the Rough Creek Graben and Rome Trough in this report will be assumed to be the same as that recommended for elsewhere in Kentucky for the background seismicity.

4.7. Background or Local Seismicity in Kentucky

Earthquakes have occurred throughout Kentucky, many of them not associated with any known seismic zone or geologic/tectonic feature. For example, the February 28, 1854, earthquake (M3.6 or $m_{b,Lg}$ 4.0) in central Kentucky is not associated with any known seismic zone. Many of these earthquakes have been recorded by the University of Kentucky Seismic and Strong-Motion Network since 1984 (Street and others, 2002), and are defined as background seismicity. In this study, an event of M4.1 ($m_{b,Lg}$ 4.5) is assumed to be the background earthquake that could occur anywhere in Kentucky, with the exception of the 28 counties highlighted on Figure 4-16. This background seismicity was used in the KTC-96-4 report and maps (Street and others, 1996).

4.7.1. Northeastern Kentucky

The largest historical earthquake in northeastern Kentucky is the M4.9 ($m_{b,Lg}$ 5.2) event on July 27, 1980, near Sharpsburg. The isoseismal for the earthquake is shown in Figure 4-17. The earthquake had a maximum MMI of VII and caused about $4 million in damage in Bath, Bourbon, Fleming, Mason, Montgomery, Nicholas, and Rowan Counties (Street, 1982). On September 7, 1988, an M4.2 ($m_{b,Lg}$ 4.6) earthquake occurred 11 km southeast of the 1980 event (Street and others, 1993). Several other minor earthquakes are also known to have occurred in northeastern Kentucky and the adjacent areas of Ohio and West Virginia (Street and others, 1993). Because of this slightly higher seismicity, an expected earthquake (EE) of M5.0 ($m_{b,Lg}$ 5.3) is used as the background or local earthquake that can be assumed to occur any time in Bath, Bracken, Boyd, Carter, Fleming, Greenup, Lewis, Mason, Menifee, Montgomery, Nicholas, Robertson, and Rowan Counties of northeastern Kentucky (Fig. 4-16). For the probable earthquake (PE) and the maximum credible earthquake (MCE) an M5.3 ($m_{b,Lg}$ 5.5) and M5.5 ($m_{b,Lg}$ 5.7) are assumed, respectively.

4.7.2. Southeastern Kentucky

Minor to moderate earthquakes have periodically occurred in Bell, Harlan, Knox, Letcher, and Whitley Counties in southeastern Kentucky (Fig. 4-16). The largest one is the M3.9 ($m_{b,Lg}$ 4.3) event near Middlesboro in 1954 (Stover and Coffman, 1993). Other earthquakes include an

M3.6 ($m_{b,Lg}$ 4.0) event near Barbourville in 1976, an M2.8 ($m_{b,Lg}$ 3.1) event in Bell County on August 28, 1983, and an M3.2 ($m_{b,Lg}$ 3.6) event in Harlan County on August 28, 1990. We recommend an event of M4.3 ($m_{b,Lg}$ 4.7) as the maximum background or local earthquake that could occur in these counties at any time. Consequently, the M4.3 earthquake is selected for the expected earthquake (EE), the probable earthquake (PE), and the maximum credible earthquake (MCE).

4.7.3. Western Kentucky

The maximum magnitude of the background or local earthquake in Ballard, Carlisle, Fulton, Graves, Hickman, Livingston, Marshall, and McCracken Counties in western Kentucky is M5.0 ($m_{b,Lg}$ 5.3). This magnitude is based on the counties' proximity to the New Madrid Seismic Zone, moderate historical events, and occasional events in the counties that have been recorded by the University of Kentucky Seismic and Strong-Motion Network, such as the June 6, 2003, Bardwell earthquake (Wang and others, 2003a). Within the eight counties, many earthquakes measuring M2.7 ($m_{b,Lg}$ 3.0) or larger have been recorded, such as the June 6, 2003, Bardwell earthquake (M4.0), which caused some damage.

The largest earthquake to occur in the Henderson area is the M4.2 ($m_{b,Lg}$ 4.6) event on September 2, 1925. Earthquakes near Henderson are generally accepted as being associated with the other seismicity in the Wabash Valley area, which was discussed in section 3.1.2. The maximum magnitude of M5.0 ($m_{b,Lg}$ 5.3) is used for the background or local earthquake in the Henderson area (Fig. 4-16) for the expected earthquake (EE), the probable earthquake (PE) and the maximum credible earthquake (MCE).

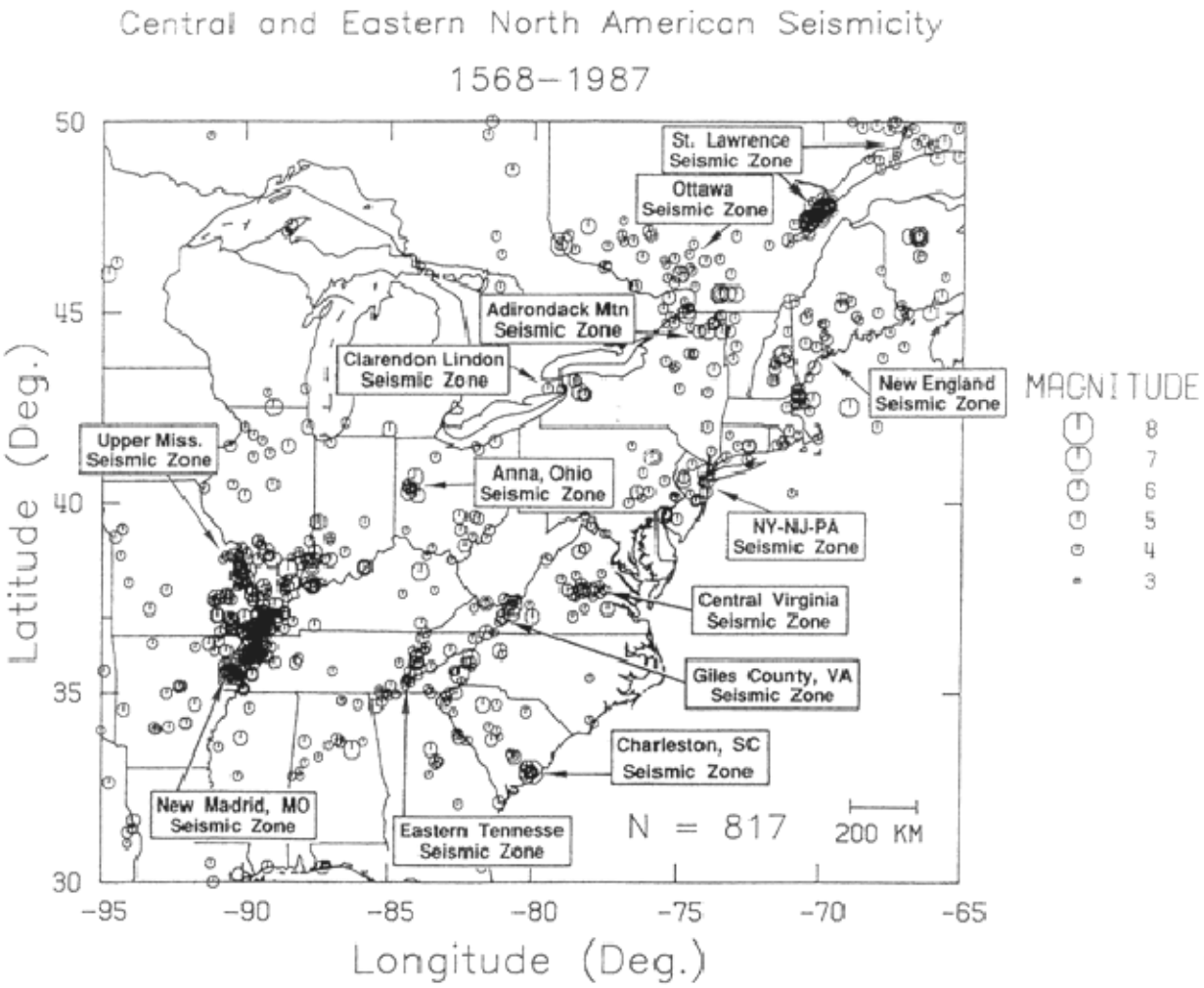

Figure 4-1. Historical seismicity in the central United States

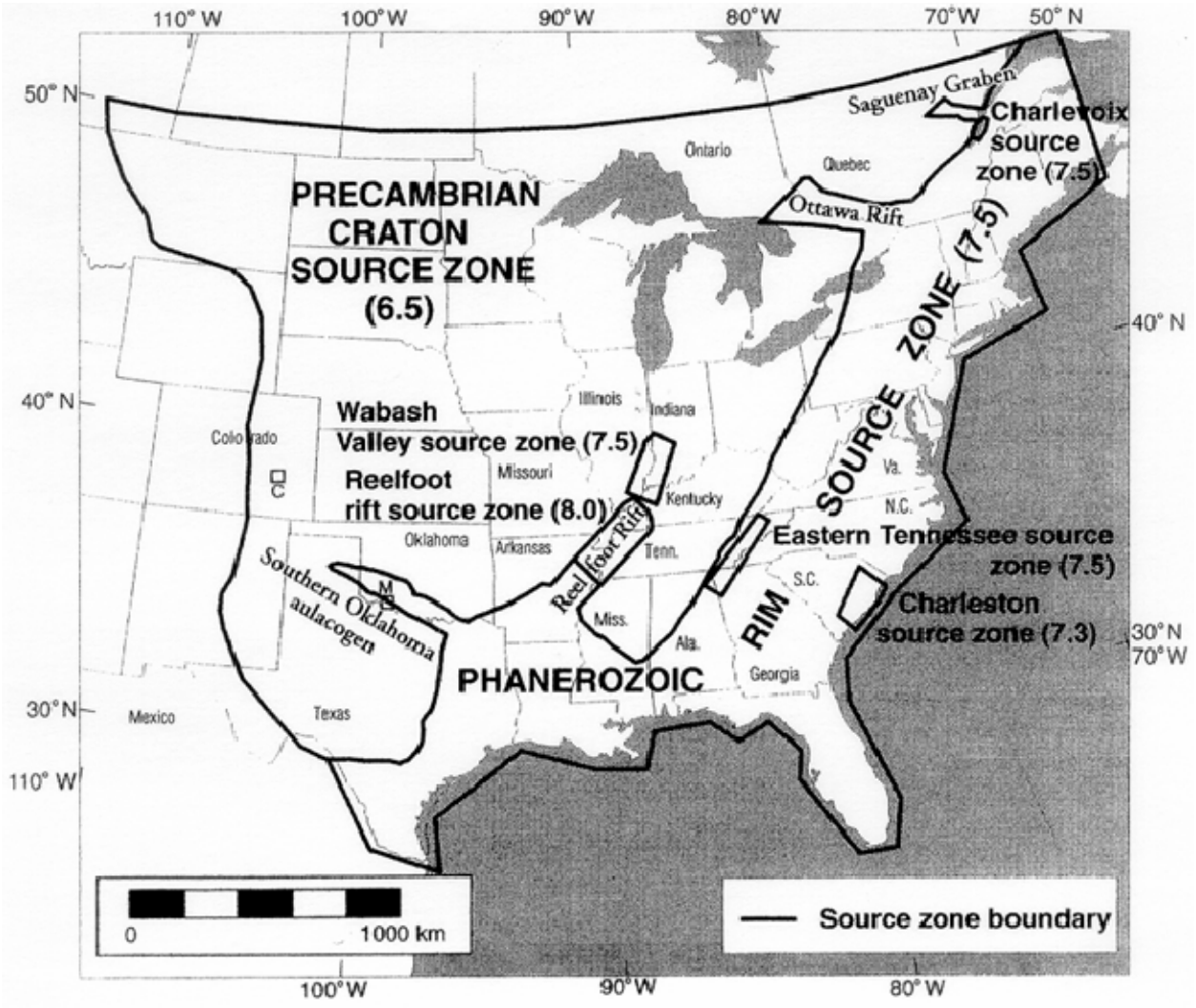

Figure 4-2. Reelfoot Rift and tectonic settings in the central United States (Wheeler and Cramer, 2002)

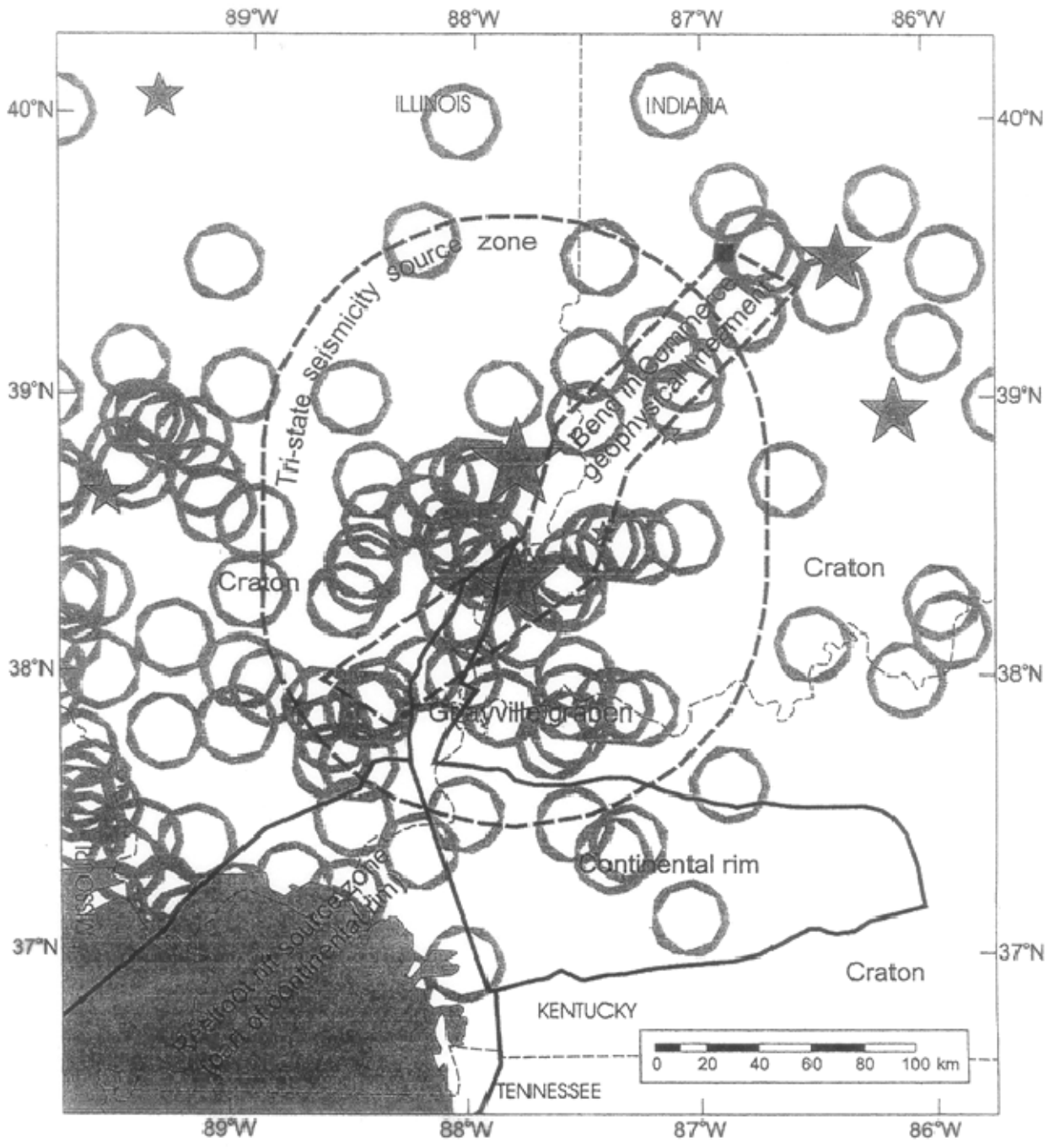

Figure 4-3. Seismicity in the tri-state area of Illinois, Indiana, and Kentucky (Wheeler and Cramer, 2002)

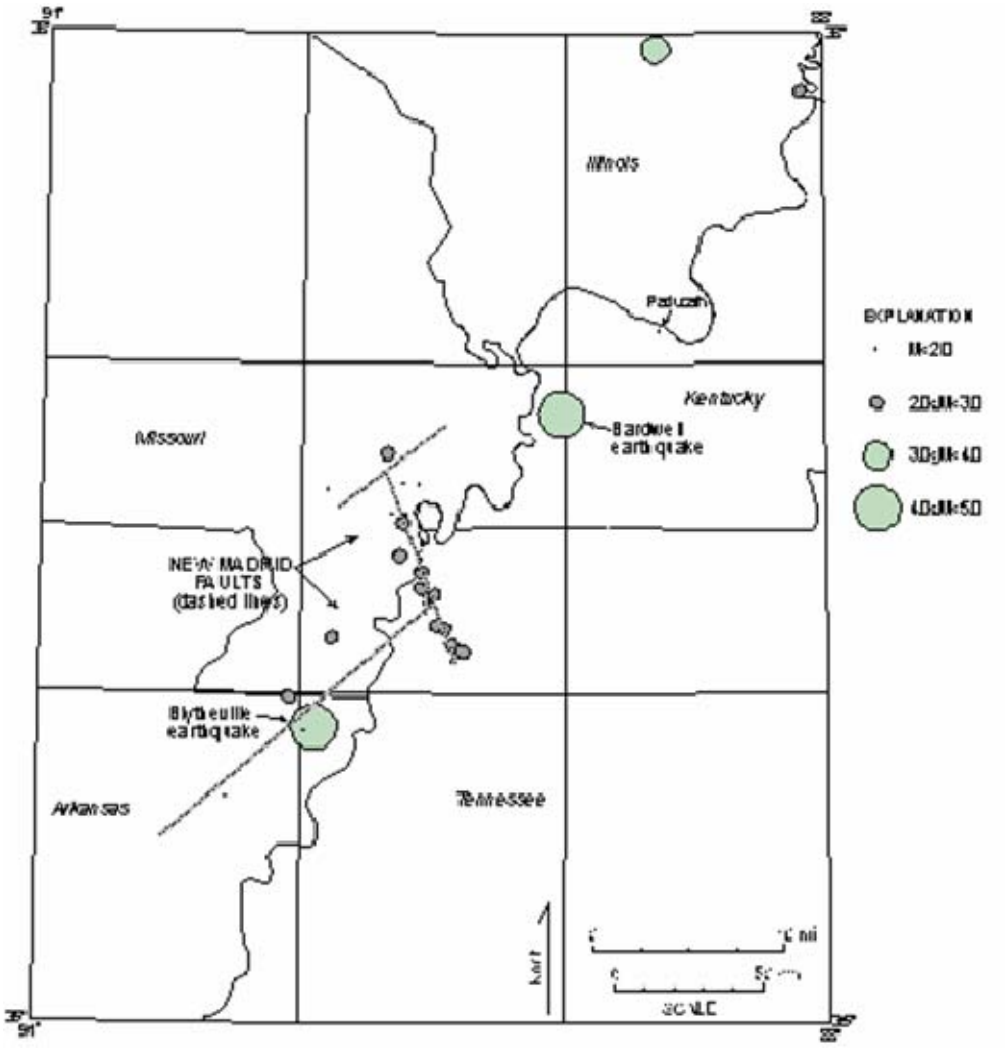

Figure 4-4. Locations of earthquakes in the New Madrid Seismic Zone between January and June 2003 (from the Center for Earthquake Research and Institute, University of Memphis)

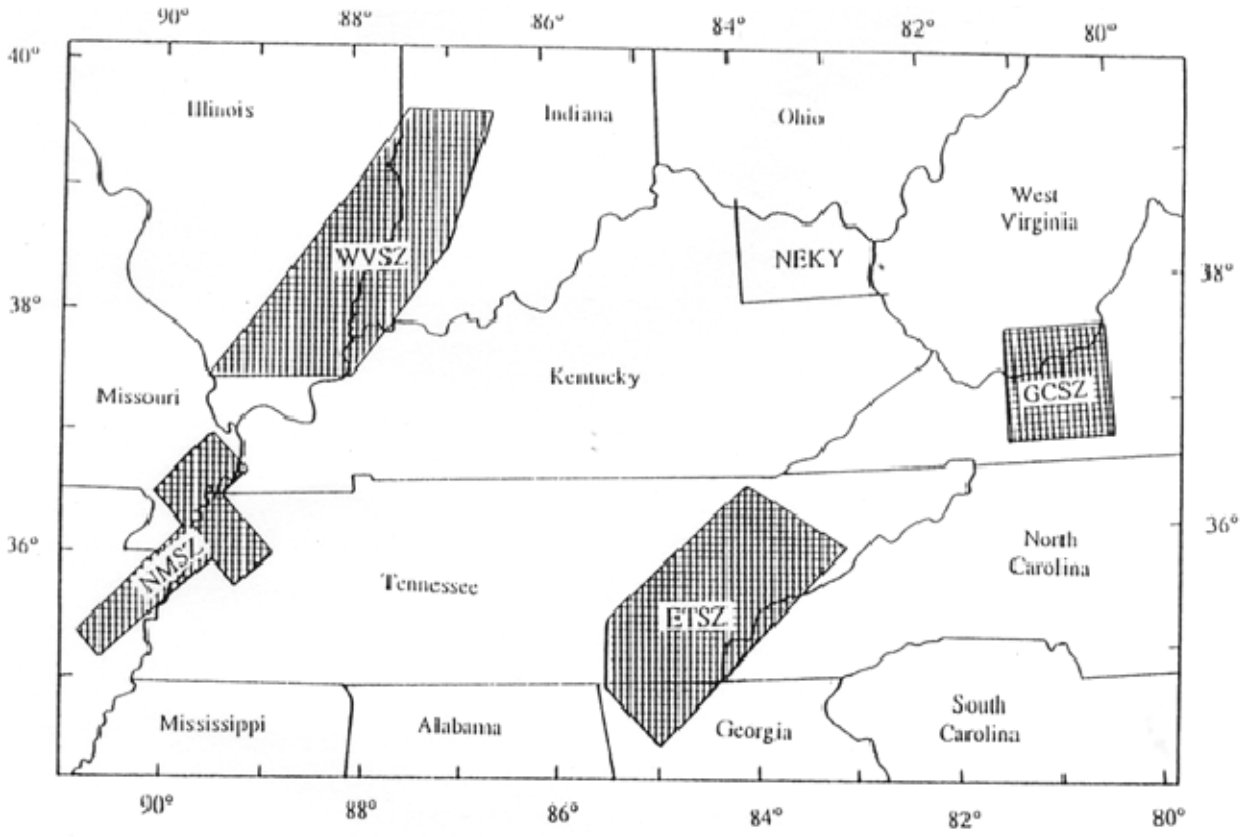

Figure 4-5. Earthquake source zones in and around Kentucky. NMSZ: New Madrid Seismic Zone; WVSZ: Wabash Valley Seismic Zone; ETSZ: Estern Tennessee Seismic Zone; NEKY: Northeastern Kentucky Seismic Zone; GCSZ: Gile County Seismic Zone

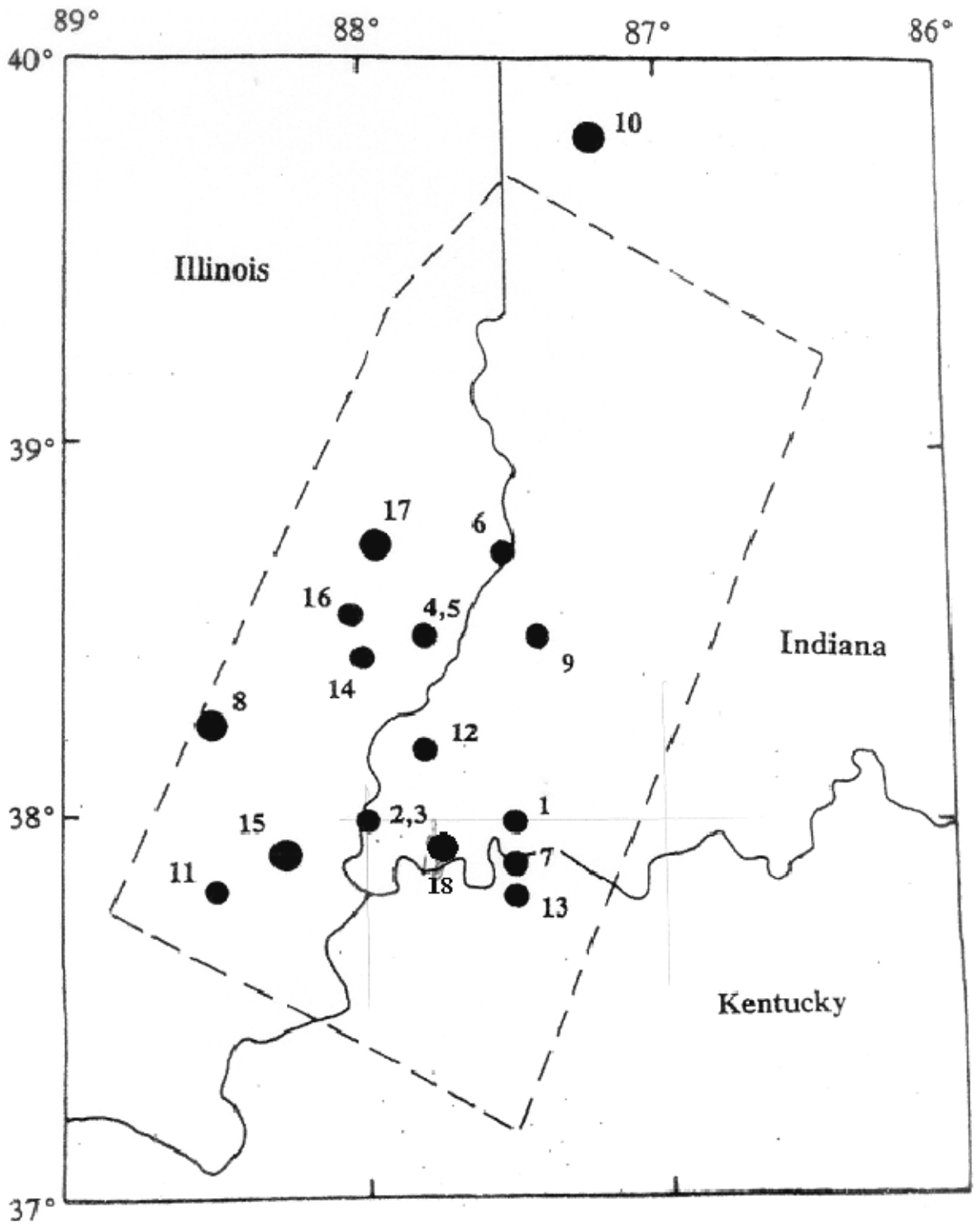

Figure 4-6. Epicentral locations of damaging earthquakes in the Wabash Valley Seismic Zone

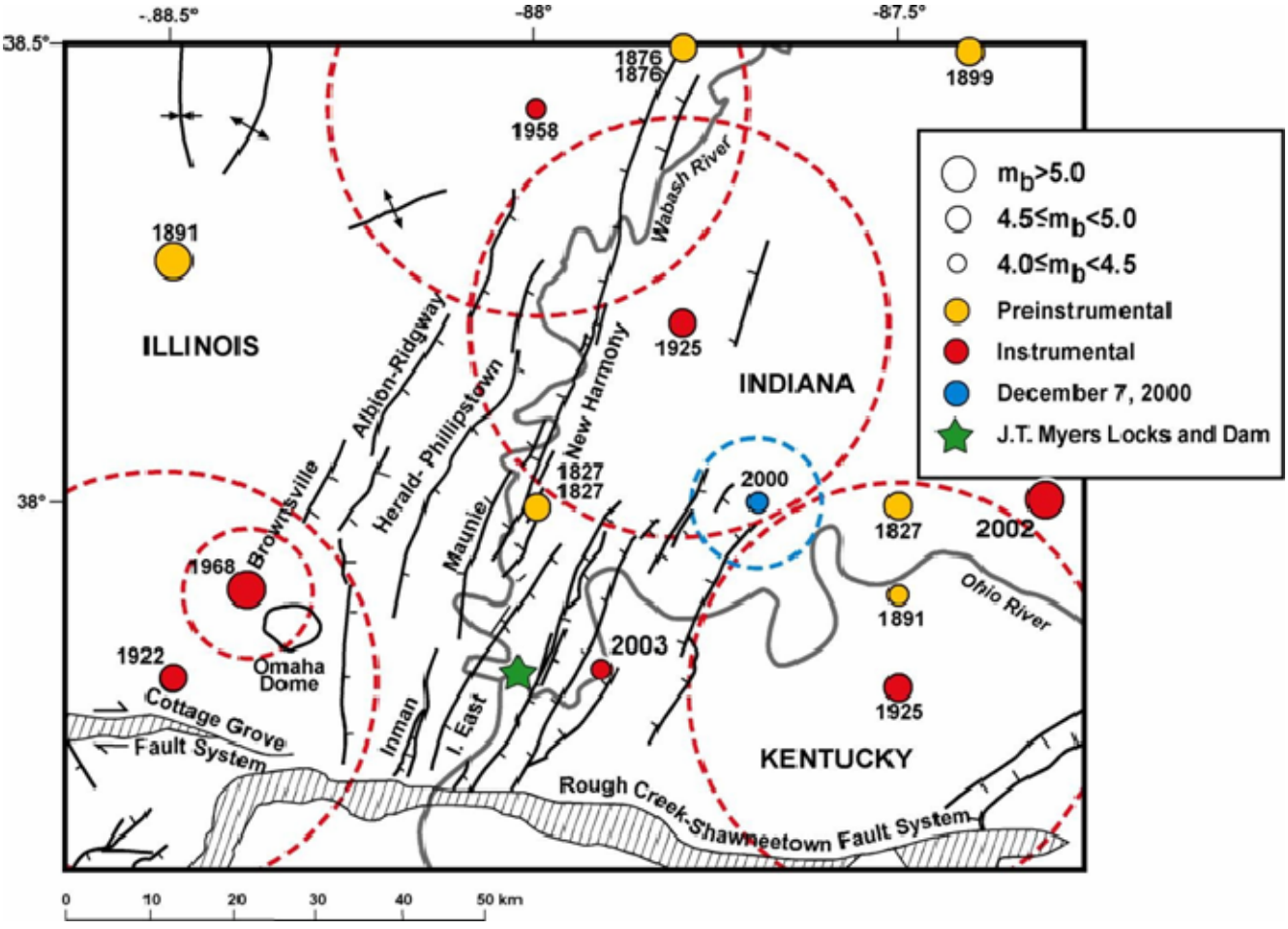

Figure 4-7. Locations of earthquakes and faults in the lower Wabash Valley

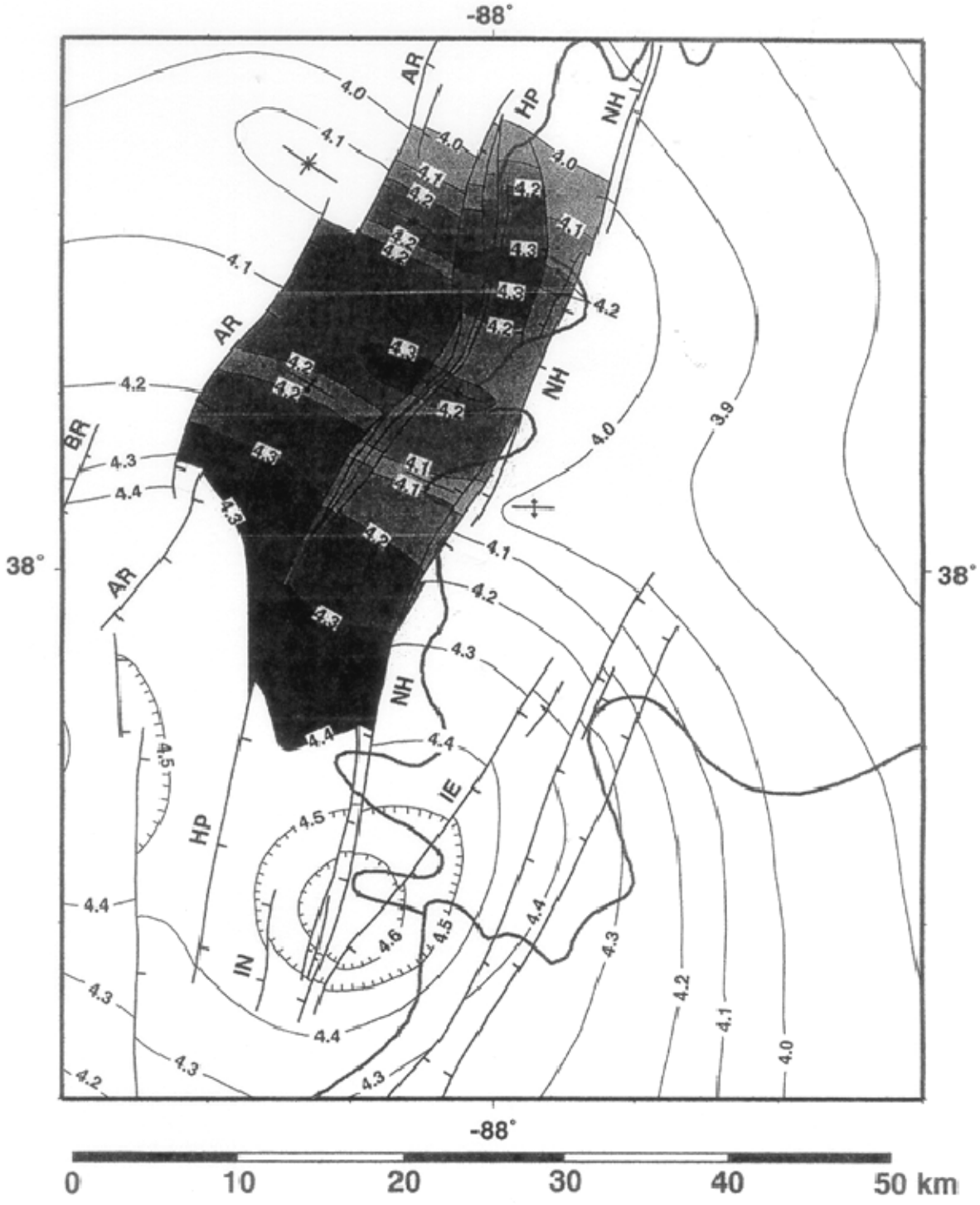

Figure 4-8. New Harmony Faults in the Wabash Valley (Sexton and others, 1996)

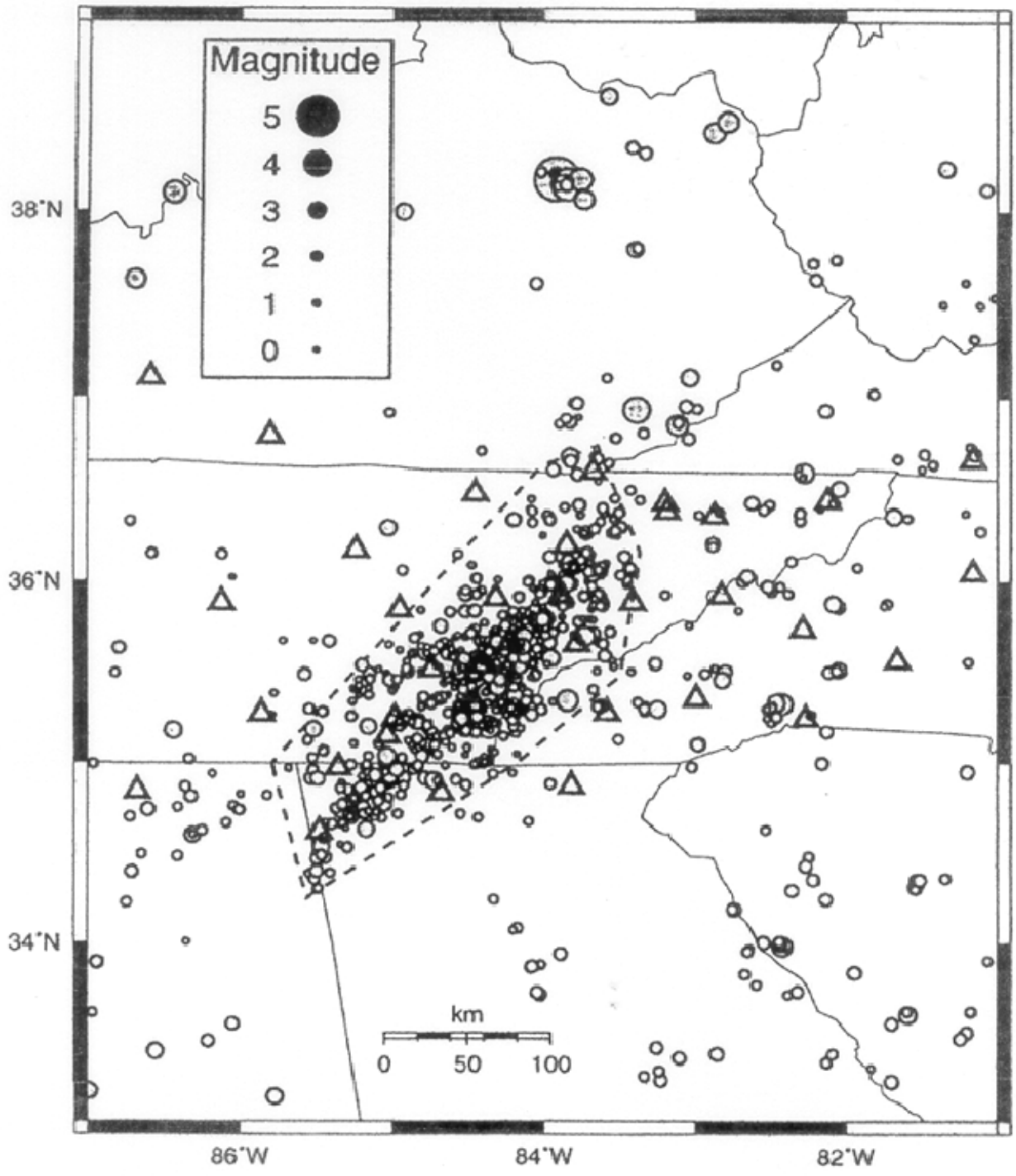

Figure 4-9. Eastern Tennessee Seismic Zone

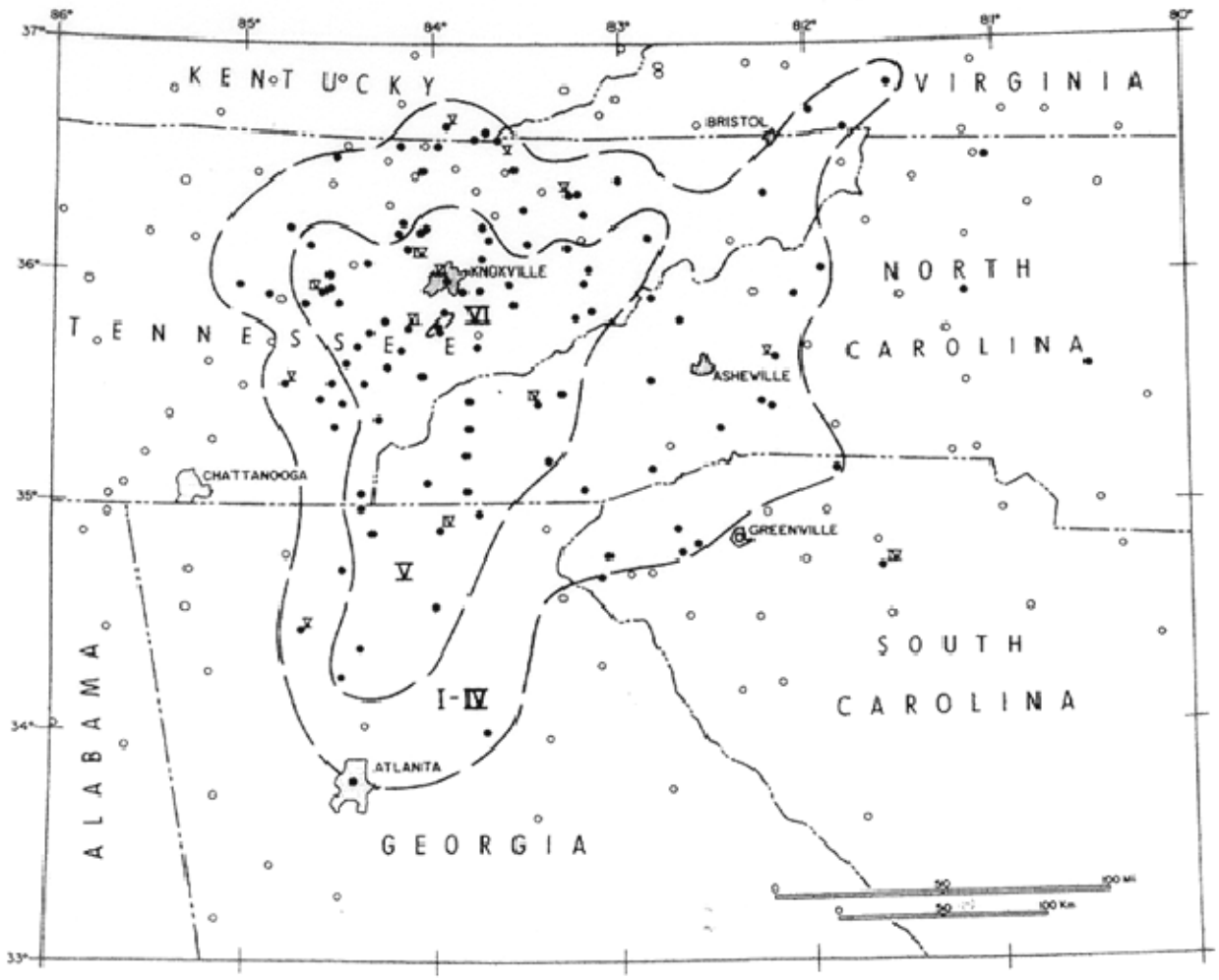

Figure 4-10. Isoseismal map of the Maryville, Tenn., earthquake of November 30, 1973

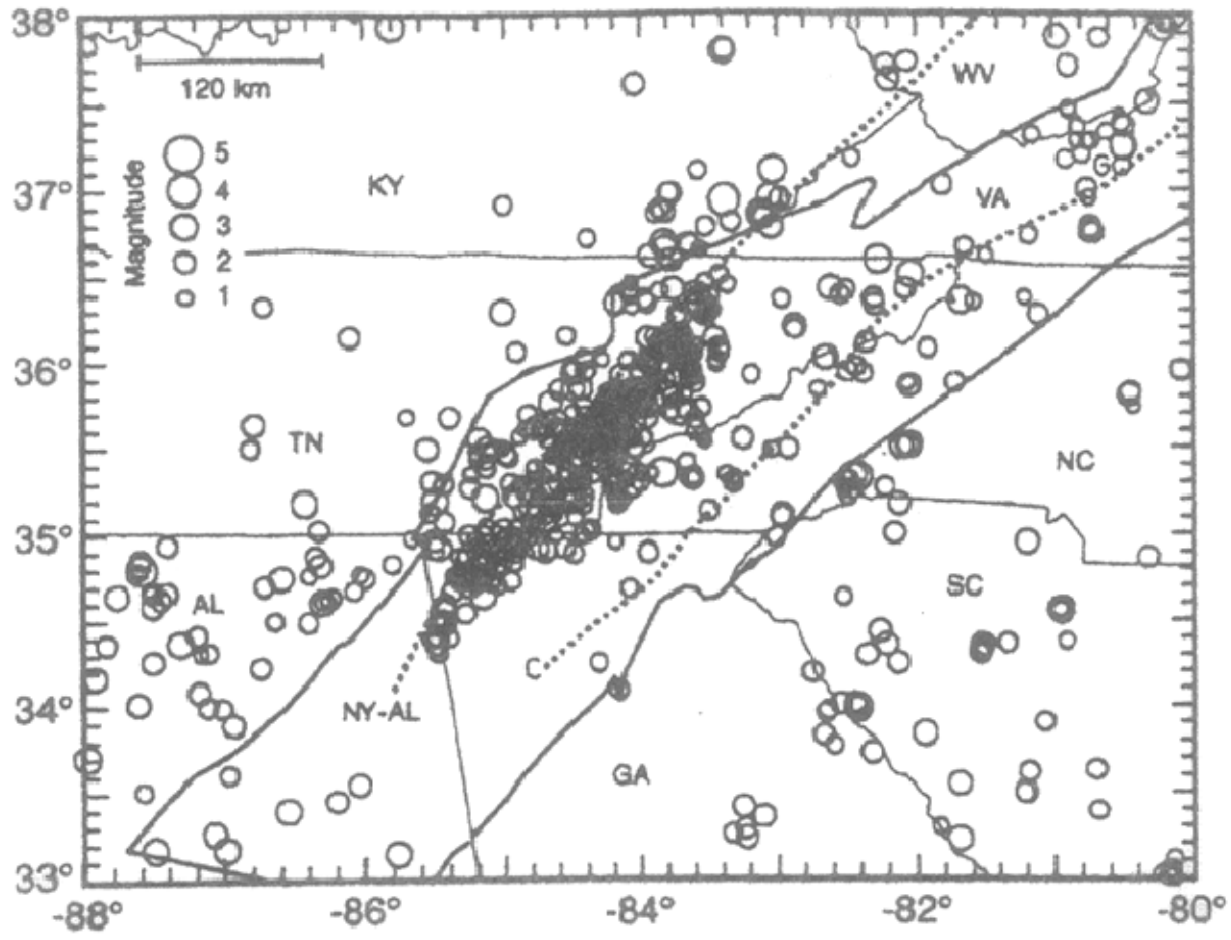

Figure 4-11. The New York–Alabama Magnetic Lineament

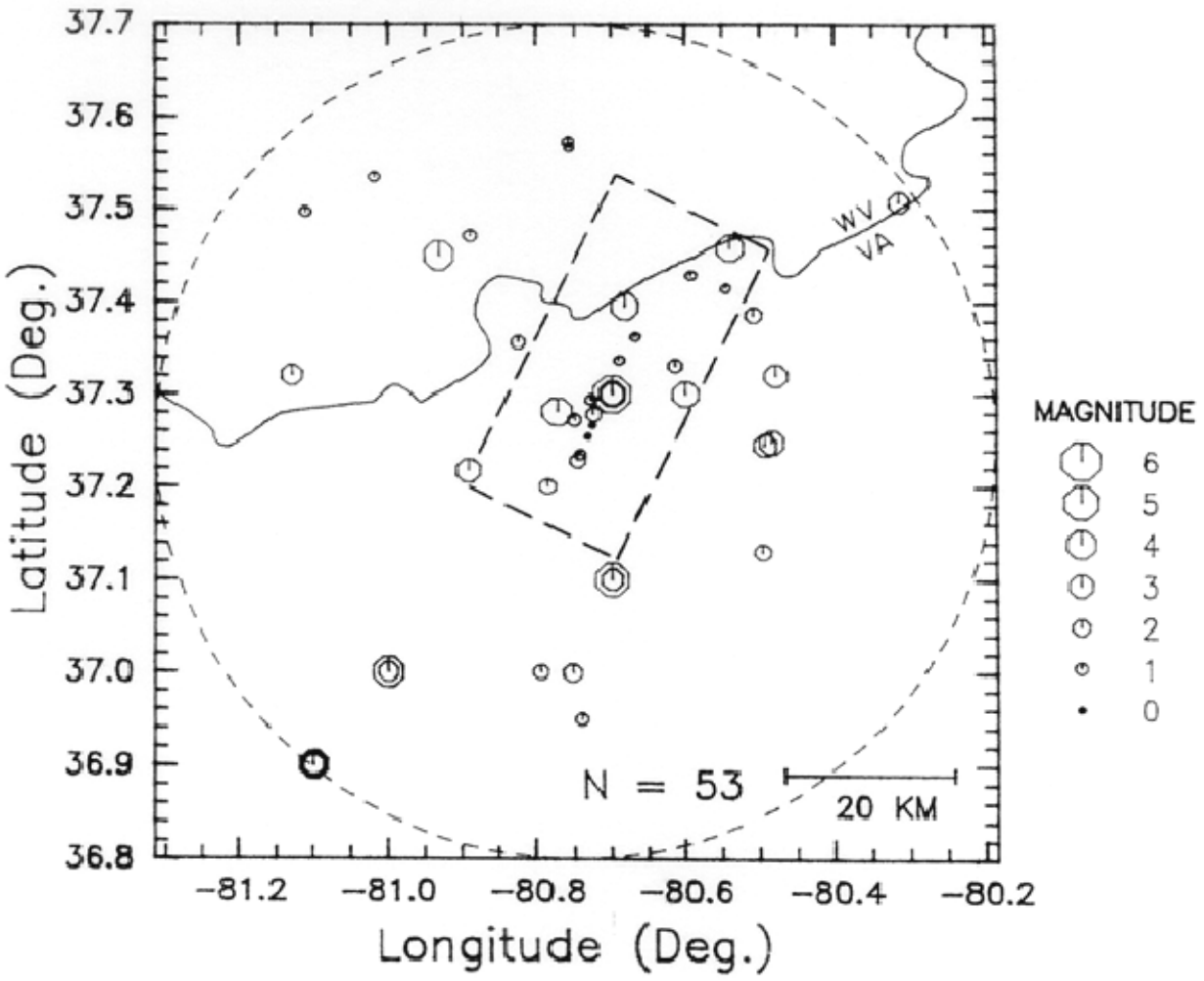

Figure 4-12. The Giles County Seismic Zone

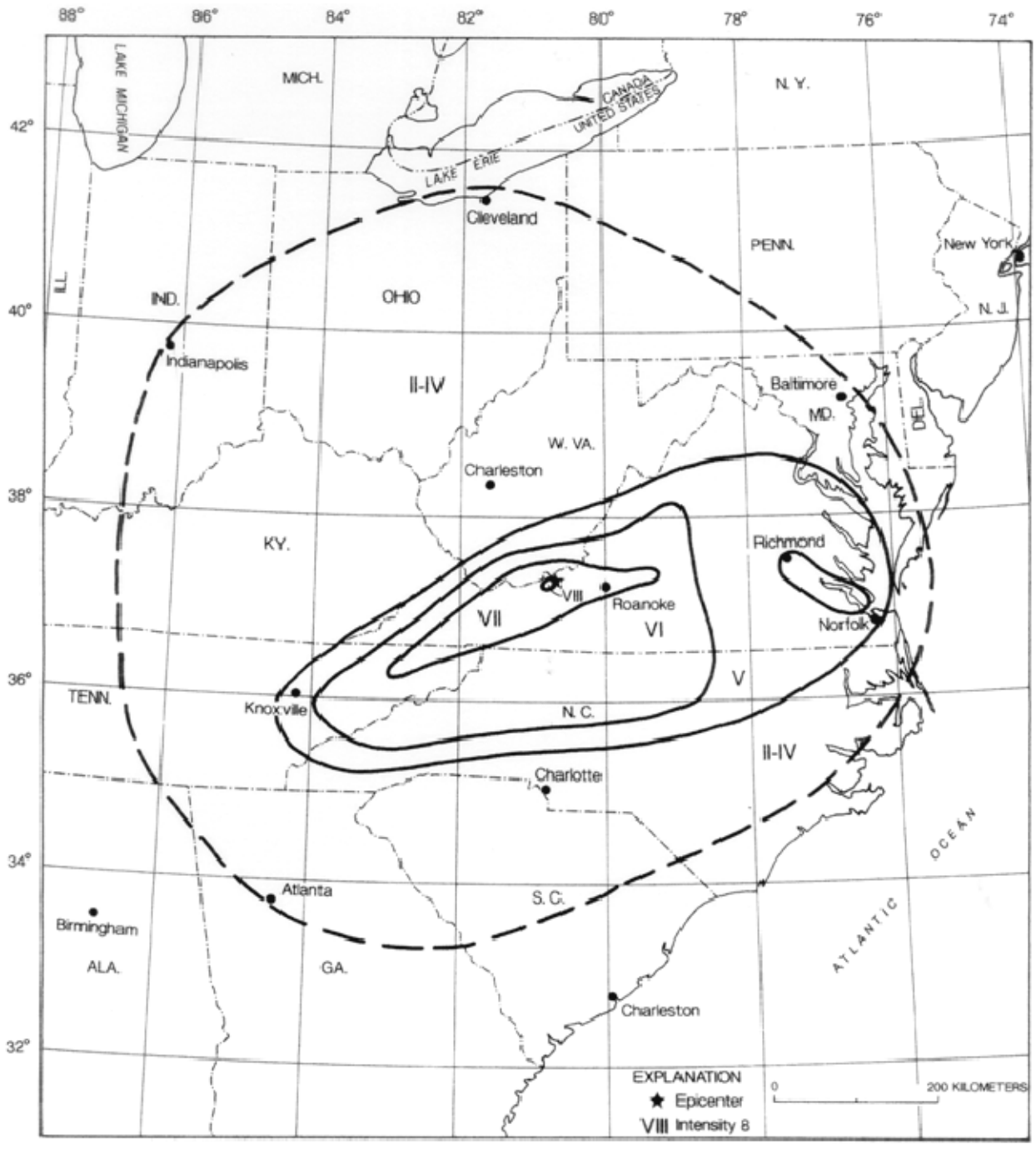

Figure 4-13. Isoseismal map of the Giles County, Va., earthquake of May 31, 1897

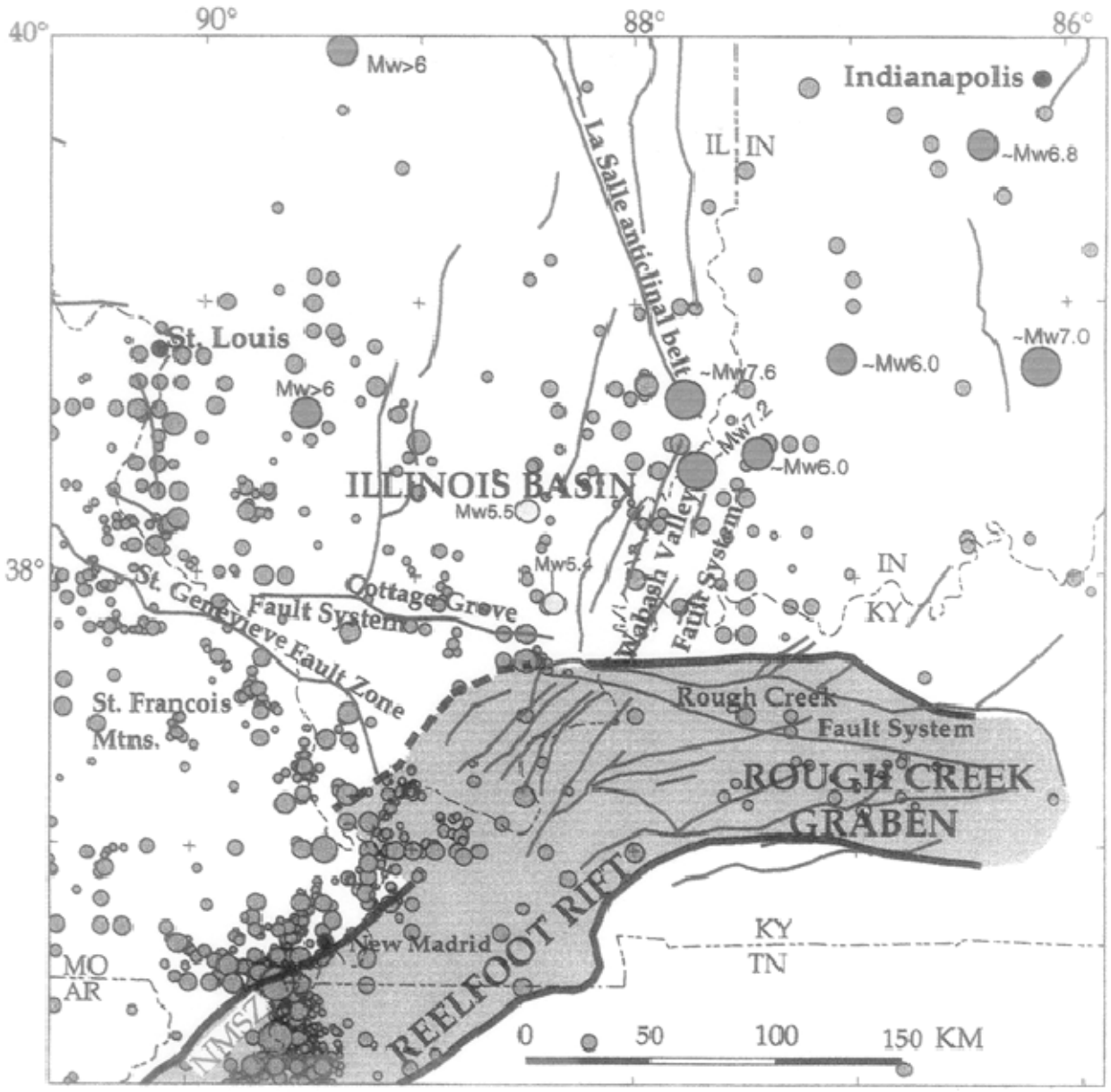

Figure 4-14. The Rough Creek Graben

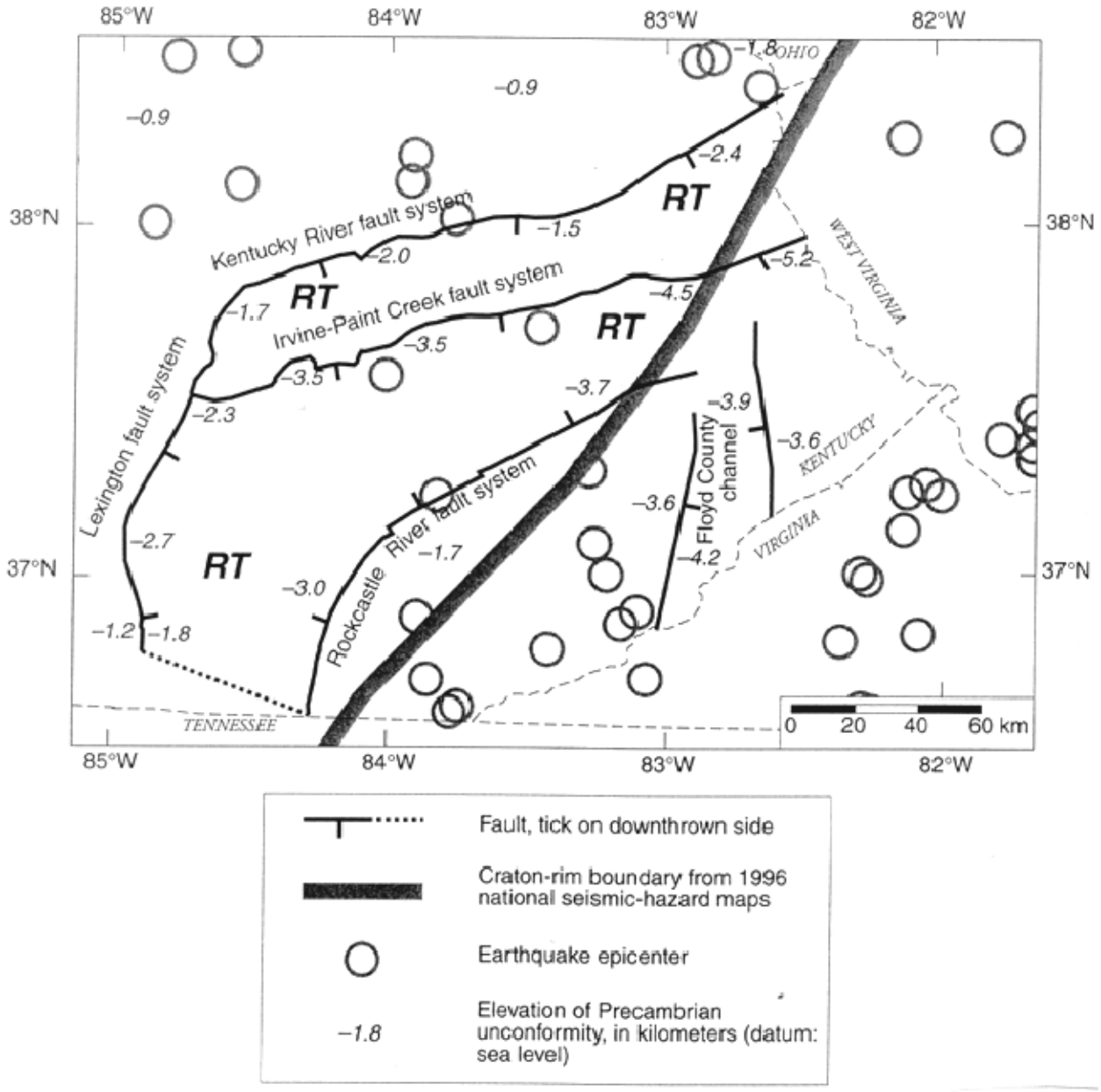

Figure 4-15. The Rome Trough in eastern Kentucky (Wheeler and Cramer, 2002)

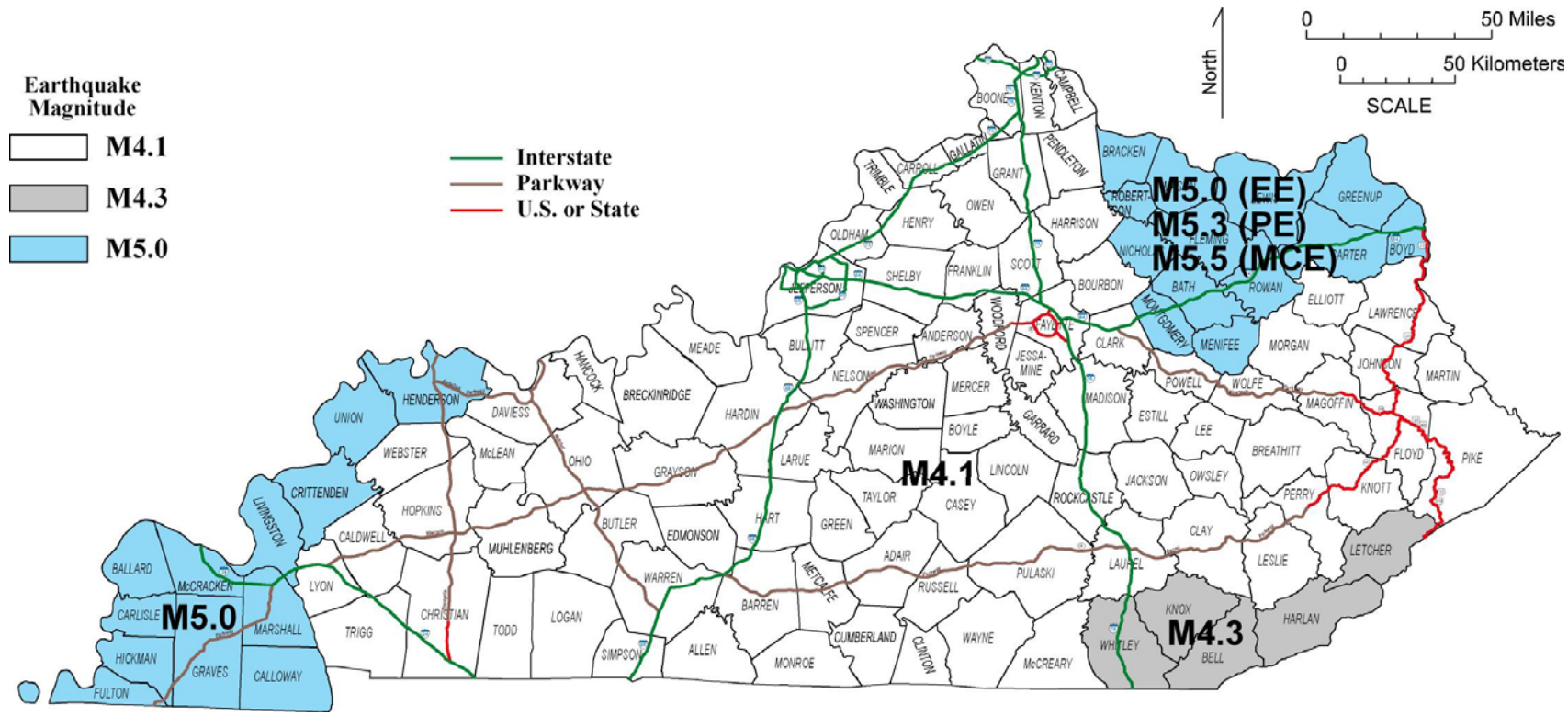

Figure 4-16. Background earthquakes in Kentucky

5. MAGNITUDE-RECURRENCE RELATIONSHIP

The number of earthquakes that occur yearly around the world varies with magnitude; the smaller earthquakes are more frequent, and the larger are less frequent. The relationship between earthquake magnitude and annual occurrence is called the magnitude-recurrence relationship, also called the Gutenburg-Richter relationship. The Gutenburg-Richter relationship is, in logarithmtic form, as follows:

$$\log_{10} N = a - bM, \qquad (5\text{-}1)$$

where N is the number of earthquakes with magnitude greater than M occurring yearly, and a and b are constants depending on the number of earthquakes in the time and region sampled. In the central United States, the Gutenburg-Richter relationship takes the form:

$$\log_{10} N = a - bm_{b,Lg}. \qquad (5\text{-}2)$$

Instrumental and historical records are insufficient to construct the magnitude-recurrence relationship for the central United States, because the seismicity is relatively low in comparison with that of California. There are no instrumental recordings for strong and large earthquakes (M > 6.0) in the central United States. Only two strong historical events (6.0 < M < 6.5), the 1843 Marked Tree, Ark., earthquake (M6.0) and the 1895 Charleston, Mo., earthquake (M6.0) (Bakun and others, 2003) have occurred. The only great events (7.0 < M < 8.0) are the 1811–1812 New Madrid events. Bakun and others (2003) suggested that the 1895 Charleston, Mo., earthquake was actually located in southern Illinois, about 100 km north of Charleston (not in the New Madrid Seismic Zone). Prehistoric records (paleoliquefaction) have been used to construct the magnitude-occurrence relationship. Figures. 5-1 and 5-2 show the magnitude-occurrence relationships for the New Madrid Seismic Zone (Frankel and others, 1996) and the Wabash Valley Seismic Zone (Wheeler and Cramer, 2002), based on instrumental, historical, and paleoliquefaction records. These figures show that (1) the annual rate derived from instrumental records and historical earthquakes is not consistent with that derived from paleoliquefaction records and (2) there is a lack of strong earthquakes of M6.0 to M7.0 (an earthquake deficit).

A *b*-value of 0.95 was used in the USGS national seismic-hazard maps for the central United States (Frankel and others, 1996, 2002). Based on instrumental and historical records, the annual occurrence of an M7.5 earthquake is less than 0.0001 (reccurence interval is longer than 10,000 years) in the New Madrid Seismic Zone (Fig. 5-1). Paleoliquefaction records revealed an annual occurrence of 0.00218 (reccurence interval of about 459 years) for an M7.5 earthquake in the New Madrid Seismic Zone, however (Fig. 5-1). According to PSHA, all earthquakes from about M4.0 to M8.0 contribute to the total hazard (Fig. 3-2). But in the central United States, there is a lack of instrumental, historical, and geologic records for earthquakes between M6.0 and M7.0. The inconsistency between the instrumental and historical rate and the geologic rate makes performing PSHA difficult in the central United States. The earthquakes that are of engineering concern are large (M7.0 or larger) and infrequent, which makes DSHA a good alternative for deriving ground motion for engineering design in the central United States.

The following magnitude-recurrence relationships were used in this study:

1. Eastern Tennessee Seismic Zone (Bollinger and others, 1989):

$$\log_{10} N = 2.75 - 0.90 m_b \qquad (6\text{-}3)$$

2. Giles County Seismic Zone (Bollinger and others, 1989):

$$\log_{10} N = 1.065 - 0.64 m_b \qquad (6\text{-}4)$$

3. Wabash Valley Seismic Zone (Nuttli and Herrmann, 1978):

$$\log_{10} N = 3.10 - 0.92 m_b \qquad (6\text{-}5)$$

4. New Madrid Seismic Zone (Nuttli and Herrmann, 1978):

$$\log_{10} N = 3.90 - 0.92 m_b \, . \qquad (6\text{-}6)$$

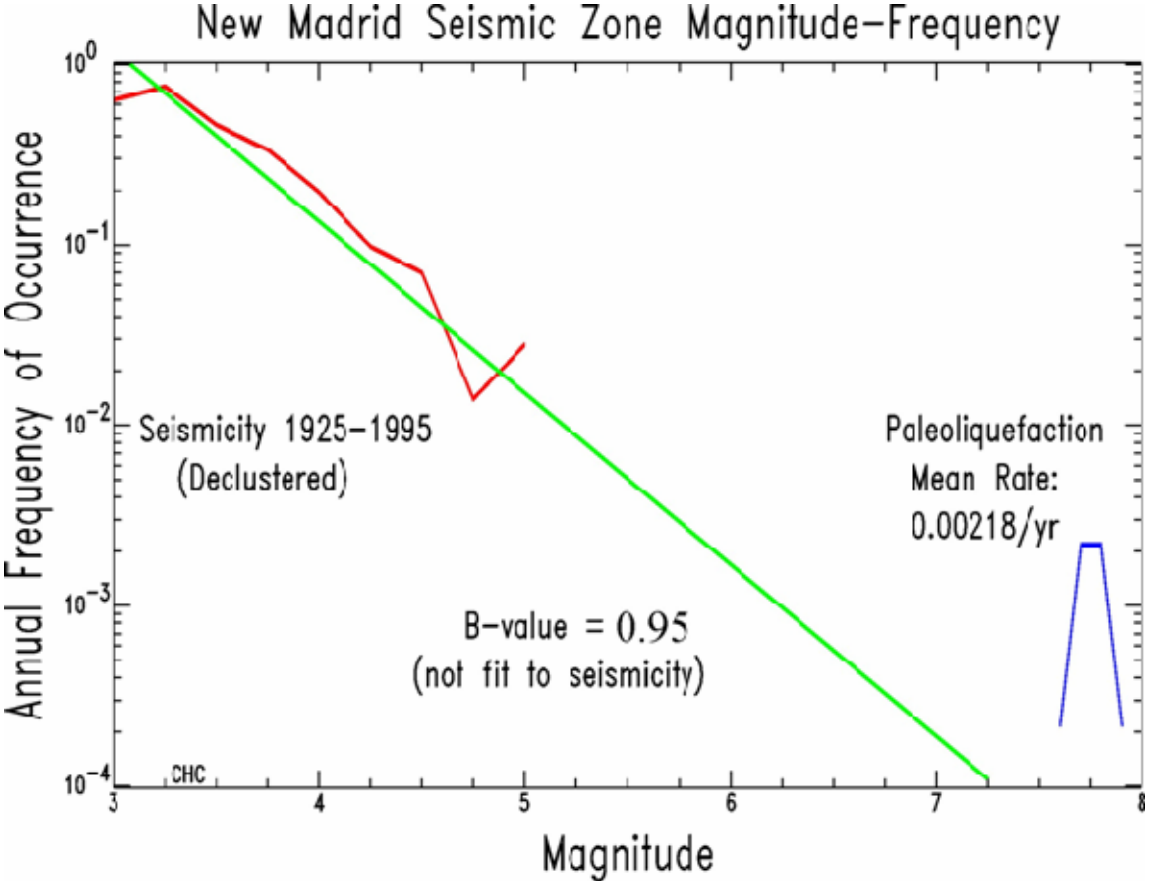

Figure 5-1. Magnitude-frequency relationship for the New Madrid Seismic Zone (Frankel and others, 1996)

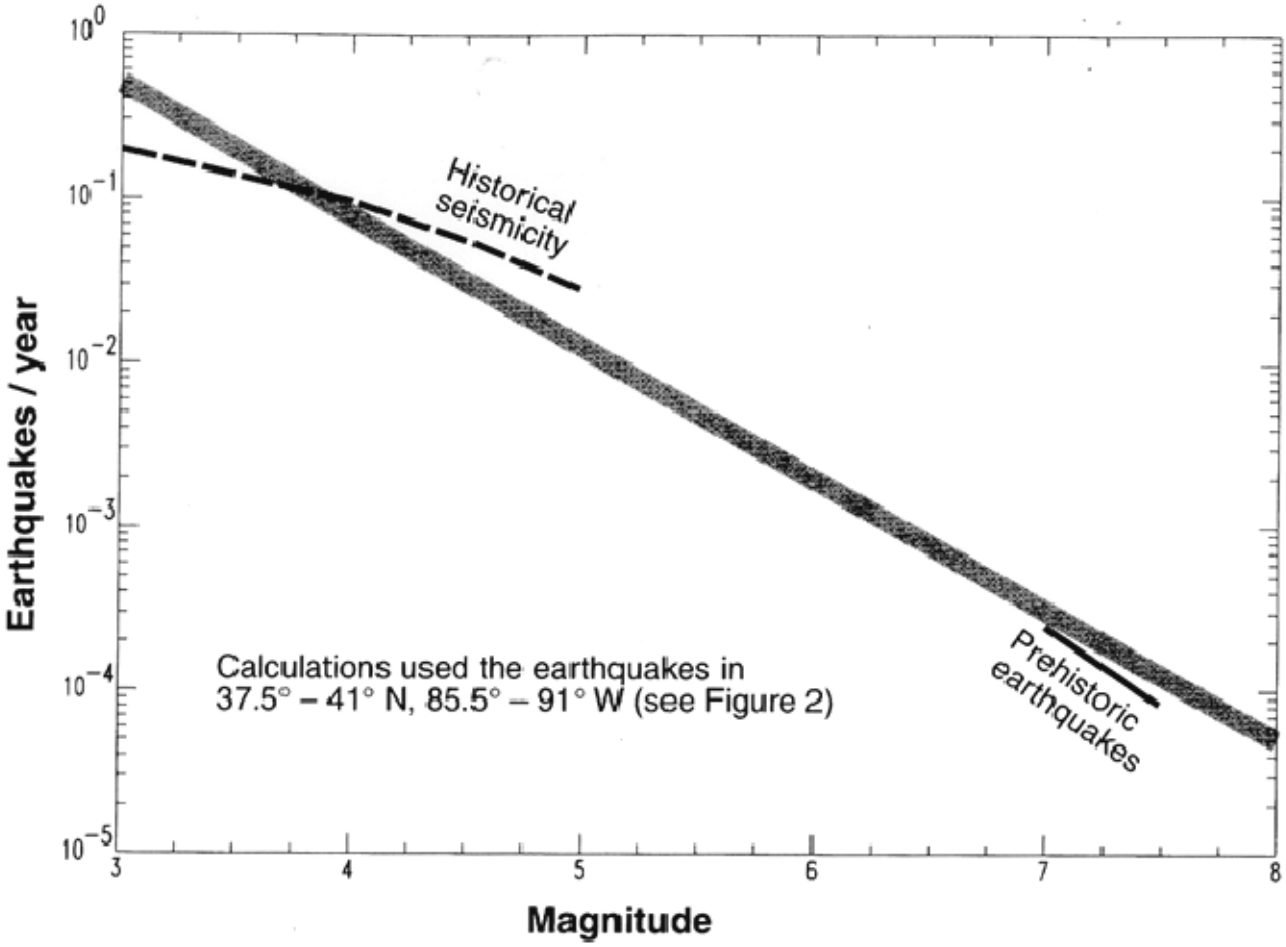

Figure 5-2. Magnitude-frequency relationship for the Wabash Valley Seismic Zone (Wheeler and Cramer, 2002)

6. GROUND-MOTION ATTENUATION RELATIONSHIP

6.1. Introduction

The ground-motion attenuation relationship is used to estimate strong ground motion for site-specific and regional seismic-hazard analyses. The relationship is a simple mathematical model that relates a ground-motion parameter to an earthquake magnitude, source-to-site distance, and other seismological parameters, such as style of faulting and local site conditions (Campbell, 2003). The most commonly predicted ground-motion parameters are peak ground acceleration (PGA), peak ground velocity (PGV), and pseudo-response spectral acceleration (PSA). In areas such as western North America and Japan, where strong-motion recordings are abundant, these attenuation relationships are developed empirically. In many regions of the world, however, including the central United States, there are not enough recordings to develop reliable empirical attenuation relationships. When the number of strong-motion recordings is limited, but good seismological data are available, it is possible to derive simple seismological models that can be used to describe how ground motion scales with earthquake source size and distance from the source.

The most widely used methods to develop the attenuation relationships are the stochastic point-source model (Hanks and McGuire, 1981; Boore, 1983; Boore and Atkinson, 1987; Toro and McGuire, 1987) and the stochastic finite-fault model (Atkinson and Silva, 1997; Beresnev and Atkinson, 1997). Stochastic models use the findings of Hanks and McGuire (1981) that stated observed ground motions can be characterized as finite-duration band-limited Gaussian noise with an amplitude spectrum specified by a simple source model (Brune model) and propagation processes. Although they have been successful and are simple, stochastic models have two obvious problems. First, the model breaks down near the source: it cannot take the near-source effects, such as rupture propagation and directivity, into consideration. Second, the models do not consider two- and three-dimensional wave propagation. Source effects and wave propagation have a significant influence on simulated ground motion.

With the improvement of computers, it has become possible to use more sophisticated numerical methods for simulating strong ground motion based on empirical or theoretical source functions and two- and three-dimensional wave propagation theory (Somerville and others, 1991; Anderson and others, 2003). Somerville and others (1991) developed a semi-empirical model that will take into account the near-source effects and three-dimensional wave propagation in detail; it has been successfully used in ground-motion simulations for many earthquakes (Somerville and others, 1991, 2001; Saikia and Somerville, 1997). A ground-motion attenuation relationship was also developed from the semi-empirical model (Somerville and others, 2001) for the central United States. Figure 6-1 shows ground-motion attenuation relationships that are widely used in seismic-hazard assessments in the central United States. Figure 6-2 shows response spectra for several ground-motion attenuation relationships for an M7.5 earthquake at a distance of 30 km. Significant differences between the stochastic models and the semi-empirical model are that semi-empirical models predict (1) much lower ground motion near the source and (2) higher ground motion far afield.

Zeng and others (1994) developed a composite source model that will take into account the near-source effects and three-dimensional wave propagation in detail. The composite source model has also been successfully used in ground-motion simulations (Yu, 1994; Zeng and others, 1994; Zeng and Anderson, 1995; Anderson, 1997; Anderson and others, 2003). Recent success in predicting ground motions for the M_W 7.9 Alaska earthquake by both the semi-empirical and composite source models (Anderson and others, 2003) demonstrates that the methods provide very reasonable simulation of ground motions for large earthquakes. The ground-motion attenuation relationship of Somerville and others (2001) was used in this study. We chose the composite source model to generate time histories because it does not require an empirical source function, nor does it require separate simulations for high and low frequencies. As Saikia and Somerville (1997) pointed out, the empirical source function is difficult to obtain because of the scarcity of strong-motion recordings in the central United States.

6.2. Composite Source Model

The composite source model (Zeng and others, 1994) uses Green's functions for the generation of synthetic strong ground-motion seismograms for a layered medium. For the Green's function synthetic computation, a generalized reflection and transmission coefficient matrix method, developed by Luco and Apsel (1983) and coded by Zeng and Anderson (1995), has been used to compute elastic wave propagation in a layered elastic half-space in frequency/wave number domain. The generalized reflection and transmission coefficient matrix method is advantageous in synthetic seismogram computation because it is based on solving the elastodynamic equation complying with the boundary conditions of the free surface, bonded motion at infinity, and continuity of the wave field across each interface. The composite source is described with superposition of a circular subevent. The number of subevents of a given radius (R) follows a power-law distribution ($\sim R^{-D}$). All the subevents have the same stress drop ($\Delta\sigma$). The largest subevent has a radius (R_{max}) that fits within the fault, and the smallest is chosen so that it does not have any effect on the numerical outcome of the computations. The total number of subevents is constrained to match the desired seismic moment of the earthquake. Thus, as $\Delta\sigma$ is increased, the overall number of subevents decreases. The subevents are placed randomly within the fault plane, and the boundaries of subevents are allowed to overlap (intersect). Each event is given a source time function defined by a Brune pulse (1970, 1971). The duration of each subevent's time function is proportional to its radius, and the amplitude is proportional to $\Delta\sigma$. Rupture on the fault starts at the hypocenter, and the radiation from each subevent begins when the rupture front, propagating at a constant rupture velocity, reaches the center of the subevent. An important feature of the composite source model is that all of its input parameters have the potential to be constrained by independent physical data. The input parameters that were used in this study are listed in Table 6-1.

Table 6-1. Parameters for ground-motion simulation

Parameter	Range of Values
Magnitude (M_w)	4.5~8.0
Fault mechanism	Strike-slip and thrust
Crust structure	USGS model[1] and Midcontinent model[2] (α, β, ρ, Q, h)
Site condition	Surface geologic and geophysical data
Centroid depth	0~30 km
Distance	0–500 km
Fault length and width	Derived from source scaling law[2]
Fault area	Derived from source scaling law[2]
Stress drop	$\Delta\sigma$=50~500 bars
R_{max} (largest radius of circular subevent)	Derived from source scaling law[2]
Slip time function	Brune's pulse (Brune, 1970, 1971)
Rupture velocity	Constant and less than shear-wave velocity
Fractal dimension	D=2
Seismic moment	Derived from moment-magnitude scale (Hanks and Kanamori, 1979)

1. Frankel and others (1996)
2. Somerville and others (2001)

The composite source model was applied to the June 18, 2003, Darmstadt, Ind., earthquake. The Kentucky Seismic and Strong-Motion Network and the U.S. Army Corps of Engineers' strong-motion stations recorded this earthquake (Wang and others, 2003c), providing a valuable ground-motion data set. The parameters used in the modelling are listed in Table 6-2. Figures 6-3 and 6-4 show the synthetic seismograms and real data recorded by the stations at J.T. Myers and Newburgh Lock and Dam, which had epicentral distances of 30 km and 35 km, respectively. In each figure, the right column shows three recorded components of acceleration and velocity time histories, and the left column gives the corresponding synthetic results. Several key parameters of the source model used for these calculations were obtained by repeated trial and by examining the resultant seismogram at the J.T. Myers and Newburgh stations.

Table 6-2. Parameters of the composite model for the June 18, 2003, Darmstadt, Ind., earthquake

Parameter	Value
L (fault length along the strike)	2.5 km
W (rupture width)	2.0 km
M_o (seismic moment)	$3.52*10^{23}$ dyne cm
Rmax (largest subevent radius)	0.5 ~0.75 km
$\Delta\sigma$ (subevent stress drop)	150 bars
V_r (rupture velocity)	2.8 km/sec
D (fractal dimension)	2.0

A composite source model simulation was also conducted for an M_w8.0 earthquake from the New Madrid Fault Zone. We used the velocity model given by the USGS (Frankel and others, 1996). The dimension of the fault is 122 km long by 36.5 km wide with a dipping angle of 60^o. The rupture breaks to the free surface with a constant stress drop of 100 bars (Shi and others,

2006). The largest radius of circular subevent derived from the source scaling relation (Somerville and others, 2001) is about 8 km. Figure 6-1 compares the simulated ground motions versus the epicentral distance using the attenuation relationship of Somerville and others (2001). The resulting peak ground accelerations are consistent with those of the empirical model of Somerville and others (2001).

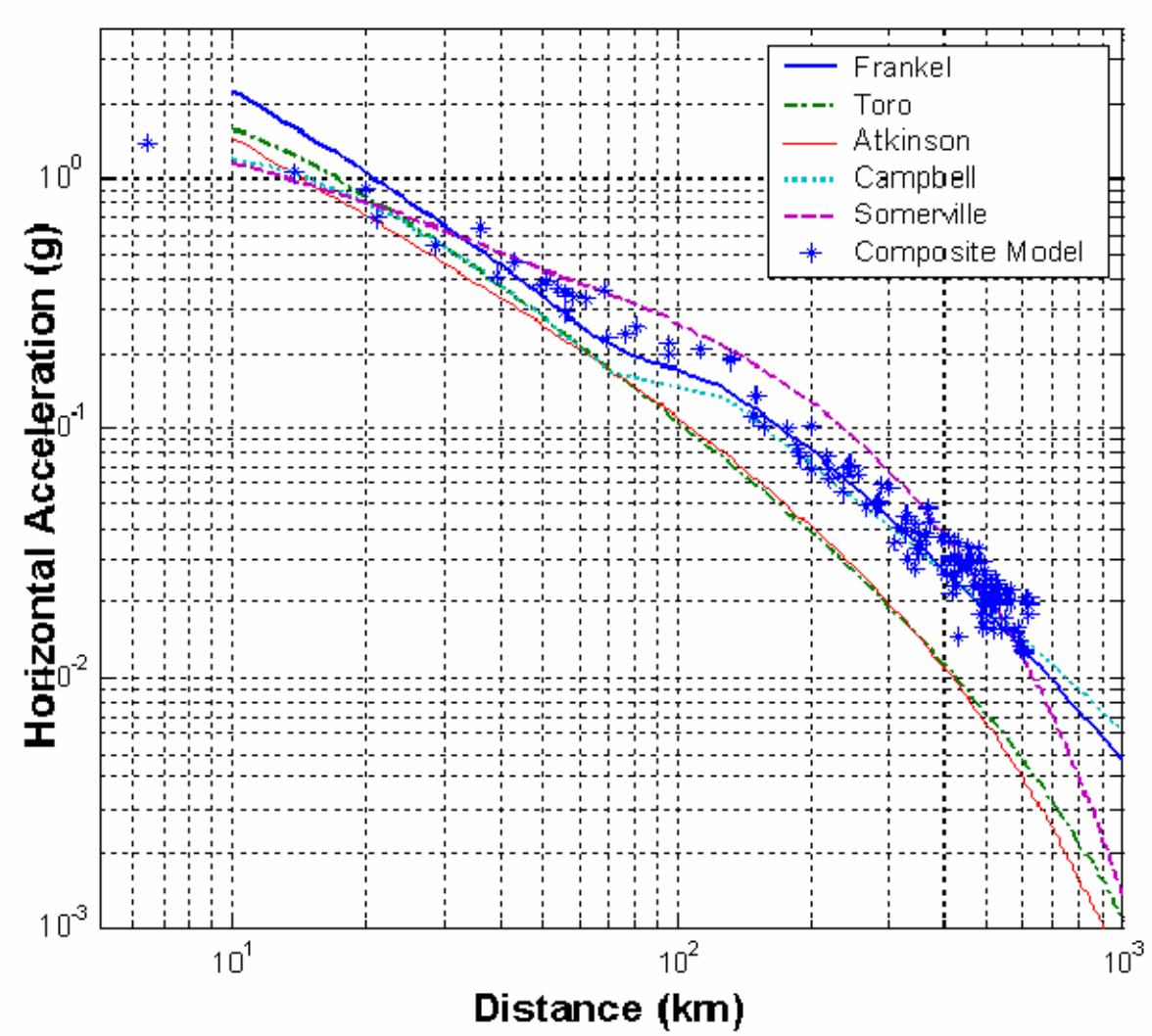

Figure 6-1. Ground-motion attenuation relationships for an M8.0 earthquake in the central United States

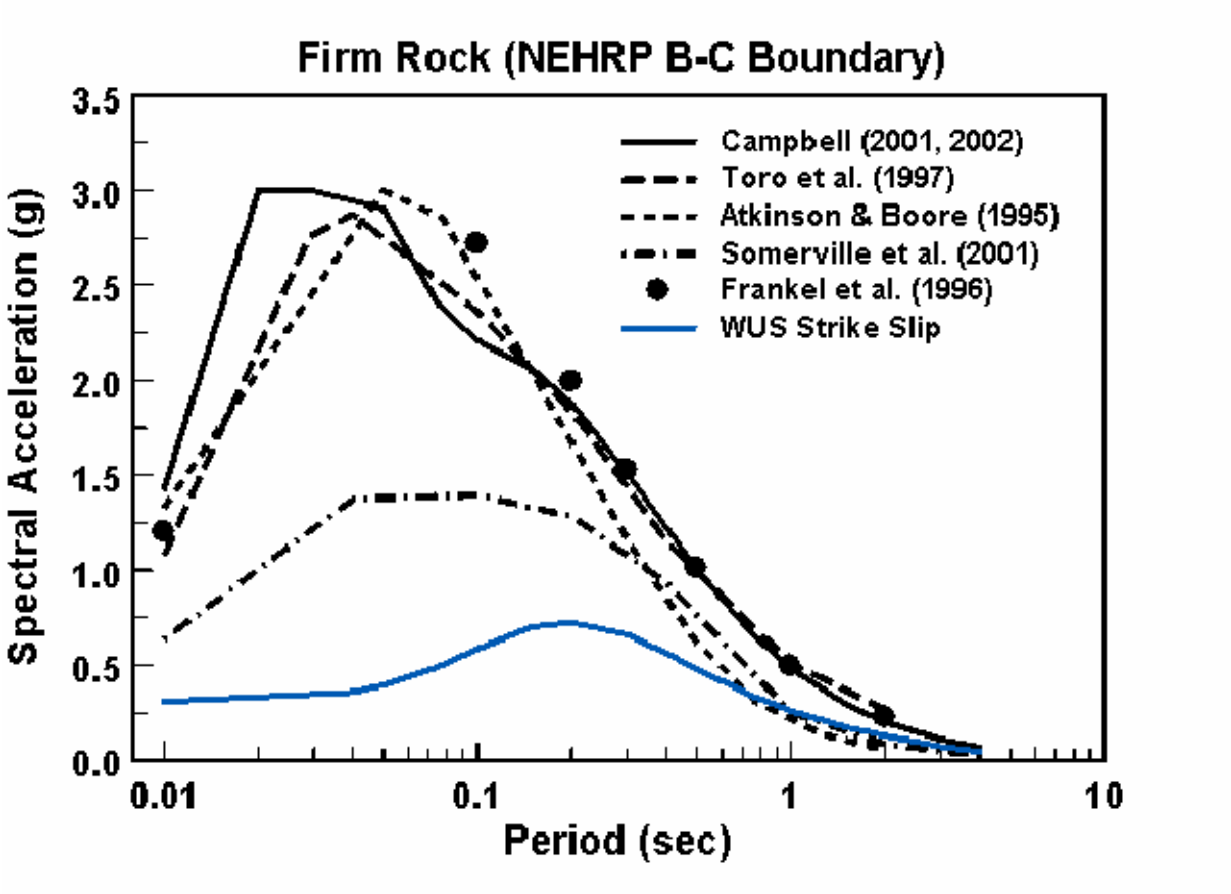

Figure 6-2. Response spectra for an M7.5 earthquake at 30 km for several attenuation relationships in the central United States

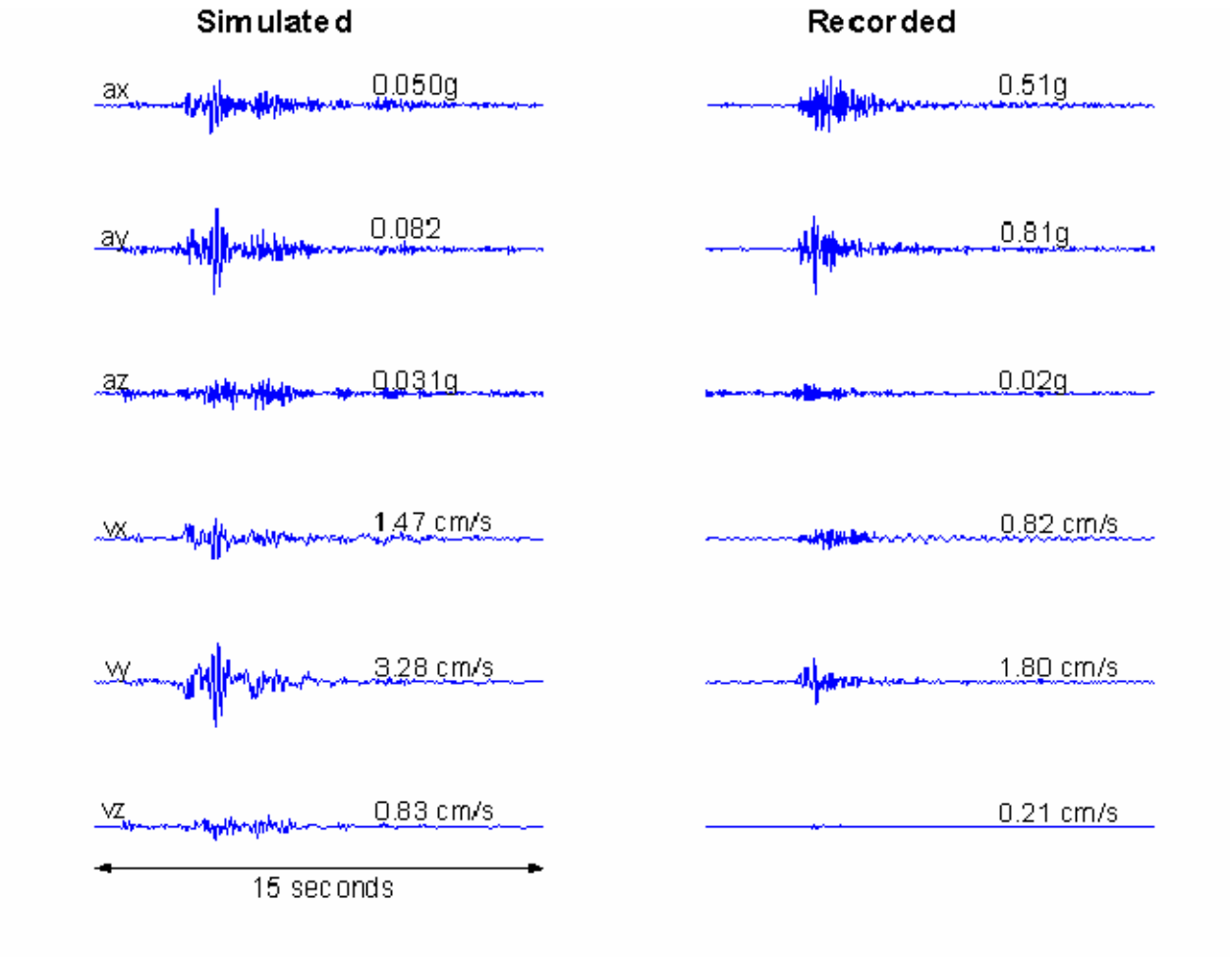

Figure 6-3. Comparison of observed and synthetic ground motion at J.T. Myers Lock and Dam. Observed acceleration and velocity are in the right column. The horizontal components a_x and a_y refer to instrument orientations, and the vertical component is denoted by a_z

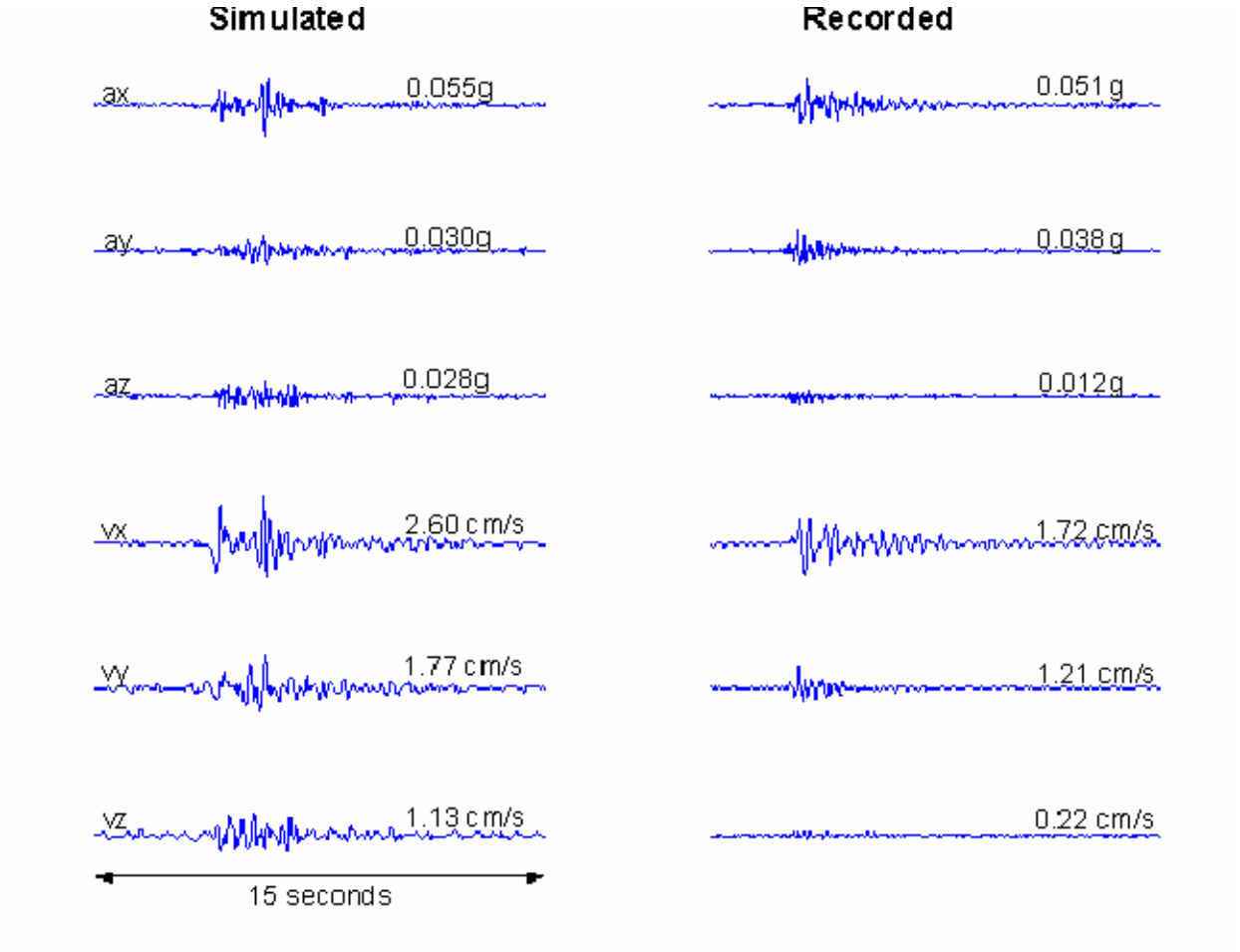

Figure 6-4. Comparison of observed and synthetic ground motion at Newburgh Lock and Dam. Observed acceleration and velocity are in the right column. The horizontal components a_x and a_y refer to instrument orientations, and the vertical component is denoted by a_z

7. DETERMINITIC SEISMIC HAZARD ANALYSIS

7.1. Expected Earthquake and the Associated Ground Motion

The *expected earthquake* is defined in this study as the earthquake that could be expected to occur in a bridge's lifetime of 75 years. The probability that EE ground motion could be exceeded over the bridge life of 75 years is about 50% (risk). EE peak ground-motion hazard maps are equivalent to the maps of horizontal peak-particle acceleration at the top of rock with a 90% probability of not being exceeded in 50 years, which were defined by Street et. al. This is equivalent to the *"small earthquake"* specified in the existing AASHTO provisions. *EE* in the study area is the background earthquakes in Kentucky and the surrounding areas. Figure 4-16 shows the *EE's* that are recommended in this study and used to generate ground motions and time histories. Table 7-1 lists the expected earthquakes for the New Madrid and other seismic zones. *EE* is similar to the "*expected earthquake"* defined in the 2003 Recommended LRFD Guidelines for the Seismic Design of Highway Bridges (MCEER, 2001), and also equivalent to the "*lower-level* earthquake" ground motion specified in the 2006 Seismic Retrofiting Manual for Highway Structures (FHWA, 2006)

Table 7-1. Expected, probable, and maximum credible earthquakes for the seismic zones

Seismic Zone	Expected Earthquake (M)	Probable Earthquake (M)	Maximum Credible Earthquake (M)
New Madrid	6.3	7.2	7.7
Wabash Valley	5.3	5.9	6.6
Eastern Tennessee	4.4	5.5	6.3
Giles County	4.1	5.2	6.3

The ground motion generated from the *expected earthquake* is called the *expected earthquake ground motion.* The *expected earthquake ground motion* is equivalent to the ground motion with a 90 percent probability of not being exceeded in 50 years, specified in the KTC-96-4 report (Street and others, 1996). The maximum median peak (horizontal) ground acceleration, and short-period (0.2 s) and long-period (1.0 s) response accelerations $\mathbf{S_S}$ and $\mathbf{S_1}$ with 5% damping, were developed in this study for expected earthquakes in Kentucky and are shown in Figures 7-1 through 7-3. Figure 7-4 shows the recommended zones of time histories and response spectra for EE. The data for the recommended time histories and response can be downloaded by following these steps: (1)- Go to web site: http://www.ktc.uky.edu/ ; (2)- Click on "Research", (3)- Click on "Reports by Section"; and (4)- Go to "Structures" and Report Number "KTC-07-07/SPR246-02-6F".

The derivation of the "Acceleration Design Response Spectrum" is presented in Appendix -I and the derivation of the "Time History" is presented in Appendix -II.

7.2. Probable Earthquake and the Associated Ground Motion

The *probable earthquake* is defined in this study as the earthquake that could be expected to occur in the next 250 years. The probability that PE ground motion could be exceeded over the bridge life of 75 years is about 26% (risk). PE peak ground-motion hazard maps are equivalent to

the maps of horizontal peak-particle acceleration at the top of rock with a 90% probability of not being exceeded in 250 years, which were defined by Street et. al. This is equivalent to the *"moderate earthquake"* applied in the existing AASHTO provisions. The *probable earthquakes* in the various seismic zones were determined from the magnitude-recurrence relationships of Bollinger and others (1989) and Nuttli and Herrmann (1978). The *probable earthquakes* that are recommended in this study are shown in Figure 4-16. Table 7-1 lists the *probable earthquakes* for the New Madrid and other seismic zones.

The ground motion generated from the *probable earthquake* is called the *probable earthquake ground motion.* The *probable earthquake ground motion* is equivalent to the ground motion with a 90 percent probability of not being exceeded in 250 years, specified in the KTC-96-4 report (Street and others, 1996). The maximum median peak (horizontal) ground acceleration, and short-period (0.2 s) and long-period (1.0 s) response accelerations $\mathbf{S_S}$ and $\mathbf{S_1}$ with 5% damping, were developed in this study for probable earthquakes in Kentucky and are shown in Figures 7-5 through 7-7. Figure 7-8 shows the recommended zones of time histories and response spectra for PE. The data for the recommended time histories and response can be downloaded by following these steps: (1)- Go to web site: http://www.ktc.uky.edu/ ; (2)- Click on "Research", (3)- Click on "Reports by Section"; and (4)- Go to "Structures" and Report Number "KTC-07-07/SPR246-02-6F".

The derivation of the "Acceleration Design Response Spectrum" is presented in Appendix -I and the derivation of the "Time History" is presented in Appendix -II.

7.3. Maximum Credible Earthquake and the Associated Ground Motion

Bollinger and others (1992) defined the maximum-magnitude earthquake as:

> (1) The largest possible earthquake that can occur given the current in-situ source conditions, or
> (2) The largest possible earthquake that might occur with a specified probability during a specified exposure time, or
> (3) The largest earthquake considered likely to occur in a "reasonable" amount of time.

Defining the maximum-magnitude earthquake for an area for which there is no clearly defined seismogenic source and only sparse seismicity is a subjective procedure. Areas can have different maximum-magnitude earthquakes. The rate of strain accumulation, the orientation, age and friction on a fault surface, material properties of the host rock, occurrence or lack of seismicity in nearby areas, etc., are some of the variables that influence the rate of seismicity and maximum-magnitude earthquake in an area.

Defining the maximum-magnitude earthquake for an area with a continuing level of seismicity and a seismogenic feature is almost as subjective as defining the maximum-magnitude earthquake for an area for which there is no clearly defined seismogenic source and only sparse seismicity. As Chinnery (1979) pointed out, there is no unequivocal way to know with certainty

if the maximum-magnitude earthquake is in a given catalog or not. At the same time, it is not necessarily correct to linearly extrapolate the magnitude-recurrence curve for an area. Youngs and Coppersmith (1985), among others, showed that the difference between the rate of historic seismicity and large characteristic earthquakes in the western United States is nonlinear.

In this study, the *maximum credible earthquake* is defined as the maximum event considered likely in a reasonable amount of time. The phrase "reasonable amount of time" is determined by the historical or geological records. For instance, the reasonable amount of time for the maximum earthquake in the New Madrid Seismic Zone is about 500 to 1,000 years, based on paleoseismic records. The reasonable amount of time for the maximum earthquake in the Wabash Valley Seismic Zone is about 2,000 to 4,000 years. Thus, the probability that MCE ground motion could be exceeded over the bridge life of 75 years varies from zone to zone, about 7% to 14% in the New Madrid Seismic Zone, 2% to 4% in the Wabash Valley Seismic Zone, and less than 2% percent in other zones.

7.3.1. New Madrid Seismic Zone

The largest earthquakes to have occurred in the New Madrid Seismic Zone are the 1811–1812 New Madrid series. Nuttli (1973a) used the falloff-of-intensity technique to estimate the $m_{b,Lg}$ magnitudes of the three largest events in the sequence (i.e., December 16, 1811, at 2:15 a.m.; January 23, 1812; and February 7, 1812) to be 7.2, 7.1, and 7.4 (M7.3, 7.2, and 7.7), respectively. Street (1982), working with a more complete set of intensity estimates, concurred with Nuttli's (1973a) magnitude estimates. Hough and others (2000) lowered several of the MM intensities assigned to communities in the central and eastern United States by Nuttli (1973a) and Street (1982), and argued that the large area of liquefaction observed in the Upper Mississippi Embayment was the result of unusually soft soil conditions. Based on these revisions, Hough and others (2000) suggested that the magnitude of the largest earthquake in the 1811–1812 New Madrid sequence, the earthquake of February 7, 1812, was approximately M7.4 to 7.5. On the other hand, Atkinson (2001) argued that the MM intensities for the New Madrid earthquakes are broadly consistent with the M8 extrapolated from the Atkinson and Boore (1995) relationship.

In this study, the maximum credible earthquake is the largest earthquake of the 1811–1812 sequence, which occurred on February 7, 1812, with a magnitude of M7.7. The maximum credible earthquake will occur along the central seismicity zone (Fig. 4-5).

7.3.2. Wabash Valley Seismic Zone

Nuttli and Herrmann (1978) concluded that the maximum-magnitude event for the Wabash Valley Seismic Zone is an $m_{b,Lg}$ 6.6 (M6.8) event. Using a very different approach, Johnston and Nava (1990) concluded that what they referred to as the “Wabash Lobe” of their seismic zone B is capable of a maximum-magnitude event of $m_{b,Lg}$ 6.5 (M6.6). Recent paleoliquefaction studies (Obermeier and others, 1991; 1993; Pond and Martin, 1997) suggested that several large earthquakes (M7.0 or larger) occurred in the geologic history. A closer examination of the paleoliquefaction studies indicated that the magnitudes are in the range of

M6.0 to 7.0, however (Street and others, 2004). Olson and others (2005) revised the magnitude estimates of Obermeier and others (1991; 1993) and Pond and Martin and gave a magnitude estimate about 0.6 unit lower. The maximum credible earthquake of $m_{b,Lg}$ 6.5 (M6.6) is used in this study for the Wabash Valley Seismic Zone.

7.3.3. Eastern Tennessee and Giles County Seismic Zones

The Eastern Tennessee and Giles County Seismic Zones are located in similar structural environments, a compressional reactivation of Iapetan faults (Wheeler, 1995). Bollinger and others (1992) considered that the two seismic zones have similar maximum-magnitude earthquakes of $m_{b,Lg}$ 6.3. This event was used as the 500-year earthquake in the KTC-96-4 report (Street and others, 1996). In this study, an event of $m_{b,Lg}$ 6.3 was the maximum credible earthquake for the Eastern Tennessee and Giles County Seismic Zones.

The ground motion generated from the *maximum credible earthquake* is called the *maximum credible earthquake ground motion. MCE* is equivalent to the ground motion with a 90 percent probability of not being exceeded in 500 years, specified in the KTC-96-4 report (Street and others, 1996). *MCE* is similar to the "*maximum considered earthquake"* ground motion defined in the 2003 Recommended LRFD Guidelines for the Seismic Design of Highway Bridges (MCEER, 2001). *MCE* is also equivalent to the "*upper-level* earthquake" ground motion specified in the 2006 Seismic Retrofiting Manual for Highway Structures (FHWA, 2006). The maximum median peak (horizontal) ground acceleration, and short-period (0.2 s) and long-period (1.0 s) response accelerations $\mathbf{S_S}$ and $\mathbf{S_1}$ with 5% damping, for the MCE were developed in this study for Kentucky and are shown in Figures 7-9 through 7-11. Figure 7-12 shows the recommended zones of time histories and response spectra for MCE. The data for the recommended time histories and response can be downloaded by following these steps: (1)- Go to web site: http://www.ktc.uky.edu/ ; (2)- Click on "Research", (3)- Click on "Reports by Section"; and (4)- Go to "Structures" and Report Number "KTC-07-07/SPR246-02-6F".

The derivation of the "Acceleration Design Response Spectrum" is presented in Appendix -I and the derivation of the "Time History" is presented in Appendix -II.

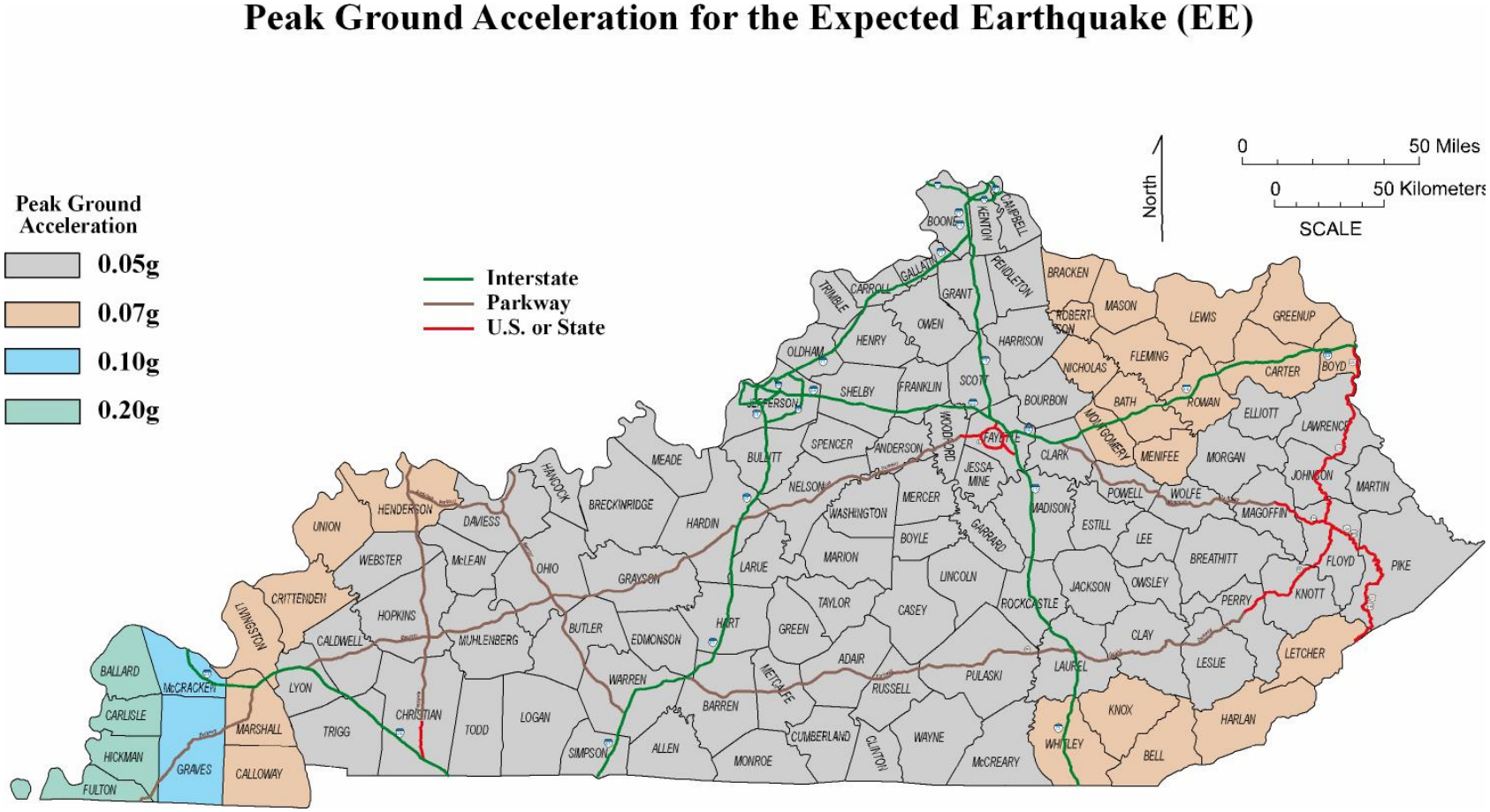

Figure 7-1. Expected Earthquake (EE) Peak Ground Acceleration for the Commonwealth of Kentucky, Site Class A (Hard Rock)

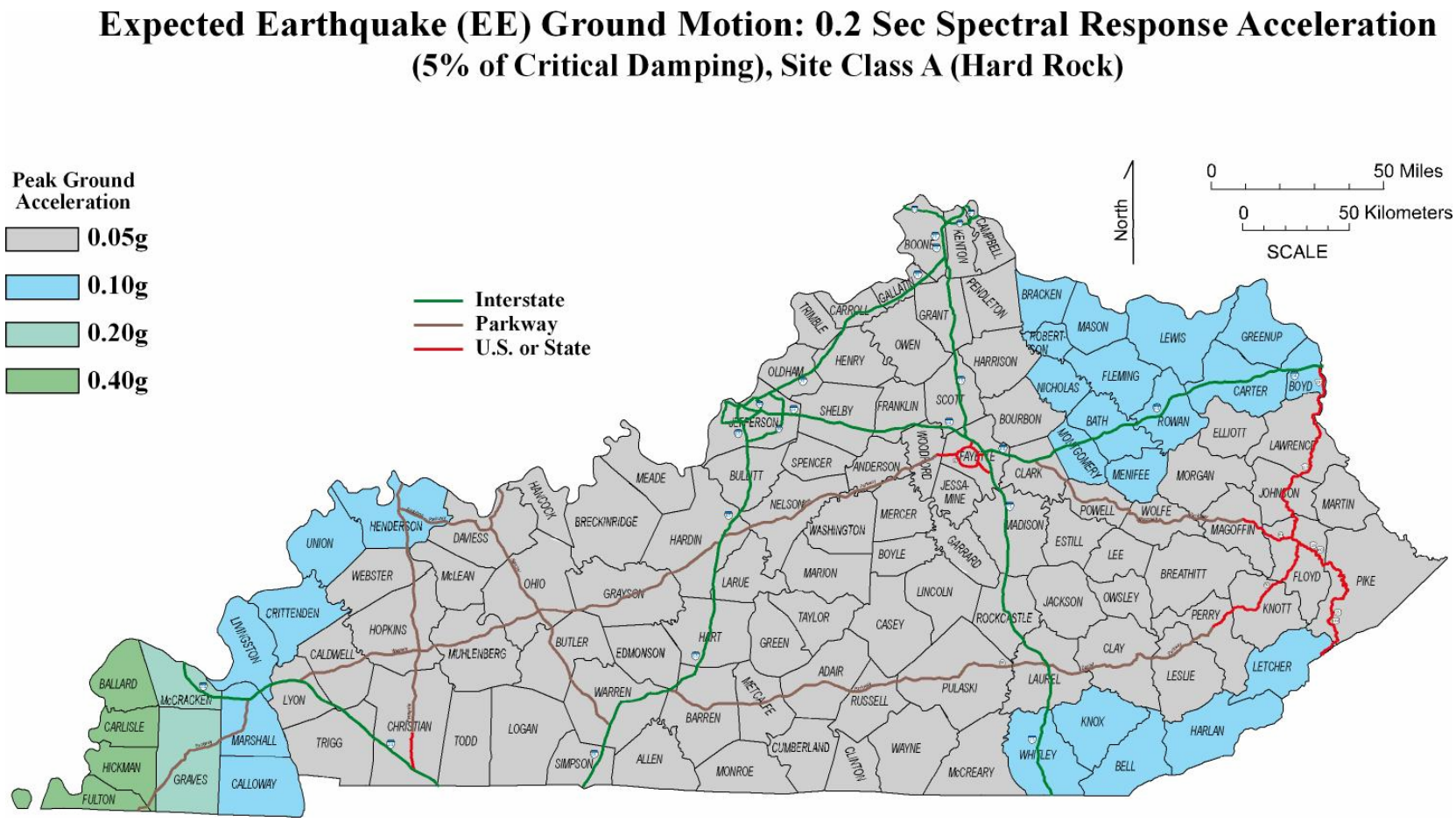

Figure 7-2. Expected Earthquake (EE) Ground Motion for the Commonwealth of Kentucky: 0.2-Sec Spectral Response Acceleration, S_s (5% of Critical Damping), Site Class A (Hard Rock)

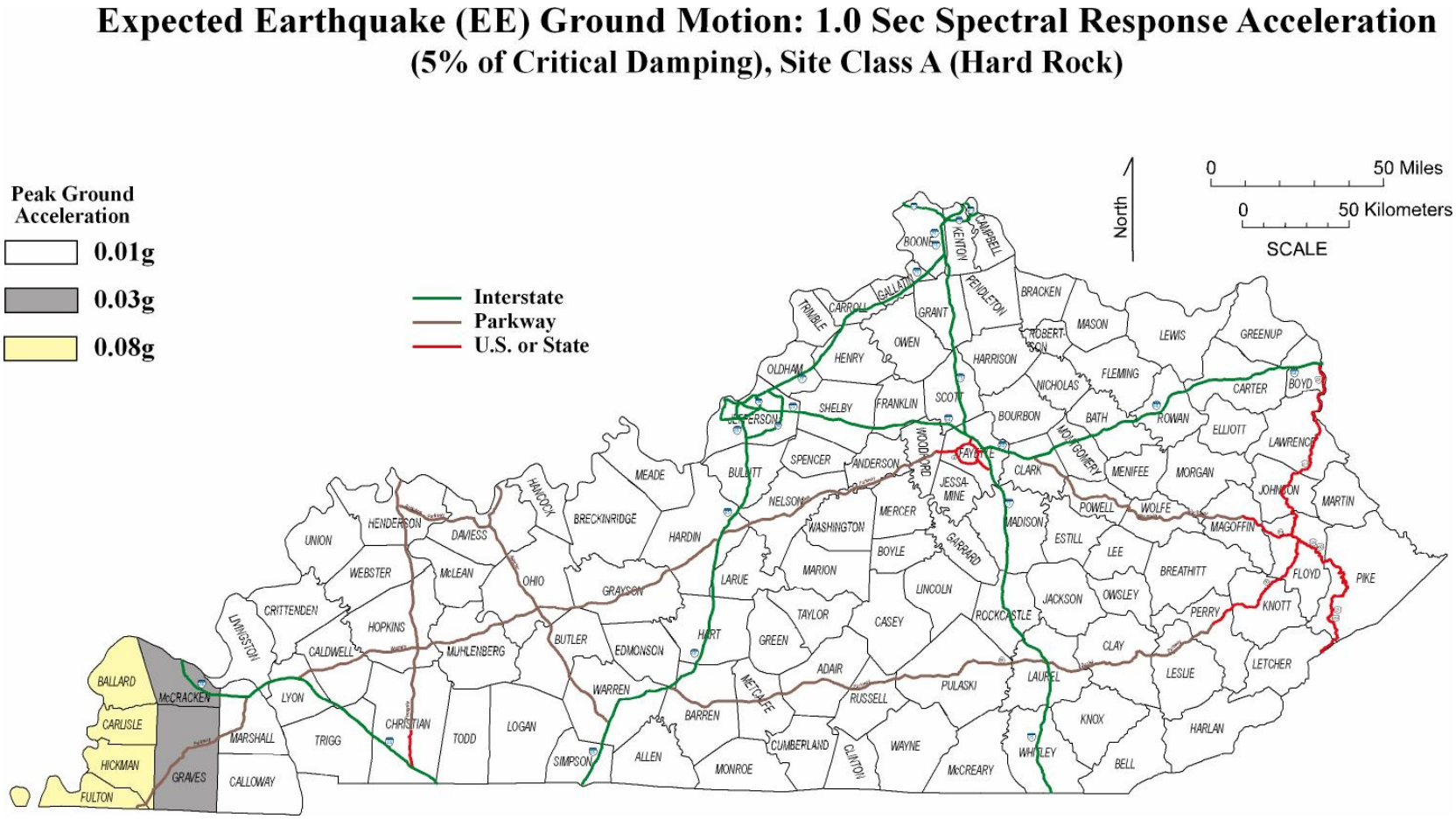

Figure 7-3. Expected Earthquake (EE) Ground Motion for the Commonwealth of Kentucky: 1.0-Sec Spectral Response Acceleration, S_1 (5% of Critical Damping), Site Class A (Hard Rock)

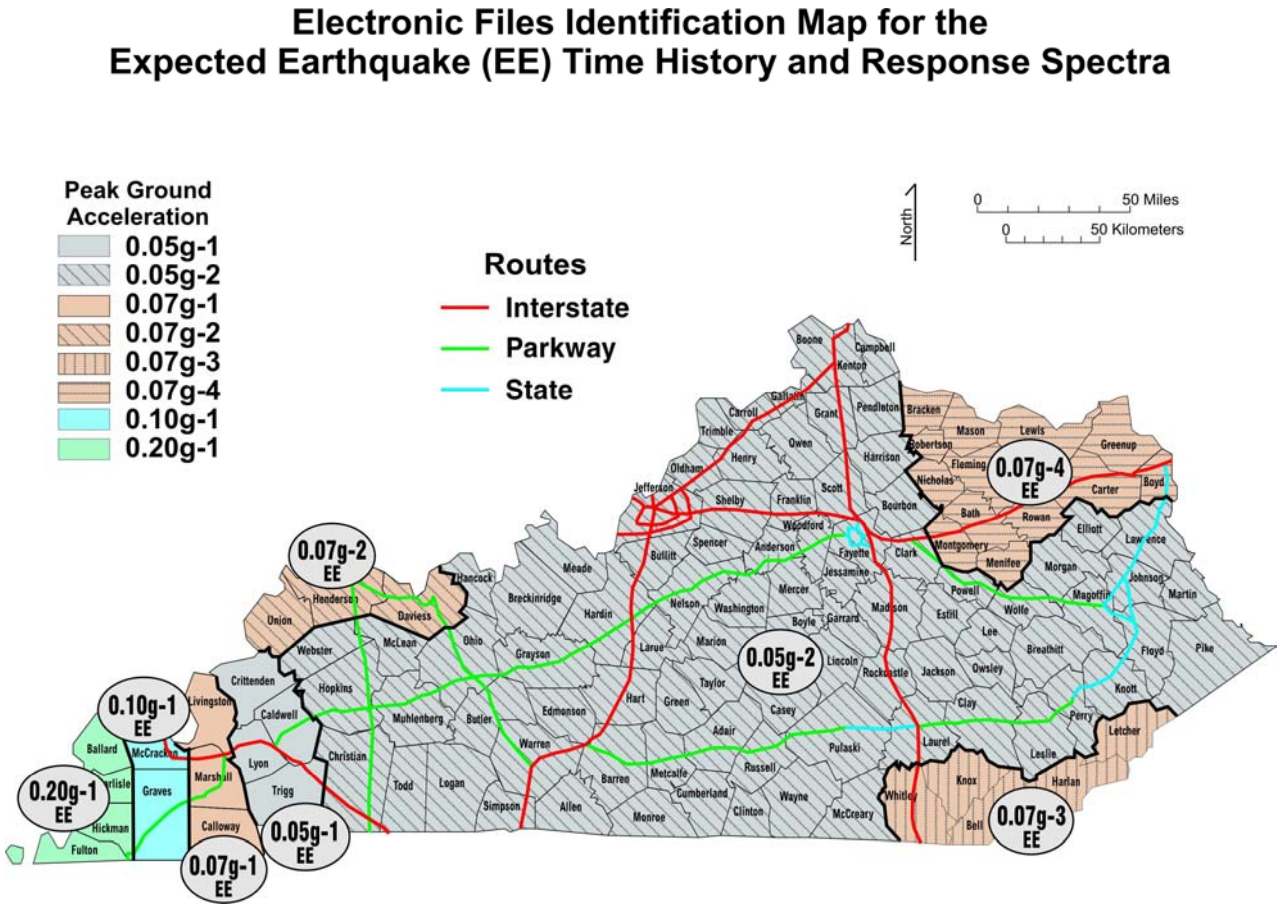

Figure 7-4. Electronic Files Identification Map for the Expected Earthquake (EE) Time History and Response Spectra for the Commonwealth of Kentucky

(Note: The data and guidelines for generating the time histories and response spectra can be downloaded by following these steps: (1)- Go to web site: http://www.ktc.uky.edu/ ; (2)- Click on "Research", (3)- Click on "Reports by Section"; and (4)- Go to "Structures" and Report Number "KTC-07-07/SPR246-02-6F")

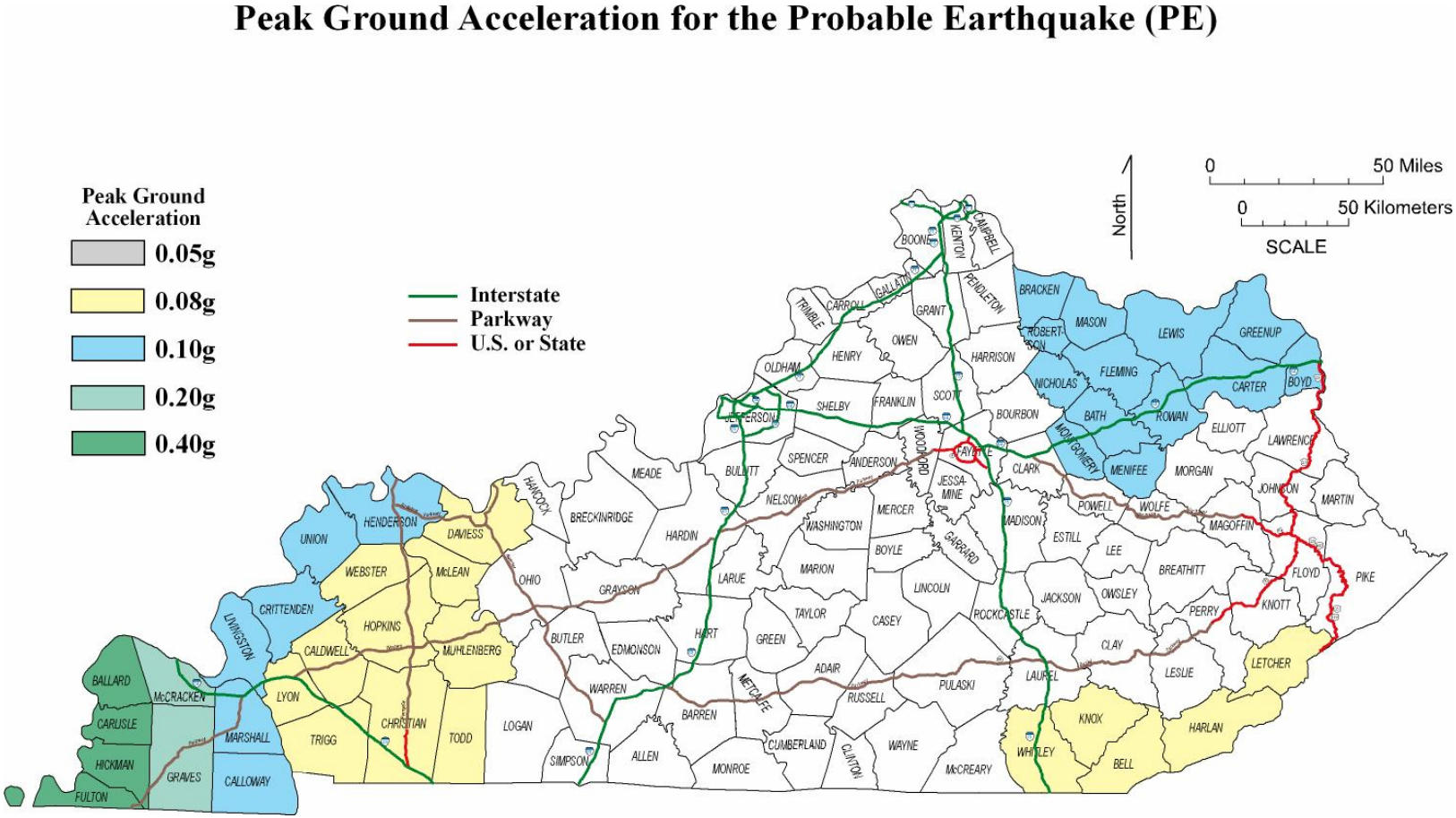

Figure 7-5. Probable Earthquake (PE) Peak Ground Acceleration for the Commonwealth of Kentucky, Site Class A (Hard Rock)

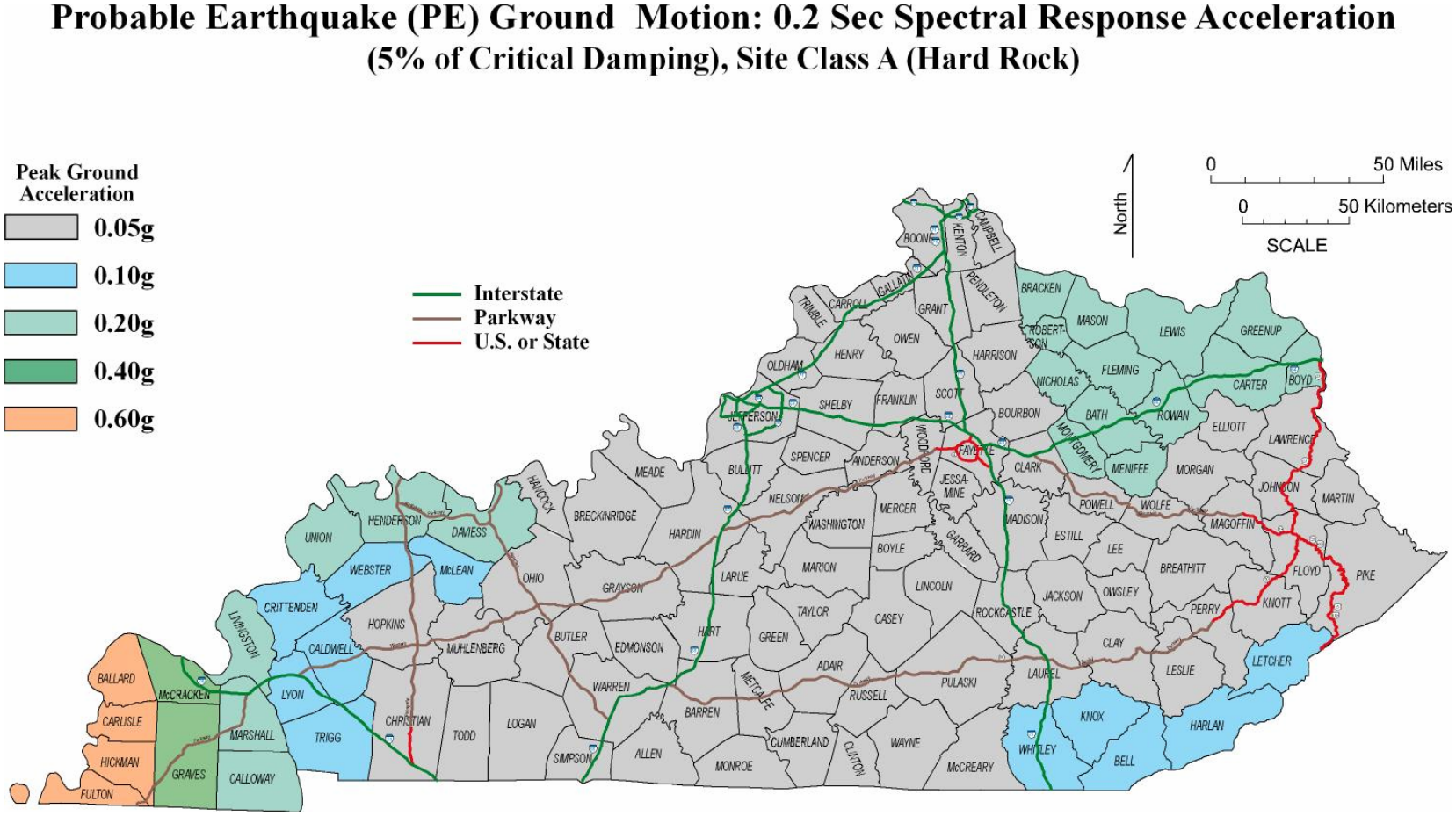

Figure 7-6. Probable Earthquake (PE) Ground Motion for the Commonwealth of Kentucky: 0.2-Sec Spectral Response Acceleration, S_s (5% of Critical Damping), Site Class A (Hard Rock)

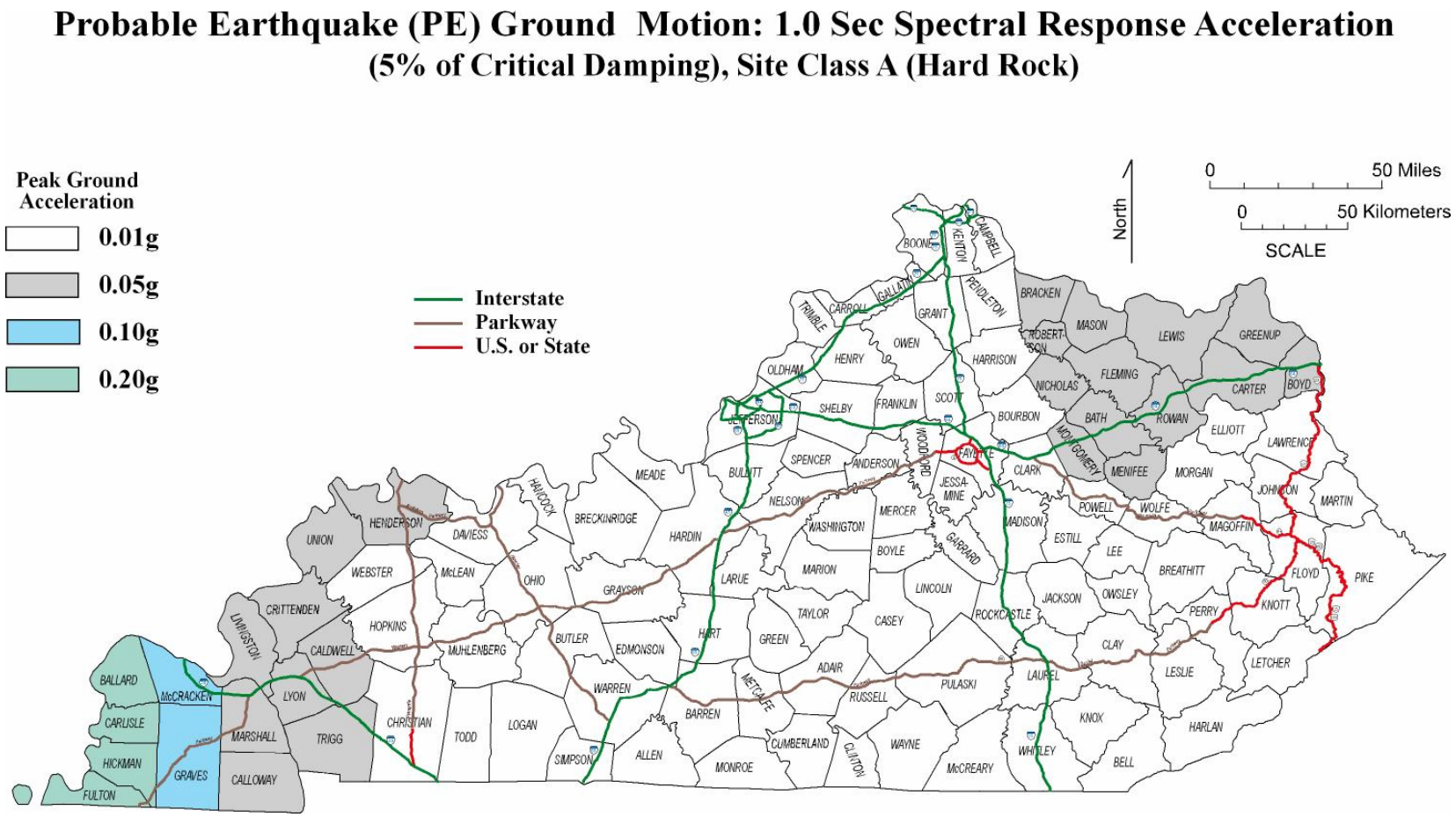

Figure 7-7. Probable Earthquake (PE) Ground Motion for the Commonwealth of Kentucky: 1.0-Sec Spectral Response Acceleration, S_1 (5% of Critical Damping), Site Class A (Hard Rock)

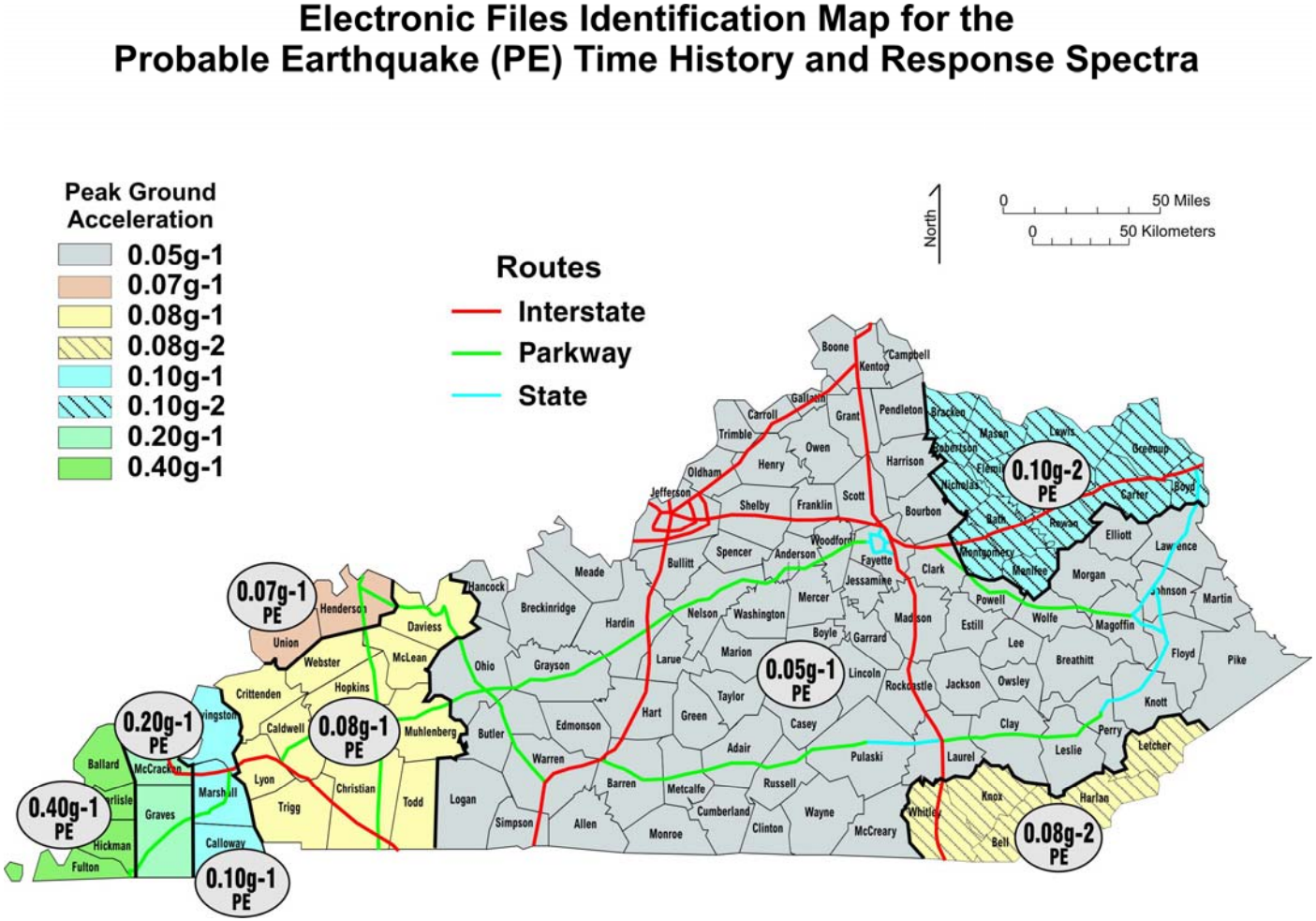

Figure 7-8. Electronic Files Identification Map for the Probable Earthquake (PE) Time History and Response Spectra for the Commonwealth of Kentucky

(Note: The data and guidelines for generating the time histories and response spectra can be downloaded by following these steps: (1)- Go to web site: http://www.ktc.uky.edu/ ; (2)- Click on "Research", (3)- Click on "Reports by Section"; and (4)- Go to "Structures" and Report Number "KTC-07-07/SPR246-02-6F")

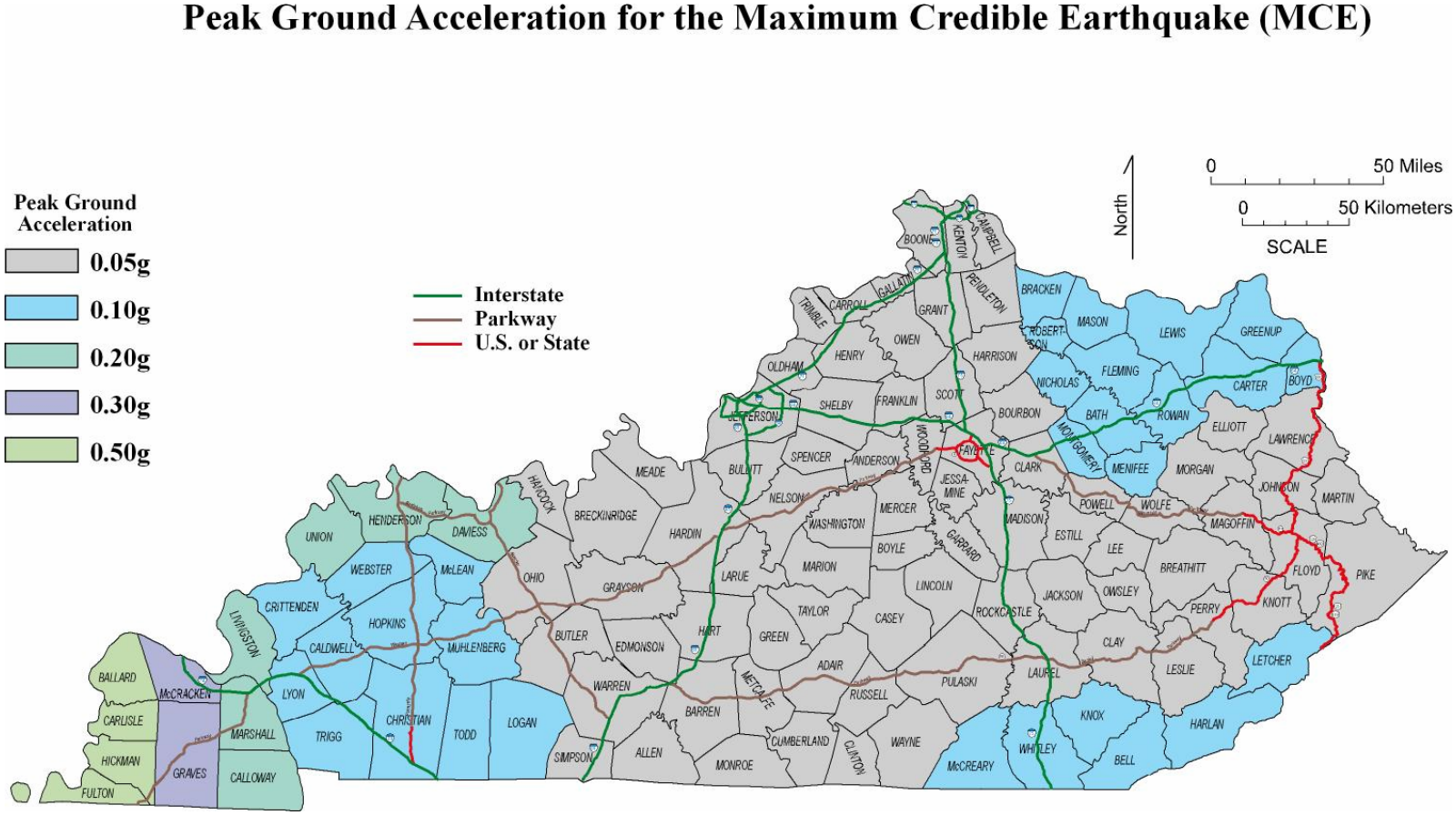

Figure 7-9. Maximum Credible Earthquake (MCE) Peak Ground Acceleration for the Commonwealth of Kentucky, Site Class A (Hard Rock)

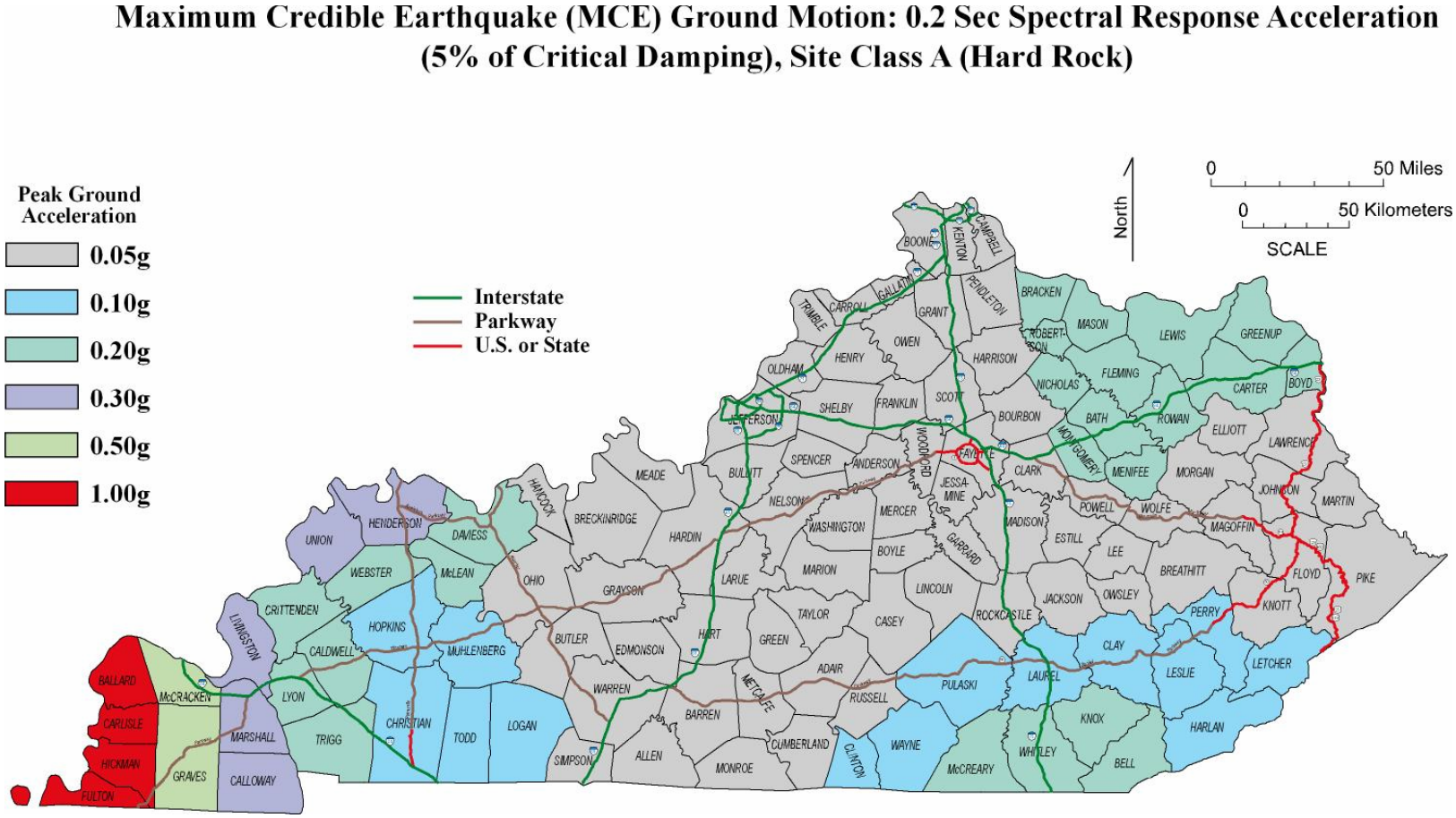

Figure 7-10. Maximum Maximum Credible Earthquake (MCE) Ground Motion for the Commonwealth of Kentucky: 0.2-Sec Spectral Response Acceleration, S_s (5% of Critical Damping), Site Class A (Hard Rock)

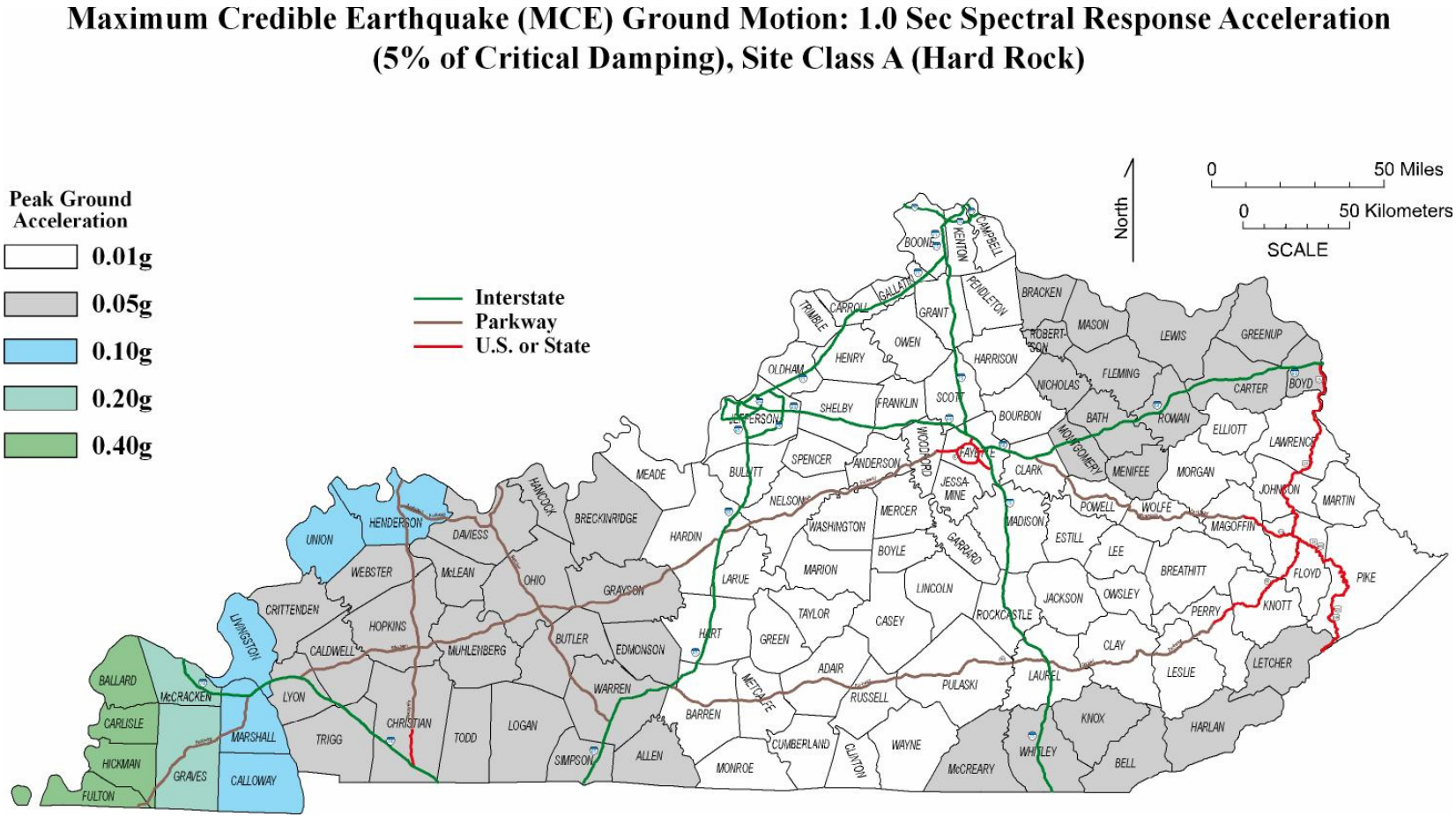

Figure 7-11. Maximum Credible Earthquake (MCE) Ground Motion for the Commonwealth of Kentucky: 1.0-Sec Spectral Response Acceleration, S_1 (5% of Critical Damping), Site Class A (Hard Rock)

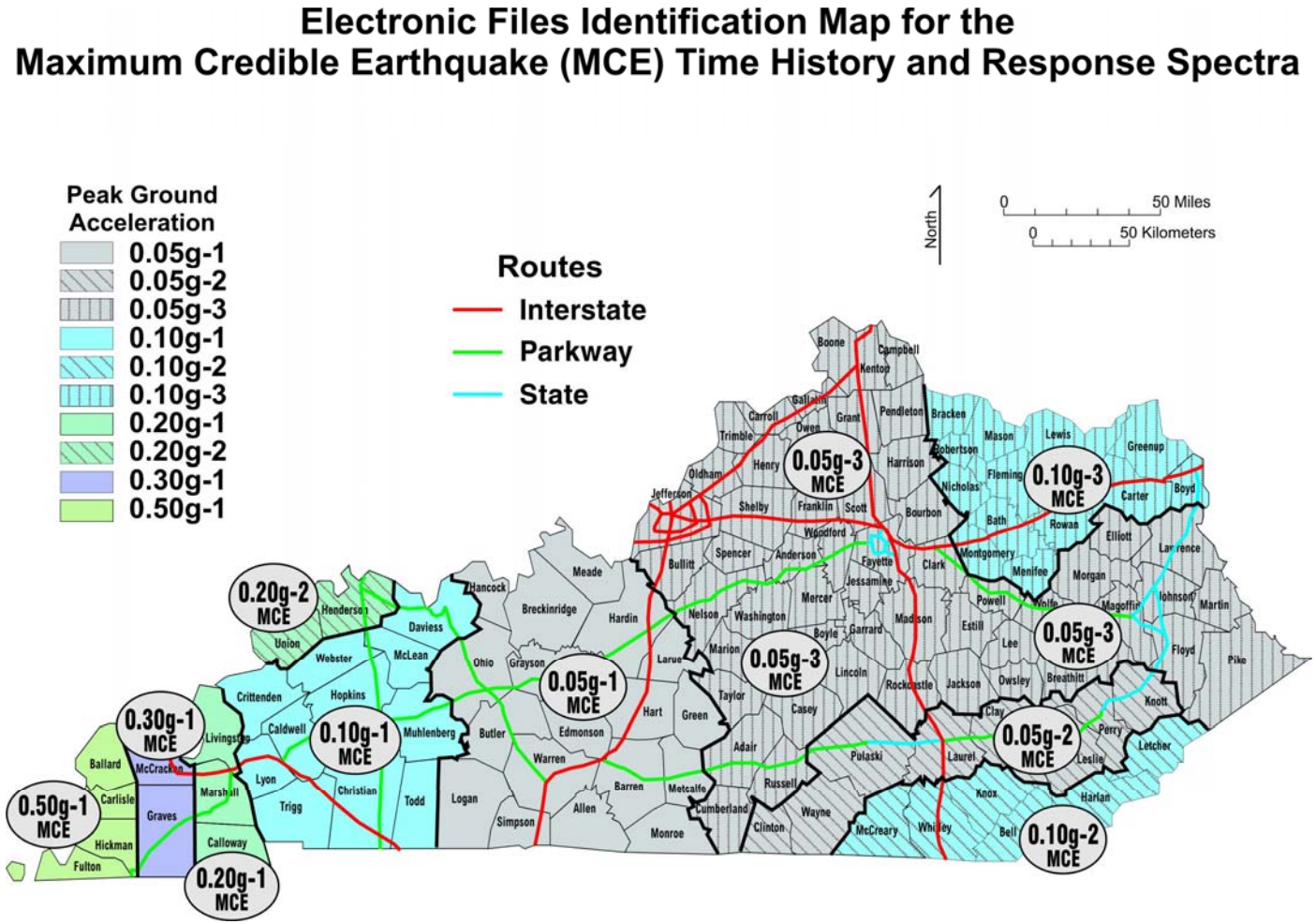

Figure 7-12. Electronic Files Identification Map for theMaximum Credible Earthquake (MCE) Time History and Response Spectra for the Commonwealth of Kentucky

(Note: The data and guidelines for generating the time histories and response spectra can be downloaded by following these steps: (1)- Go to web site: http://www.ktc.uky.edu/ ; (2)- Click on "Research", (3)- Click on "Reports by Section"; and (4)- Go to "Structures" and Report Number "KTC-07-07/SPR246-02-6F")

8. CONCLUSIONS AND RECOMMENDATIONS

In Kentucky, as well as in the central United States, the question is not "do we have earthquakes, seismic hazards, and risk?" but "where, how big, how often, and how strong?" Even though the New Madrid Seismic Zone in the central United States is well known and well studied, we still do not fully understand many aspects of earthquakes here, including source mechanics and location. The biggest historical earthquakes to have occurred in the central United States were the 1811–1812 New Madrid events. The estimated magnitude ranged from about M7 to M8—a large range, though it has been well studied. Earthquakes are also infrequent, especially large earthquakes that have significant impacts on humans and structures. Limited paleoseismic data suggest the recurrence intervals for large earthquakes in the New Madrid Seismic Zone are about 500 to 1,000 years and about 2,000 to 4,000 years in the Wabash Valley Seismic Zone; they are even longer in other zones. There is no ground-motion record from large earthquakes for the central United States. All the ground-motion attenuation relationships were developed based on numerical modeling and sparse strong-motion records from small earthquakes. All these models show that there is a large uncertainty inherent in seismic-hazard and risk estimates in Kentucky.

Seismic hazard and risk are two fundamentally different concepts. Seismic hazard describes ground motion and its associated return period, whereas seismic risk describes probability of a ground motion being exceeded over a period. The relationship between seismic hazard and risk is complicated and must be treated very cautiously. Seismic risk depends not only on seismic hazard and exposure, but also on the models (i.e., time-independent [Poisson] and time-dependent) that could be used to describe the occurrences of earthquakes. There is still confusion between seismic hazard and risk, however. For example, maps showing ground motions with 10, 5, and 2 percent PE in 50 years depict seismic risk by definition, but have been called hazard maps (Frankel and others, 1996, 2002). This project is an effort to predict or estimate seismic hazard: the ground motions that could be expected in Kentucky in a certain period, 75, 250, and 500 to several thousand years.

The purpose of seismic-hazard analysis, either PSHA or DSHA, is to provide an estimate of seismic hazard: a level of ground motion and its return period or annual probability of exceedance. Although PSHA is the most widely used method to assess seismic hazard, it contains some technical difficiencies (Wang and others, 2003, 2005; Wang, 2005, 2006; Wang and Ormsbee, 2005). These technical difficiencies make PSHA difficult to use and understand (Wang and others, 2003, 2005; Wang, 2005, 2006; Wang and Ormsbee, 2005). DSHA develops a particular seismic scenario upon which a ground-motion hazard evaluation is based. The scenario consists of the postulated occurrence of an earthquake of a specified size at a specified location. DSHA addresses the ground motion from individual (i.e., maximum magnitude, maximum credible or maximum considered) earthquakes. Ground motion derived from DSHA represents ground motion from an individual earthquake. In the central United States, the earthquakes that are of engineering significance are infrequent and large. Therefore, DSHA is more appropriate for use in the central United States.

This study determined the ground-motion hazard for three earthquake scenarios (*expected earthquake*, *probable earthquake*, and *maximum credible earthquake*) on the free surface in hard

rock (shear-wave velocity >1,500 m/s) using deterministic seismic-hazard analysis. Response spectra and time histories were derived as part of this study. The results are based on (1) historical observations, (2) instrumental records, and (3) our best understanding of the earthquake source, recurrence, and ground-motion attenuation relationship in the central United States. There are uncertainties in the results because of uncertainties inherent in the input parameters, such as earthquake location, magnitude, and frequency. The emphasis of this study is on earthquakes that would have major impacts. The study provides ground-motion parameters for the seismic design of highway structures and bridges in Kentucky.

The ground-motion parameters, including time histories, are intended for use at sites where the structure is assumed to be situated at the top of a bedrock foundation. For sites underlain by soils, and in particular for sites underlain by poorly consolidated soils, we recommend that site-specific investigations be conducted by qualified professionals in order to determine the possibilities of amplification, liquefaction, slope failure, and other problems when subjected to ground motion.

REFERENCES CITED

Anderson, J.G., 1997, Seismic energy and stress-drop parameters for a composite source model: Bulletin of the Seismological Society of America, v. 87, p. 85–96.

Anderson, J.G., Graves, R., Zeng, Y., and Somerville, P., 2003, Blind prediction of near-fault strong ground motions caused by the Mw 7.9 Alaska earthquake: Seismological Research Letters, v. 74, p. 244–245.

Atkinson, G.M., 2001, Linking historical intensity observations with ground-motion relations for eastern North America: Seismological Research Letters, v. 72, p. 560–574.

Atkinson, G., and Boore, D., 1995, New ground-motion relations for eastern North America: Bulletin of the Seismological Society of America, v. 85, p. 17–30.

Atkinson, G.M., and Silva, W., 1997, An empirical study of earthquake source spectra for California earthquakes: Bulletin of the Seismological Society of America, v. 87, p. 97–113.

Bakun, W.H., and Hopper, M.G., 2004, Historical seismic activity in the central United States: Seismological Research Letters, v. 75, p. 564–574.

Bakun, W., Johnston, A.C., and Hopper, M.G., 2003, Estimating locations and magnitudes of earthquakes in eastern North America from modified Mercalli intensities: Bulletin of the Seismological Society of America, v. 93, p. 190–202.

Bear, G.W., Rupp, J.A., and Rudman, A.J., 1997, Seismic interpretations of the deep structure of the Wabash Valley Fault System: Seismological Research Letters, v. 68, p. 624–640.

Beresnev, I.A., and Atkinson, G.M., 1997, Modeling finite-fault radiation from ωn spectrum: Bulletin of the Seismological Society of America, v. 87, p. 67–84.

Bollinger, G.A., Davison, F.C., Sibol, M.S., and Birch, J.B. 1989, Magnitude recurrence relations for the southeastern U.S. and its subdivisions: Journal of Geophysical Research, v. 94, p. 2857–2873.

Bollinger, G.A., Sibol, M.S., and Chapman, M.C., 1992, Maximum magnitude estimation for an intraplate setting—Example: The Giles County, Virginia, Seismic Zone: Seismological Research Letters, v. 63, p. 139–152.

Bollinger, G.A., and Wheeler, R.L., 1983, The Giles County, Virginia, Seismic Zone: Science, v. 219, p. 1063–1065.

Boore, D.M., 1983, Stochastic simulation of high-frequency ground motions based on seismological models of radiated spectra: Bulletin of the Seismological Society of America, v. 73, p. 1865–1894.

Boore, D.M., and Atkinson, G.A., 1987, Stochastic prediction of ground motion and spectral response parameters at hard-rock sites in eastern North America: Bulletin of the Seismological Society of America, v. 77, p. 440–467.

Brune, J.N., 1970, Tectonic stress and the spectra of seismic shear waves from earthquakes: Journal of Geophysical Research, v. 75, p. 4997–5009.

Brune, J.N., 1971, Correction: Journal of Geophysical Research, v. 76, p. 5002.

Building Seismic Safety Council (BSSC), 1998, NEHRP recommended provisions for seismic regulations for new buildings [1997 ed.]: Federal Emergency Management Agency, 337p.

Caltrans, 1999, Seismic design methodology, memo to designers 20-1, January 1999.

Campbell, K.W., 2003, Prediction of strong ground motion using the hybrid empirical method and its use in the development of ground motion (attenuation) relations in eastern North America: Bulletin of the Seismological Society of America, v. 93, p. 1012–1033.

Chapman, M.C., Powell, C.A., Vlahovic, G., and Sibol, M.S., 1997, A statistical analysis of earthquake focal mechanisms and epicenter locations in the Eastern Tennessee Seismic Zone: Bulletin of the Seismological Society of America, v. 87, p. 1522–1536.

Chinnery, M.A., 1979, Investigations of the seismological input to the safety design of nuclear power reactors in New England: U.S. Nuclear Regulatory Commission, NUREG/CR-0563, 72 p.

Chiu, J.-M., Johnston, A.C., and Yang, Y.T., 1992, Imaging the active faults of the central New Madrid Seismic Zone using PANDA array data: Seismological Research Letters, v. 63, p. 375–393.

Cornell, C.A., 1968, Engineering seismic risk analysis: Bulletin of the Seismological Society of America, v. 58, p. 1,583–1,606.

Cornell, C.A., and Winterstein, S.R., 1986, Applicability of the Poisson earthquake-occurrence model, *in* Seismic hazard methodology for the central and eastern United States: Electric Power Research Institute, EPRI Research Report NP-4726.

Esteva, L., 1970, Seismic risk and seismic design decisions, *in* Hansen, R.J., ed., Seismic design of nuclear power plants: Cambridge, Mass., MIT Press.

Federal Highway Administration (FHWA), 2006, Seismic Retrofiting Manual for Highway Structures: Part 1-Bridge, Publication No. FHWA-HRT-06-032, 610p.

Frankel, A., 1995, Mapping seismic hazard in the central and eastern United States: Seismological Research Letters, v. 66, p. 8–21.

Frankel, A., 2004, How can seismic hazard around the New Madrid Seismic Zone be similar to that in California?: Seismological Research Letters, v. 75, p. 575–586.

Frankel, A., Mueller, C., Barnhard, T., Perkins, D., Leyendecker, E.V., Dickman, N., Hanson, S., and Hopper, M., 1996, National seismic-hazard maps—Documentation June 1996: U.S. Geological Survey Open-File Report 96-532, 70 p.

Frankel, A., Petersen, M., Mueller, C., Haller, K., Wheeler, R., Leyendecker, E.V., Wesson, R., Harmsen, S., Cramer, C., Perkins, D., and Rukstales, K., 2002, Documentation for the 2002 update of the national seismic hazard maps: U.S. Geological Survey Open-File Report 02-420, 33 p.

Gupta, R.S.,1989, Hydrology and hydraulic systems: Englewood Cliffs, N.J., Prentice-Hall, 739p.

Hanks, T.C., and Kanamori, H., 1979, A moment magnitude scale: Journal of Geophysical Research, v. 84, p. 2348–2360.

Hanks, T.C., and McGuire, R.K., 1981, The character of high frequency strong ground motion: Bulletin of the Seismological Society of America, v. 71, p. 2071–2095.

Hanson, R.D., Anderson, R.W., Bollinger, G.A., Dodry, R., Huang, J.L., and Ward, D.B., 1980, Reconnaissance report, northern Kentucky earthquake, July 27, 1980: EERI, September 1980, 69 p.

Harmsen, S., Perkins, D., and Frankel, A., 1999, Deaggregation of probabilistic ground motions in the central and eastern United States: Bulletin of the Seismological Society of America, v. 89, p. 1–13.

Hawman, R.B., Chapman, M.C., Powell, C.A., Clippand, J.E., and Ahmed, H.O., 2001, Wide-angle reflection profiling with quarry blasts in the Eastern Tennessee Seismic Zone: Seismological Research Letters, v. 72, p. 108–122.

Herrmann, R.B., and Ammon, C.J., 1997, Faulting parameters of earthquakes in the New Madrid, Missouri, region: Engineering Geology, v. 46, p. 299–311.

Herrmann, R.B., Langston, C.A., and Zollweg, J.E., 1982, The Sharpsburg, Kentucky, earthquake of 27 July, 1980: Bulletin of the Seismological Society of America, v. 72, p. 1219–1239.

Holbrook, J., Autin, W.J., Rittenour, T.M., Marshak, S., and Goble, R.J., 2006, Stratigraphic evidence for millennial-scale temporal clustering of earthquakes on a continental-interior fault: Holocene Mississippi River floodplain deposits, New Madrid seismic zone, USA, Tectonophysics, v. 420, p. 431–454.

Hough, S., Armbruster, J.G., Seeber, L., and Hough, J.F., 2000, On the modified Mercalli intensities and magnitudes of the 1811/1812 New Madrid, central United States earthquakes: Journal of Geophysical Research, v. 105, p. 23,839–23,864.

International Code Council (ICC), 2000, International Building Code.

Johnston, A.C., 1996, Seismic moment assessment of earthquakes in stable continental regions—I. Instrumental seismicity: Journal of Geophysics, v. 124, p. 314–344.

Johnston, A.C., and Nava, S.J., 1990, Seismic hazard assessment in the central United States, *in* Krinitzsky, E.I., and Slemmons, D.B., eds., Neotectonics in earthquake evaluation: Review in Engineering Geology, v. 8, p. 47–58.

Johnston, A.C., Reinbold, D.J., and Brewer, S.I., 1985, Seismotectonics of the southern Appalachians: Bulletin of the Seismological Society of America, v. 75, p. 291–312.

Kafka, A.L., and Levin, S.Z., 1999, Does the spatial distribution of smaller earthquakes delineate areas when larger earthquakes are likely to occur [abs.]: Seismological Research Letters, v. 70, p. 237–238.

Kafka, A.L., and Walcott, J.R., 1998, How well does the spatial distribution of smaller earthquakes forecast the locations of larger earthquakes in the northeastern United States: Seismological Research Letters, v. 69, p. 428–440.

Kim, W., 2003, June 18, 2002 Evansville, Indian Earthquake: Reactivation of ancient rift in the Wabash Valley fault zone?, *Bull. Seism. Soc. Am*., v. 93, p.2201–2211.

Leyendecker, E.V., Hunt, R.J., Frankel, A.D., and Rukstales, K.S., 2000, Development of maximum considered earthquake ground motion maps: Earthquake Spectra, v. 16, p. 21–40.

Liu, H., 1991, Wind engineering, a handbook for structural engineers: Englewood Cliffs, N.J., Prentice-Hall, 209p.

Luco, J.E., and Apsel, R.J., 1983, On the Green's function for a layered half space: Bulletin of the Seismological Society of America, v. 73, p. 909–929.

Malhotra, P.K., 2006, Seismic Risk and Design Loads: *Earthquake Spectra*, v.22, p115–128.

McBride, J.H., Hildenbrand, T.G., Stephenson, W.J., and Potter, C.J., 2002, Interpreting the earthquake source of the Wabash Valley Seismic Zone (Illinois, Indiana, and Kentucky) from seismic reflection, gravity, and magnetic intensity data: Seismological Research Letters, v. 73, p. 660–686.

McGuire, R.K., 2004, Seismic Hazard and Risk Analysis: *Earthquake Engineering Research Institute MNO-10*, 221p.

Milne, W.G., and Davenport, A.G., 1969, Distribution of earthquake risk in Canada: Bulletin of the Seismological Society of America, v. 59, p. 729–754.

Mueller, K. and Pujol, J., 2001, Three-dimensional geometry of the reelfoot blind thrust: Implications for moment release and earthquake magnitude in the New Madrid Seismic Zone: Bulletin of the Seismological Society of America, v. 91, p.1563–1573.

Multidisciplinary Center for Earthquake Engineering Research (MCEER), 2001, Recommended LRFD Guidelines for Seismic Design of Highway Bridges, Part I: Specifications, November 2001.

Munson, P.J., Obermeier, S.F., Munson, C.A., Hajic, E.R., 1997, Liquefaction evidence for Holocene and latest Pleistocene earthquakes in the southern halves of Indiana and Illinois: Apreliminary overview: Seismological Research Letters, v. 68, p. 521–536.

National Research Council, 1988, Probabilistic Seismic Hazard Analysis: Washington, D.C.National Academy Press, 97p.

Nuttli, O.W., 1973a, The Mississippi Valley earthquakes of 1811–1812: Intensities, ground motion and magnitudes: Bulletin of the Seismological Society of America, v. 63, p. 227–248.

Nuttli, O.W., 1973b, Seismic wave attenuation and magnitude relations for eastern North America: Journal of Geophysical Research, v. 78, p. 876–885.

Nuttli, O.W., 1976, Comment on "Seismic intensities, 'size' of earthquakes and related problems" by Jack Evernden: Bulletin of the Seismological Society of America, v. 66, p. 331–338.

Nuttli, O.W., and Herrmann, R.B., 1978, Credible earthquakes in the central United States, *in* State-of-the art for assessing earthquake hazards in the United States: U.S. Army Corps of Engineers Geotechnical Lab Report 12, 99 p.

Obermeier, S.F., Bleuer, N.R., Munson, C.A., Munson, P.J., Martin, W.S., McWilliams, K.M., Tabacznski, D.A., Odum, J.K., Rubin, M., and Eggert, D.L., 1991, Evidence of strong earthquake shaking in the Lower Wabash Valley from prehistoric liquefaction features: Science, v. 251, p. 1061–1063.

Powell, C.A., Bollinger, G.A., Chapman, M.C., Sibol, M.S., Johnston, A.C., and Wheeler, R.L., 1994, A seismotectonic model for the 300-kilometer-long Eastern Tennessee Seismic Zone: Science, v. 264, p. 686–688.

Reiter, L., 1990, Earthquake hazard analysis, issues and insights: New York, Columbia University Press, 254 p.

Saikia, C.K., and Somerville, P.G., 1997, Simulated hard-rock motions in Saint Louis, Missouri, from large New Madrid earthquakes (Mw>=6.5): Bulletin of the Seismological Society of America, v. 87, p. 123–139.

Senior Seismic Hazard Analysis Committee, 1997, Recommendations for probabilistic seismic hazard analysis: Guidance on uncertainty and use of experts: Lawrence Livermore National Laboratory, NUREG/CR-6372, 81 p.

Sexton, J.L., Braile, L.W., Hinze, W.J., and Campbell, M.J., 1996, Seismic reflection profiling studies of a buried Precambrian rift beneath the Wabash Valley Fault Zone: Geophysics, v. 51, p. 640–660.

Shi, B., Wang, Z., and Woolery, E.W., 2006, Source scaling, subevent distributions, and ground-motion simulation in the composite source model: Kentucky Geological Survey, ser. 12, Report of Investigations 14, 16 p.

Somerville, P., Collins, N., Abrahamson, N., Graves, R., and Saikia, C., 2001, Ground motion attenuation relations for the central and eastern United States: Final report to U.S. Geological Survey.

Somerville, P.G., Sen, M.K., and Cohee, B., 1991, Simulation of strong ground motions recorded during the 1985 Michoacan, Mexico, and Valparasio, Chile, earthquakes: Bulletin of the Seismological Society of America, v. 81, p. 1–27.

Stein, R.S., Toda, S., and Parsons, T., 2005, A new probabilistic seismic hazard ssessment for

greater Tokyo [abs.]: 2005 American Geophysical Union Fall Meeting, San Francosco, Calif.

Stein, S., and Wysession, M., 2003, An introduction to seismology, earthquakes, and earth structure: Maldem, Mass., Blackwell Publishing, 498 p.

Stover, C.W., and Coffman, J.L., 1993, Seismicity of the United States, 1568–1989 [reved.]: U.S. Geological Survey Professional Paper 1527, 418 p.

Street, R., 1979, An instrumental $m_{b,Lg}$ magnitude estimate of the 1897 Giles County, Virginia, earthquake: Earthquake Notes, v. 50, no. 2, p. 21–23.

Street, R., 1980, The southern Illinois earthquake of September 27, 1891: Bulletin of the Seismological Society of America, v. 70, p. 915–920.

Street, R., 1982, A contribution to the documentation of the 1811–1812 Mississippi Valley earthquake sequence: Earthquake Notes, v. 53, no. 2, p. 39–52.

Street, R., Bollinger, G.A., and Woolery, E., 2002, Blasting and other mining-related activities in Kentucky: A source of earthquake misidentification: Seismological Research Letters, v. 73, p. 739–750.

Street, R., Bauer, R.A., and Woolery, E.W., 2004, A short note on the magnitude scaling of the prehistorical earthquakes in the Wabash Valley Seismic Zone of the central United States: Seismological Research Letters, v. 75, p. 637–641.

Street, R., and Foley, W., 1982, Architectural and structural damage, and ground effects resulting from the July 27, 1980 Sharpsburg, Ky., earthquake: NITS Publication PBB2-246794, 60 p.

Street, R., and Green, R.F., 1984, The historical seismicity of the central United States, 1811–1928: Contract report for the U.S. Geological Survey, contract 14-08-21251, 550 p.

Street, R., Taylor, K., Jones, D., Harris, J., Steiner, G., Zekulin, A., and Zhang, D., 1993, The 4.6 $m_{b,Lg}$ northeastern Kentucky earthquake of September 7, 1988: Seismological Research Letters, v. 64, p. 187–199.

Street, R., and Turcotte, F.T., 1977, A study of northeastern North American spectral moments, magnitudes and intensities: Bulletin of the Seismological Society of America, v. 67, p. 599–614.

Street, R., Wang, Z., Harik, I.E., Allen, D.L., and Griffin, J.J., 1996, Source zones, recurrence rates, and time histories for earthquakes affecting Kentucky: Kentucky Transportation Center, KTC-96-4, 187 p.

Street, R., Zekulin, A., and Harris, J., 1991, The Meade County, Kentucky, earthquakes of January and March 1990: Seismological Research Letters, v. 62, p. 105–111.

Toro, G.R., Abrahamson, N.A., and Schneider, J.E.F., 1997, Models of strong ground motions from earthquakes in central and eastern North America: Best estimates and uncertainties: Seismological Research Letters, v. 68, p. 41–57.

Toro, G.R., and McGuire, R.K., 1987, An investigation into earthquake ground motion characteristics in eastern North America: Bulletin of the Seismological Society of America, v. 77, p. 468–489.

Tuttle M.P., and Schweig, E.S., 1996, Archaeological and pedological evidence for large prehistoric earthquakes in the New Madrid Seismic Zone, central United States: Geology, v. 23, p. 253–256.

Tuttle, M.P., Schweig, E.S., Sims, J.D., Lafferty, R.H., Wolf, L.W., and Haynes, M.L., 2002, The earthquake potential of the New Madrid Seismic Zone: Bulletin of the Seismological Society of America, v. 92, p. 2080–2089.

Vere-Jones, D., and Ozaki, T., 1982, Some examples of statistical estimation applied to earthquake data, I, Cyclic Poisson and self-exciting models: Annuals of the Institute of Statistics and Mathematics, v. 34, pt. B, p. 189–207.

Wald, D.J., Quitoriano, V., Heaton, T.H., and Kanamori, H., 1999, Relationships between peak ground acceleration, peak ground velocity, and modified Mercalli intensity in California: Earthquake Spectra, v. 15, no. 3, p. 557–564.

Wang, Z., 2006, Understanding Seismic Hazard and Risk Assessments: An Example in the New Madrid Seismic Zone of the Central United States: Proceedings of the 8th National Conference on Earthquake Engineering, April 18-22, 2006, San Francisco, Calif., Paper 416, 10p.

Wang, Z., 2005, Comment on J.U. Klügel's: Problems in the Application of the SSHAC Probability Method for Assessing Earthquake Hazards at Swiss Nuclear Power Plants, in Engineering Geology, vol. 78, pp. 285-307, Engineering Geology, 82**,** p. 86-88.

Wang, Z., and Ormsbee, L., 2005, Comparison between probabilistic seismic hazard analysis and flood frequency analysis: EOS, Transactions of the American Geophysical Union, v. 86, p. 45, 51–52.

Wang, Z., Woolery, E.W., Shi, B., and Kiefer, J.D., 2005, Comment on "How Can Seismic Hazard around the New Madrid Seismic Zone Be Similar to that in California?" by Arthur Frankel: Seismological Research Letters, v. 76, p. 466–471.

Wang, Z., Woolery, E.W., and Shi, B., 2003a, Observed seismicity (earthquake activity) in the Jackson Purchase Region of western Kentucky: January through June 2003: Kentucky Geological Survey, ser. 12, Special Publication 6, 16 p.

Wang, Z., Woolery, E.W., Shi, B., and Kiefer, J.D., 2003b, Communicating with uncertainty: A Critical Issue with Probabilistic seismic hazard analysis: EOS, 84, 501, 506, 508.

Wang, Z, Woolery, E.W., and Schaeffer, J.A., 2003c, A Short Note on Ground-Motion Recordings from the June 18, 2002, Darmstadt, Ind., Earthquake: Seismological Research Letters, 72, p.148-152.

Wheeler, R.L., 1995, Earthquakes and the cratonward limit of Iapetan faulting in eastern North America: Geology, v. 23, p. 105–108.

Wheeler, R.L., 1997, Boundary separating the seismically active Reelfoot Rift from the sparsely seismic Rough Creek Graben, Kentucky and Illinois: Seismological Research Letters, v. 63, p. 586–598.

Wheeler, R.L., and Cramer, C.H., 2002, Updated seismic hazard in the southern Illinois Basin—Geological and geophysical foundations for use in the 2002 USGS national seismic-hazard maps: Seismological Research Letters, v. 73, p. 776–791.

Wheeler, R.L., and Frankel, A., 2000, Geology in the 1996 USGS seismic-hazard maps, central and eastern United States: Seismological Research Letters, v. 71, p. 273–282.

Wood, H.O., and Neumann, F., 1931, Modified Mercalli intensity scale of 1931: Bulletin of the Seismological Society of America, v. 21, p. 277–283.

Woolery, E.W., 2005, Geophysical and geological evidence of Neotectonic deformation along the Hovey Lake fault, Lower Wabash Valley fault system: Bulletin of the Seismological Society of America, v. 95, p. 1193–1201.

Youngs, R.R., and Coppersmith, K.J., 1985, Implications of fault slip rates and earthquake recurrence models to probabilistic seismic hazard estimates: Bulletin of the Seismological Society of America, v. 75, p. 939–964.

Yu, G., 1994, Some aspects of earthquake seismology: Slip partitioning along major convergent plate boundaries; composite source model for estimation of strong motion; and nonlinear soil response modeling: Reno, University of Nevada, Ph.D. dissertation.

Zeng, Y., and Anderson, J.G., 1995, A method for direct computation of the differential seismogram with respect to the velocity change in a layered elastic solid: Bulletin of the Seismological Society of America, v. 85, p. 300–307.

Zeng, Y., Anderson, J.G., and Yu, G., 1994, A composite source model for computing realistic synthetic strong ground motions: Geophysical Research Letters, v. 21, p. 725–728.

Zoback, M.D., Prescott, W.H., and Kroeger, S.W., 1985. Evidence for lower crustal ductile strain localization in southern New York: Nature, v. 317, p. 705–707.

Zoback, M.D., Zoback, M.L., Mount, V.S., Suppe, J., Eaton, J.P., Healy, J.H., Oppenheimer, D., Reasenberg, P., Jones, L., Raleigh, C.B., Wong, I.G., Scotti, O., and Wentworth, C., 1987, New evidence on the state of stress of the San Andreas Fault System: Science, v. 238, p. 1105–1111.

Appendix I

Derivation of the Acceleration Design Response Spectrum

Acceleration Response Spectra Generation
For Counties in the Commonwealth of Kentucky

Example: Generate the Maximum Credible Earthquake Acceleration Response Spectra for McCracken County, KY.

I. Electronic File Identification Map

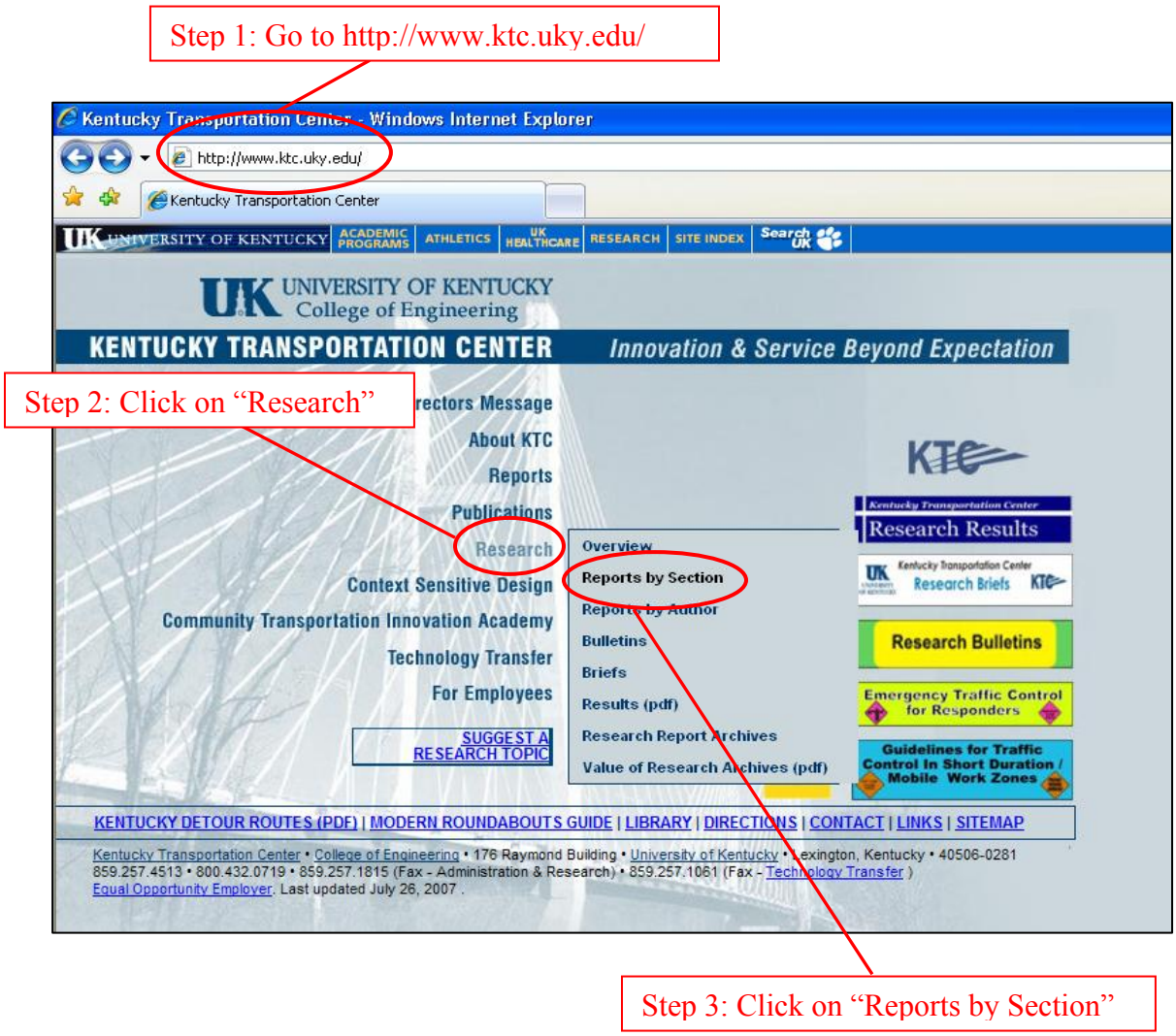

Step 4: Scroll down to “Structures”

Step 5: Go to Report Number "KTC-07-07/SPR246-02-6F"

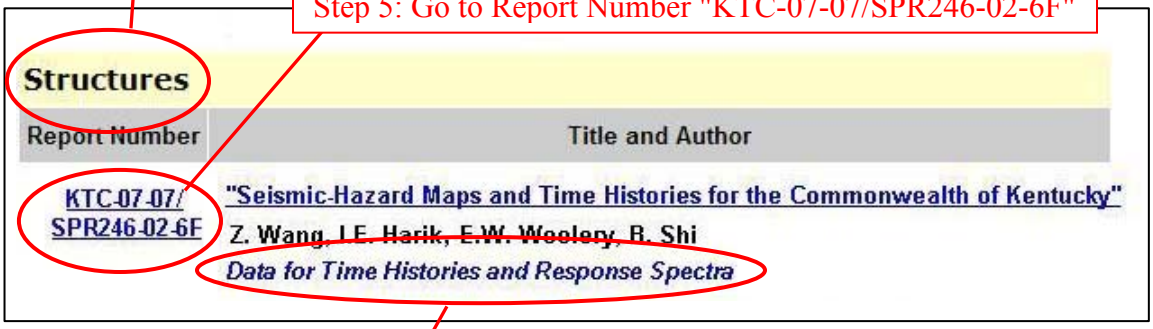

Step 6: Click on “*Data for Time Histories and Response Spectra*”

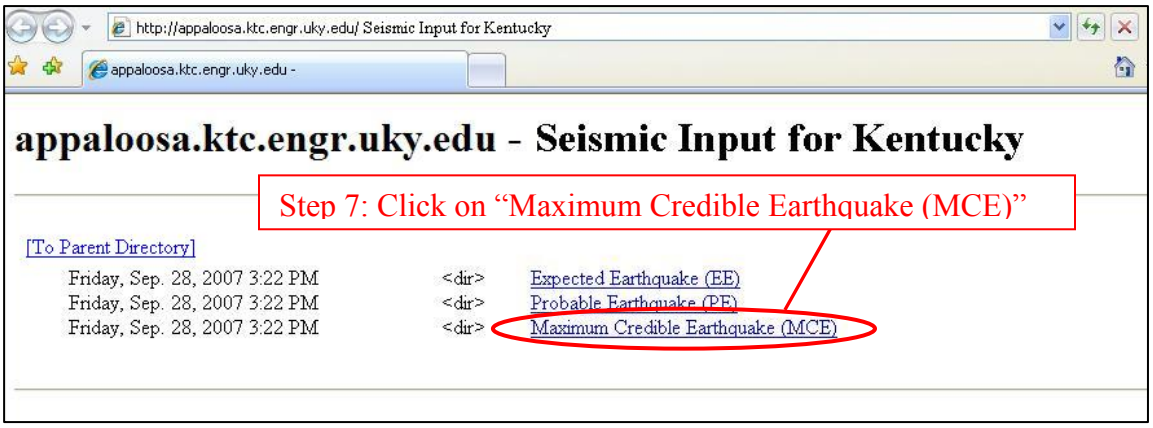

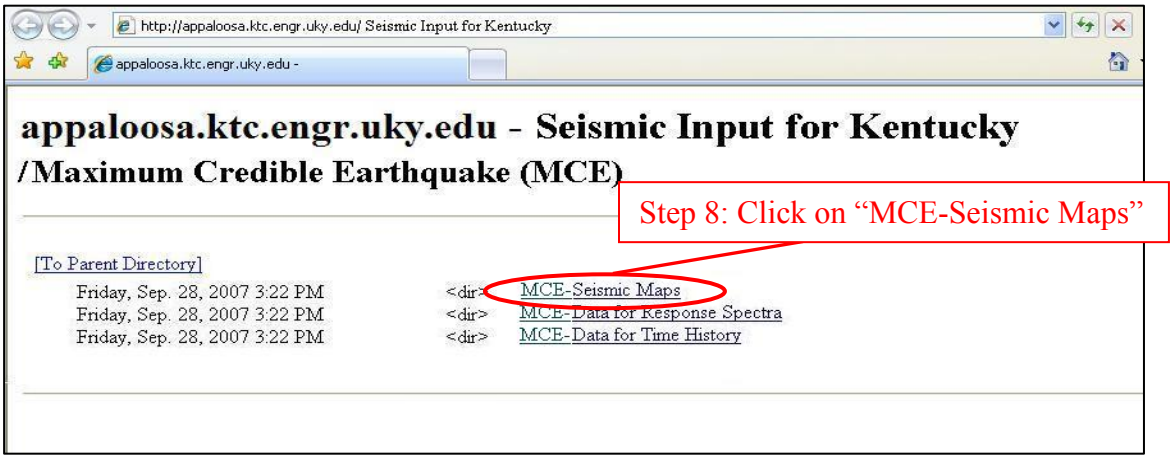

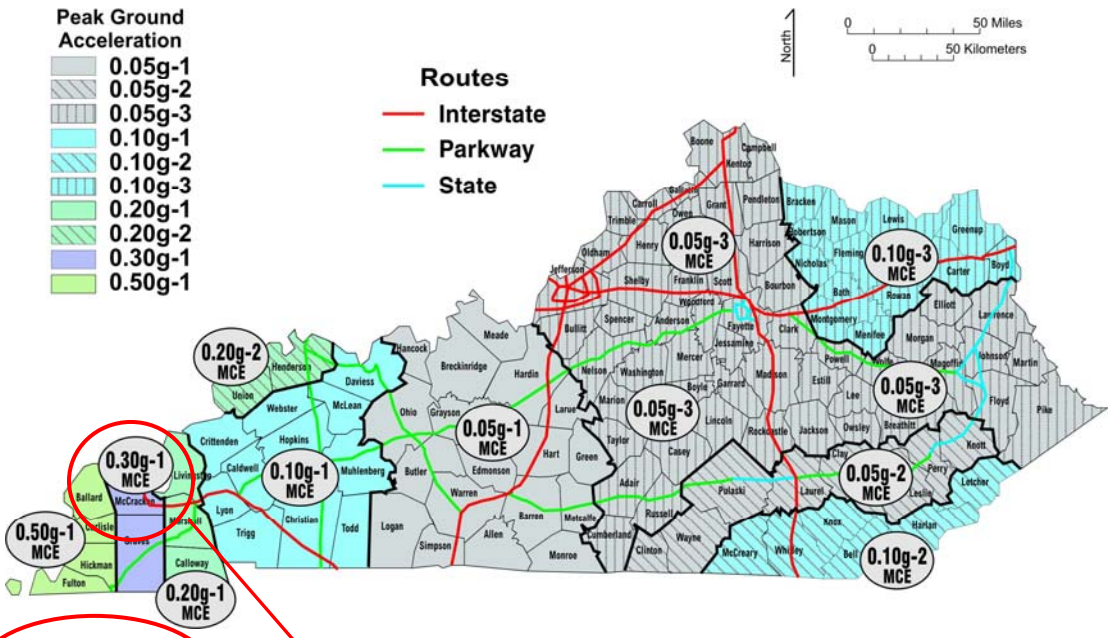

Figure 5-MCE. Electronic Files Identification Map for the Maximum Credible Earthquake (MCE) Time History and Response Spectra for the Commonwealth of Kentucky

Step 9: Go to Figure 5-MCE

Step 10: Locate "*McCracken County, KY*" and the corresponding "Peak Ground Acceleration" (0.30g-1 MCE for this example)

II. Acceleration Response Spectra

Step 11: Go back to the "Maximum Credible Earthquake (MCE)" Screen

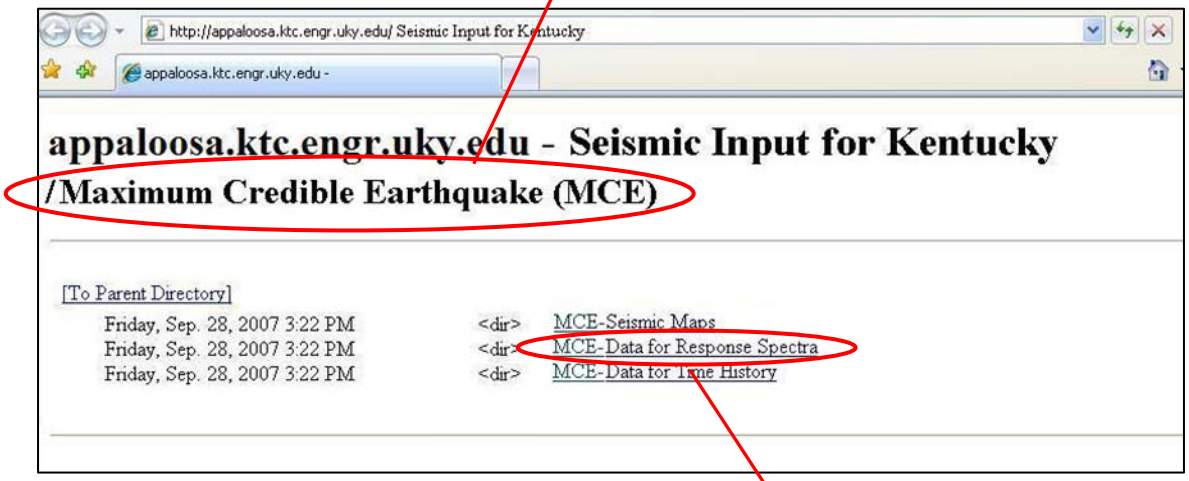

Step 12: Click on "MCE-Data for Response Spectra"

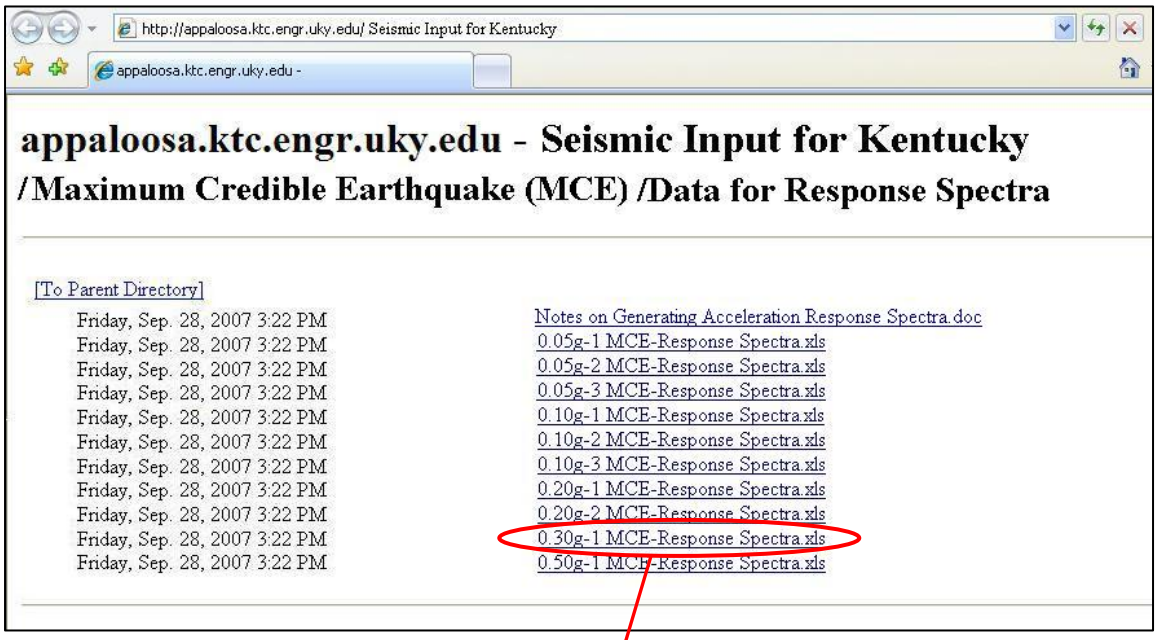

Step 13: Click on "0.30g-1 MCE-Response Spectra.xls"

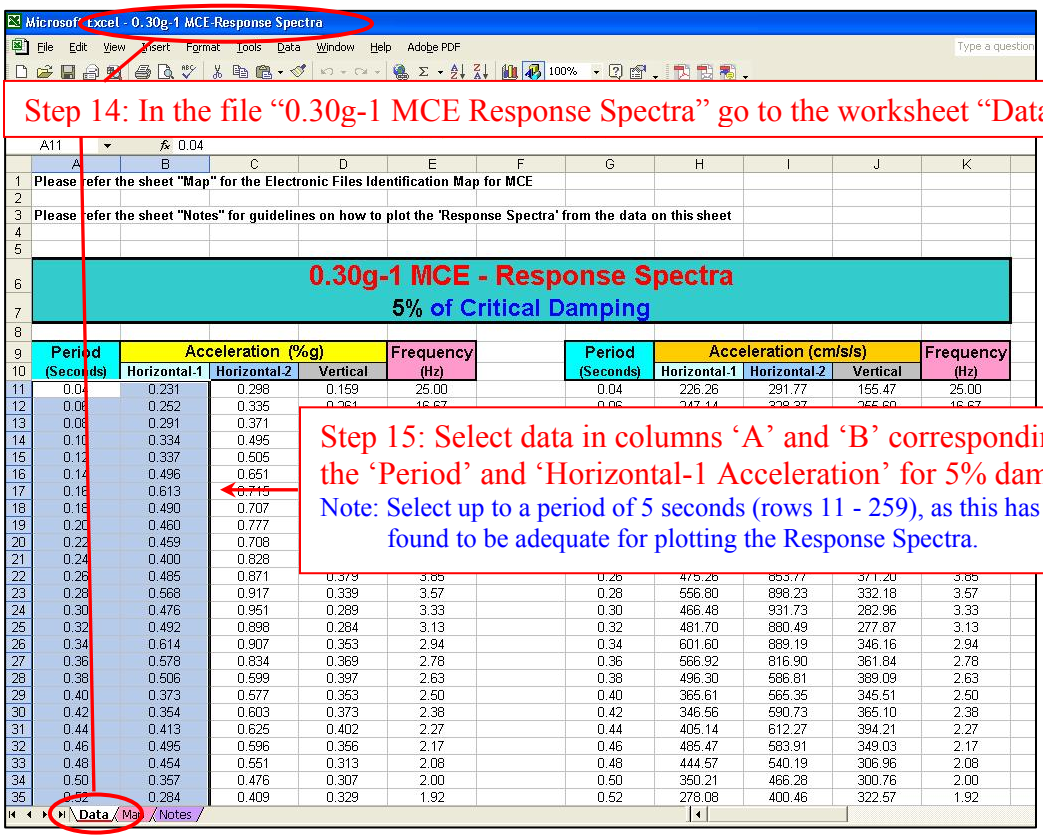

Step 14: In the file "0.30g-1 MCE Response Spectra" go to the worksheet "Data"

Step 15: Select data in columns 'A' and 'B' corresponding to the 'Period' and 'Horizontal-1 Acceleration' for 5% damping

Note: Select up to a period of 5 seconds (rows 11 - 259), as this has been found to be adequate for plotting the Response Spectra.

Step 16: Click "Chart Wizard" button or on the menu click *Insert* → *chart*

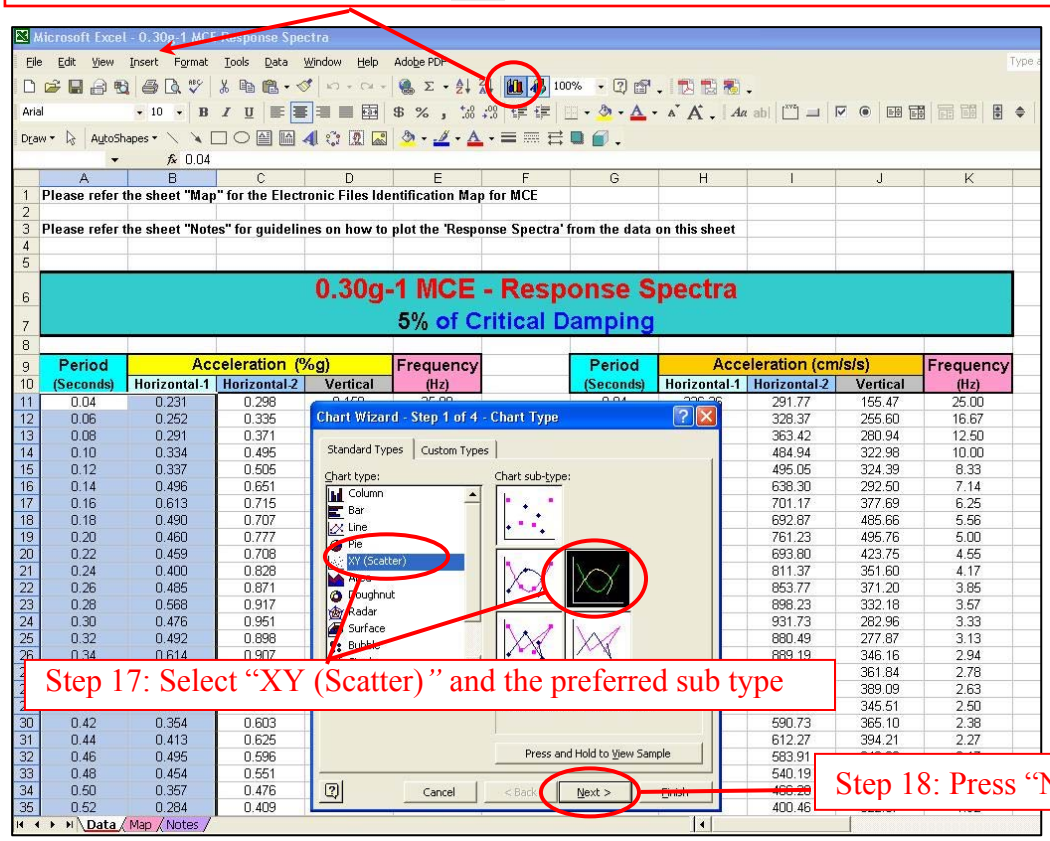

Step 17: Select "XY (Scatter)" and the preferred sub type

Step 18: Press "Next"

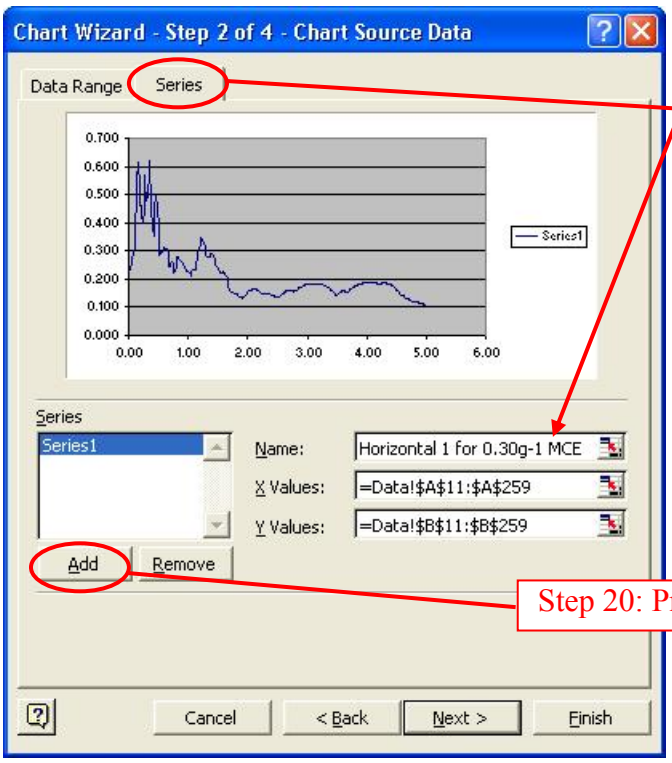

Step 19: Press "Series" tab and enter 'Name' of Series 1

Step 20: Press *"Add"* to enter Series 2

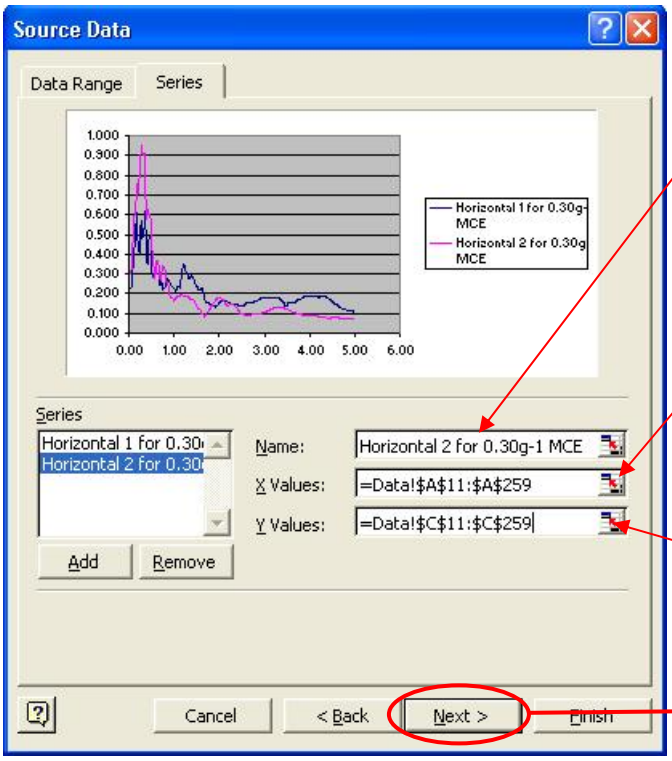

Step 21: Enter 'Name' of Series 2

Step 22: Press and select data for 'Period' in column A (row 11-259) for 'X-Values' (refer to step 14)

Step 23: Press and select data for 'Horizontal-2 Acceleration' in column C (row 11-259) for 'Y-Values' (refer to step 14)

Step 24: Press "Next"

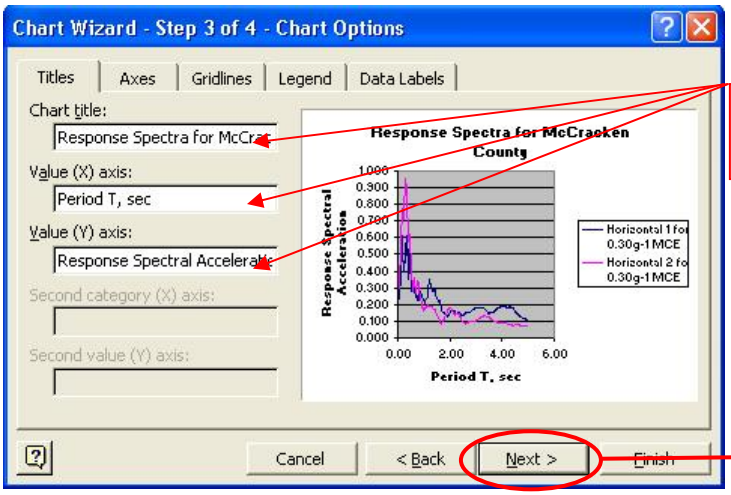

Step 25: Enter 'Chart Title' and X, Y axis titles

Step 26: Press "Next"

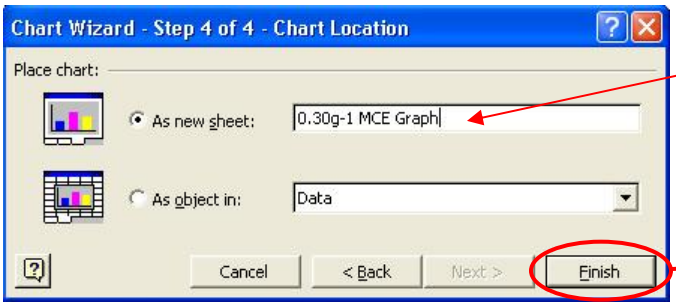

Step 27: Select "As new sheet" and enter name e.g.: 0.30g-1 MCE Graph

Step 28: Press "Finish"

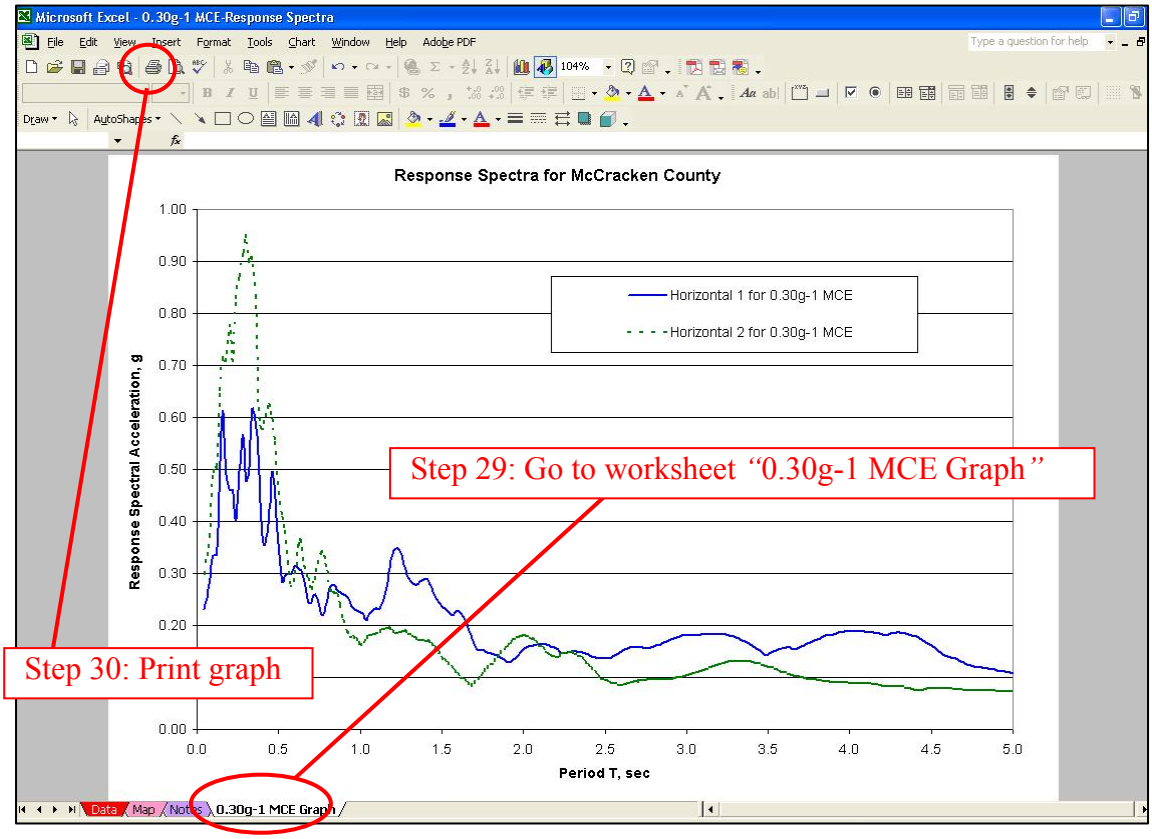

Step 29: Go to worksheet "0.30g-1 MCE Graph"

Step 30: Print graph

III. Design Response Spectra

Step 31: Plot manually or in Microsoft Excel the 'Design Response Spectra'

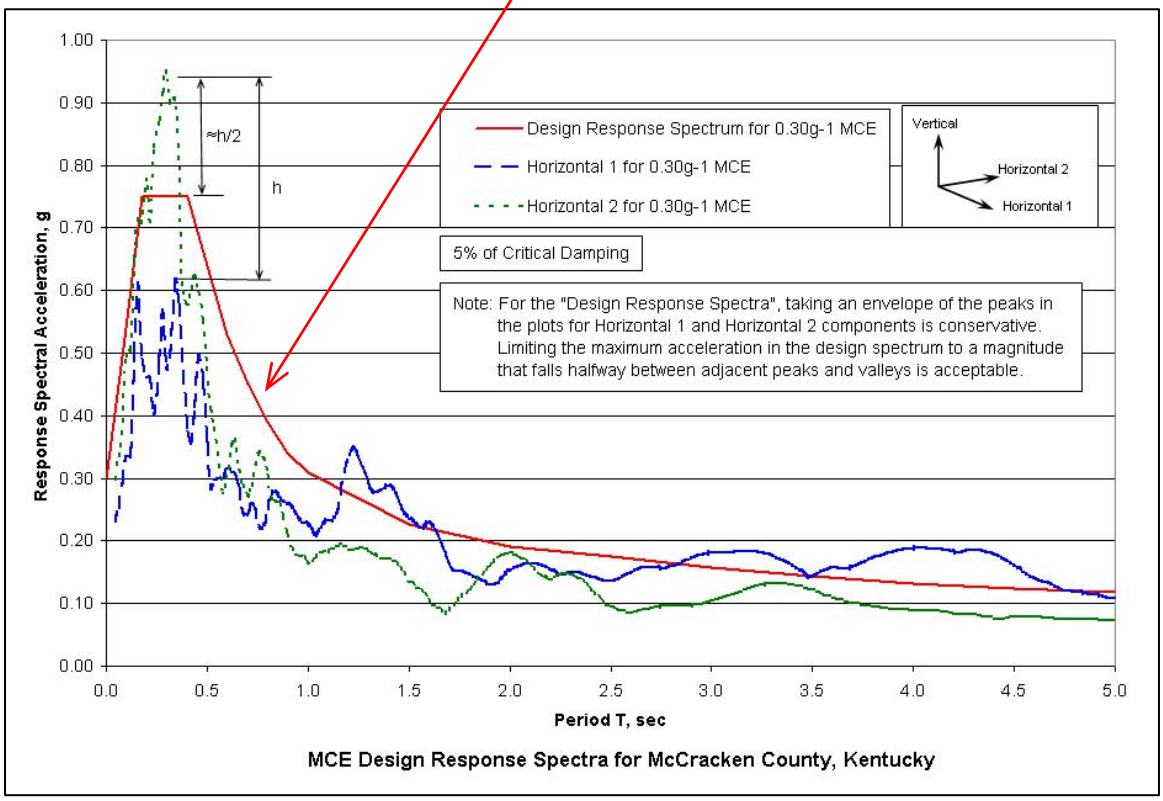

Appendix II

Derivation of the Time History

Time History Generation
For Counties in the Commonwealth of Kentucky

Example: Generate the Expected Earthquake Horizontal-1 Acceleration Time History for McCracken County, KY.

I. Electronic File Identification Map

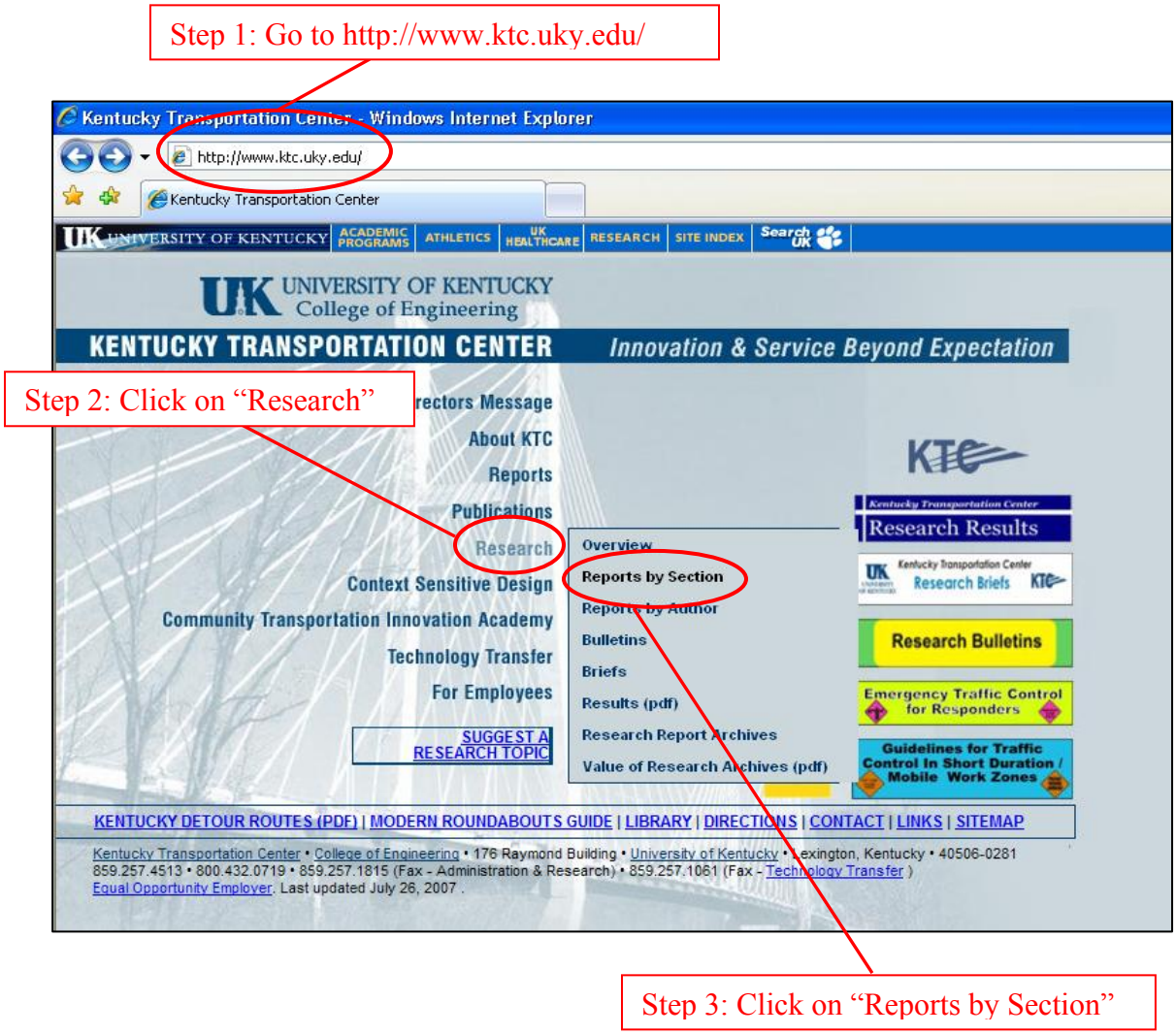

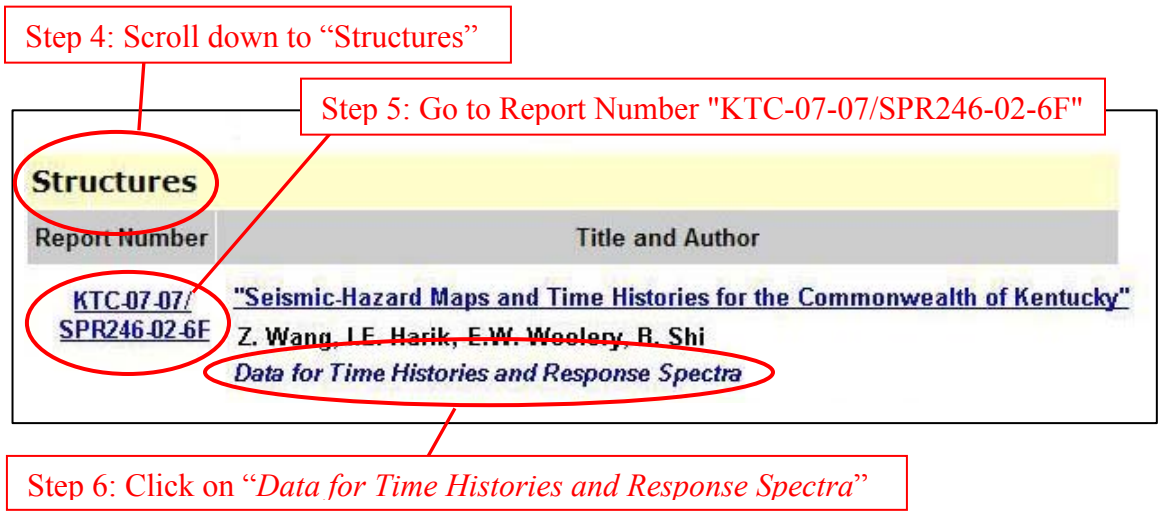
Step 4: Scroll down to “Structures”
Step 5: Go to Report Number "KTC-07-07/SPR246-02-6F"
Structures
Report Number
Title and Author
KTC-07-07/ SPR246-02-6F
"Seismic-Hazard Maps and Time Histories for the Commonwealth of Kentucky"
Z. Wang, I.E. Harik, E.W. Woolery, B. Shi
Data for Time Histories and Response Spectra
Step 6: Click on “Data for Time Histories and Response Spectra”

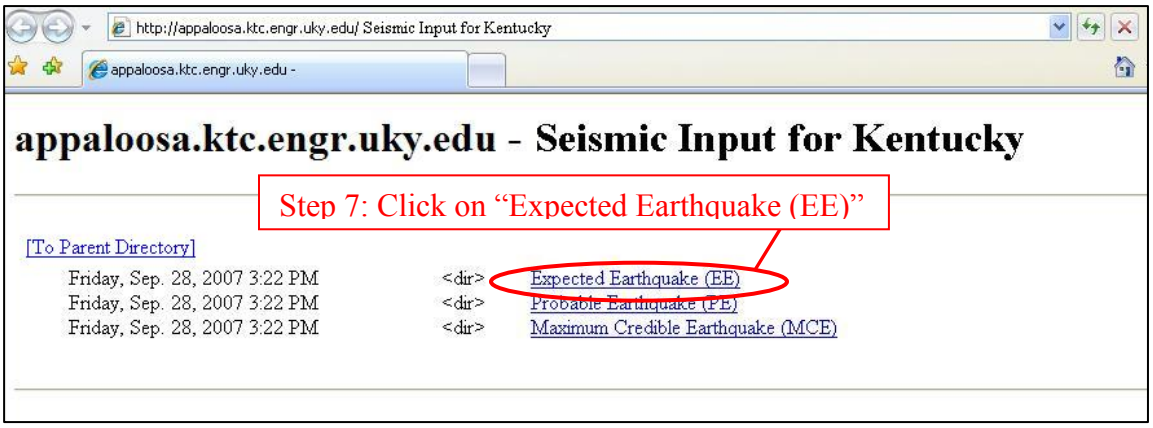
http://appaloosa.ktc.engr.uky.edu/ Seismic Input for Kentucky
appaloosa.ktc.engr.uky.edu -
appaloosa.ktc.engr.uky.edu - Seismic Input for Kentucky
Step 7: Click on “Expected Earthquake (EE)”
[To Parent Directory]
Friday, Sep. 28, 2007 3:22 PM <dir> Expected Earthquake (EE)
Friday, Sep. 28, 2007 3:22 PM <dir> Probable Earthquake (PE)
Friday, Sep. 28, 2007 3:22 PM <dir> Maximum Credible Earthquake (MCE)

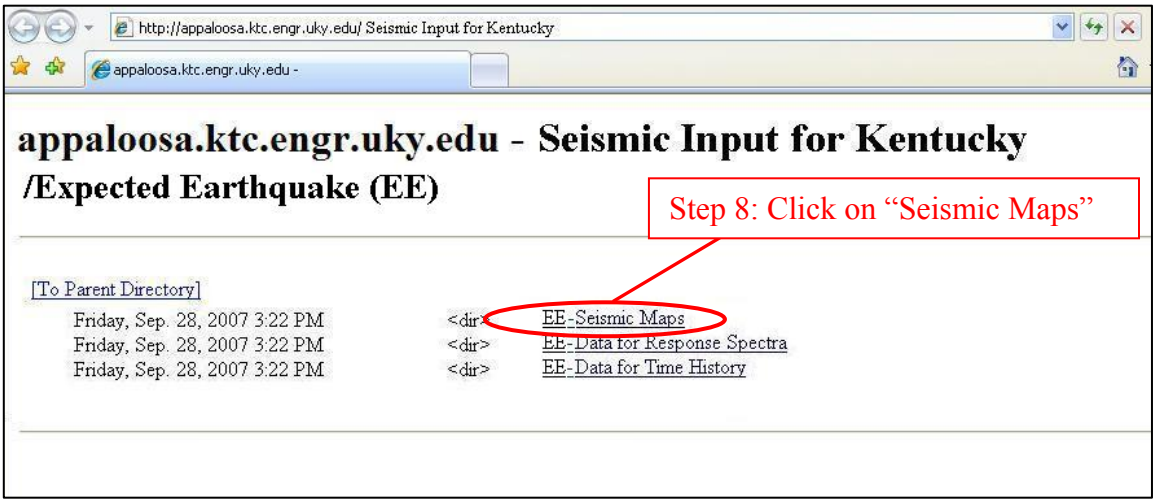
http://appaloosa.ktc.engr.uky.edu/ Seismic Input for Kentucky
appaloosa.ktc.engr.uky.edu -
appaloosa.ktc.engr.uky.edu - Seismic Input for Kentucky
/Expected Earthquake (EE)
Step 8: Click on “Seismic Maps”
[To Parent Directory]
Friday, Sep. 28, 2007 3:22 PM <dir> EE-Seismic Maps
Friday, Sep. 28, 2007 3:22 PM <dir> EE-Data for Response Spectra
Friday, Sep. 28, 2007 3:22 PM <dir> EE-Data for Time History

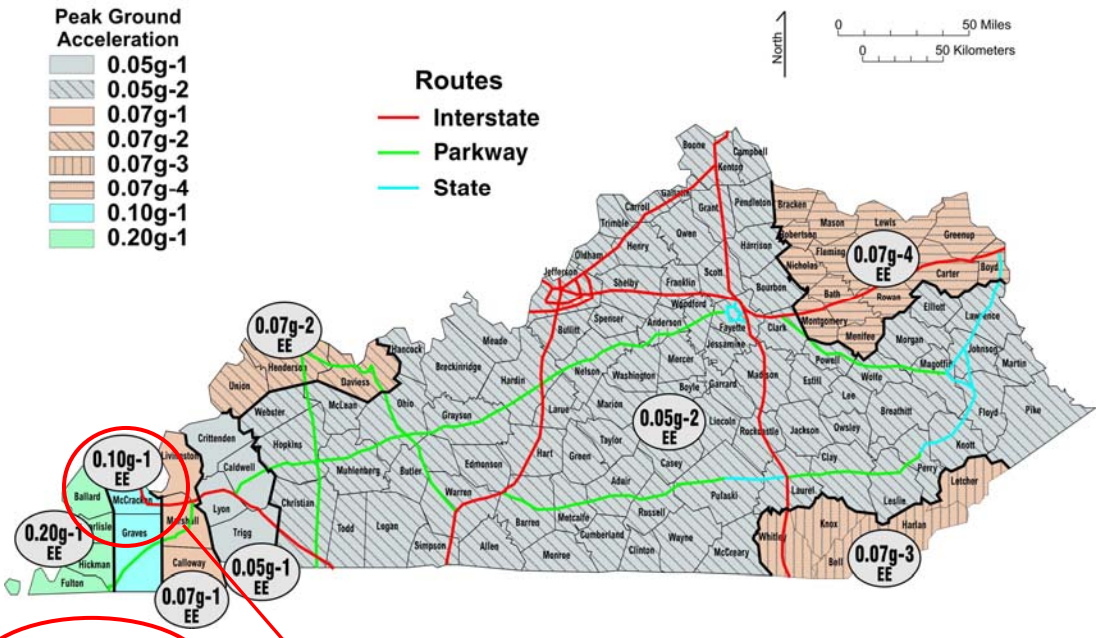

Figure 5-EE. Electronic Files Identification Map for the Expected Earthquake (EE) Time History and Response Spectra for the Commonwealth of Kentucky

Step 9: Go to Figure 5-EE

Step 10: Locate "*McCracken County, KY*" and the corresponding "Peak Ground Acceleration" (0.10g-1 EE for this example)

II. Time History

Step 11: Go back to the "Expected Earthquake (EE)" Screen

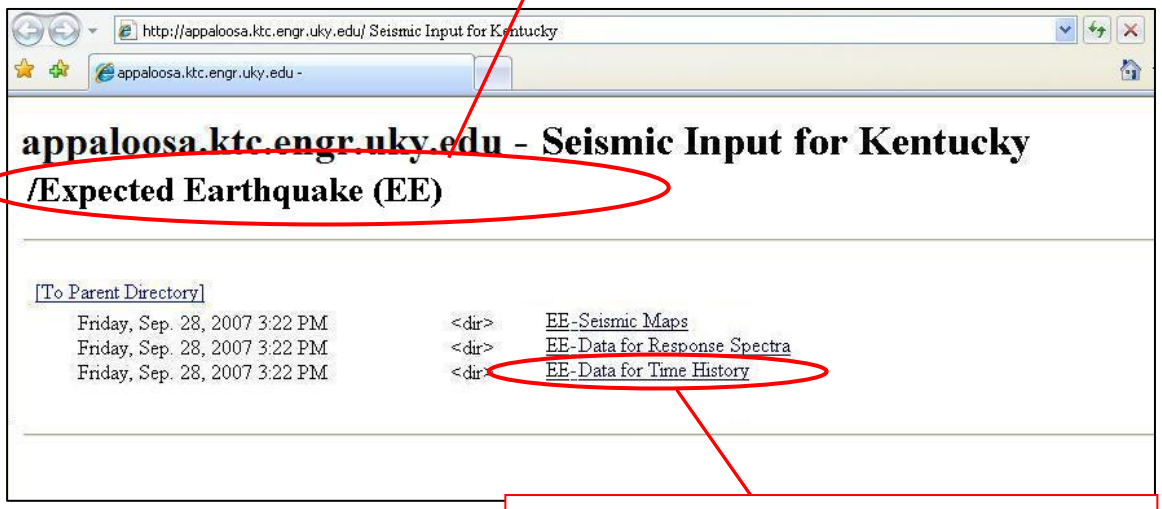

Step 12: Click on "EE- Data for Time History"

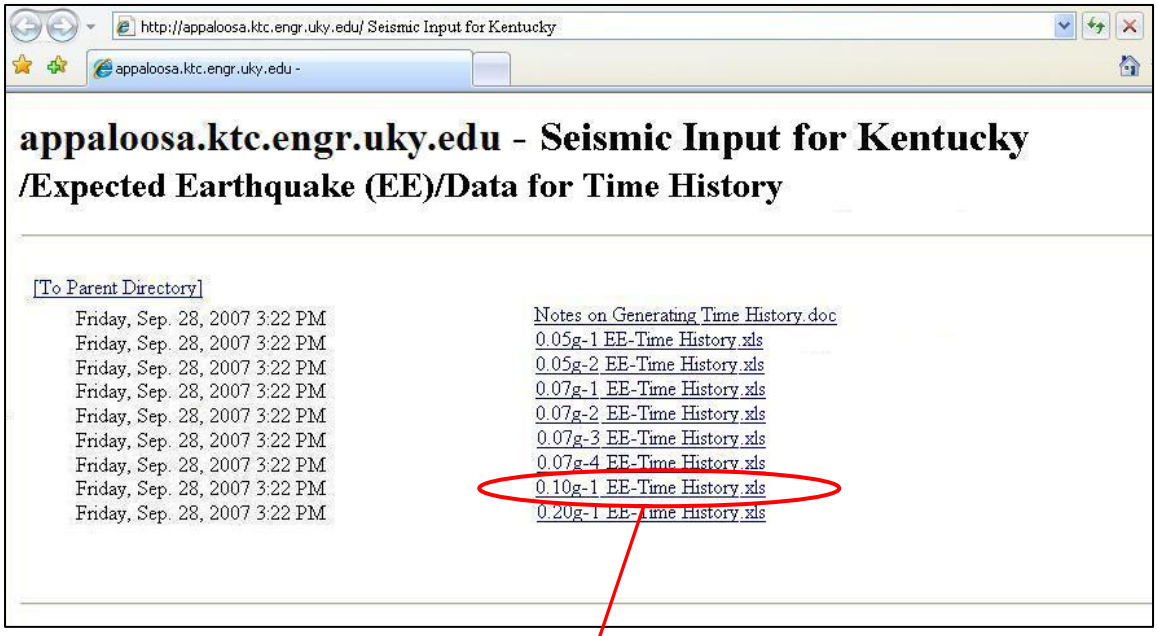

Step 13: Click on "0.10g-1 EE-Time History.xls"

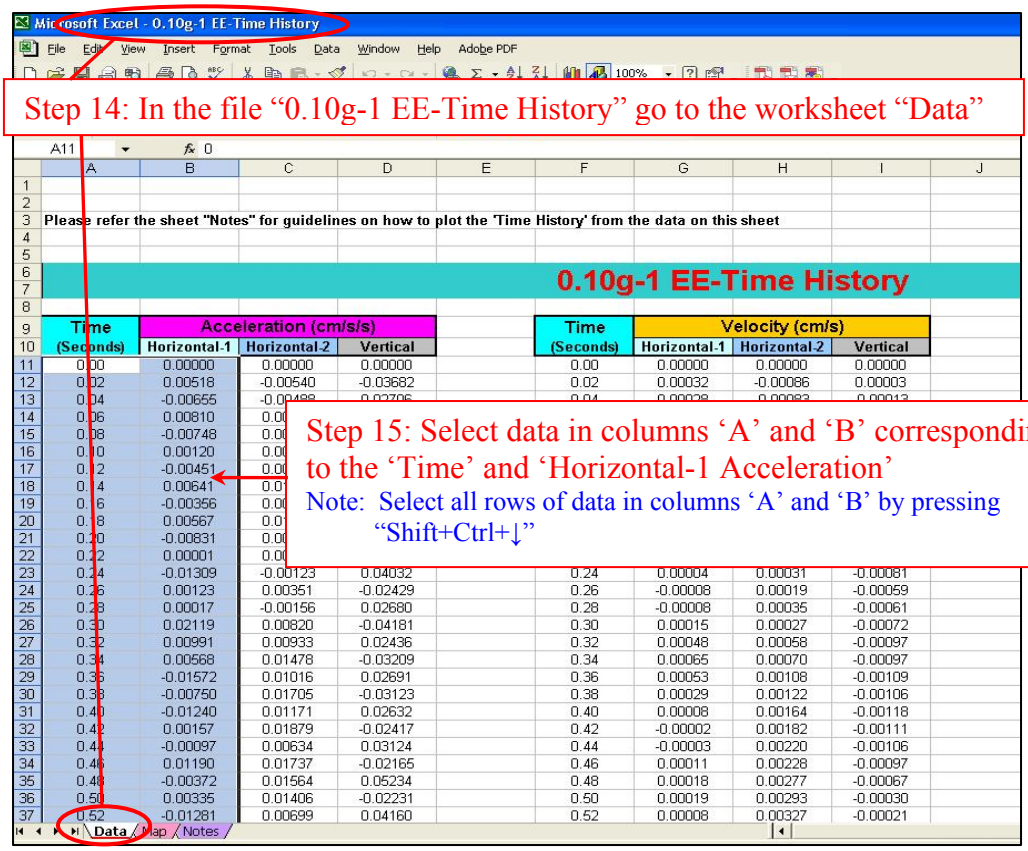
Microsoft Excel - 0.10g-1 EE-Time History
Step 14: In the file "0.10g-1 EE-Time History" go to the worksheet "Data"
Please refer the sheet "Notes" for guidelines on how to plot the 'Time History' from the data on this sheet
0.10g-1 EE-Time History
Time (Seconds)
Acceleration (cm/s/s)
Horizontal-1
Horizontal-2
Vertical
Velocity (cm/s)
Step 15: Select data in columns 'A' and 'B' corresponding to the 'Time' and 'Horizontal-1 Acceleration'
Note: Select all rows of data in columns 'A' and 'B' by pressing "Shift+Ctrl+↓"
Data
Map
Notes

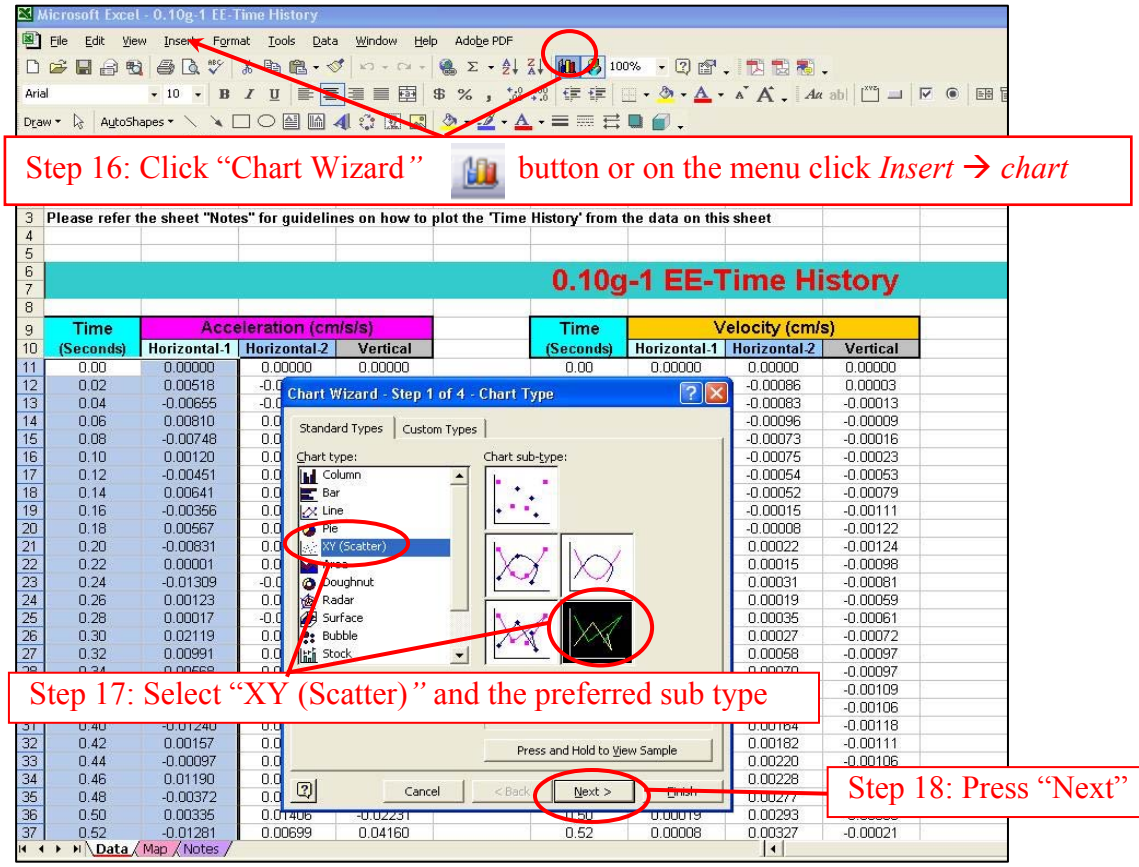
Microsoft Excel - 0.10g-1 EE-Time History
Step 16: Click "Chart Wizard" button or on the menu click Insert → chart
Please refer the sheet "Notes" for guidelines on how to plot the 'Time History' from the data on this sheet
0.10g-1 EE-Time History
Chart Wizard - Step 1 of 4 - Chart Type
Standard Types
Custom Types
Chart type:
Chart sub-type:
Column
Bar
Line
Pie
XY (Scatter)
Doughnut
Radar
Surface
Bubble
Stock
Press and Hold to View Sample
Cancel
< Back
Next >
Finish
Step 17: Select "XY (Scatter)" and the preferred sub type
Step 18: Press "Next"
Data
Map
Notes

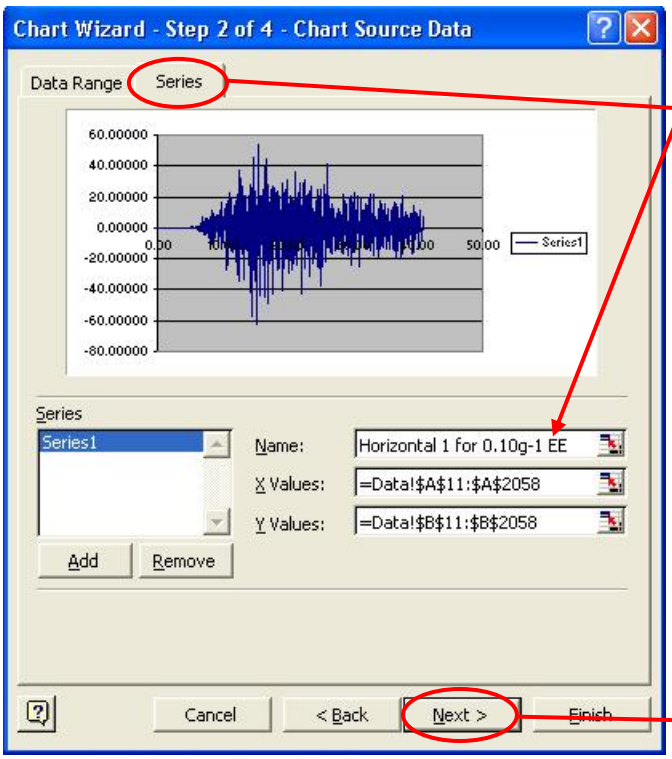

Step 19: Press "Series" tab and enter 'Name' of Series 1

Step 20: Press "Next"

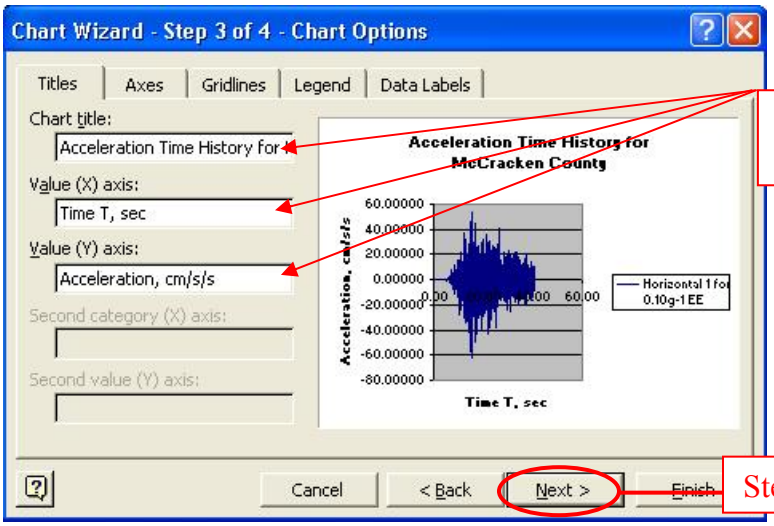

Step 21: Enter 'Chart Title' and X, Y axis titles

Step 22: Press "Next"

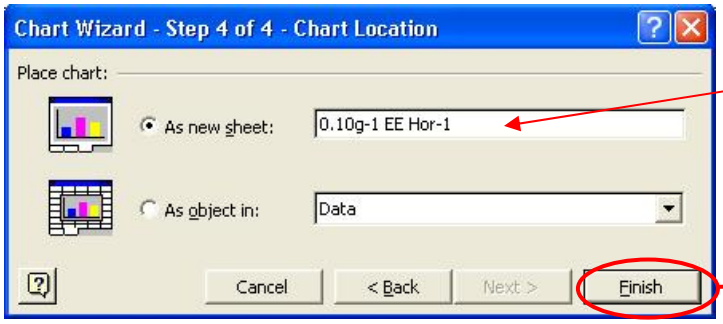

Step 23: Select "As new sheet" and enter name e.g.: 0.10g-1 EE Hor 1

Step 24: Press "Finish"

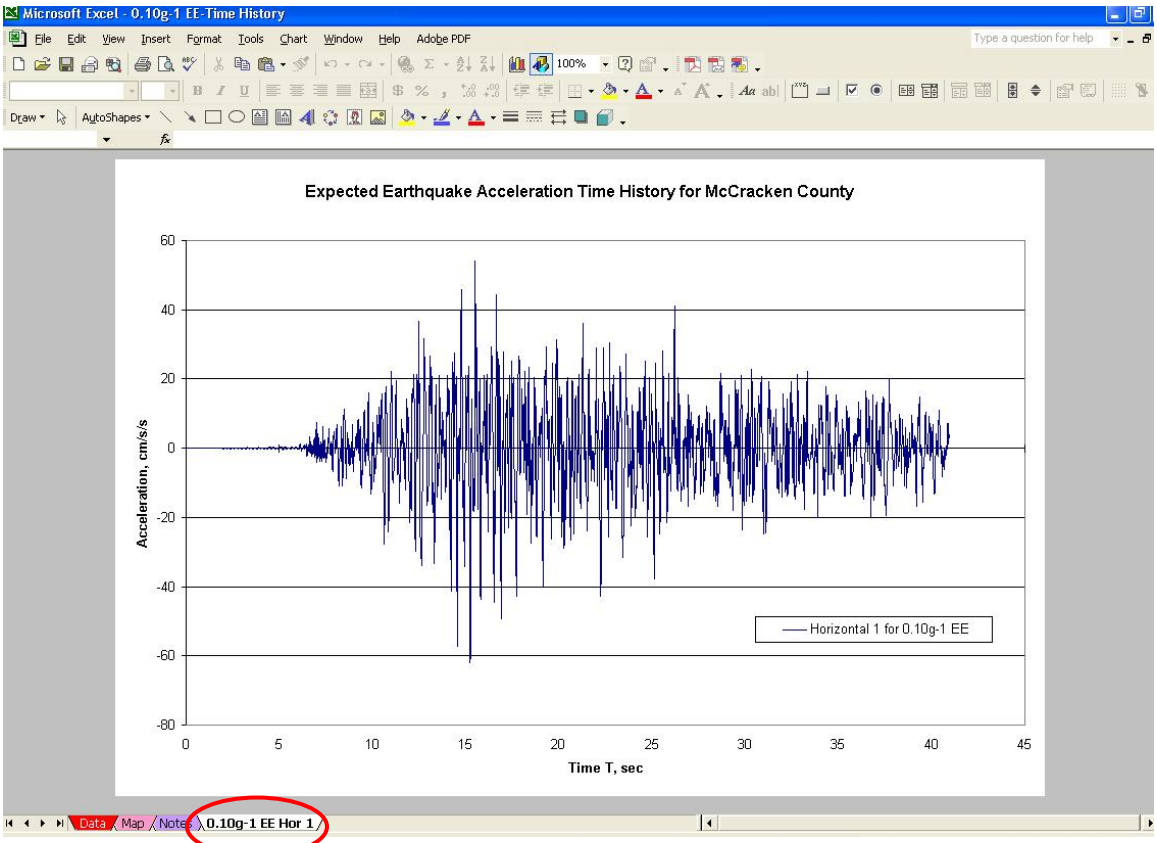

Step 25: Go to worksheet "0.10g-1 EE Hor 1"

Note : To plot any other Time History, for example the Expected Earthquake Horizontal-2 Velocity Time History go back to step 15, select data in columns 'F' and 'H' and repeat the above process.

For more information or a complete publication list, contact us at:

KENTUCKY TRANSPORTATION CENTER

176 Raymond Building
University of Kentucky
Lexington, Kentucky 40506-0281

(859) 257-4513
(859) 257-1815 (FAX)
1-800-432-0719
www.ktc.uky.edu
ktc@engr.uky.edu